

SYNTHETIC, STRUCTURAL, SPECTROSCOPIC,
CATALYTIC AND MECHANISTIC STUDIES OF
PALLADIUM COMPLEXES WITH BIDENTATE
CARBENE LIGANDS

By

SRI SKANDARAJA SUBRAMANIAM

Bachelor of Science in Chemistry
University of Kelaniya
Kelaniya, Sri Lanka
2003

Submitted to the Faculty of the
Graduate College of the
Oklahoma State University
in partial fulfillment of
the requirements for
the Degree of
DOCTOR OF PHILOSOPHY
May, 2011

SYNTHETIC, STRUCTURAL, SPECTROSCOPIC,
CATALYTIC AND MECHANISTIC STUDIES OF
PALLADIUM COMPLEXES WITH BIDENTATE
CARBENE LIGANDS

Dissertation Approved:

Dr. LeGrande M. Slaughter

Dissertation Adviser

Dr. Richard A. Bunce

Dr. Kevin D. Ausman

Dr. Stacy D. Benson

Dr. James P. Wicksted

Outside Committee Member

Dr. Mark E. Payton

Dean of the Graduate College

DEDICATION

I dedicate this thesis to my loving parents the late Ramasamy Subramaniam and the late Kasi Mariya Sarojani. Thank you for all your love and unconditional support.

ACKNOWLEDGEMENTS

The time I spent at Oklahoma State University has been the most enjoyable and biggest learning experience for me as a person and as a professional. I consider it a privilege to acknowledge many people who have encouraged, inspired, and guided me throughout my stay at Oklahoma State University. First, I would like to express my deepest gratitude to my advisor, Dr. LeGrande M. Slaughter, for his excellent guidance, caring, patience, and providing me with an excellent atmosphere for doing research. Thank you for all the advice, guidance and encouragement. I would also like to thank my thesis committee members, Dr. Richard A. Bunce, Dr. Kevin D. Ausman, Dr. Stacy D. Benson, and Dr. James P. Wicksted for all their guidance, advice, and motivation given to me. I am thankful to Dr. LeGrande M. Slaughter and Mr. Eli Sluch for their help in X-ray crystallography. I am also thankful to Dr. Margaret Eastman and Ms. Gianna Bell-Eunice for their help in NMR spectroscopy. I would like to thank Anju (Dr. Yoshitha Wanniarachchi) for her help and support in learning new techniques and adjusting to the new lab environment. I would like to thank all the former and current members of Dr. Slaughter's research group; Dr. Anthea, Dr. Dipesh, Eli, Chase, Chris, Yohan, Sachin, Aaron, Evangeline and James for their friendship and help given to me when needed. I also wish to thank the Faculty and Staff of the Department of Chemistry for giving me the opportunity to follow my dreams.

Finally, I wish to thank the people who are most responsible for my achievements, my parents, the late Ramasamy Subramaniam and the late Kasi Mariya Sarojani for their love, encouragement and for guiding me throughout my life. Even though I feel very sad that you are not with me to see the achievement, I am very happy to fulfill one of your dreams. I love you very much. Finally, I thank my sisters Subashine and Shanthi and brother, Ananda, for all the help and support given to me.

TABLE OF CONTENTS

Chapter	Page
I. LITERATURE REVIEW AND INTRODUCTION	1
Introduction.....	1
Carbenes.....	4
Types of carbenes	6
N-heterocyclic carbenes (NHCs)	9
Synthesis of NHC precursors and free NHCs.....	14
Synthesis of NHC metal complexes	17
Bis(NHC) complexes.....	18
Acyclic diaminocarbenes (ADC).....	21
References.....	23
II. SYNTHESIS OF METHYLPALLADIUM BIS(NHC) COMPLEXES AND INVESTIGATION OF CARBONYLATION REACTIONS RELEVANT TO CO / ALKENE COPOLYMERIZATION.....	31
Introduction.....	32
Results and discussion	34
Summary and conclusion.....	70
Experimental.....	71
References.....	86
III. SYNTHESIS AND CHARACTERIZATION OF DICATIONIC BIS(METHYLISOCYANIDE) ADDUCTS OF PALLADIUM(II) BIS(CARBENE) AND BIS(PHOSPHINE) COMPLEXES.....	90
Introduction.....	91
Results and discussion	94
Summary and conclusion.....	164
Experimental.....	165
References.....	180

Chapter	Page
IV. CORRELATION OF LIGAND DONICITY WITH CATALYTIC ACTIVITY FOR ELECTROPHILIC CATIONIC BIS(CARBENE) PALLADIUM(II) COMPLEXES.....	187
Introduction.....	188
Results and discussion	190
Summary and conclusion.....	220
Experimental.....	221
References.....	227
V. POLARIZED NAZAROV CYCLIZATIONS CATALYZED BY CATIONIC BIS(CARBENE) PALLADIUM(II) COMPLEXES AND SILVER SALTS	230
Introduction.....	231
Results and discussion	234
Summary and conclusion.....	248
Experimental.....	249
References.....	258

LIST OF TABLES

Table	Page
2.1. Selected bond lengths (Å) and bond angles (°) of complex 3	40
2.2. Crystal data and structure refinement details for complex 3	41
2.3. Selected bond lengths (Å) and bond angles (°) of complex 4	45
2.4. Crystal data and structure refinement details for complex 4	46
2.5. Equilibrium data between 4 and 5	48
3.1. ¹ H NMR spectral data for bis(NHC) bis(methylisocyanide) palladium(II) complexes.	99
3.2. ¹³ C NMR spectral data for bis(NHC) bis(methylisocyanide) palladium(II) complexes.	100
3.3. Selected bond lengths (Å) and bond angles (°) of complex 26a	104
3.4. Crystal data and structure refinement details for complex 26a	105
3.5. Selected bond lengths (Å) and bond angles (°) of complex 26b	107
3.6. Crystal data and structure refinement details for complex 26b	108
3.7. Selected bond lengths (Å) and bond angles (°) of complex 26c	110
3.8. Crystal data and structure refinement details for complex 26c	111

Table	Page
3.9. Selected bond lengths (Å) and bond angles (°) of complex 26d	113
3.10. Crystal data and structure refinement details for complex 26d	114
3.11. Infrared spectral data for bis(NHC) palladium bis(methylisocyanide) complexes	116
3.12. Selected bond lengths (Å) and bond angles (°) of complex 26e	121
3.13. Crystal data and structure refinement details for complex 26e	122
3.14. Selected bond lengths (Å) and bond angles (°) of complex 26f	127
3.15. Crystal data and structure refinement details for complex 26f	128
3.16. Selected bond lengths (Å) and bond angles (°) of complex 28b	133
3.17. Crystal data and structure refinement details for complex 28b	134
3.18. Selected bond lengths (Å) and bond angles (°) of complex 28c	138
3.19. Crystal data and structure refinement details for complex 28c	139
3.20. Selected bond lengths (Å) and bond angles (°) of complex 28e	143
3.21. Crystal data and structure refinement details for complex 28e	144
3.22. Selected bond lengths (Å) and bond angles (°) of complex 28f	147
3.23. Crystal data and structure refinement details for complex 28f	148
3.24. Selected bond lengths (Å) and bond angles (°) of complex 29b	155
3.25. Crystal data and structure refinement details for complex 29b	156
3.26. Selected bond lengths (Å) and bond angles (°) of complex 30b	159
3.27. Crystal data and structure refinement details for complex 30b	160
4.1. Summary of NMR scale catalytic cyclization of 2-(phenylethynyl)benzaldehyde with different catalysts	194
4.2. Solvent effect on the cyclization of S1 with catalyst 31f	196

Table	Page
4.3. Use of methanol as a solvent for cyclization of S1 to produce P1 and P2	197
4.4. Temperature effect on the cyclization of S1 with catalyst 31f in DCE	197
4.5. Catalytic reaction data for cyclization of S1 with varies catalyst together with IR stretching frequency for analogous methylisocyanide adduct.....	200
4.6. Results for catalytic mesitylene (1 equivalent) addition to propiolic acid (1.4 equivalent)	212
4.7. Pd-catalyzed hydroarylation between mesitylene (2 equiv) and propiolic acid (1 equiv) correlated with IR stretching frequencies for analogous (ligand) Pd ²⁺ methylisocyanide adducts	213
5.1. $\Delta\nu_{\text{MeNC}}$ values for bis(ADC) complexes with Hammett constant	236
5.2. Catalytic reaction data for cyclization of S2 with different bis(ADC) complexes together with IR stretching frequency for analogous methylisocyanide adduct	238
5.3. Lower catalytic loading with <i>p</i> -CF ₃ bis(ADC) complex	240
5.4. Substrate scope with <i>p</i> -CF ₃ bis(ADC) complex	242
5.5. Substrate scope with <i>p</i> -OCH ₃ bis(ADC) complex	243
5.6. Substrate scope with rigid bis(NHC) complex 21	245
5.7. Nazarov cyclization of substrate S2 with different silver salts.....	246
5.8. Substrate scope with AgSbF ₆ as catalyst	247

LIST OF FIGURES

Figure	Page
1.1. Electronic configuration and geometry of singlet and triplet carbenes	5
1.2 (i) Orbital diagram of a carbene containing σ -electron withdrawing substituents, (ii) electronegativity effect on ground state	6
1.3. Electron donation and resonance structures of a Fischer carbene ligand	8
1.4 Electron donation in a Schrock carbene complex	9
1.5. Electronic stabilization of N-heterocyclic carbenes.....	12
1.6 Structures of the most common five membered NHC subclasses.....	13
1.7. Determination of orientation by linker length: (A) in-plane conformation (shorter linkage); (B) perpendicular orientation (longer linker).....	19
1.8 Steric interactions between (A) N-substituents and coligands (B) N- substituents and N-substituents.....	19
2.1. Molecular structure of complex 3 with 50% probability ellipsoids	39
2.2. Molecular structure of complex 4 with 50% probability ellipsoids	44
2.3. Van't Hoff plot for equilibrium between 4 and 5	48
2.4. Kinetic plot for methyl migration in 4 at 0.5 atm and - 50°C of CO	50
2.5. Kinetic plot for methyl migration in 4 at 1 atm and - 50°C of CO	51
3.1. Molecular structure of complex 26a with 50% probability ellipsoids	103
3.2. Molecular structure of complex 26b with 50% probability ellipsoids	106
3.3. Molecular structure of complex 26c with 50% probability ellipsoids	109

Figure	Page
3.4. Molecular structure of complex 26b with 50% probability ellipsoids	112
3.5. Variation of donicity with dihedral angle and bite angle for complexes 26a-26d	115
3.6. Molecular structure of complex 26e with 50% probability ellipsoids	120
3.7. Molecular structure of complex 26f with 50% probability ellipsoids	126
3.8. Molecular structure of complex 28b with 50% probability ellipsoids	132
3.9. Molecular structure of complex 28c with 50% probability ellipsoids	137
3.10. Molecular structure of complex 28e with 50% probability ellipsoids	142
3.11. Molecular structure of complex 28f with 50% probability ellipsoids	146
3.12. Structure of five- and seven-membered chelate bis(ADC) palladium(II) bis(methylisocyanide) complexes	149
3.13. Molecular structure of complex 29b with 50% probability ellipsoids	154
3.14. Molecular structure of complex 30b with 50% probability ellipsoids	158
3.15. Donor scale versus ligand structure for bis(carbene) and bis(phosphine) ligands.....	162
4.1. Cyclization rate of alkenylaldehyde versus Δv_{MeNC} for various (chelate) Pd ²⁺ complexes	201
4.2. Cyclization rate of alkenylaldehyde versus Δv_{MeNC} for the rigid, non-labile DPPBen complex and bis(carbene) complexes.....	203
4.3. Virtual LUMO energies from optimized (bisNHC)Pd ²⁺ (B3LYP/CEP-31G(d), Gaussian03) together with experimental and catalytic rate data	205
4.4. Calculated $G_{Pd(L)}$ and G_γ together with other stereoelectronic parameters	207
4.5. Effects on reaction rate of varying concentration of S1, CH ₃ CN, Pd catalyst, and CH ₃ OH	209
4.6. Reaction mechanism for cyclization of 2-(phenylethynyl)benzaldehyde	210

Figure	Page
4.7. Hydroarylation rate versus Δv_{MeNC} for bis(NHC) Pd ²⁺ catalysts	214
5.1. Nazarov cyclization mechanism.....	231
5.2. Effects of different substituent pattern on the catalytic activity.....	232
5.3. Nazarov cyclization rate versus $\Delta v_{\text{N=C}}$ with bis(ADC) palladium catalysts	239
5.4. Dimeric analogue of <i>p</i> -CF ₃ bis(ADC) complex with bridging chloride	240

CHAPTER I

LITERATURE REVIEW AND INTRODUCTION

Introduction

Currently, carbenes are an extremely important class of ligands in metal-catalyzed reactions. They have been shown to be superior to other ligands in scope and activities of several catalytic reactions. This is due to several reasons, primarily the strong donor abilities of carbene ligands. Metal carbene complexes have found use in a wide variety of catalytic applications. This chapter will provide an introduction to carbene structure, types of carbenes, their metal complexes, and their usage in catalytic reactions. Chapter II will describe the synthesis of neutral and cationic methylpalladium complexes of bis(N-heterocyclic carbenes), or bis(NHCs), and their use in mechanistic studies of methyl migration to CO, a key step in alkene / CO copolymerization. Chapter III will focus on the use of methylisocyanide as an IR probe to evaluate the trans effect in bis(NHC) and bis(phosphine) containing palladium bis(methylisocyanide) complexes, which allows correlation of ligand donicity with structural features. Chapter IV will discuss catalytic activities of bis(NHC) and bis(phosphine) palladium complexes in electrophilic reaction and correlations of their catalytic activities with ligand donicity. Finally, Chapter V describes Nazarov cyclization reactions catalyzed by bis(acyclic diaminocarbene), or [bis(ADC)], palladium complexes and the role of silver salts in these reactions.

The stereoelectronic properties of ligands have a great influence on the reactivities and properties of transition metal complexes. N-heterocyclic carbenes (NHCs) are one of the most popular classes of ligand in metal catalyzed reactions. The electronic properties of NHCs were investigated by CO stretching frequencies,¹⁻³ calorimetric studies,⁴ theoretical pK_a values⁵ and NMR spectroscopic studies. The steric parameters of NHCs were commonly examined by Tolman cone angle θ ,⁶ solid angles

Ω ,⁷ and % V_{Bur} .⁸ All most all these studies focus on mono-NHC ligands, and there were few studies on mono-ADC ligand.^{5,9} Even though correlations between mono-NHC donor and structural parameters were extensively investigated, their correlation with catalytic activity has rarely been studied. In addition, little attention was focused toward studying the stereoelectronic properties of chelating bis(NHCs).

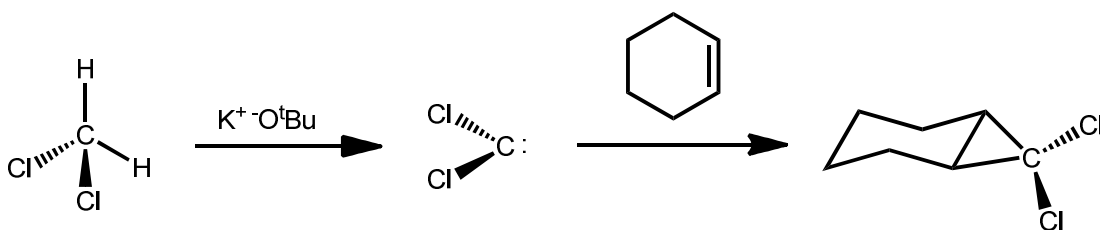
In the current study, comparisons of σ -donicity of bis(NHCs) with bis(ADCs) and the more commonly used bis(phosphine) ligands were made using an IR probe ligand. Chelating bis(NHC) ligands having various alkane bridges, azole rings, and binding position (C2, C3, and C4) were prepared to assess their donicity as a function of different structural parameters. Comparisons of these electronic and structural parameters were done using IR probe and X-ray crystallography studies.

Even though the stretching frequency of CO (ν CO) in various transition metal-carbonyl complexes is the most widely used method for comparing the electronic properties of NHC and phosphine ligands, this method has the disadvantage of not separating σ -donor and π -acceptor effects. Methyl isocyanide is a stronger σ -donor and weaker π -acceptor ligand than CO.¹⁰ Therefore, replacing CO with isoelectronic methylisocyanide will provide a more useful assessment of relative σ -donor strength of ligands *trans* to it. Comparison of donicity was performed by attaching various bis(NHC), bis(phosphine) and bis(ADC) ligands to cationic bis(methyl isocyanide) palladium(II) complexes. These ligands donicity and structural parameters were directly correlated to their catalytic activities in bis(acetonitrile) palladium(II) complexes. This investigation successfully predicted catalytic activities of catalysts containing homologous ligand series using methylisocyanide as an IR probe. However, other

parameters such as steric hindrance and electronic structure have to be considered when predicting the catalytic activity for different series of ligands. Finally, the catalytic activities of a series of palladium complexes of electronically tunable bis(ADC) ligands were predicted using methylisocyanide as an IR probe.

Carbenes

Carbenes have been involved in many synthetic reactions during the past six decades after their introduction to organic chemistry by Doering in the 1950s¹¹ and to organometallic chemistry by Fischer in 1964.¹² Their electronic structure plays a vital role in their properties and applications. In the early days, carbenes were considered as highly reactive transient intermediates, which were rarely stable in the free state and only generated in a reaction mixture. Geuther in 1862 was first to propose the dichlorocarbene can exist as a reaction intermediate.¹³ However, it was Doering in 1954 who synthesized dichlorocarbene and trapped it with olefins to generate cyclopropane derivatives (Scheme 1.1).¹



Scheme 1.1. In-situ generation of dichlorocarbene and trapping with cyclohexene.

(Adapted from Reference 11)

Most carbenes have a bent geometry, with sp² hybridization and an unhybridized P_y (P_π) orbital.¹⁴ The ground state spin multiplicity can be either singlet or triplet, based

on the orbital location of the two non bonding electrons and depending on the relative energies of the sp^2 (σ) and P_π orbitals. A singlet state carbene has two non bonding electrons in one of the σ orbitals with anti-parallel spin, usually with more than a 2.0 eV energy gap between the σ and P_π orbitals. A triplet carbene has two non bonding electrons located separately in σ and P_π orbitals with parallel spin, usually with less than a 1.5 eV energy gap between the σ and P_π orbitals. The electronic (inductive and mesomeric) and steric effects of the neighboring groups determine the spin multiplicity via this energy gap. It is well known that σ -electron withdrawing substituents favor the singlet over the triplet state; for example the ground state changes from triplet to singlet when the substituent changes from electropositive lithium to electronegative fluorine.¹⁴ This reduces the energy of the non-bonding σ -orbital (HOMO) of the carbene and increases the σ and P_π energy gap. This stabilizes the singlet state of the carbene.

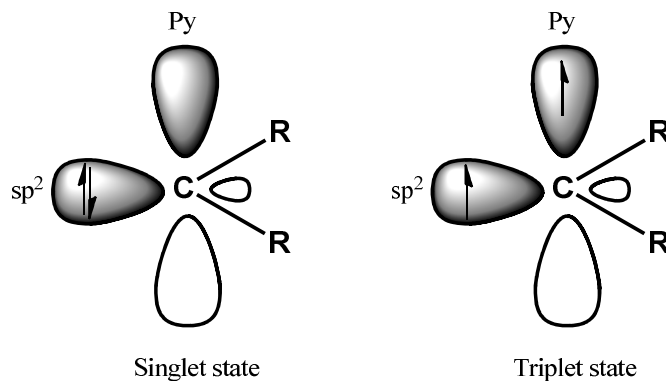


Figure 1.1. Electronic configuration and geometry of singlet and triplet carbenes (adapted from reference 14)

Carbenes can be kinetically stabilized by bulky substituents. When electronic effects are negligible, steric effects can determine the spin multiplicity. Bulkier substituents favor the linear geometry and increase the carbene bond angle; therefore the triplet ground state is favored.¹⁴ For example, di(*tert*-butyl)¹⁵ and diadamantyl¹⁶ carbenes are triplet and dimethylcarbene¹⁷ is singlet.

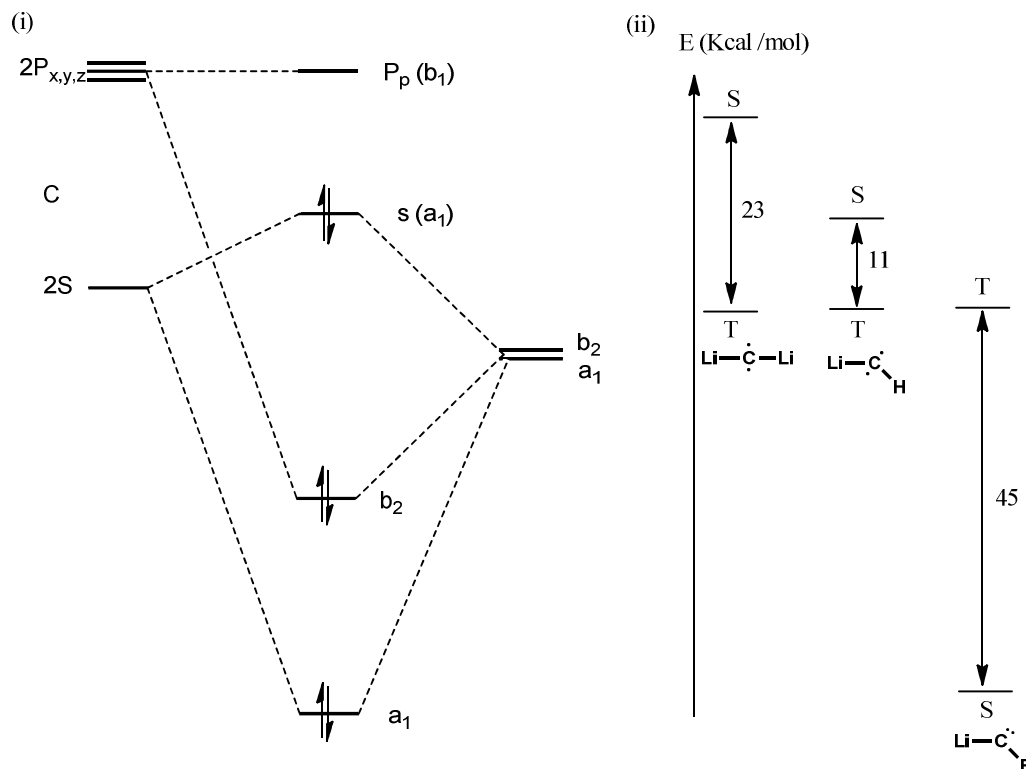
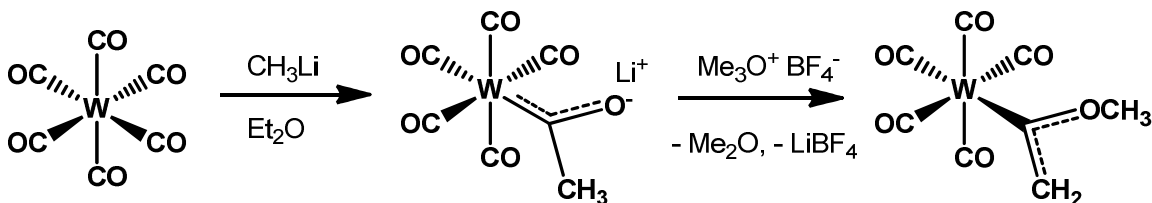


Figure 1.2. (i) Orbital diagram of a carbene containing σ -electron withdrawing substituents, (ii) electronegativity effect on ground state. (adapted from Reference 14)

Types of carbenes

Carbene ligands coordinated to metal centers have been divided into two main categories, Fischer and Schrock carbenes. Fischer carbenes are considered as singlet, electrophilic carbenes and Schrock carbenes as triplet, nucleophilic carbenes. Both

carbenes have different types of bonding to the metal. Fisher in 1964 synthesized the first stable Fischer carbene complex with tungsten (Scheme 1.2).¹²



Scheme 1.2. Synthesis of the first Fischer carbene complex. (Adapted from reference 12)

Fischer carbenes can be found in early or late transition metals in low oxidation state, with π -donor substituents such as $-\text{OMe}$ or $-\text{NMe}_2$ bound to the carbene carbon. Fischer carbene formation is facilitated by the presence of π -acceptor ligands on the metal. Fischer carbenes are neutral, two-electron donor ligands. Fischer carbenes are predominantly σ -donors to the metal via the lone pair present in an sp^2 hybrid orbital. The empty P_π orbital can act as a weak acceptor for π back donation from metal d_π electrons. This makes the carbene electrophilic, because $\text{C} \rightarrow \text{M}$ donation is partially cancelled by $\text{M} \rightarrow \text{C}$ backdonation.¹⁸ The lone pairs on the carbene π -substituent and the filled d_π orbitals can compete for donation to the empty P_π orbital on the Fischer carbene, which produces two possible resonance structures (Figure 1.3). Resonance structure (c) in Figure 1.3 is a reasonable description of real structures determined by X-ray crystallography, which showed short C-O and long M-C bonds.¹⁸ This indicates low π back donation from metal to carbene.

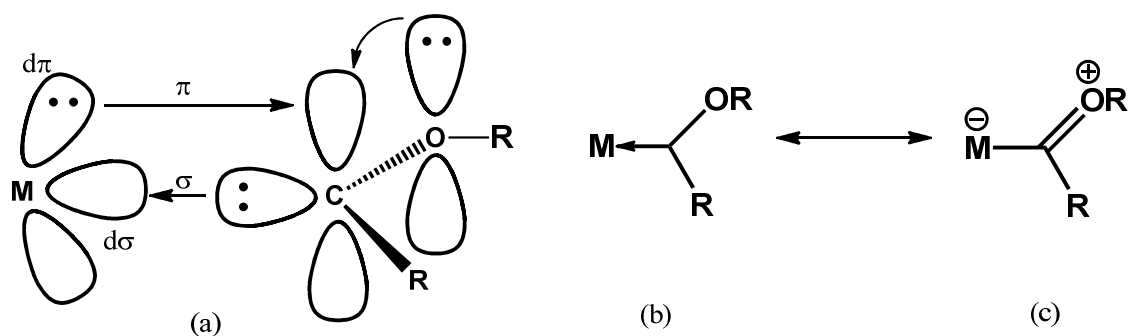
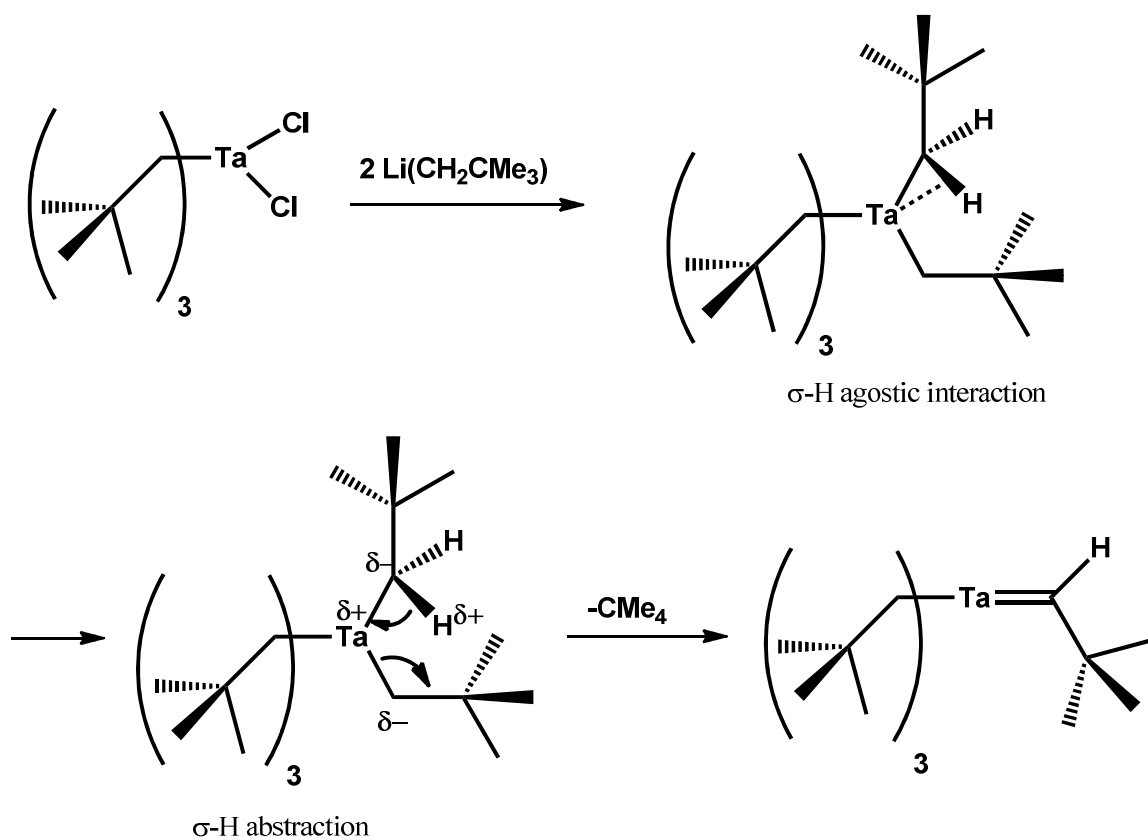


Figure 1.3. Electron donation and resonance structures of a Fischer carbene ligand.



Scheme 1.3. Synthesis of a Schrock carbene complex. Adapted from Reference 20.

Schrock in 1974 discovered Schrock carbenes in an attempt to synthesize $\text{Ta}(\text{CH}_2\text{CMe}_3)_5$.¹⁹ The treatment of $\text{Ta}(\text{CH}_2\text{CMe}_3)_3\text{Cl}_2$ with 2 equivalents of

$\text{Li}(\text{CH}_2\text{CMe}_3)$ resulted in the first stable Schrock carbene complex $(\text{CH}_2\text{CMe}_3)_3\text{Ta}(\text{CHCMe}_3)$. This carbene complex forms through a $\text{Ta}(\text{CH}_2\text{CMe}_3)_5$ intermediate, in which Ta forms an α -agostic interaction with one of the neighboring C-H groups followed by α -hydrogen abstraction to form the carbene complex (Scheme 1.3).²⁰

Schrock carbenes are commonly known as ‘alkylidenes’. Schrock carbenes can be found in early transition metal complexes with higher oxidation states, such as Ta(V), Ti(IV) and W(V). Usually, these complexes lack π -acceptor ligands and do not need π -donor substituents on the carbene to stabilize it. The bonding between metal and carbene takes place by interaction between two unpaired electrons on the carbene and the metal each. This results in the formation of two covalent bonds. Therefore, the carbene can be considered as a formally -2 ligand. The carbon is more electronegative than the metal; therefore, the covalent bonds are polarized toward carbon, producing a nucleophilic carbene.

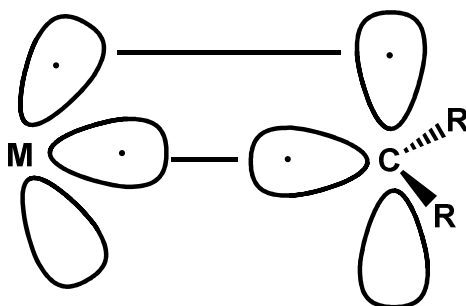
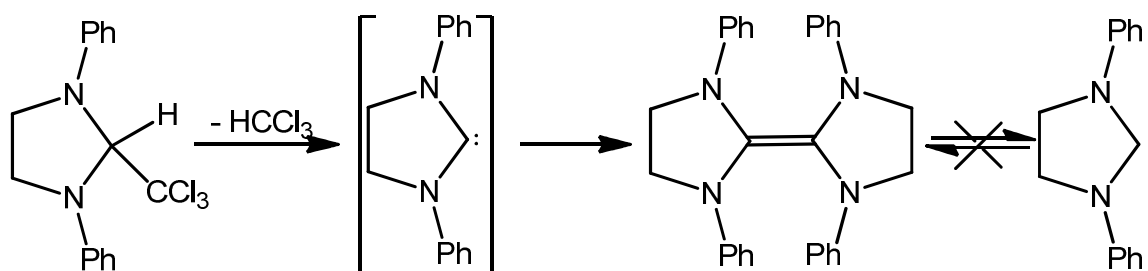


Figure 1.4. Electron donation in a Schrock carbene complex. Adapted from Reference 18

N-Heterocyclic carbenes (NHCs)

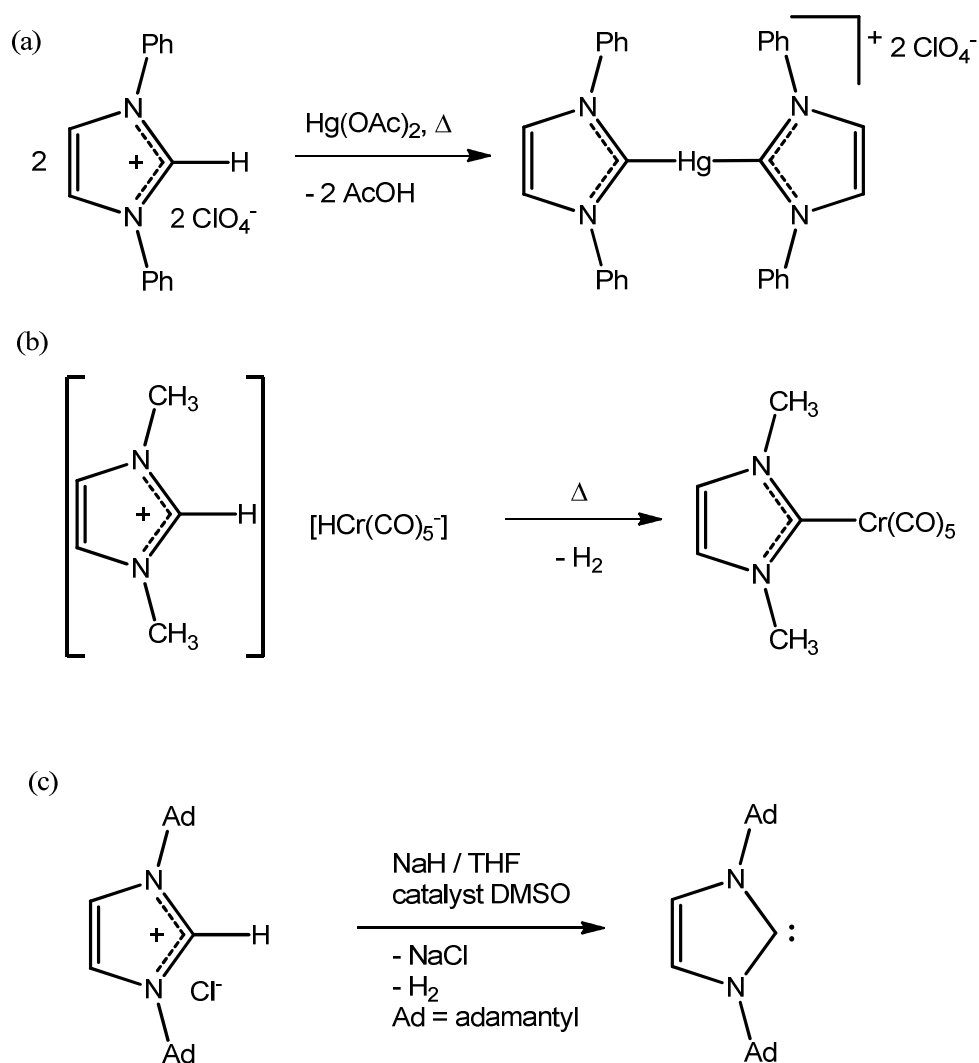
NHCs are considered singlet neutral carbenes, with at least one nitrogen atom within a heterocyclic ring connected to the divalent carbene.²¹ They can also be described

as an extreme type of Fisher carbene.¹⁸ In the early 1960s, Wanzlick suggested the existence of NHCs and a way to synthesize them in reaction media.²² The attempt to synthesize free NHC from the thermal elimination of chloroform from 2-trichloromethyl dihydroimidazoles instead produced a dimeric electron-rich olefin (Scheme 1.4).²³⁻²⁵ At that time, crossover experiments did not support an equilibrium between this dimer and the free carbene,²⁶⁻²⁸ but recently Denk et al. provided some evidence for this equilibrium.²⁹



Scheme 1.4. Attempted free NHC synthesis by Wanzlick et al. adapted from Reference 23

Subsequently, Wanzlick³⁰ and Ofele³¹ in 1968 independently reported NHCs as ligands in Cr(0) and Hg(II) complexes (Scheme 1.5). In 1991, Arduengo et al. isolated and fully characterized the first free NHC, 1.3-di(adamantyl)imidazol-2-ylidene (IAd), through deprotonation of its imidazolium precursor (Scheme 1.5 c).³² The colorless crystals of free NHC showed thermal stability up to the melting point of 240-241 °C without decomposition. This is the breakthrough point of NHC chemistry, after which there was tremendous growth in the field of NHCs as ligands in metal catalyzed reactions.



Scheme 1.5. Synthesis of first NHC complexes ((a) and (b)) and isolation of the first stable free NHC (c).

The electronic structure of NHCs is similar to that of Fischer carbenes, but with an insignificant amount of backbonding. The carbene carbon has a planar geometry with sp^2 hybridization. The energy gap between occupied sp^2 (σ) and unoccupied P_π orbitals is larger than 2 eV.³³ This stabilizes the singlet ground state. The s character of the σ orbital of the carbene is increased due to the inductive effects and electron-withdrawing power

of neighboring N atoms, with minimal effect on the P_π orbital. However, the N atoms can π -donate into the empty P_π orbital on the carbene.³⁴ These electronic effects will stabilize the singlet NHC by lowering the HOMO and increasing the singlet-triplet energy gap.

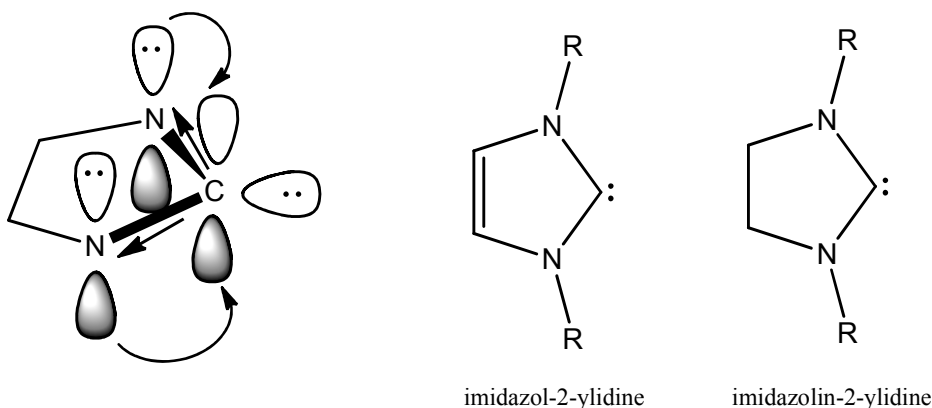
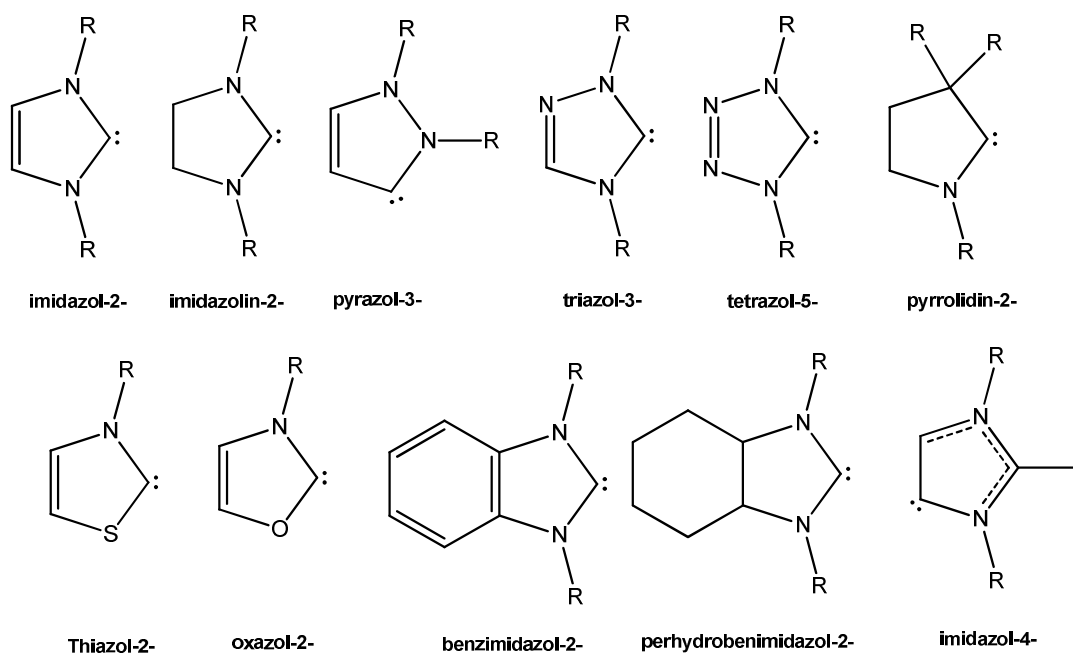


Figure 1.5. Electronic stabilization of N-heterocyclic carbenes

The electron pairs on nitrogen donate significant electron density into the P_π orbital on the carbene, which consequently minimizes π -back donation from metal toward the carbene.³⁴ Therefore, NHCs are considered as strong σ -donors with no or negligible π -back donation from the metal. However, there is some evidence which indicates considerable backdonation toward NHCs in some cases.³⁵⁻³⁷ The presence of a C=C bond in the heterocycle neighboring N can supply additional stabilization, as indicated by the higher stability of imidazol-2-ylidene than imidazolin-2-ylidene.³⁸ Bulky N-substituents can supply kinetic stabilization to free NHCs³², but free NHCs with very small methyl substituents³⁹ are also known. Therefore, the stability of NHC arises from both steric and electronic properties, but electronics have a major contribution.

Unlike other carbenes, NHCs are electron-rich nucleophilic species, which arises from the electronic stabilization. NHCs are strong σ -donor ligands and therefore form stronger bonds with metals than most other ligands such as phosphines.⁴⁰⁻⁴⁴ Initially, NHCs were considered as structural mimics to phosphine ligands, but eventually it was found that NHC-metal catalysts are superior in scope and activity.⁴⁵ NHCs have several advantages over phosphines, such as reduced need for excess ligand in catalytic reactions and improved air and moisture stability.⁴⁶ NHCs provide better steric protection to the metal active site because N-substituents shield the metal in a fence- or fan-like fashion. This is different from the cone-like steric shielding provided by tertiary phosphines.



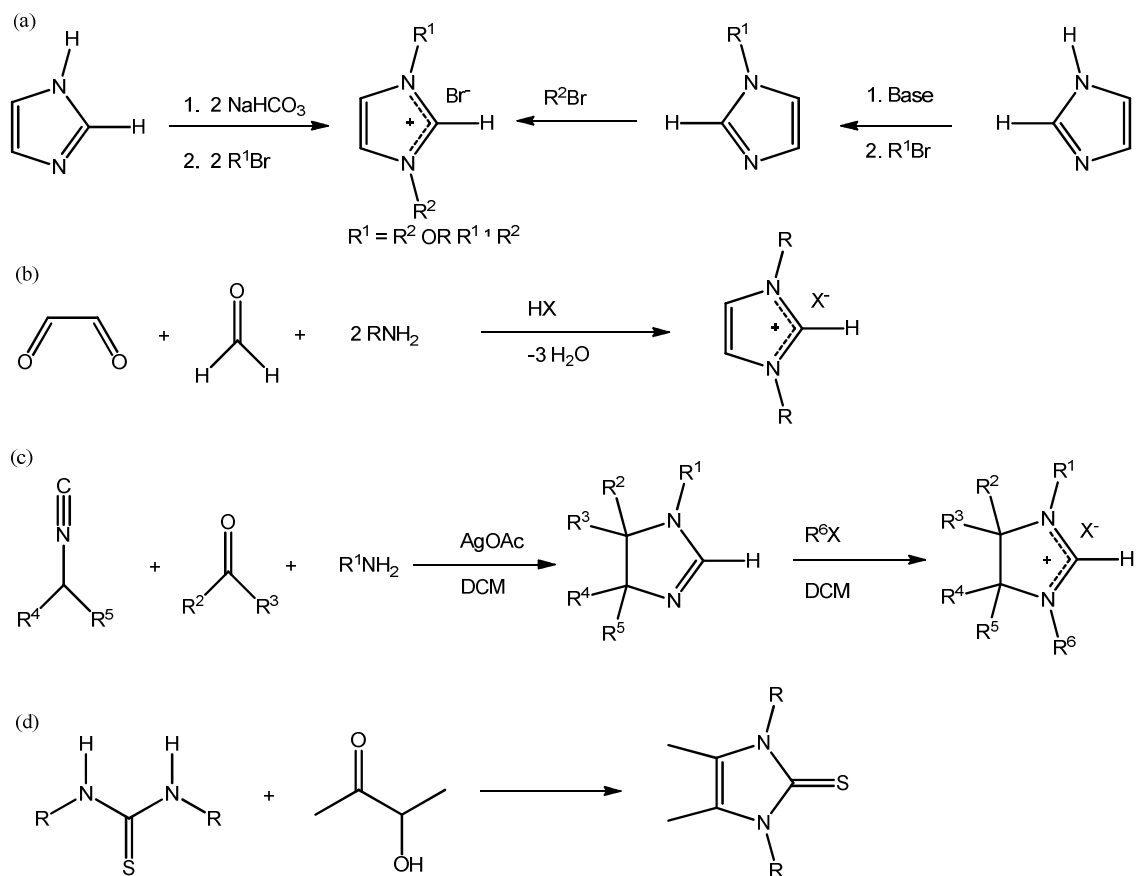
^a The suffix 'ylidene' should be added to the end of the subclass name to get generic name

Figure 1.6. Structures of the most common five membered NHC subclasses^a

As NHCs have become more popular ligands, access to a wide variety of NHCs with different electronic and steric properties has become possible. Even though three, four, five, six, and seven membered NHCs are known,^{33,34} only five membered NHCs are used in most applications. The most common subclasses of five membered NHCs are shown in Figure 1.6. The imidazol-2-ylidene is the most widely used one among them.

Synthesis of NHC precursors and free NHCs

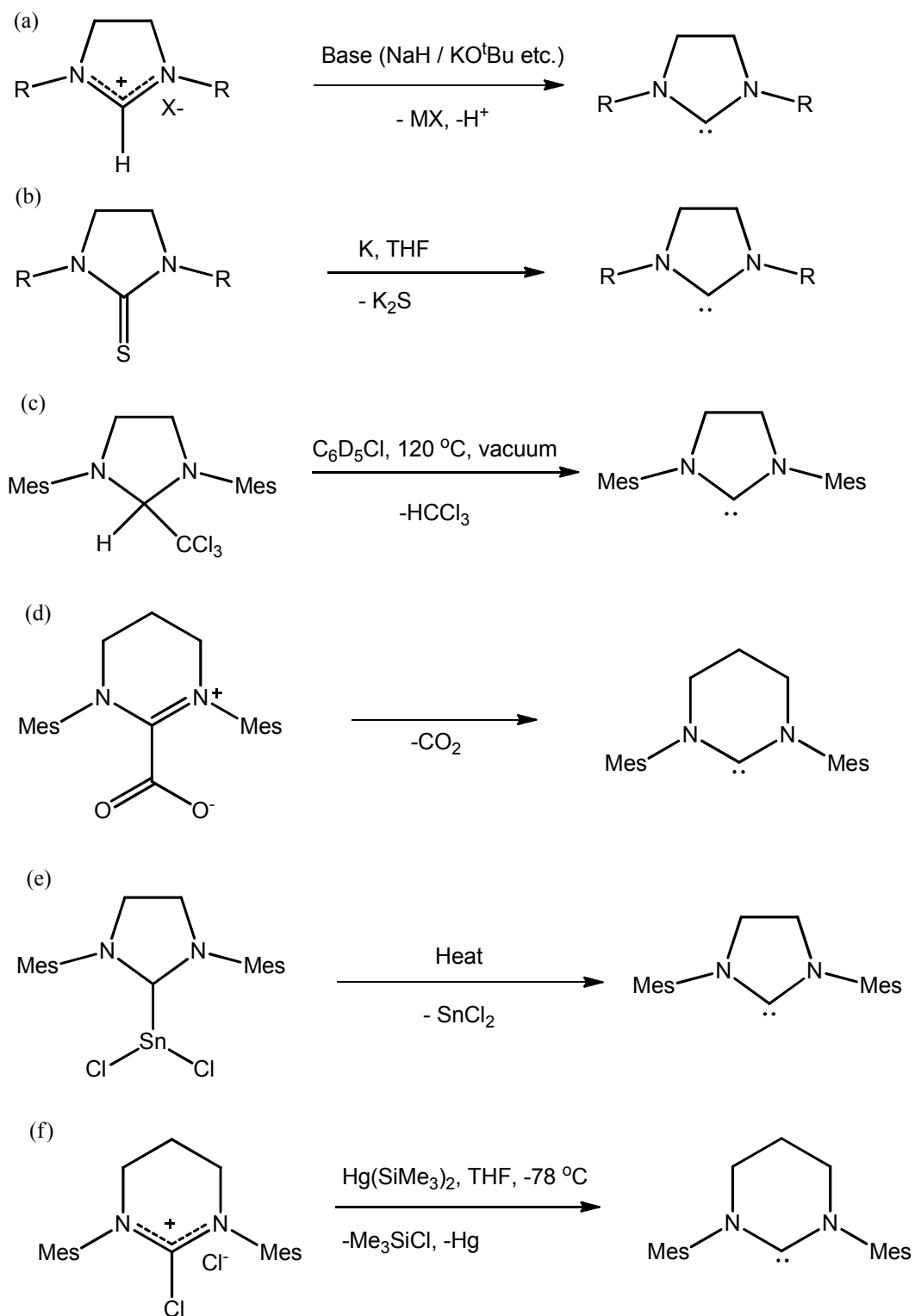
There are numerous methods available to synthesize NHC precursor salts (Scheme 1.6). The easiest and most common route is alkylation reactions at the nitrogen atoms of imidazole.⁴⁷ The other common method is multicomponent reactions.⁴⁸ Both methods are suitable for the synthesis of symmetric and asymmetric N,N'-substituted NHC salts. For example, Scheme 1.6c shows a multicomponent reaction with isocyanides leading to saturated backbone-containing unsymmetrical NHC salts.⁴⁹ Thiourea derivatives are alternative precursors for the synthesis of NHCs, and cyclic thioureas are easily accessible through the reaction of σ -hydroxyketones with suitable 2-thiones (Scheme 1.6 b & d).⁵⁰ Triazolium salts, thiazolium salts, and benzimidazol-2-thione derivatives are a few other salt precursors used to synthesize NHCs.^{34,51}



Scheme 1.6. Synthesis of NHC precursors, (a),(b) & (c): imidazolium salt, (d): thiourea.

Adapted from reference 34.

Typically, free NHCs are obtained by deprotonation of the NHC (azolium) salt precursors with suitable bases such as DMSO / NaH in THF, NaH, KO^tBu, liquid ammonia, or KHMDS. A few other methods include: reduction of thioureas with molten potassium,⁵² vacuum pyrolysis of volatile adducts of NHCs,⁵³ reductions of chloroformamidinium salts with Hg(TMS)₂,⁵⁴ and in-situ generation of NHC from NHC-CO₂ or NHC-metal adducts (Scheme 1.7).⁵⁵



Scheme 1.7. Synthesis of free NHCs

Synthesis of NHC metal complexes

There are numerous ways to achieve NHC complexes that have arisen after Wanzlick³⁰ and Ofele's³¹ initial reports of mercury and chromium complexes. The most commonly used method is in situ deprotonation of azolium salts in the presence of suitable metal precursors. The basic ligands (OAc or H^- or OR^-)⁵⁶⁻⁵⁸ present in the metal precursor can act as an internal base, or external bases⁵⁹ such as NaOAc or KO^tBu can be added for in situ deprotonation. In this method, prior isolation of the free NHC is not necessary, and this is therefore the most popular method to prepare NHC complexes.

Reaction of the free NHC⁵⁹ or its enetetramine dimer⁶⁰ with suitable metal precursors is the simplest route to NHC complexes. The isolated free NHCs are reacted with metal precursors, usually at low temperature. The cleavage of an NHC enetetramine dimer in the presence of coordinatively unsaturated metal precursors has been used to synthesize benzimidazol-2-ylidene complexes.⁶⁰

Trans metalation (carbene transfer reaction) using silver-NHC complexes is another popular method. This method was introduced by Lin et al. in 1998.⁶¹ The silver NHC complexes can be prepared by in-situ deprotonation of azolium salts using Ag_2O . The labile silver carbene bond allows transfer of NHCs to another metal center. This method has several advantages, such as the air stability of silver complexes, and carbene formation occurs at the C2 position regardless of the presence of acidic protons. This method is usually employed when other methods are not successful.

Another method is the oxidative addition of C2-X (X = H, R, halogen) bonds of azolium salts to metal complex. DFT calculations suggest that addition of azolium salts to electron rich d^8 or d^{10} metal centers proceeds most rapidly and with more favorable

reaction enthalpy (exothermic).⁶² When the C2 position is functionalized with halogens, the reaction proceeds faster than in other cases. Hahn et al. reported template controlled cyclization of β -functionalized isocyanides to produce 'protic' NHC complexes which are not very stable.⁶³ These can be converted to classical NHC complexes by stepwise alkylation.

Bis(NHC) complexes

More types of NHC structures have been explored as the application of NHCs has grown. NHCs have typically been considered as strong donor ligands which always produce electron rich metal centers. Variations in N-substituent⁴² or backbone⁴⁴ on mono-NHC have very little effect on the donor ability. Chelating bis(NHCs) provide an excellent way to alter the denticity by variation of bite angle, dihedral angle (σ angle), in plane distortion of NHC (θ (yaw) angle), and length and type of linkage between two azole rings. Bis(NHCs) also supply extra stability to a complex by the chelate effect. The azole ring in a mono-NHC usually is orientated with its slim axis in the bulky planar of the complex. However, bis(NHCs) can chelate in either *cis* or *trans* fashion to one metal or bridge between two metals. In chelate bis(NHC) complexes, metal-NHC rotation is hindered, and the bulky part of the ligand might have steric interactions with the sterically crowded coordination plane. Peris et al. in 2009 reviewed how these factors affect the structural parameters of bis(NHC) complexes.⁶⁴ Several studies have been done to identify the steric factors influencing the binding of bis(NHC)s.⁶⁵⁻⁶⁸ It was identified for pseudo-square planar complexes that shorter alkylene linkers prefer in-plane

conformation, whereas longer alkylene linkers prefer a perpendicular orientation as shown in Figure 1.7.

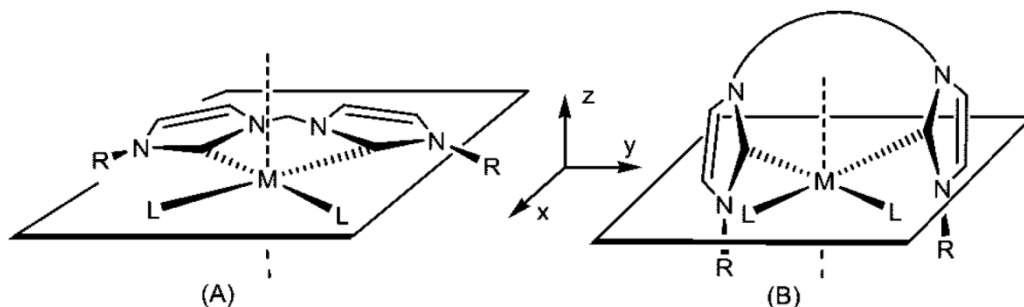


Figure 1.7. Determination of orientation by linker length: (A) in-plane conformation (shorter linkage); (B) perpendicular orientation (longer linker). Adapted from Reference 64.

However, the N-substituents of bis(NHCs) and the nature of the coligands in the complex also play a vital role in its stability (Figure 1.8). Bulky N-substituents (R) and coligands (L) will prevent formation of chelating complexes for larger linker sizes due to steric repulsion. Therefore, the sizes of the linker, N-substituents and coligands all determine the stability of bis(NHC) complexes.

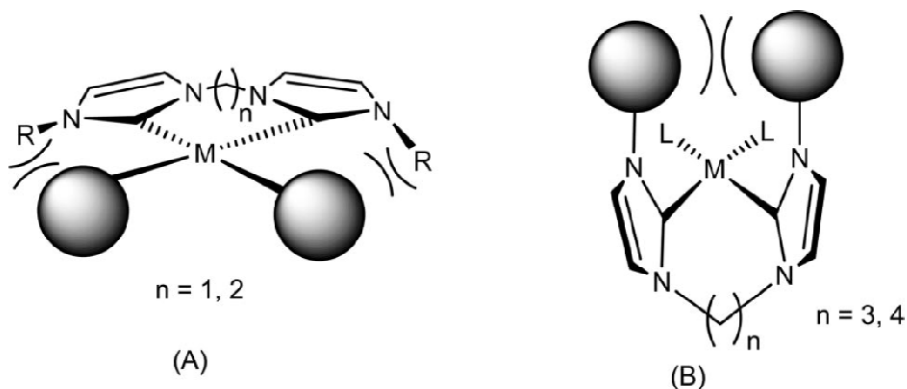
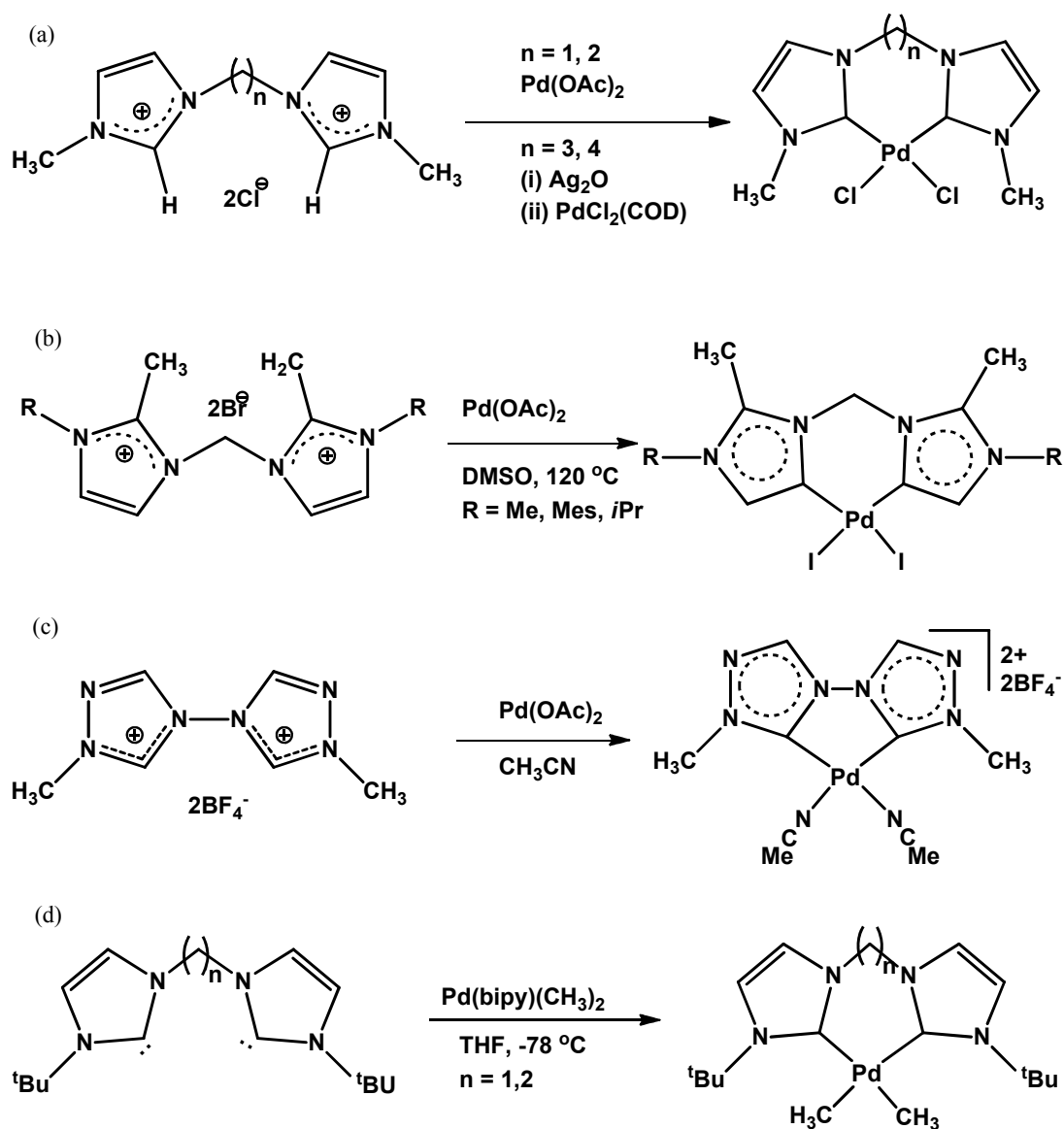


Figure 1.8. Steric interactions between (A) N-substituents and coligands (B) N-substituents and N-substituents. Adapted from reference 64.

Bis(NHC) complexes with alkylene linkages were the first known complexes of chelating NHCs.⁶⁹ Subsequently, linkers such as ethers,⁷⁰ amines,⁷¹ and aromatic rings⁷² in bis(NHC) complexes were developed. The synthetic routes for these complexes vary based on the type of azole ring, N-substituents, linkages and metals. Scheme 1.8^{49,67,73,74} summarizes the synthetic routes used for bis(NHC) palladium complexes relevant to the current study, many of which are similar to syntheses of mono-NHC complexes.

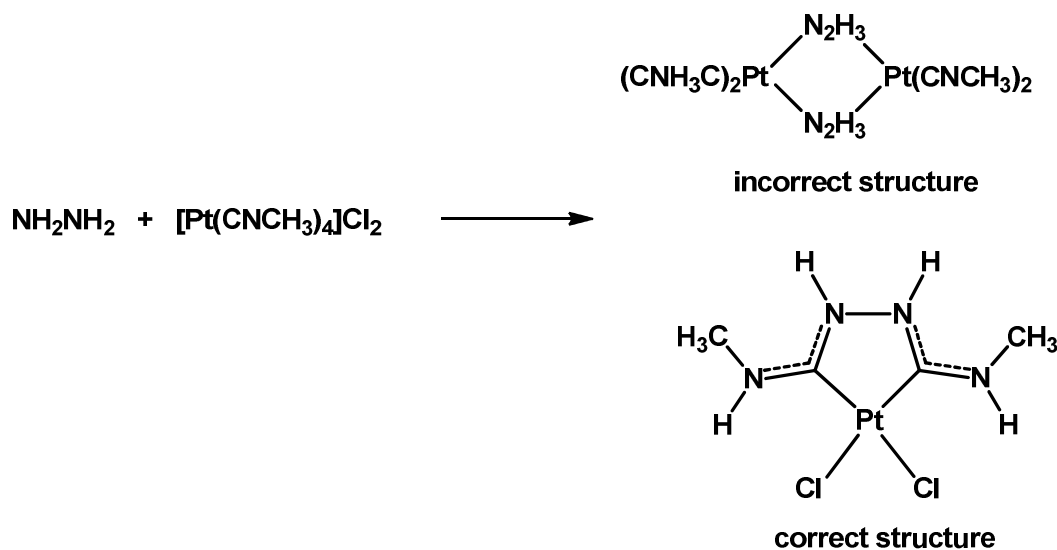


Scheme 1.8. Synthesis of bis(NHC) palladium complexes.

It is well known that NHC complexes catalyze a wide variety of organic reactions. Bis(NHC) containing palladium complexes catalyze coupling reactions,⁷⁵ olefin hydrogenations,⁷⁶ copolymerizations,⁷⁷ and C-H activation reactions such as conversion of methane to methanol⁶⁷ and Fujiwara hydroarylation.⁷⁸

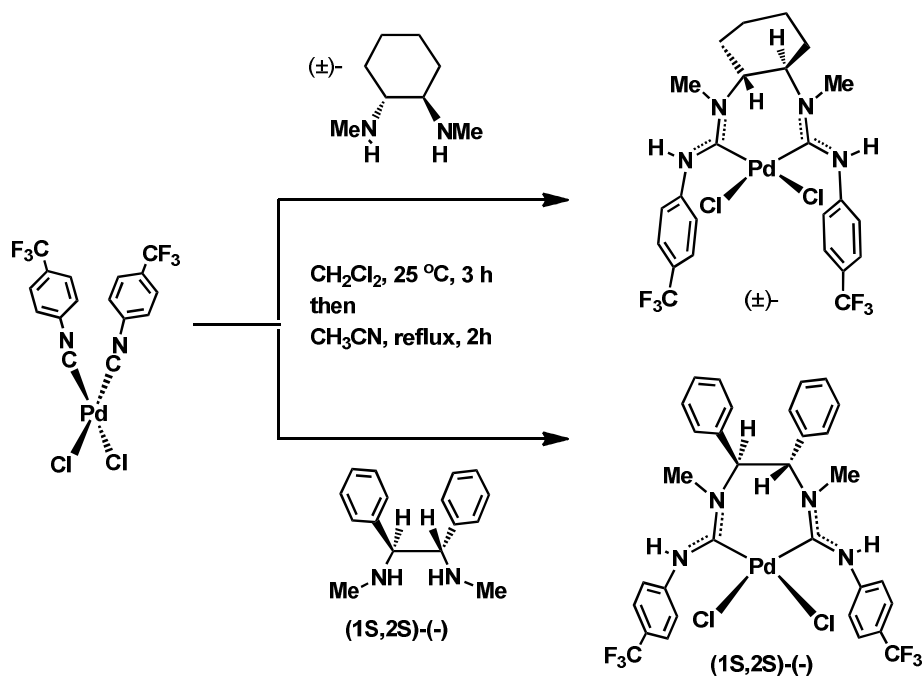
Acyclic diaminocarbenes (ADCs)

ADCs are electronically similar to NHC ligands⁷⁹⁻⁸¹ but have found less attention as ancillary ligands than NHCs, even though they are considered as stronger donors than NHCs.⁴⁴ This is due to their relative instability in the free carbene state.^{54,82} In spite of little attention in earlier years, ADC complexes have recently found interesting applications in catalysis.⁸³⁻⁸⁶ The strong σ -donor ability, increased NCN bond angle, and presence of N-substituents close to the metal centre, allow steric tuning⁸⁷ of ADC complexes and introduction of chirality.



Scheme 1.9. The synthesis of Chugaev's bis(ADC) complex

There are a few different methods available for the synthesis of ADC complexes.⁸⁸ The first ADC complex was synthesized by Chugaev in 1915,⁸⁹ but its structure was incorrectly assigned based on available techniques at that time. A correct structure was assigned by Shaw et al.⁹⁰ and Burke et al.⁹¹ using spectroscopic and X-ray crystallographic studies respectively in the 1970s. The 1,2-addition of protic amines to metal coordinated isocyanides produces ADC complexes. Slaughter et al.⁹² used this synthetic method to prepare a series of Chugaev-type bis(ADC) complexes of palladium. These complexes showed moderate catalytic activity in Suzuki-Miyaura cross coupling reactions under air. This method was subsequently extended to the synthesis of the first chiral bis(ADC) complex.⁹³ A palladium bis(arylisocyanide) synthon was used to synthesize novel bis(ADC) complexes with a variety of chiral backbone.^{88,93,94} These complexes show activity in enantioselective aza-Claisen rearrangements.⁹⁴



Scheme 1.10. Synthesis of chiral palladium bis(ADC) complexes. Adapted from references 88.

Preliminary methylisocyanide IR probe studies showed that the bis(ADC) ligands could be weaker donors than bis(NHC) or bis(phosphines).⁹⁴ However it, is not clear to what extent this reflects on the intrinsic donicity of the ligands, as these ligand had different chelating ring sizes.

References

- (1) Dorta, R.; Stevens, E. D.; Hoff, C. D.; Nolan, S. P. *J. Am. Chem. Soc.* **2003**, *125*, 10490.
- (2) Dorta, R.; Stevens, E. D.; Scott, N. M.; Costabile, C.; Cavallo, L.; Hoff, C. D.; Nolan, S. P. *J. Am. Chem. Soc.* **2005**, *127*, 2485.
- (3) Chianese, A. R.; Li, X. W.; Janzen, M. C.; Faller, J. W.; Crabtree, R. H. *Organometallics* **2003**, *22*, 1663.
- (4) Huang, J. K.; Schanz, H. J.; Stevens, E. D.; Nolan, S. P. *Organometallics* **1999**, *18*, 2370.
- (5) Magill, A. M.; Cavell, K. J.; Yates, B. F. *J. Am. Chem. Soc.* **2004**, *126*, 8717.
- (6) Tolman, C. A. *Chem. Rev.* **1977**, *77*, 313.
- (7) Guzei, I. A.; Wendt, M. *Dalton Transactions* **2006**, 3991.
- (8) Hillier, A. C.; Sommer, W. J.; Yong, B. S.; Petersen, J. L.; Cavallo, L.; Nolan, S. P. *Organometallics* **2003**, *22*, 4322.
- (9) Alder, R. W.; Allen, P. R.; Murray, M.; Orpen, A. G. *Angew. Chem.-Int. Edit. Engl.* **1996**, *35*, 1121.

- (10) Treichel, P. M.; Wagner, K. P. *Journal of Organometallic Chemistry* **1973**, *61*, 415.
- (11) Doering, W. V.; Hoffmann, A. K. *J. Am. Chem. Soc.* **1954**, *76*, 6162.
- (12) Fischer, E. O.; Maasbol, A. *Angewandte Chemie-International Edition* **1964**, *3*, 580.
- (13) Geuther, A. *Ann.* **1862**, *123*, 121.
- (14) Bourissou, D.; Guerret, O.; Gabbai, F. P.; Bertrand, G. *Chem. Rev.* **2000**, *100*, 39.
- (15) Myers, D. R.; Senthilnathan, V. P.; Platz, M. S.; Jones, M. *J. Am. Chem. Soc.* **1986**, *108*, 4232.
- (16) Gano, J. E.; Wettach, R. H.; Platz, M. S.; Senthilnathan, V. P. *J. Am. Chem. Soc.* **1982**, *104*, 2326.
- (17) Richards, C. A.; Kim, S. J.; Yamaguchi, Y.; Schaefer, H. F. *J. Am. Chem. Soc.* **1995**, *117*, 10104.
- (18) Crabtree, R. H. *The Organometallic Chemistry of the Transition Metals*; Wiley International: New York, 2001.
- (19) Schrock, R. R. *J. Am. Chem. Soc.* **1974**, *96*, 6796.
- (20) Schrock, R. R. *Journal of the Chemical Society-Dalton Transactions* **2001**, 2541.
- (21) Benhamou, L.; Chardon, E.; Lavigne, G.; Laponnaz, S. B.; Cesar, V. *Chem. Rev.* **2011**, *111*, 2705.
- (22) Wanzlick, H. W. *Angewandte Chemie-International Edition* **1962**, *1*, 75.
- (23) Wanzlick, H-W.; Schikora, E. *Angew. Chemie.* **1960**, *72*, 494.
- (24) Wanzlick, H. W.; Esser, F.; Kleiner, H. J. *Chem. Ber.-Recl.* **1963**, *96*, 1208.

- (25) Wanzlick, H. W.; Kleiner, H. J. *Angewandte Chemie-International Edition* **1961**, 73, 493.
- (26) Lemal, D. M.; Lovald, R. A.; Kawano, K. I. *J. Am. Chem. Soc.* **1964**, 86, 2518.
- (27) Winberg, H. E.; Carnahan, J. E.; Coffman, D. D.; Brown, M. *J. Am. Chem. Soc.* **1965**, 87, 2055.
- (28) Wiberg, N. *Angewandte Chemie-International Edition* **1968**, 7, 766.
- (29) Denk, M. K.; Hatano, K.; Ma, M. *Tetrahedron Lett.* **1999**, 40, 2057.
- (30) Wanzlick, H. W.; Schonher, H. *Angewandte Chemie-International Edition* **1968**, 7, 141.
- (31) Ofele, K. *Journal of Organometallic Chemistry* **1968**, 12, 42.
- (32) Arduengo, A. J.; Kline, M.; Calabrese, J. C.; Davidson, F. *J. Am. Chem. Soc.* **1991**, 113, 9704.
- (33) Viciu, M. S.; Nolan, S. P. *Topics in Organometallic chemistry* **2005**, 14, 241.
- (34) Jahnke, M. C.; Hahn, F. E. *Topics in Organometallic chemistry* **2010**, 30, 95.
- (35) Fantasia, S.; Petersen, J. L.; Jacobsen, H.; Cavallo, L.; Nolan, S. P. *Organometallics* **2007**, 26, 5880.
- (36) Khramov, D. M.; Lynch, V. M.; Bielawski, C. W. *Organometallics* **2007**, 26, 6042.
- (37) Khramov, D. M.; Rosen, E. L.; Er, J. A.; Vu, P. D.; Lynch, V. M.; Bielawski, C. W. *Tetrahedron* **2008**, 64, 6853.
- (38) Heinemann, C.; Muller, T.; Apeloig, Y.; Schwarz, H. *J. Am. Chem. Soc.* **1996**, 118, 2023.

- (39) Arduengo, A. J.; Dias, H. V. R.; Harlow, R. L.; Kline, M. *J. Am. Chem. Soc.* **1992**, *114*, 5530.
- (40) Huang, J. K.; Schanz, H. J.; Stevens, E. D.; Nolan, S. P. *Organometallics* **1999**, *18*, 2370.
- (41) Dorta, R.; Stevens, E. D.; Scott, N. M.; Costabile, C.; Cavallo, L.; Hoff, C. D.; Nolan, S. P. *J. Am. Chem. Soc.* **2005**, *127*, 2485.
- (42) Dorta, R.; Stevens, E. D.; Hoff, C. D.; Nolan, S. P. *J. Am. Chem. Soc.* **2003**, *125*, 10490.
- (43) Chianese, A. R.; Li, X. W.; Janzen, M. C.; Faller, J. W.; Crabtree, R. H. *Organometallics* **2003**, *22*, 1663.
- (44) Magill, A. M.; Cavell, K. J.; Yates, B. F. *J. Am. Chem. Soc.* **2004**, *126*, 8717.
- (45) Kelly, R. A.; Clavier, H.; Giudice, S.; Scott, N. M.; Stevens, E. D.; Bordner, J.; Samardjiev, I.; Hoff, C. D.; Cavallo, L.; Nolan, S. P. *Organometallics* **2008**, *27*, 202.
- (46) Diez-Gonzalez, S.; Nolan, S. P. *Coord. Chem. Rev.* **2007**, *251*, 874.
- (47) Herrmann, W. A.; Goossen, L. J.; Spiegler, M. *Journal of Organometallic Chemistry* **1997**, *547*, 357.
- (48) Bohm, V. P. W.; Weskamp, T.; Gstottmayr, C. W. K.; Herrmann, W. A. *Angewandte Chemie-International Edition* **2000**, *39*, 1602.
- (49) Bon, R. S.; de Kanter, F. J. J.; Lutz, M.; Spek, A. L.; Jahnke, M. C.; Hahn, F. E.; Groen, M. B.; Orru, R. V. A. *Organometallics* **2007**, *26*, 3639.
- (50) Kuhn, N.; Kratz, T. *Synthesis-Stuttgart* **1993**, 561.

- (51) Enders, D.; Breuer, K.; Raabe, G.; Runsink, J.; Teles, J. H.; Melder, J. P.; Ebel, K.; Brode, S. *Angewandte Chemie-International Edition* **1995**, *34*, 1021.
- (52) Denk, M. K.; Hezarkhani, A.; Zheng, F. L. *European Journal of Inorganic Chemistry* **2007**, 3527.
- (53) Nyce, G. W.; Csihony, S.; Waymouth, R. M.; Hedrick, J. L. *Chemistry-a European Journal* **2004**, *10*, 4073.
- (54) Otto, M.; Conejero, S.; Canac, Y.; Romanenko, V. D.; Rudzevitch, V.; Bertrand, G. *J. Am. Chem. Soc.* **2004**, *126*, 1016.
- (55) Bantu, B.; Pawar, G. M.; Decker, U.; Wurst, K.; Schmidt, A. M.; Buchmeiser, M. R. *Chemistry-a European Journal* **2009**, *15*, 3103.
- (56) Kocher, C.; Herrmann, W. A. *Journal of Organometallic Chemistry* **1997**, 532, 261.
- (57) Hahn, F. E.; Holtgrewe, C.; Pape, T.; Martin, M.; Sola, E.; Oro, L. A. *Organometallics* **2005**, *24*, 2203.
- (58) Weskamp, T.; Bohm, V. P. W.; Herrmann, W. A. *Journal of Organometallic Chemistry* **2000**, *600*, 12.
- (59) Douthwaite, R. E.; Green, M. L. H.; Silcock, P. J.; Gomes, P. T. *Journal of the Chemical Society-Dalton Transactions* **2002**, 1386.
- (60) Lappert, M. F. *Journal of Organometallic Chemistry* **1988**, *358*, 185.
- (61) Wang, H. M. J.; Lin, I. J. B. *Organometallics* **1998**, *17*, 972.
- (62) McGuinness, D. S.; Cavell, K. J.; Yates, B. F.; Skelton, B. W.; White, A. H. *J. Am. Chem. Soc.* **2001**, *123*, 8317.
- (63) Kosterke, T.; Pape, T.; Hahn, F. E. *J. Am. Chem. Soc.* **2011**, *133*, 2112.

- (64) Poyatos, M.; Mata, J. A.; Peris, E. *Chem. Rev.* **2009**, *109*, 3677.
- (65) Mata, J. A.; Chianese, A. R.; Miecznikowski, J. R.; Poyatos, M.; Peris, E.; Faller, J. W.; Crabtree, R. H. *Organometallics* **2004**, *23*, 1253.
- (66) Leung, C. H.; Incarvito, C. D.; Crabtree, R. H. *Organometallics* **2006**, *25*, 6099.
- (67) Ahrens, S.; Zeller, A.; Taige, M.; Strassner, T. *Organometallics* **2006**, *25*, 5409.
- (68) Viciano, M.; Poyatos, M.; Sanau, M.; Peris, E.; Rossin, A.; Ujaque, G.; Lledos, A. *Organometallics* **2006**, *25*, 1120.
- (69) Herrmann, W. A.; Elison, M.; Fischer, J.; Kocher, C.; Artus, G. R. J. *Angewandte Chemie-International Edition.* **1995**, *34*, 2371.
- (70) Nielsen, D. J.; Cavell, K. J.; Skelton, B. W.; White, A. H. *Organometallics* **2006**, *25*, 4850.
- (71) Houghton, J.; Dyson, G.; Douthwaite, R. E.; Whitwood, A. C.; Kariuki, B. M. *Dalton Transactions* **2007**, 3065.
- (72) Baker, M. V.; Skelton, B. W.; White, A. H.; Williams, C. C. *Journal of the Chemical Society-Dalton Transactions* **2001**, 111.
- (73) Heckenroth, M.; Kluser, E.; Neels, A.; Albrecht, M. *Angewandte Chemie-International Edition* **2007**, *46*, 6293.
- (74) Poyatos, M.; McNamara, W.; Incarvito, C.; Clot, E.; Peris, E.; Crabtree, R. H. *Organometallics* **2008**, *27*, 2128.
- (75) Weskamp, T.; Bohm, V. P. W.; Herrmann, W. A. *Journal of Organometallic Chemistry* **1999**, *585*, 348.
- (76) Heckenroth, M.; Kluser, E.; Neels, A.; Albrecht, M. *Angewandte Chemie-International Edition* **2007**, *46*, 6293.

- (77) Gardiner, M. G.; Herrmann, W. A.; Reisinger, C. P.; Schwarz, J.; Spiegler, M. *Journal of Organometallic Chemistry* **1999**, 572, 239.
- (78) Jia, C. G.; Piao, D. G.; Oyamada, J. Z.; Lu, W. J.; Kitamura, T.; Fujiwara, Y. *Science* **2000**, 287, 1992.
- (79) Tolman, C. A. *Chem. Rev.* **1977**, 77, 313.
- (80) Alder, R. W.; Allen, P. R.; Murray, M.; Orpen, A. G. *Angewandte Chemie-International Edition.* **1996**, 35, 1121.
- (81) Alder, R. W.; Blake, M. E. *Chemical Communications* **1997**, 1513.
- (82) Alder, R. W.; Blake, M. E.; Chaker, L.; Harvey, J. N.; Paolini, F.; Schutz, J. *Angewandte Chemie-International Edition* **2004**, 43, 5896.
- (83) Seo, H.; Roberts, B. P.; Abboud, K. A.; Merz, K. M.; Hong, S. W. *Organic Letters* **2010**, 12, 4860.
- (84) Rosen, E. L.; Sung, D. H.; Chen, Z.; Lynch, V. M.; Bielawski, C. W. *Organometallics* **2010**, 29, 250.
- (85) Yu, I.; Wallis, C. J.; Patrick, B. O.; Diaconescu, P. L.; Mehrkhodavandi, P. *Organometallics* **2010**, 29, 6065.
- (86) Hashmi, A. S. K.; Hengst, T.; Lothschutz, C.; Rominger, F. *Adv. Synth. Catal.* **2010**, 352, 1315.
- (87) Collins, M. S.; Rosen, E. L.; Lynch, V. M.; Bielawski, C. W. *Organometallics* **2010**, 29, 3047.
- (88) Slaughter, L. M. *Comments on Inorganic Chemistry* **2008**, 29, 46.
- (89) Tschugajeff (Chugaev), L.; Skanawy-Grigorjewa, M. *J. Russ. Chem. Soc.* **1915**, 47, 776.

- (90) Rouschia.G; Shaw, B. L. *Journal of the Chemical Society D-Chemical Communications* **1970**, 183.
- (91) Burke, A.; Balch, A. L.; Enemark, J. H. *J. Am. Chem. Soc.* **1970**, 92, 2555.
- (92) Moncada, A. I.; Khan, M. A.; Slaughter, L. M. *Tetrahedron Lett.* **2005**, 46, 1399.
- (93) Wanniarachchi, Y. A.; Slaughter, L. M. *Chemical Communications* **2007**, 3294.
- (94) Wanniarachchi, Y. A.; Kogiso, Y.; Slaughter, L. M. *Organometallics* **2008**, 27, 21.

CHAPTER II

SYNTHESIS OF METHYLPALLADIUM BIS(NHC) COMPLEXES AND
INVESTIGATION OF CARBONYLATION REACTIONS RELEVANT
TO
CO/ALKENE COPOLYMERIZATION

Introduction

Since the discovery of stable N-heterocyclic carbene (NHC) ligands, there has been increased attention on using these as ancillary ligands in metal-catalyzed reactions.¹ NHC ligands are considered as structural mimics to phosphine ligands^{2,3} and there is increasing experimental evidence suggesting that NHCs are superior to phosphines in both catalytic activity and scope.^{1,4,5} This is due to the improved thermal stability⁶ and superior donor ability of NHCs compared to phosphines.⁷ Therefore, NHCs have replaced phosphines as ligands in several catalytic reactions such as coupling reactions,^{8,9} olefin metathesis,¹⁰ hydroarylation¹¹ and polymerization.¹² Alternating copolymerization of CO and ethylene is a commercially important polymerization reaction,¹³⁻¹⁵ which typically uses neutral bidentate donor ligands such as diimines^{14,16} and diphosphines.¹⁷ The highest activity for CO / ethylene copolymerization was reported for a palladium complex of 1,2-bis(diphenylphosphino)propane (DPPP) by Drent and co-workers.¹⁸ One possible way to improve these catalytic systems is to replace phosphines or imines with stronger donor NHC ligands. Cationic methylpalladium species are highly active initiators for this CO / ethylene copolymerization.¹⁴ However, NHC-containing methylpalladium complexes are known to decompose via reductive elimination of 2-alkylimidazolium salts.¹⁹ This instability of methylpalladium NHC complexes affects the development of NHC-based catalytic systems for copolymerization.

In 1999, Herrmann and co-workers reported CO / ethylene copolymerization initiated by a dicationic palladium complex containing the bidentate bis(NHC) ligand 1,1'-dimesityl-3,3'-methylenediimidazol-2,2'-diylidene.¹² The results showed this catalytic system produced high average molecular weight polyketones, but with low turnover

numbers. Since Herrmann's initial studies, there have been only two more reports on CO / alkene copolymerization by palladium-NHC systems.^{20,21} The selection of the NHC ligand is important in these catalytic systems, as methylpalladium complexes containing monodentate NHCs decompose rapidly via reductive elimination,^{19,22} and this process is more rapid for cationic species.²³ It is reported that bidentate or 'pincer'-type tridentate chelating NHCs can prevent this decomposition.^{24,25} Several stable cationic methylpalladium-NHC complexes were produced in this way,^{20,26-29} but they contain mixed chelates of NHCs with other donors. There are only two example of bidentate bis(NHC) containing methylpalladium complexes.³⁰ Even though mechanistic and kinetic details were studied and active species were identified in CO / alkene copolymerization reactions with diimine³¹⁻³³ and phosphines³⁴⁻³⁸ complexes, there are no such studies involving NHC-containing systems that provide information on key catalytic steps or the nature of active species. Simple insertion reactions of CO and olefins with methylpalladium-NHC complexes have also not been observed. One attempt at such a study with a mono-NHC ligand resulted in formation of 2-acylimidazolium salts by CO insertion followed by reductive elimination.²³

This study focused on CO insertion into methylpalladium bis(NHC) systems, which required the synthesis of stable neutral and cationic methylpalladium-bis(NHC) complexes. The N-substituent on the NHC ligand is important to stabilize the methylpalladium species. According to Cavell's study of a series of cationic methylpalladium complexes with tridentate pyridyl bis(NHC) ligands,²⁸ steric shielding provided by mesityl groups appear to stabilize the methylpalladium better than methyl or *tert*-butyl groups. Therefore, the mesityl substituted bis(NHC) ligand, 1,1'-dimesityl-3,3'-

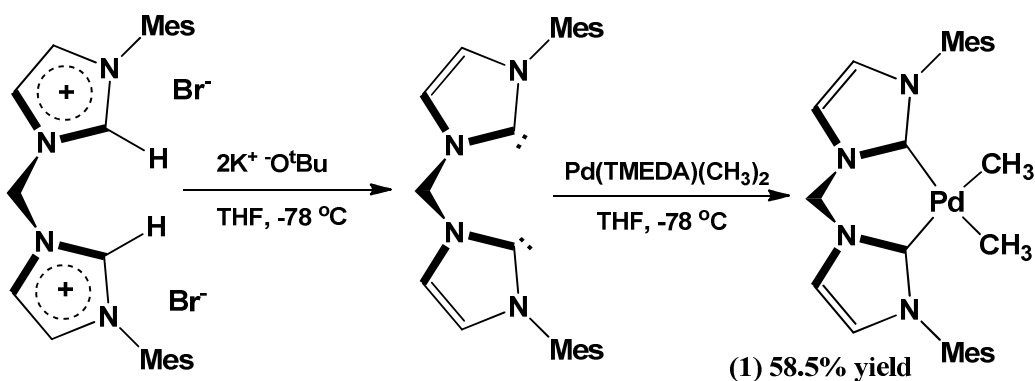
methylenediimidazol-2,2'-diylidene, previously reported by Herrmann,¹² and variations of this ligand with longer linkers, were used for the current study. Herrmann's ligand is referred to as DIMes^{Me}, and the superscript is changed according to the length of the linkage between the two imidazole rings (ethylene→ DIMes^{Et}, propylene→ DIMes^{Pr}, butylene→ DIMes^{Bu}).

Results and discussion

Synthesis and characterization of [(DIMes^{Me})Pd(CH₃)₂] (1)

Complex **1** was synthesized using the in situ generated free carbene by reaction with a dimethylpalladium precursor. This synthesis started by placing one molar equivalent of the bis imidazolium salt of DIMes^{Me} and two molar equivalents of potassium *tert*-butoxide in a 3-neck round bottom flask fixed with a septum and a needle valve. Dry THF was distilled onto the mixture under vacuum at – 78 °C, and the mixture was stirred for 45 minutes to form the free bis(carbene). The resultant cloudy, light pink suspension was transferred to a solution of [(TMEDA)Pd(CH₃)₂] in THF at – 78 °C via cannula, and the resulting mixture was stirred for another 45 minutes. The volatiles were removed under vacuum, the residue was extracted with methylene chloride, and diethyl ether was added to obtain white crystals. This complex was stable under air for a couple of hours, but then started to darken and decompose. However, it can be stored for a couple of months at – 35 °C under inert atmosphere. The ¹H NMR spectrum in DMSO showed two sets of doublets for the imidazole protons at 7.57 and 7.04 ppm and a singlet each for aromatic and methylene protons at 6.90 and 6.19 ppm, respectively. These

values are slightly downfield compared to the dibromide version of the complex.¹² Methyl protons in the mesityl groups showed two singlets at 2.51 and 1.96 ppm with a 6:12 integration ratio. The palladium-bound methyl protons showed an upfield singlet at -1.11 ppm. In the ^{13}C NMR spectrum, the carbene peak appeared at 189.1 ppm. The four imidazole carbons showed two peaks at 121.7 and 119.9 ppm, aromatic carbons showed four peaks, and the linkage methylene showed a peak at 62.5 ppm. The mesityl methyl carbons showed two peaks at 20.59 and 18.05 ppm. An upfield resonance at -5.38 ppm appeared for the palladium-bound methyl carbons. These NMR data suggest a twofold symmetric molecule in solution.

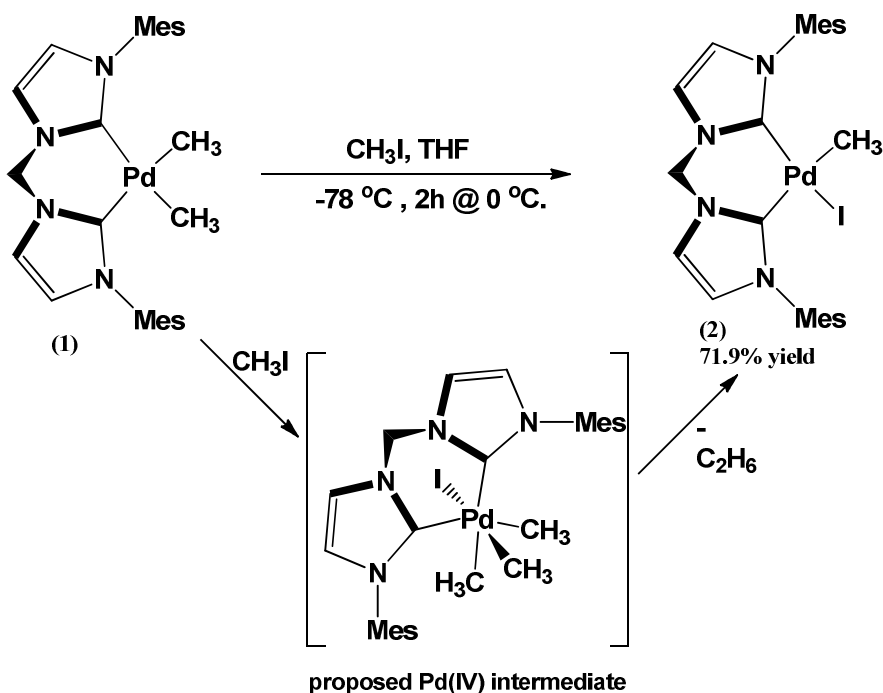


Scheme 2.1. Synthesis of $[(\text{DIMes}^{\text{Me}})\text{Pd}(\text{CH}_3)_2]$ (**1**)

Synthesis and characterization of $[(\text{DIMes}^{\text{Me}})\text{Pd}(\text{CH}_3)(\text{I})]$ (**2**)

A sample of $[(\text{DIMes}^{\text{Me}})\text{Pd}(\text{CH}_3)_2]$ was placed in a two-neck round bottom flask fixed with a septum and a needle valve. Dry THF was distilled into the flask under vacuum at -78 °C, and excess methyl iodide was added via syringe under inert atmosphere. The reaction mixture was warmed to 0 °C and stirred for one hour to give a bright white precipitate with liberation of ethane. This is similar to a procedure published by van Koten to produce $[(\text{TMEDA})\text{Pd}(\text{CH}_3)(\text{Br} / \text{I})]$, which involved intermediate

Pd(IV) species.³⁹ This complex is very unstable and darkened rapidly with decomposition upon standing at room temperature for more than one hour, even in inert atmosphere. This prevented characterization by elemental analysis. The complex was only soluble in DMSO, but it decomposed rapidly in solution, making it very difficult to obtain adequate ¹³C NMR data. The complex can be stored at -35 °C for several weeks without significant decomposition. The ¹H NMR spectrum in DMSO-*d*₆ showed four resonances for the four imidazole protons at 7.80, 7.71, 7.35 and 7.20 ppm. Two singlets were observed for the four aromatic protons with a 2:2 integration ratio at 6.98 and 6.96 ppm. The methylene resonance was observed at 6.40 ppm, slightly upfield compared to [(DImes^{Me})Pd(CH₃)₂]. Three singlets were observed for mesityl methyl protons at 2.27, 2.03 and 1.95 ppm, with a 6:6:6 integration ratio. An upfield signal at -0.54 ppm was found for the palladium-bound methyl protons, which is slightly downfield compared to [(DImes^{Me})Pd(CH₃)₂]. These data suggest an unsymmetric molecule in solution.



Scheme 2.2. Synthesis of [(DImes^{Me})Pd(CH₃)(I)] (2)

Synthesis and characterization of [(DIMes^{Me})Pd(CH₃)(CH₃CN)][BF₄] (**3**)

A sample of [(DIMes^{Me})Pd(CH₃)(I)] was suspended in acetonitrile under inert conditions. One molar equivalent of AgBF₄ was added to the reaction flask, and the mixture was stirred for one hour to give an ash brown precipitate. The precipitate was removed by filtration through celite, volatiles were removed under vacuum, and the residue was dried for an additional two hours. The solid was redissolved in acetonitrile and filtered through celite to remove residual AgI. The solution was then concentrated, and diethyl ether was added to obtain white crystals, which were isolated by filtration. Complex **3** is stable at room temperature and soluble in polar solvents such as dimethylsulfoxide, acetonitrile, dichloromethane and tetrahydrofuran, but insoluble in hydrocarbon solvents. The ¹H NMR spectrum in CD₂Cl₂ or CD₃CN had the same resonance pattern observed for [(DIMes^{Me})Pd(CH₃)(I)], but with a new singlet for the methyl protons of acetonitrile. The ¹³C NMR spectrum in CD₂Cl₂ showed two carbene carbon signals at 186.02 and 167.31 ppm. Four resonances were observed for the four imidazole carbons at 124.6, 123.3, 122.7, and 122.0 ppm. Two sets of signals were observed for the two mesityl aromatic carbons. Four resonances were observed for the *ortho* and *para* methyl substituents on the two mesityl groups. Singlets were observed for acetonitrile and the palladium-bound methyl carbons at 3.3 and – 8.5 ppm, respectively. X-ray quality transparent crystals were grown by slow diffusion of diethyl ether into an acetonitrile solution of [(DIMes^{Me})Pd(CH₃)(CH₃CN)][BF₄]. This crystal structure belonged to the monoclinic P2₁/n space group. One acetonitrile solvent molecule was present in the unit cell per molecule. The palladium-carbene distance for C2 [2.098(2)] is significantly longer than that for C1 [1.967(1)] because of the very

strong *trans* influence of the methyl ligand. The elongated *trans* Pd-carbene bond length is similar to that reported for dimethylpalladium complexes with bis(NHC) ligands.⁴⁰ The Pd-C_{methyl} distance of 2.064(2) Å is also long and similar to those in analogous complexes with phosphine-NHC and diphosphine ligands.³⁸ The Pd-N_{acetonitrile} distance of 2.051(1) Å is similar to that found in a reported bis(acetonitrile) adduct of a Pd-bis(NHC) complex.¹² The bis(NHC) bite angle (C_{carbene}-Pd-C_{carbene}) of 87.86(6)° is slightly larger than that found in methylene bridged N-methyl substituted bis(NHC) palladium complexes with two acetonitrile¹² or two isocyanide ligands.⁴¹ This may be arise from the greater steric demand of N-mesityl compared to N-methyl groups. N-C_{carbene}-N angles in the imidazole rings were shorter than those in N-methyl bis(NHC) palladium complexes¹² but comparable to those in an N-*tert*-butyl bis(NHC) palladium complex.⁴⁰

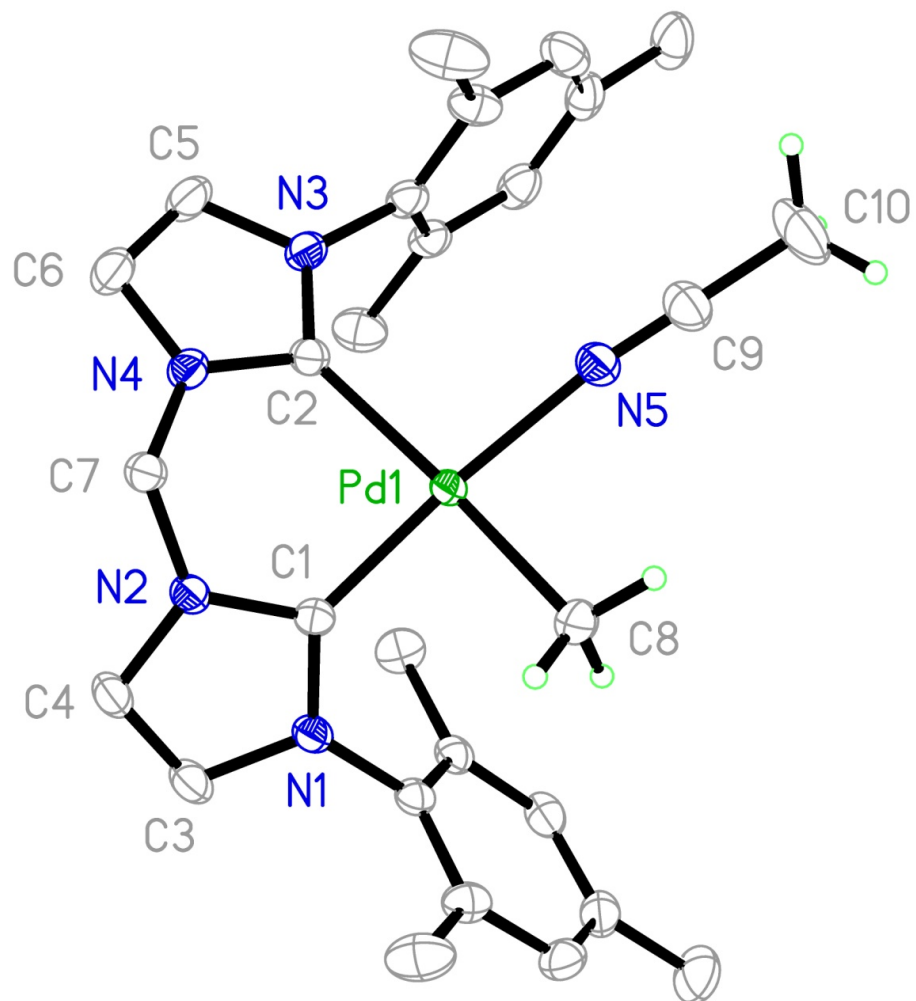


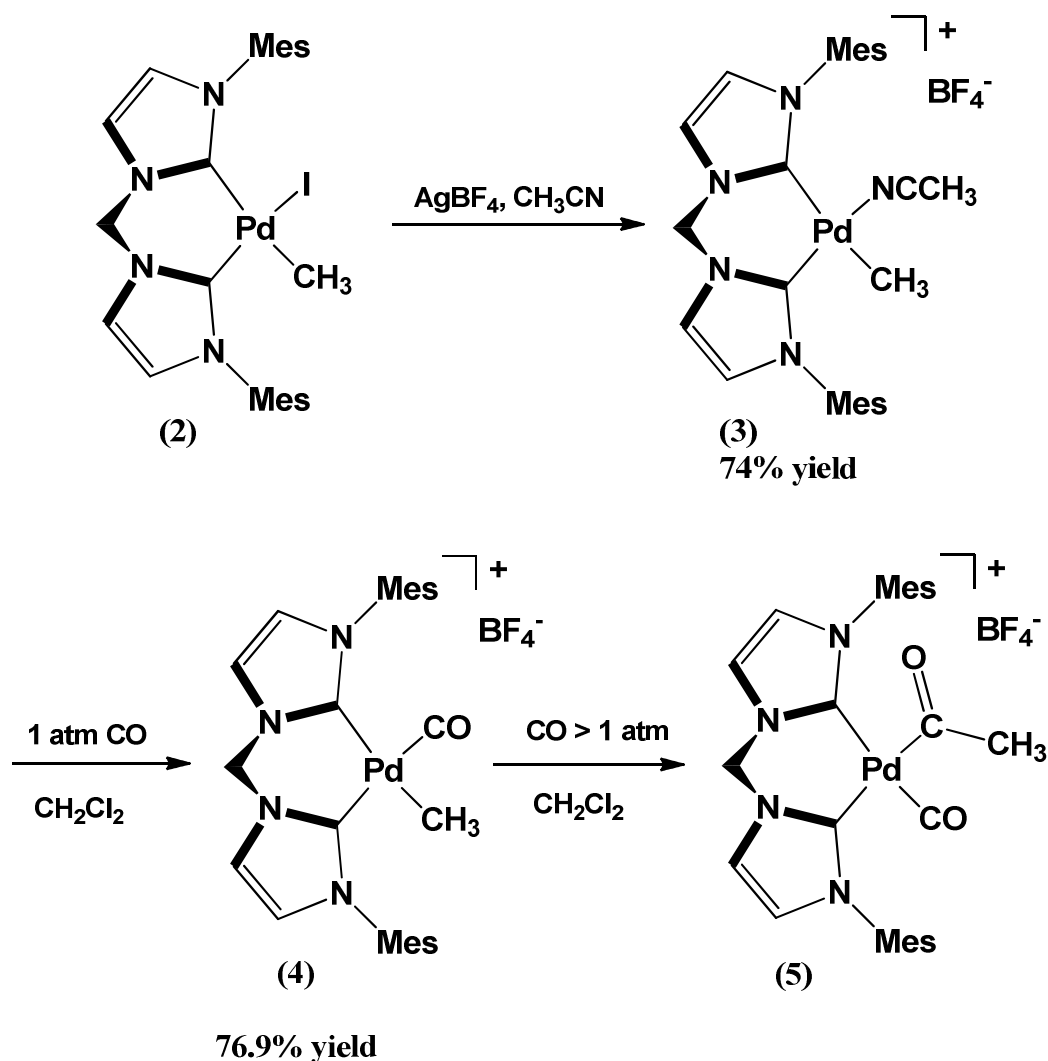
Figure 2.1. Molecular structure of complex **3** with 50% probability ellipsoids. The tetrafluoroborate counter ion and acetonitrile solvent were omitted for clarity.

Table 2.1. Selected bond lengths (Å) and bond angles (°) of complex **3**

	Bond Lengths (Å)
Pd(1)-C(1)	1.9672(14)
Pd(1)-C(2)	2.0980(15)
Pd(1)-C(8)	2.0635(15)
Pd(1)-C(12)	2.0521(13)
C(1)-N(1)	1.3582(18)
C(1)-N(2)	1.3558(18)
C(2)-N(3)	1.3559(19)
C(2)-N(4)	1.3549(18)
C(9)-N(5)	1.135(2)
	Bond angles (°)
C(1)-Pd(1)-C(2)	87.38(6)
C(8)-Pd(1)-N(5)	88.06(6)
C(1)-Pd(1)-C(8)	89.75(6)
C(2)-Pd(1)-N(5)	96.42(6)
C(1)-Pd(1)-N(5)	174.65(6)
C(2)-Pd(1)-C(8)	170.76(6)
N(1)-C(1)-N(2)	103.89(12)
N(3)-C(2)-N(4)	103.36(12)

Table 2.2. Crystal data and structure refinement details for complex **3**

Empirical formula	C ₃₀ H ₃₇ BF ₄ N ₆ Pd
Formula weight	674.87
Crystal system	Monoclinic
Space group	P2 ₁ /n
Unit cell dimensions	a = 11.5389(1) Å α = 90 ° b = 19.0724(2) Å β = 108.068 ° c = 15.1677 (2) Å γ = 90 °
Volume	3173.43(6) Å ³
Z	4
Density (calculated)	1.413 Mg/m ³
Absorption coefficient	0.638 mm ⁻¹
Crystal size	0.43 x 0.23 x 0.20 mm
θ range for data collection	1.77 – 30.86 °
Index range	-16 ≤ h ≤ 16 -21 ≤ k ≤ 27 -20 ≤ l ≤ 21
Temperature	115(2) K
Wave length	0.71073 Å
Reflections collected	54834
Independent reflections	9914 (R _{int} = 0.0325)
Final R indices [I > 2σ(I)]	R1 = 0.0278 wR2 = 0.0682
R indices (all data)	R1 = 0.0364 wR2 = 0.0726
Goodness-of-fit on F ²	1.060



Scheme 2.3. Synthesis of cationic bis(NHC) methylpalladium complexes (3), (4) and (5)

Synthesis and characterization $[(\text{DMe}^{\text{Me}})\text{Pd}(\text{CH}_3)(\text{CO})][\text{BF}_4]$ (4)

A sample of $[(\text{DMe}^{\text{Me}})\text{Pd}(\text{CH}_3)(\text{CH}_3\text{CN})][\text{BF}_4]$ was dissolved in CH_2Cl_2 in a sealable thick-walled glass reaction vessel, and 1 atm of CO was admitted. The solution was stirred for 15 minutes, volatiles were removed, and the resulting solid was dried under vacuum overnight to form a transparent residue. The residue was dissolved in CH_2Cl_2 , and the solution was filtered through celite to remove any palladium black formed. Diethyl ether and hexanes were added, forming white crystals that were collected

by filtration. This complex is stable at room temperature under inert atmosphere. The ^1H NMR and ^{13}C NMR spectra in CD_2Cl_2 showed resonance patterns similar to those of $[(\text{DIMes}^{\text{Me}})\text{Pd}(\text{CH}_3)(\text{CH}_3\text{CN})][\text{BF}_4]$ for aromatic, imidazole, methylene and N-methyl groups. A new CO peak appeared at 183.01 ppm in the ^{13}C NMR spectrum. The CH_3 resonance shifted slightly downfield relative to $[(\text{DIMes}^{\text{Me}})\text{Pd}(\text{CH}_3)(\text{CH}_3\text{CN})][\text{BF}_4]$ in the ^1H NMR spectrum (-0.29 ppm) and upfield in the ^{13}C NMR (-13.16 ppm) spectrum. The IR spectrum showed a stretching frequency at 2105 cm^{-1} for CO. This value is substantially lower than the range of $2122\text{--}2136\text{ cm}^{-1}$ seen in analogous complexes with nitrogen³¹ or phosphorous³⁸ chelating ligands. This suggests a higher donicity and *trans* influence from the bis(NHC) ligand.

X-ray quality transparent crystals were grown by slow diffusion of diethyl ether into a dichloromethane solution of $[(\text{DIMes}^{\text{Me}})\text{Pd}(\text{CH}_3)(\text{CO})][\text{BF}_4]$. The crystal structure was belonged to the triclinic $\text{P}\bar{1}$ space group. The elongated Pd-carbene bond lengths to C1 [2.047(3) Å] and C2 [2.062(3) Å] indicated a similar degree of *trans* influence from the CH_3 and CO ligands. The short C-O bond length of 1.095(5) Å suggests little or no π -backbonding from palladium to CO. The Pd- CH_3 bond length of 2.069(4) Å is similar to values found in cationic methylpalladium complexes with bis(phosphine) ligands³⁸ and $[(\text{DIMes}^{\text{Me}})\text{Pd}(\text{CH}_3)(\text{CH}_3\text{CN})][\text{BF}_4]$. Stable methyl carbonyl palladium(II) complexes are extremely rare in the literature, as there are only two reports of structurally characterized complexes. $[(\text{DIMes}^{\text{Me}})\text{Pd}(\text{CH}_3)(\text{CO})][\text{BF}_4]$ is the first methyl carbonyl palladium(II) complex with an NHC ligand. A slightly smaller bite angle of $86.9(1)^\circ$ is seen compared to $[(\text{DIMes}^{\text{Me}})\text{Pd}(\text{CH}_3)(\text{CH}_3\text{CN})][\text{BF}_4]$, possibly indicating more steric repulsion from the CO ligand compared to a CH_3CN ligand.

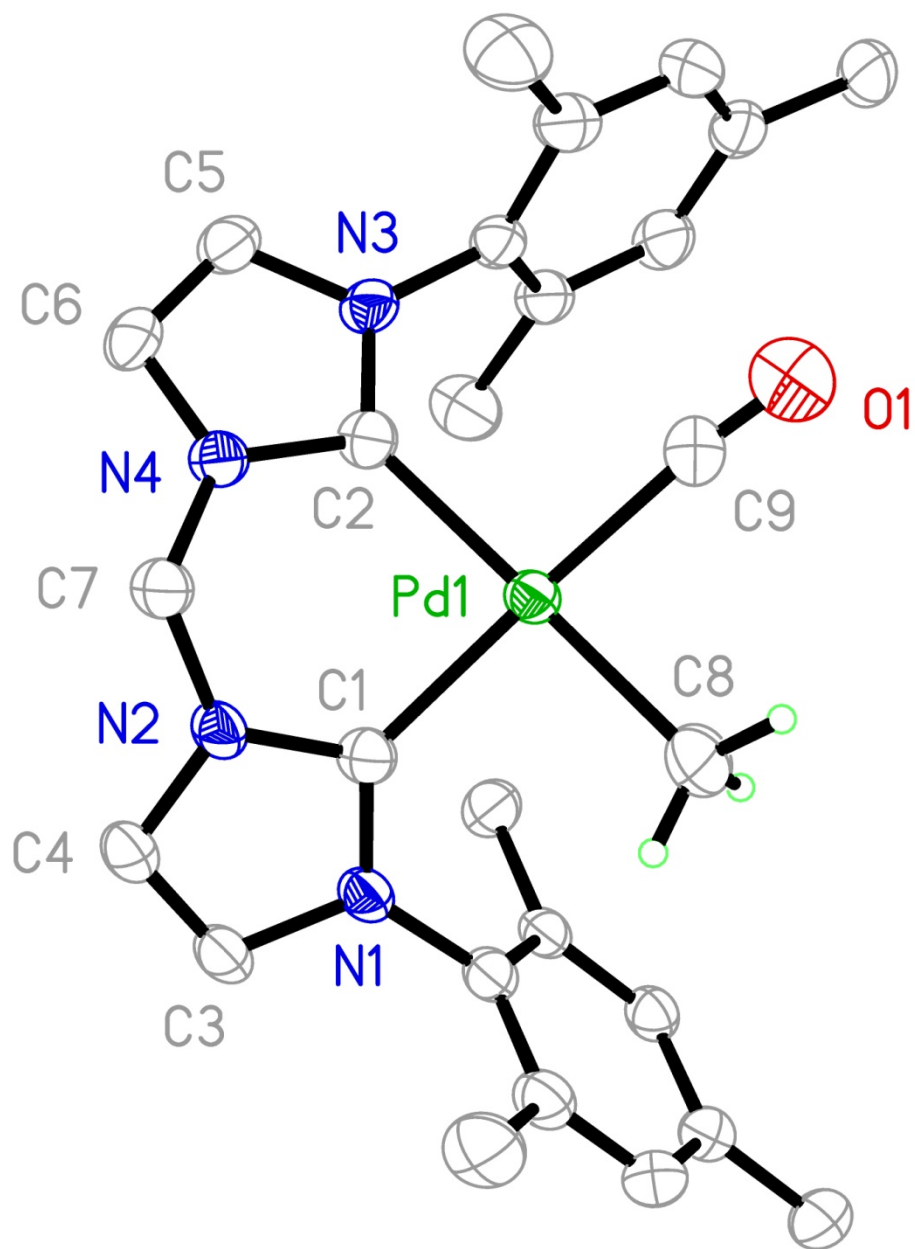


Figure 2.2. Molecular structure of complex **4** with 50% probability ellipsoids.

The tetrafluoroborate counter ion is omitted for clarity.

Table 2.3. Selected bond lengths (Å) and bond angles (°) of complex **4**

	Bond Lengths (Å)
Pd(1)-C(1)	2.034(5)
Pd(1)-C(2)	2.081(5)
Pd(1)-C(8)	2.101(5)
Pd(1)-C(9)	1.918(6)
C(1)-N(1)	1.352(6)
C(1)-N(2)	1.351(6)
C(2)-N(3)	1.350(6)
C(2)-N(4)	1.349(6)
C(9)-O(1)	1.118(6)
	Bond angles (°)
C(1)-Pd(1)-C(2)	85.42(19)
C(8)-Pd(1)-C(9)	85.30(20)
C(1)-Pd(1)-C(8)	90.90(20)
C(2)-Pd(1)-C(9)	98.50(20)
C(1)-Pd(1)-C(9)	175.80(20)
C(2)-Pd(1)-C(8)	174.20(20)
N(1)-C(1)-N(2)	104.50(40)
N(3)-C(2)-N(4)	104.00(40)

Table 2.4. Crystal data and structure refinement details for complex **4**

Empirical formula	C ₂₇ H ₃₁ BF ₄ N ₄ Pd
Formula weight	620.77
Crystal system	Triclinic
Space group	P $\bar{1}$
Unit cell dimensions	a = 10.7458(3) Å α = 68.230 (2) ° b = 12.1565(4) Å β = 73.986 (2) ° c = 12.6369 (4) Å γ = 67.495 (2) °
Volume	1398.94(8) Å ³
Z	2
Density (calculated)	1.474 Mg/m ³
Absorption coefficient	0.717 mm ⁻¹
Crystal size	0.13 x 0.10 x 0.03 mm
θ range for data collection	1.76 – 23.54 °
Index range	-12 ≤ h ≤ 12 -13 ≤ k ≤ 13 -14 ≤ l ≤ 14
Temperature	115(2) K
Wave length	0.71073 Å
Reflections collected	15017
Independent reflections	4140 (R _{int} = 0.0468)
Final R indices [I > 2σ(I)]	R1 = 0.0467 wR2 = 0.1121
R indices (all data)	R1 = 0.0637 wR2 = 0.1209
Goodness-of-fit on F ²	1.038

Equilibrium between [Pd(DIMes^{Me})(CH₃)(CO)][BF₄] (4**) and [Pd(DIMes^{Me})(COCH₃)(CO)][BF₄] (**5**).**

Exposure of a dichloromethane solution of **4** to > 1 atm of CO produces [(DIMes^{Me})Pd(CO)(COCH₃)][BF₄] quantitatively in the solution. However, crystals obtained by layering diethyl ether over the reaction mixture always contained ~5% of complex **4**, preventing the characterization of complex **5** by elemental analysis. This suggested an equilibrium between complex **4** and **5** which was confirmed by an NMR experiment with 1 atm of CO in a J Young NMR tube. This temperature dependent equilibrium was measured using variable temperature ¹H NMR spectroscopy from 4 °C to 25 °C. Complex **4** was dissolved in 0.7 mL of CD₂Cl₂ in a J Young NMR tube, and 1 atm of CO was added at 25 °C. After 15 min, CO was added again to adjust the pressure to exactly 1 atm. The sample tube was placed in the NMR probe set at the desired temperature (probe temperature pre-calibrated). The sample was equilibrated for 20 min at each temperature before taking data. Only **4** and **5** were detected under these conditions. The solubility of CO in CD₂Cl₂ at 1 atm was calculated using Bryndza's equation⁴², which also accounts for the temperature dependence of CO concentration.

$$\text{Bryndza's equation: } [\text{CO}]_{1\text{atm}} = 2.75 \times 10^{-6} [T] + 6.45 \times 10^{-3}$$

[CO] in molarity and T in °C

Calculated K_{eq} for different temperatures are shown in Table 2.5, together with concentrations of different species. A Van't Hoff plot (Figure 2.3) of the K_{eq} data was used to calculate ΔH° = - 17(1) kcal mol⁻¹ and ΔS° = - 42(4) cal mol⁻¹ K⁻¹. These values were consistent with an enthalpically driven bimolecular reaction. Uncertainties are

reported at the 95% confidence level. These were derived from a least-squares linear regression analysis of the temperature dependence of K_{eq} .

Table 2.5. Equilibrium data between **4** and **5**

Temperature		[4] mol / dm ⁻³	[5] mol / dm ⁻³	[CO] mol / dm ⁻³	K_{eq}
°C	K	(x 10 ⁵)	(x 10 ⁵)	(x 10 ⁵)	(dm ³ / mol)
4.1	277.3	5.32	441.89	646.12	12845
9.3	282.5	9.79	437.46	647.55	6895.0
14.5	287.7	15.39	431.87	648.97	4324.3
19.7	292.9	25.27	421.99	650.40	2567.1
24.85	298	42.27	404.99	651.83	1469.9

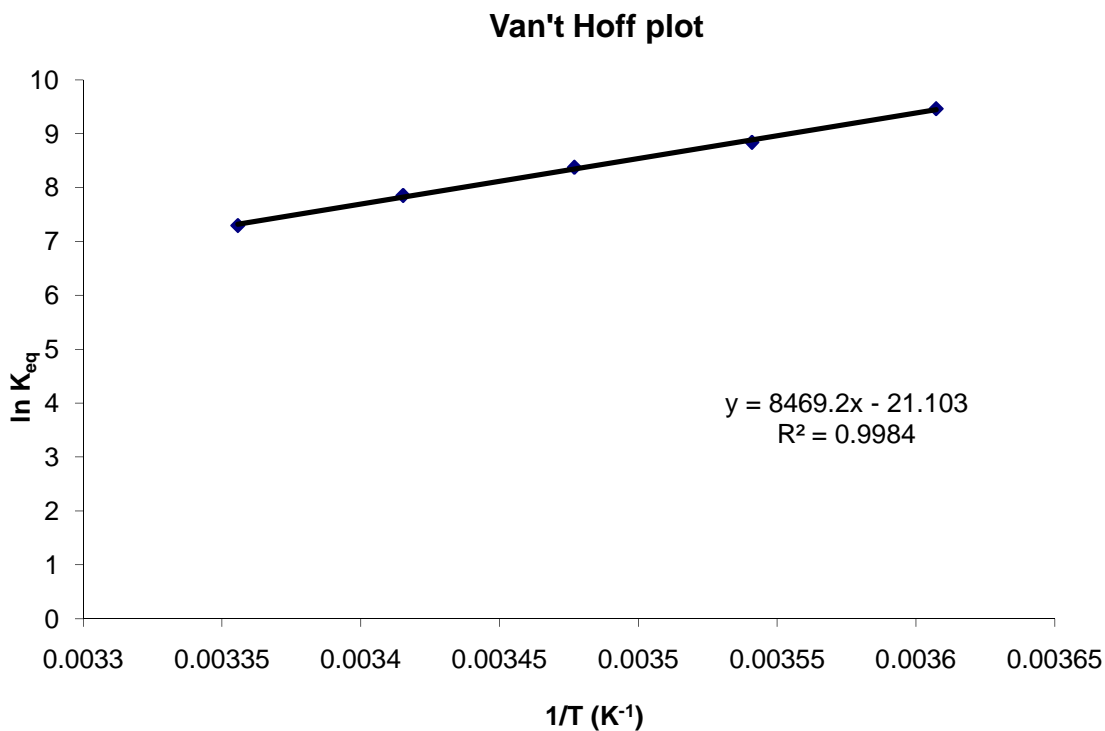


Figure 2.3. Van't Hoff plot for the equilibrium between **4** and **5**

Synthesis and characterization of [(DIMEs^{Me})Pd(CO)(COCH₃)] [BF₄] (5)

Exposure of a solution of **4** to higher CO pressure (> 1 atm) produced complex **5** quantitatively in the solution. This allowed characterization of the complex by spectroscopic methods. The ¹H NMR spectrum in CD₂Cl₂ showed an acyl CH₃ resonance at 1.29 ppm. Acyl resonances in the ¹³C NMR appeared at 234.52 (acyl CO) and 44.30 (acyl CH₃) ppm, but no resonance was identified for the Pd-bound CO because of its fast exchange with free CO. The other resonance patterns are similar to those found for complex **3** and **4**. IR signals for the Pd-COCH₃ (1667 cm⁻¹) and Pd-CO (2112 cm⁻¹) ligands were identified, and they are substantially lower than those seen in analogous phosphorous³⁸ or nitrogen³¹ complexes.

Kinetics of methyl migratory insertion into CO in [Pd(DIMEs^{Me})(CH₃)(CO)] [BF₄] (4)

Approximately 2.5 mg of complex **4** was dissolved in 0.7 mL of CD₂Cl₂ under vacuum in a J Young NMR tube. An initial ¹H NMR spectrum was taken after equilibration for 20 minutes at -50 °C. This was used to establish the initial concentration of complex **4** in the solution. The NMR tube with the sample was then cooled to -84 °C using an ethyl acetate slush bath. CO (1 atm or 0.5 atm) was added to the NMR tube while the liquid was held at -84 °C. In the J Young NMR tube used, this corresponded to 22 equivalent of CO per mole of complex **4** at 1 atm and 11 equiv of CO at 0.5 atm. The sample was shaken a couple of times while preventing warming and then placed in the pre-cooled, calibrated NMR probe at -50 °C. The reaction mixture was equilibrated for 5 minutes, and data collection was started. The residual NMR solvent

peak (CHDCl_2) was used as an internal standard to convert the integrated intensity of the methyl peak of **4** into concentration units. Data were collected for disappearance of **4** over 4.7 hours at 1 atm CO (3.8 half-lives) and 0.5 atm (3 half-lives). Assuming pseudo-first order kinetics (i.e. constant $[\text{CO}]$), graphs of $\ln[\mathbf{4}]$ versus time were plotted and are shown in Figure 2.4 (1 atm CO) and Figure 2.5 (0.5 atm CO). The plots allowed calculation of the observed rate constants (k_{obs}) as $1.58(1) \times 10^{-4} \text{ s}^{-1}$ at 1 atm of CO and $1.18(2) \times 10^{-4} \text{ s}^{-1}$ at 0.05 atm of CO.

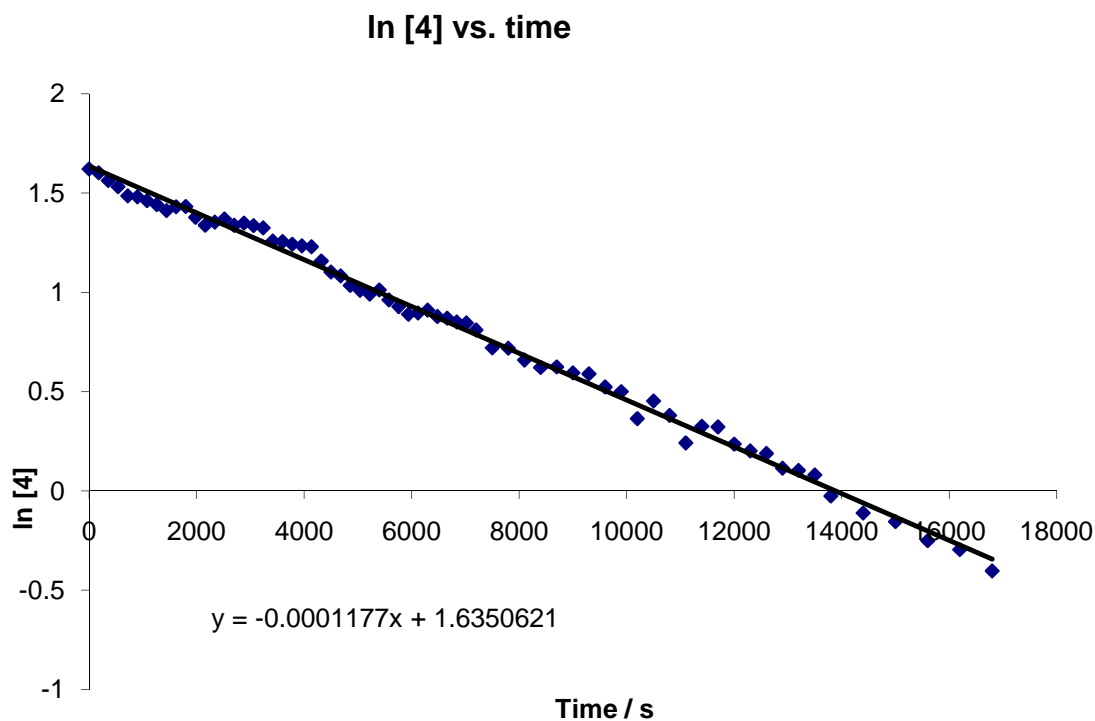


Figure 2.4. Kinetic plot for methyl migration in **4** at 0.5 atm of CO and -50°C

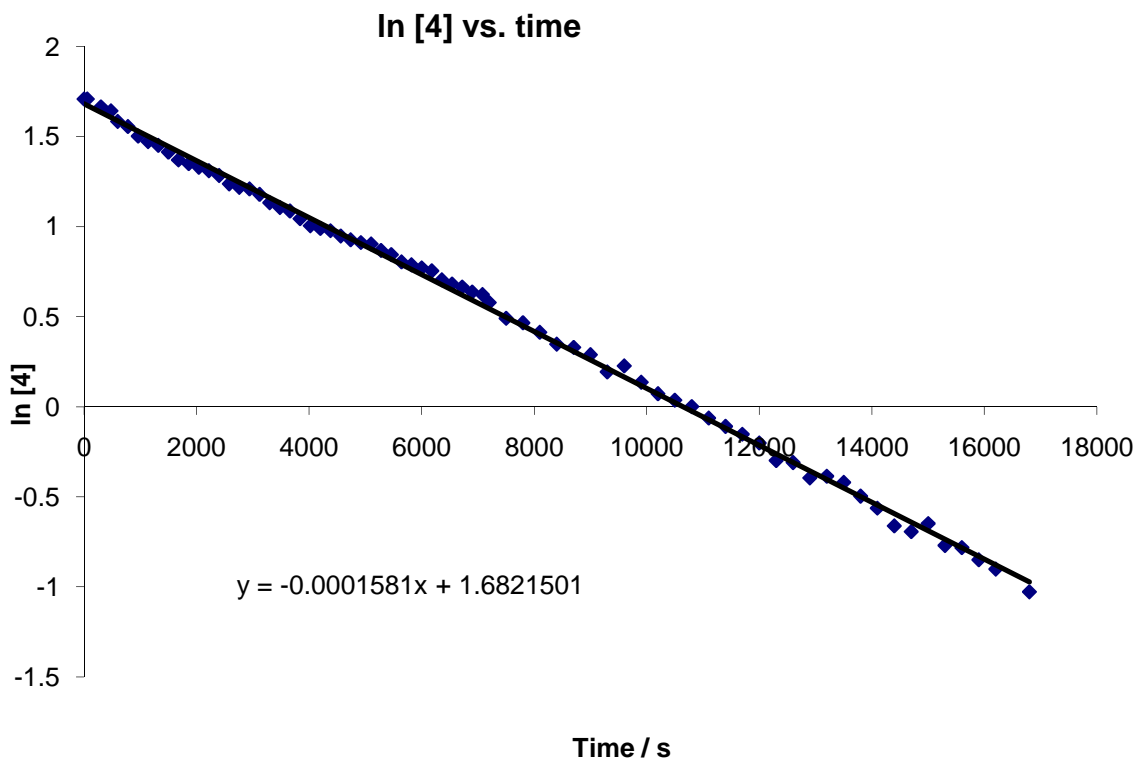
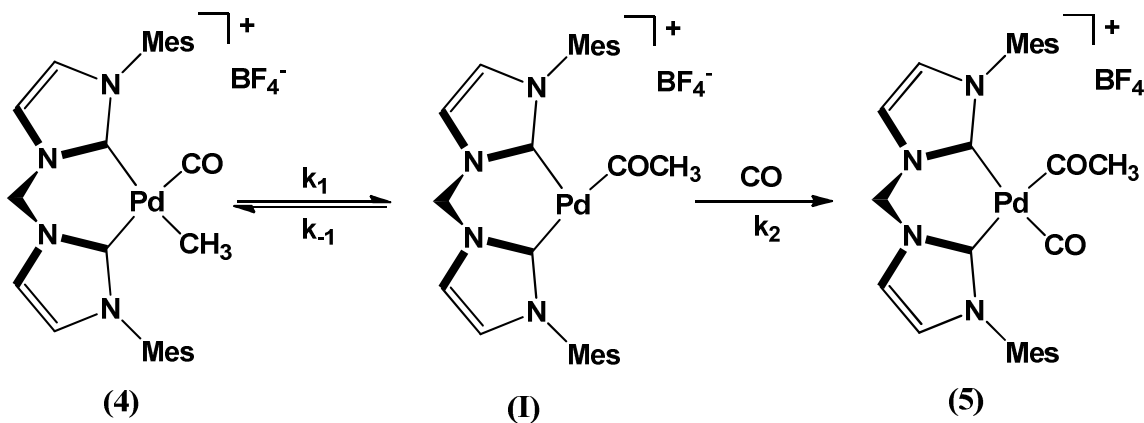


Figure 2.5. Kinetic plot for methyl migration in **4** at 1 atm of CO and - 50°C

This system is likely to follow a mechanism earlier proposed for similar diimine and bis(phosphine) palladium systems based on kinetic studies.^{31, 38} In this mechanism, reversible methyl migration to the Pd-CO gives an unsaturated acyl intermediate (k_1) which is then trapped by CO ($k_2[\text{CO}]$) (Scheme 2.4). The k_{obs} dependence on CO concentration indicates that the rate of the reverse methyl migration from acyl to Pd (k_{-1}) must be comparable to $k_2[\text{CO}]$ at the pressures used. If $k_2[\text{CO}] \gg k_{-1}$, k_{obs} should not depend on $[\text{CO}]$. On the other hand, if incoming CO associates with Pd prior to or during the methyl migration step in the mechanism, this should give k_{obs} at 0.5 atm of CO roughly one half the value observed at 1.0 atm of CO (i.e. perfect 1st order

dependence on [CO]). Assuming [CO] at 0.5 atm is one half of its value at 1 atm and using the steady state approximation, a value for k_1 was derived.



Scheme 2.4. Proposed mechanism for methyl migration in **4** and trapping by CO to form **5**.

$$\text{rate} = \frac{d[5]}{dt} = k_2[\text{CO}][\text{I}]$$

At steady state approximation for I (acyl intermediate)

$$\frac{d[\text{I}]}{dt} = k_1[4] - k_{-1}[\text{I}] - k_2[\text{CO}][\text{I}] = 0$$

$$[\text{I}] = \frac{k_1[4]}{k_{-1} + k_2[\text{CO}]}$$

$$\frac{d[5]}{dt} = \frac{k_1 k_2 [\text{CO}][4]}{k_{-1} + k_2 [\text{CO}]} \quad k_{\text{obs}} = \frac{k_1 k_2 [\text{CO}]}{k_{-1} + k_2 [\text{CO}]}$$

[CO] at $-50\text{ }^{\circ}\text{C}$ and 1 atm was estimated using Bryndza's equation⁴². [CO] at 0.5 atm was assumed to be one-half its value at 1.0 atm CO using Henry's Law behavior for CO.

$$\frac{k_{\text{obs}}(1.0\text{ atm})}{k_{\text{obs}}(0.5\text{ atm})} = \frac{k_1 k_2 (0.00631)}{k_{-1} + k_2 (0.00631)} \times \frac{k_{-1} + k_2 (0.00316)}{k_1 k_2 (0.00316)} = \frac{1.58(1) \times 10^{-4} \text{ s}^{-1}}{1.18(2) \times 10^{-4} \text{ s}^{-1}} = 1.43(2)$$

$$k_{-1} = [0.00326(22)]k_2$$

This expression was plugged into the k_{obs} with the concentration of CO at 1 atm and $-50\text{ }^{\circ}\text{C}$:

$$[\text{CO}]_{1\text{atm}, -50\text{ }^{\circ}\text{C}} = 0.00631 \text{ M}$$

$$k_{\text{obs}} = 1.58(1) \times 10^{-4} \text{ s}^{-1} = \frac{k_1 k_2 [0.00631]}{([0.00326(22)]k_2) + k_2 [0.00631]}$$

$$k_1 = \frac{1.58(1) \times 10^{-4}}{0.659(15)} \text{ s}^{-1} = 2.40(6) \times 10^{-4} \text{ s}^{-1}$$

For pseudo-first order conditions, the kinetic plot should have the following form:

$$\ln[\mathbf{4}] = -k_{\text{obs}}t + \ln[\mathbf{4}]_0$$

As shown below, the y-intercepts of the kinetic plots were very close to the expected values of $\ln[\mathbf{4}]_0$ based on starting concentrations. This indicates that the steady state model shown above, with the k_2 step effectively irreversible, is very likely valid under the conditions used.

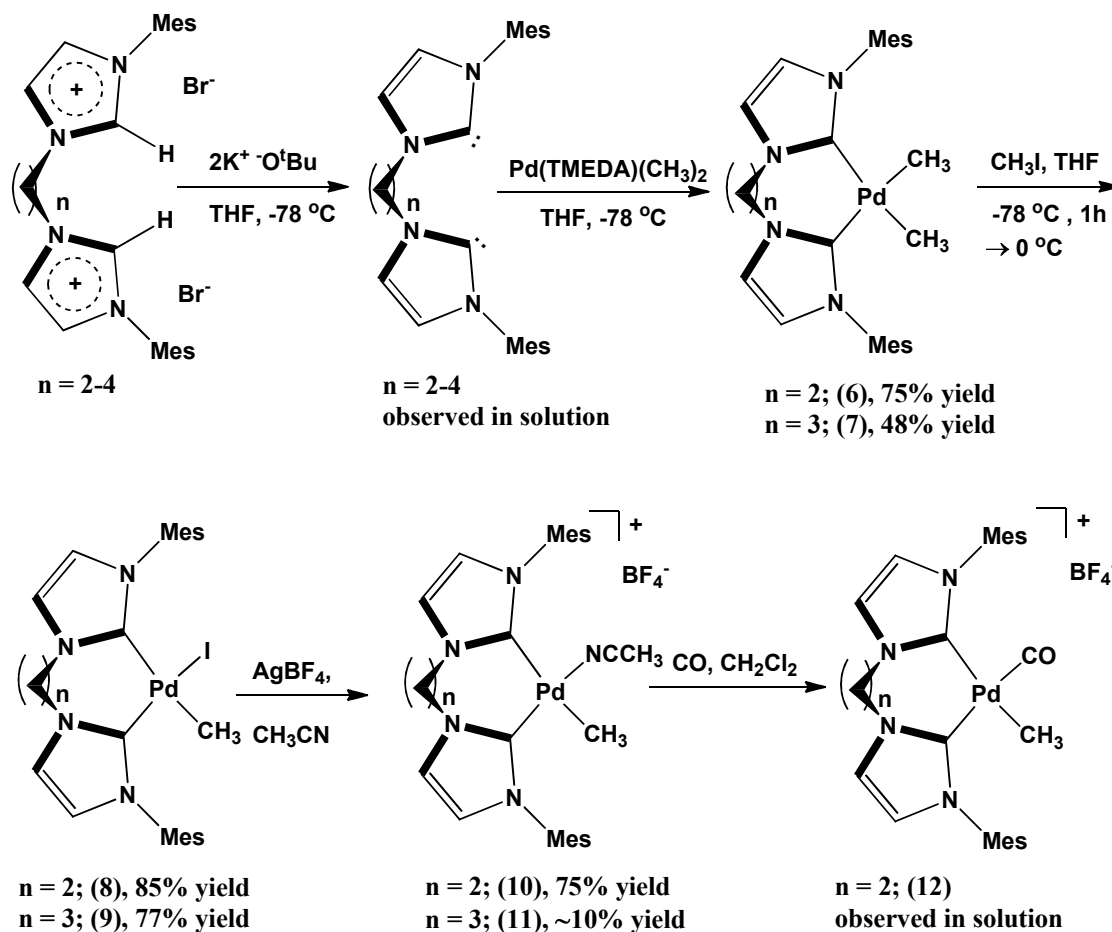
<i>PCO</i>	y intercept	expected ln[4] ₀
1.0 atm	1.68(1)	1.71
0.5 atm	1.64(2)	1.62

The rate constant (k_1) of $2.40(6) \times 10^{-4} \text{ s}^{-1}$ for the methyl migration step is comparable with the analogous DPPE palladium complex. Both DPPE and DIMes^{Me} form palladium complexes with similar bite angles ($90^\circ <$), even though DPPE forms a five-membered chelating ring complex and DIMes^{Me} forms a six-membered chelating ring complex. The small bite angle in **3** and **4** is due to incorporation of a less flexible imidazolylidene ring into the chelate ring. The six membered chelating ring bis(phosphine) ligands, DⁱPPP (bis(diisopropylphosphino)propane) and DPPP (bis(diphenylphosphino)propane), formed complexes that showed a significantly larger rate for methyl migration. These bis(phosphine) ligands showed larger bite angles of $\sim 97^\circ$, and even the methylpalladium CO complexes showed measurable insertion rates even at -82°C . A plausible explanation for the lower methyl migration rate in **4** is the smaller C-Pd-C bite angle of the bis(NHC) ligand, since it is well known that the bis(phosphine) systems show higher methyl migration rate with increasing P-Pd-P bite angle.³⁸ Therefore, a larger bite angle chelating bis(NHC) is necessary to achieve the higher activity shown by the DPPP systems.

Increasing the chelate ring size of bis(NHC) ligand.

The linkage between the two imidazole rings was changed from methylene to larger alkylene linkages to obtain larger chelate ring sizes. The synthetic approach

followed for the DIMes^{Me} complexes was used to synthesize these complexes (Scheme 2.5).



Scheme 2.5. Synthesis of larger chelate ring size bis(NHC) methylpalladium complexes

Synthesis and characterization of $[(\text{DIMes}^{\text{Et}})\text{Pd}(\text{CH}_3)_2]$ (6) and $[(\text{DIMes}^{\text{Pr}})\text{Pd}(\text{CH}_3)_2]$ (7).

These ethylene and propylene linkage bis(NHC) dimethylpalladium complexes were synthesized using an approach similar to that used for the DIMes^{Me} complex but

with some modifications. Longer reaction times were given for the free carbene formation step, the reaction of DIMes^{Et} (3 h) and DIMes^{Pr} (4 h) dibromide salts with potassium *tert*-butoxide. These dimethyl complexes decomposed very rapidly in dichloromethane. Therefore, this solvent was avoided during extraction, and tetrahydrofuran, diethyl ether and hexanes were used for the recrystallization process. One molar equivalent of bis(imidazolium) salt and two molar equivalents of potassium *tert*-butoxide were placed in a two neck round bottom flask fixed with a septum and a needle valve. Dry THF was distilled onto the mixture under vacuum at $-78\text{ }^{\circ}\text{C}$, and the mixture was stirred for $\sim 3 - 4$ hours to form the free bis(carbene). The resultant cloudy, light pink suspension was transferred onto a solution of [(TMEDA)Pd(CH₃)₂] in THF at $-78\text{ }^{\circ}\text{C}$ via cannula, and the resulting mixture was stirred for another 3 hours. The volatiles were removed under vacuum, the residue was extracted with THF, and diethyl ether and hexanes were added to get white crystals. These complexes were more unstable than the analogous DIMes^{Me} complex, but they can be stored at $-35\text{ }^{\circ}\text{C}$ under inert conditions. The instability of bis(NHC) dimethyl palladium complexes increased with increasing chelate ring size. Both complexes showed same resonance pattern found for the DIMes^{Me} dimethylpalladium complex in their ¹H NMR spectra taken in DMSO-*d*₆. The ethylene linkage in DIMes^{Et} showed a very broad peak from 4-6 ppm, and the propylene linkage in DIMes^{Pr} showed two resonances at 5.91 ppm and 4.54-4.20 ppm with a 4:2 integration ratio. The Pd-CH₃ resonances were observed at upfield values of -1.15 and -1.18 ppm for complex **6** and **7**, respectively. The ¹³C NMR spectrum of the DIMes^{Et} complex showed a carbene carbon signal at 189.7 ppm. The instability of the DIMes^{Pr} complex in solution prevented its characterization by ¹³C NMR.

The attempted synthesis of a DIMes^{Bu} dimethylpalladium complex failed using this synthetic route. In an NMR tube experiment at room temperature, the ¹H NMR spectrum showed formation of the free carbene DIMes^{Bu}, but addition of dimethylpalladium(TMEDA) did not result in any recognizable peaks in the spectrum, indicating that both reactants had decomposed into unidentified products.

Synthesis and characterization of [(DIMes^{Et})Pd(CH₃)(I)] (8) and [(DIMes^{Pr})Pd(CH₃)(I)] (9).

These complexes were synthesized similarly to [(DIMes^{Me})Pd(CH₃)(I)]. The bis(NHC) dimethyl palladium complex was placed in a two neck round bottom flask fixed with a septum and a swivel frit. Dry THF was distilled onto the reactants under vacuum at -78 °C, and excess methyl iodide was added via syringe under inert atmosphere. The reaction mixture was warmed to 0 °C and stirred for one hour to give a bright white precipitate with liberation of ethane. The product was isolated by filtration and washed with diethyl ether. These complexes are very unstable and darkened rapidly with decomposition upon standing at room temperature, even in inert atmosphere. These complexes were only soluble in DMSO, but they decomposed very rapidly in solution, making it very difficult to obtain adequate NMR data. Only the DIMes^{Et} complex was characterized by ¹H NMR. These complexes can be stored at -35 °C for several weeks without significant decomposition.

Synthesis and characterization of [(DIMes^{Et})Pd(CH₃)(CH₃CN)][BF₄] (10) and [(DIMes^{Pr})Pd(CH₃)(CH₃CN)][BF₄] (11).

Following a synthetic route similar to that used for the synthesis of [(DIMes^{Me})Pd(CH₃)(CH₃CN)][BF₄] at room temperature did not lead to isolable products. During the recrystallization step, the formation of white crystals of the complexes with DIMes^{Et} and DIMes^{Pr} ligands was observed, but the complexes started to decompose rapidly during isolation. Therefore, the reactions were carried out at lower temperatures using pre-cooled solvents under inert conditions. Complex [(DIMes^{Et})Pd(CH₃)(I)] was suspended in pre-cooled acetonitrile at – 35 °C under inert condition. One molar equivalent of AgBF₄ was added to the reaction flask, and the mixture was stirred for one hour at – 35 °C to give an ash-brown precipitate. The precipitate was removed by filtration through celite. A small amount of pre-cooled diethyl ether was added to the filtrate to precipitate any silver salt present, and the mixture was filtered through celite. Pre-cooled diethyl ether was then layered on the filtrate, and the mixture was kept in the glove box freezer at – 35 °C to form crystals. White crystals formed after standing at – 35 °C for a couple of hours. Products were isolated by filtration while maintaining the low temperature of the solution. [(DIMes^{Et})Pd(CH₃)(CH₃CN)][BF₄] is very unstable at room temperature, but it can be stored at – 35 °C. The ¹H NMR spectrum in CD₃CN showed broad peaks with a resonance pattern similar to that of [(DIMes^{Me})Pd(CH₃)(CH₃CN)][BF₄], but the complex decomposed during data collection, preventing full characterization by ¹³C NMR. White crystals of [(DIMes^{Et})Pd(CH₃)(CH₃CN)][BF₄] were isolated in < 10% yield. However, the complex decomposed very quickly in NMR solution, preventing characterization.

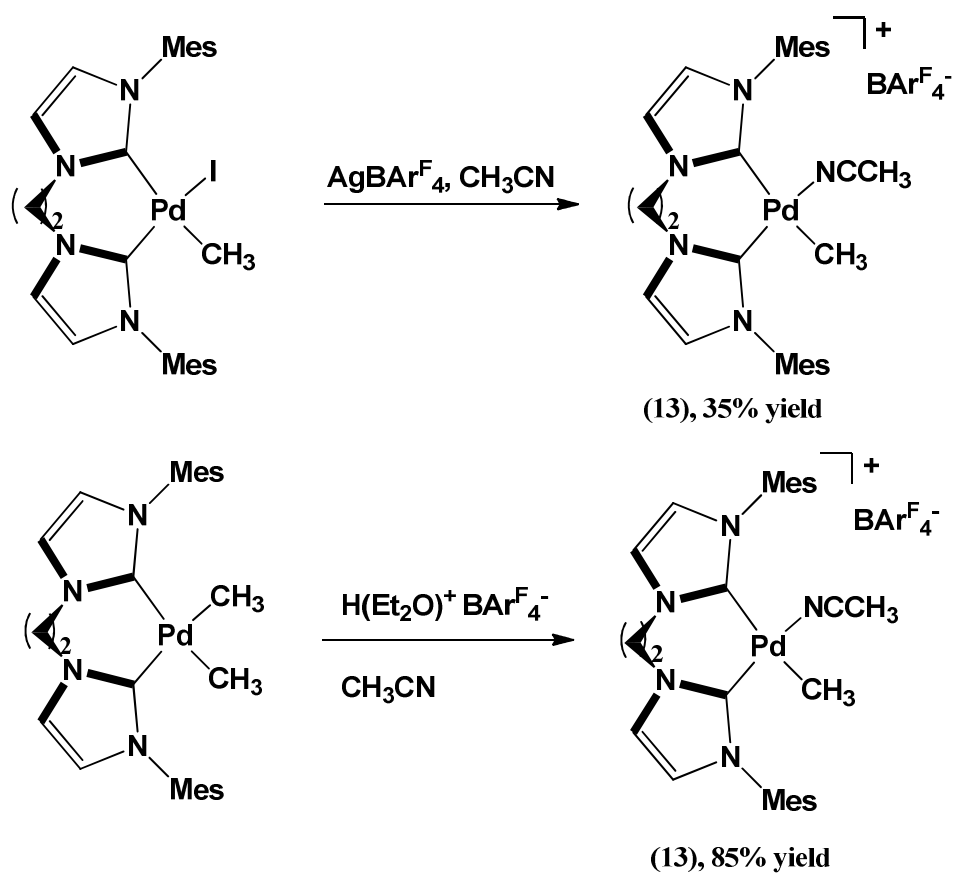
Synthesis of [(DIMes^{Et})Pd(CH₃)(CO)][BF₄] (12) and kinetic studies on methyl migration

[(DIMes^{Et})Pd(CH₃)(CH₃CN)][BF₄] was dissolved in CD₂Cl₂ in a J Young NMR tube, and the solution was cooled to – 84 ° C using an ethyl acetate slush bath. CO (1 atm) was added to the NMR tube while the liquid was held at -84 °C. The NMR tube was then placed in a pre-cooled NMR probe – 50 °C. The starting methyl complex was found to be completely converted to the acyl product [(DIMes^{Et})Pd(COCH₃)(CO)][BF₄] **12a**, indicating a faster methyl migration step compared to the DIMes^{Me} complex. In the attempted synthesis of [(DIMes^{Et})Pd(CH₃)(CO)][BF₄] **12**, the desired product was observed in the crude NMR spectrum, but it decomposed slowly with formation of palladium black. It was hypothesized that replacing the small non-coordinating anion BF₄⁻ with the large non-coordinating anion BAr^F₄⁻ could stabilize the cationic, large chelate ring size bis(NHC) methylpalladium complexes.

Synthesis and characterization of cationic, large chelate ring size bis(NHC) methylpalladium complexes with the BAr^F₄ anion (13)

[(DIMes^{Et})Pd(CH₃)(I)] was suspended in acetonitrile under inert atmosphere. One molar equivalent of AgBAr^F₄ was added to the reaction flask, and the mixture was stirred for one hour to give an ash brown precipitate. The precipitate was removed by filtration through celite, volatiles were removed under vacuum, and the residue was dried for an additional two hours. The solid was dissolved in diethyl ether and filtered through celite to remove residual AgI. The solution was then concentrated, hexanes was layered top of the filtrate, and the solution was kept at -35 °C to form crystals. Crystals were isolated by

filtration. The $^1\text{H NMR}$ spectrum in $\text{CD}_3\text{CN}-d_3$ confirmed the formation of $[(\text{DIMes}^{\text{Et}})\text{Pd}(\text{CH}_3)(\text{CH}_3\text{CN})][\text{BAr}_4^{\text{F}}]$. Even though the complex is stable at room temperature, the high solubility of $\text{AgBAr}_4^{\text{F}}$ and the product, as well as the presence of AgI , interfered with isolation of pure product in good yield. Therefore, an alternative synthetic route was used for the synthesis of $[(\text{DIMes}^{\text{Et}})\text{Pd}(\text{CH}_3)(\text{CH}_3\text{CN})][\text{BAr}_4^{\text{F}}]$. Equal equivalents of $(\text{DIMes}^{\text{Et}})\text{Pd}(\text{CH}_3)_2$ and $[\text{H}(\text{Et}_2\text{O})_2][\text{BAr}_4^{\text{F}}]$ were placed in a round-bottom flask fixed to a swivel frit, and acetonitrile was distilled onto the reactants at $-78\text{ }^\circ\text{C}$. The reaction mixture was stirred for one hour at $-78\text{ }^\circ\text{C}$ and then warmed to room temperature. The reaction produced the desired product with liberation of methane gas, and the product was isolated by layering diethyl ether onto the reaction mixture. The product was very stable at room temperature.



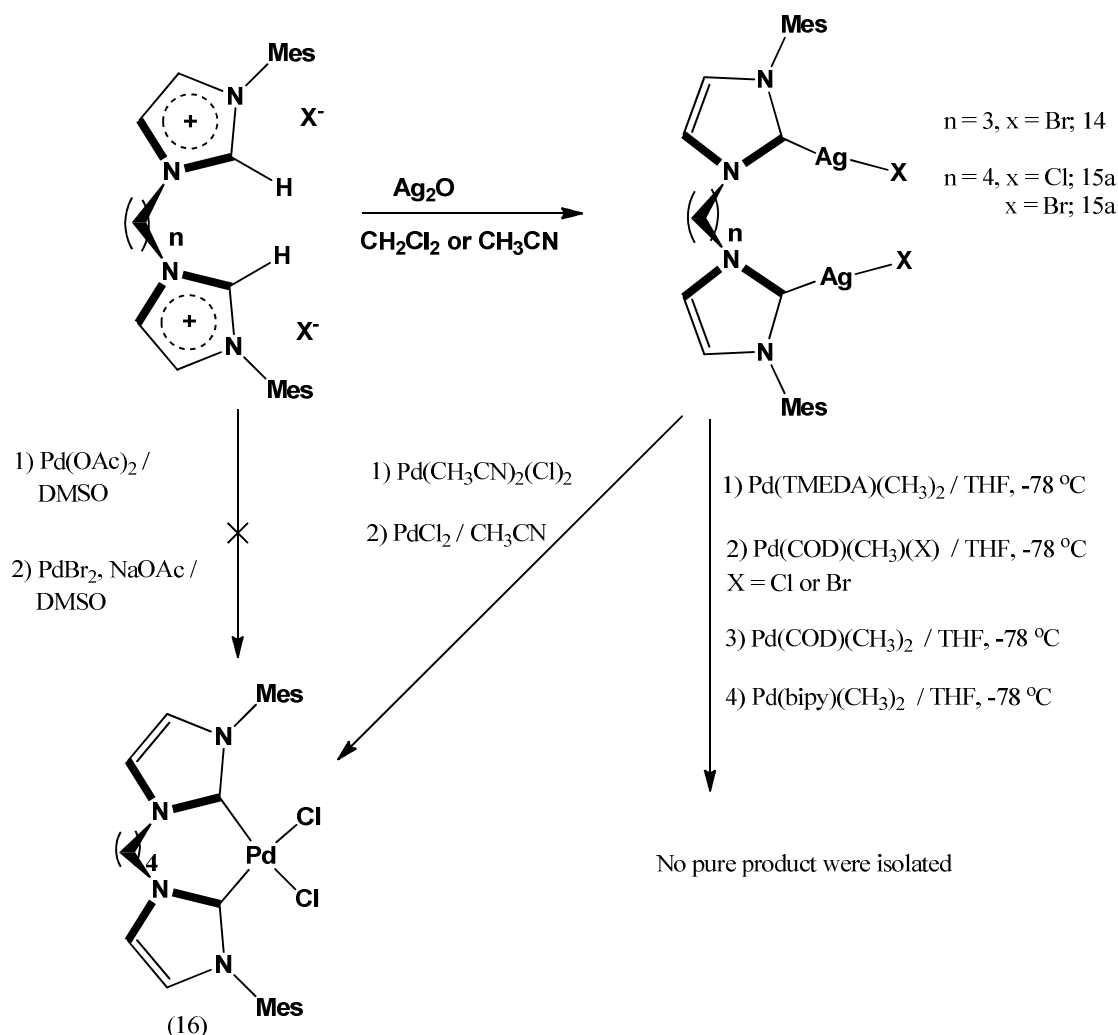
Scheme 2.6. Synthesis of $[\text{Pd}(\text{DIMes}^{\text{Et}})(\text{CH}_3)(\text{CH}_3\text{CN})][\text{BAR}^{\text{F}}_4]$ complex (**13**)

Attempted synthesis of large chelate ring bis(NHC) methylpalladium complexes by transmetalation with silver complexes

Because of lower yield and synthetic problems during the synthesis of large chelate ring (propylene and ethylene linkage) bis(NHC) methylpalladium complexes, we searched for alternative synthetic approaches. First, we investigated the applicability of silver bis(NHC) complexes for transmetalation to produce methylpalladium complexes. Di silver dihalide complexes of the bis(NHC) ligands DIMes^{Pr} and DIMes^{Bu} , $\{\text{Ag}_2(\text{DIMes}^{\text{Pr}})\text{Br}_2$ (**14**), $(\text{Ag}_2(\text{DIMes}^{\text{Bu}})\text{Cl}_2$ (**15a**), and $(\text{Ag}_2(\text{DIMes}^{\text{Bu}})\text{Br}_2$ (**15b**) were synthesized in good yield using a procedure published for less bulky bis(NHC)

complexes by Ahrens et al in 2006.⁴³ Transmetalation with methylpalladium precursors such as Pd(TMEDA)(CH₃)₂, Pd(COD)(CH₃)₂, Pd(bipy)(CH₃)₂, Pd(COD)(CH₃)(Br), and Pd(COD)(CH₃)(Cl) failed to produce the desired bis(NHC) methylpalladium complexes in pure form. Most of these reactions produced mixtures of products in moderate yields, but isolation of the pure bis(NHC) methylpalladium complexes failed.

A second approach focused on synthesis of bis(NHC) palladium dihalide complexes. It was thought that these complexes could be used to synthesize methylpalladium complexes via reaction with methylation reagents such as Sn(CH₃)₄, Mg(CH₃)(Br), Zn(CH₃)₂, and Al(CH₃)₃. However, all synthetic attempts with Pd(OAc)₂ and PdBr₂ failed to produce desired product in pure form. Isolation of pure products from mixtures of products failed. However, reactions of (DIMes^{Bu})Ag₂Cl₂ with Pd(CH₃CN)₂Cl₂ or PdCl₂ in solvents such as CH₂Cl₂ and CH₃CN did produce (DIMes^{Bu})PdCl₂ at room temperature. Equival molar equivalents of Pd(CH₃CN)₂Cl₂ (PdCl₂) and (DIMes^{Bu})Ag₂Cl₂ were placed in a round bottom flask fixed to a needle valve, and CH₂Cl₂ was distilled onto the reactants under vacuum. The reaction mixture was stirred overnight under exclusion of light. The unreacted materials were filtered off through celite. After reduction of solvent volume under reduced pressure, addition of diethyl ether produced the desired product as a pale yellow solid, which was isolated by filtration. The ¹H NMR spectrum showed the presence of two isomers in a 1: 19 ratio, which may arise from two different orientation of the butylene linkage.



Scheme 2.7. Synthesis of silver bis(NHC) complexes and their attempted transmetalation reactions

A rigid backbone, bulky bis(NHC) complex:

Synthesis and characterization of (1,1'-bis(2,4,6-trimethylbenzyl)-3,3'-(1,2-phenylene)diimidazolium dibromide salt (17)

Benzene was used as a linkage between two imidazole rings to get a rigid backbone. This will reduce the flexibility of ligand and result in formation of large bite angle. 2,4,6-trimethylbenzyl groups were incorporated as N-substituents in order to

produce steric shielding. One molar equivalent of 1-(bromomethyl)-2,4,6-trimethylbenzene, 0.55 molar equivalent of 1,1'-(1,2-phenylene)bis(imidazole), and toluene solvent were placed in a thick-walled glass vessel. The reaction mixture was heated at 100 °C for 24 hours, during which time white solids formed. After cooling the reaction mixture to room temperature, the solids were isolated by filtration and then washed with THF. The product was recrystallized using dichloromethane as a solvent. ¹H and ¹³C spectra indicate a symmetric molecule, and the acidic imidazole protons were observed at 9.19 ppm.

Synthesis of (1,1'-bis(2,4,6-trimethylbenzyl)-3,3'-(1,2-phenylene)diimidazol-2,2'-diylidene) (18)

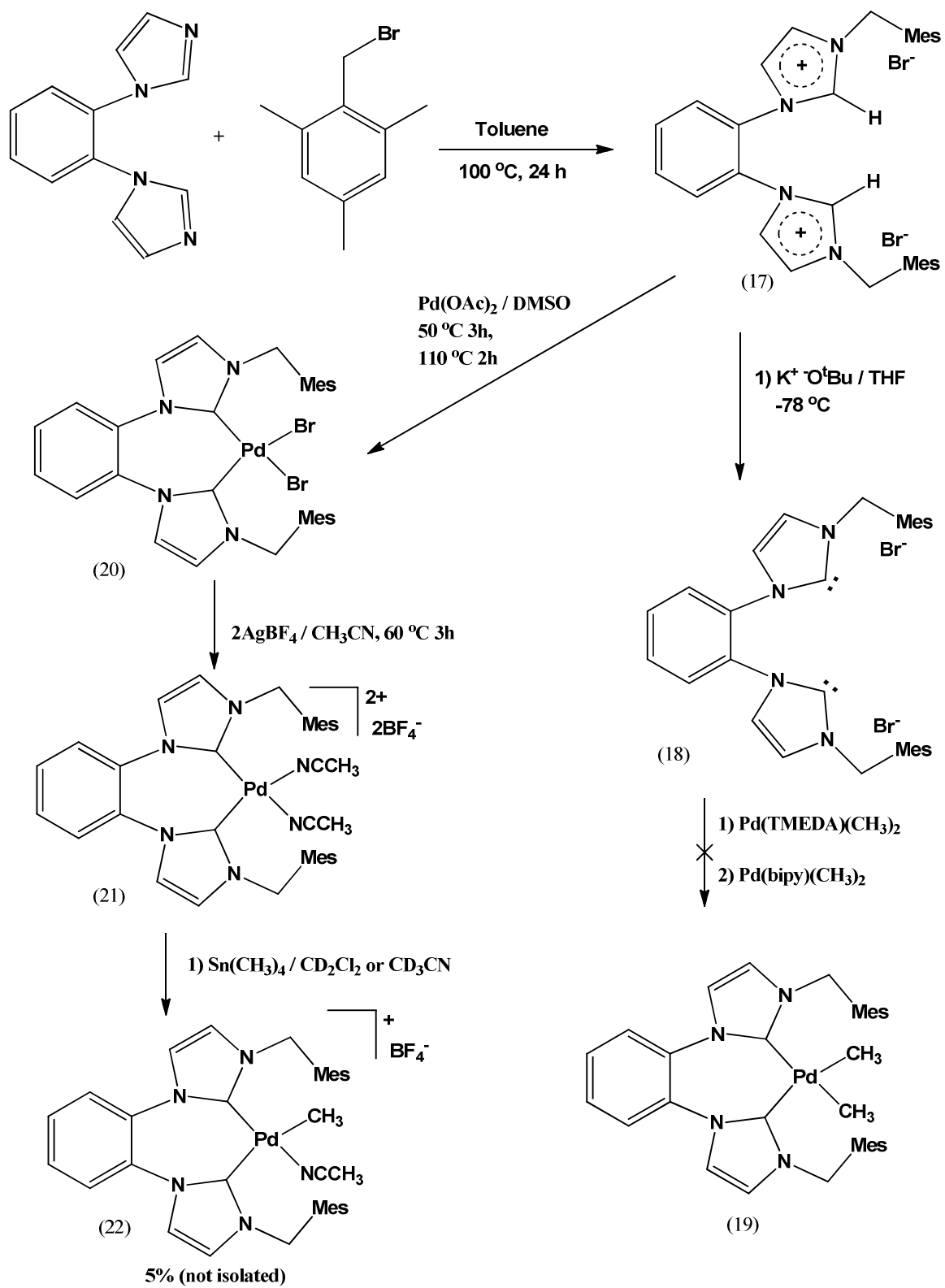
Attempted synthesis of the (1,1'-bis(2,4,6-trimethylbenzyl)-3,3'-(1,2-phenylene)diimidazol-2,2'-diylidene) Pd (CH₃)₂ complex using a procedure similar to that used for the synthesis of complexes **1**, **6** and **7** failed. However, the free carbene **18** was isolated from the reaction between **17** and K⁺O⁻tBu in THF. One molar equiv of **17** and two molar equiv of K⁺O⁻tBu were placed in a round bottom flask fitted to a swivel frit. THF was distilled into the flask at -78 °C, and the mixture was stirred at the same temperature for 4 hours. It was then allowed to warm up to room temperature, which resulted in a cloudy yellow solution. The reaction mixture was filtered to remove KBr byproduct, volatiles were stripped under vacuum, and the residue was dried for an additional two hours. The solid was extracted with hexanes, and the extract was concentrated. The concentrated solution was kept at -35°C for a couple of days to produce yellow crystals, which were isolated by filtration.

Free carbene **18** did not react with methylpalladium precursors like Pd(THEDA)(CH₃)₂ and Pd(bipy)(CH₃)₂ in THF or benzene, even upon heating up to 50 °C. Monitoring the reaction by ¹H NMR using C₆D₆ as an NMR solvent revealed that no reaction occurred at room temperature, and decomposition of the methylpalladium precursors and the free carbene occurred at higher temperatures. Free carbene **18** was stable at room temperature during the reaction period, but started to form a new set of peaks at 50 °C. However, these peaks cannot be assigned to complex **19** because of the absence of a methylpalladium signal. Free carbene **18** was stable at room temperature under inert atmosphere and solutions of **18** in C₆D₆ were stable for 8-10 hours under air. However, solid samples were not stable under air.

Synthesis and characterization of [Pd(1,1'-bis(2,4,6-trimethylbenzyl)-3,3'-(1,2-phenylene)diimidazol-2,2'-diylidene)Br₂] (20**)**

The synthesis of **20** followed a procedure reported for a similar type of less bulky bis(NHC) complex.⁴³ Equal molar equivalents of imidazolium salt **17** and Pd(OAc)₂ were mixed in a thick-walled glass vessel, and wet DMSO was added as a solvent. The sealed vessel containing the reaction mixture was initially heated at 50 °C for 3 hours, followed by 110 °C for 2 hours. Cooling to room temperature produced a small amount of solids, and addition of dichloromethane increased the solid formation. Solids were isolated by filtration and washed with dichloromethane and diethyl ether to remove unreacted starting material. Complex **20** was insoluble in most solvents but very slightly soluble in DMSO. This low solubility prevented characterization by ¹³C NMR spectroscopy. The ¹H NMR spectrum showed two slightly broad singlet peaks for imidazole protons at 7.70 and

6.53 ppm, with a 1:1 integration ratio. The linkage phenylene showed two sets of multiplets ranging from 7.88 to 7.86 and 7.79 to 7.71 ppm. The diastereotopic methylene protons showed an AB pattern at 6.05-5.41 ppm. Aromatic mesityl protons showed a singlet at 7.00 ppm, and the methyl protons showed 2 singlets at 2.27 and 2.23 ppm with a 6:12 integration ratio.



Scheme. 2.8. Synthesis of rigid backbone bis(NHC) complexes

Synthesis and characterization of [Pd(1,1'-bis(2,4,6-trimethylbenzyl)-3,3'-(1,2-phenylene)diimidazol-2,2'-diylidene)(CH₃CN)₂][BF₄]₂ (21**)**

Dicationic, bulky, rigid backbone-containing bis(NHC) complex **21** was synthesized as a possible precursor for a cationic methylpalladium complex. One molar equivalent of complex **20** and two molar equivalents of AgBF₄ were placed in a thick walled glass vessel with acetonitrile. The sealed vessel was heated at 60 °C for three hours. The resultant reaction mixture was filtered through celite to remove silver salts. The solvent was removed from the filtrate under vacuum, and the residue was dried for an additional two hours. The resultant solid was redissolved in acetonitrile, the solution was filtered through celite, the solvent was removed under vacuum, and the residue was dried under vacuum. This sequence was repeated one more time. This sequence is very important in order to remove all silver salts present in the product. Finally, white crystalline products were isolated by layering ether onto the solution in acetonitrile.

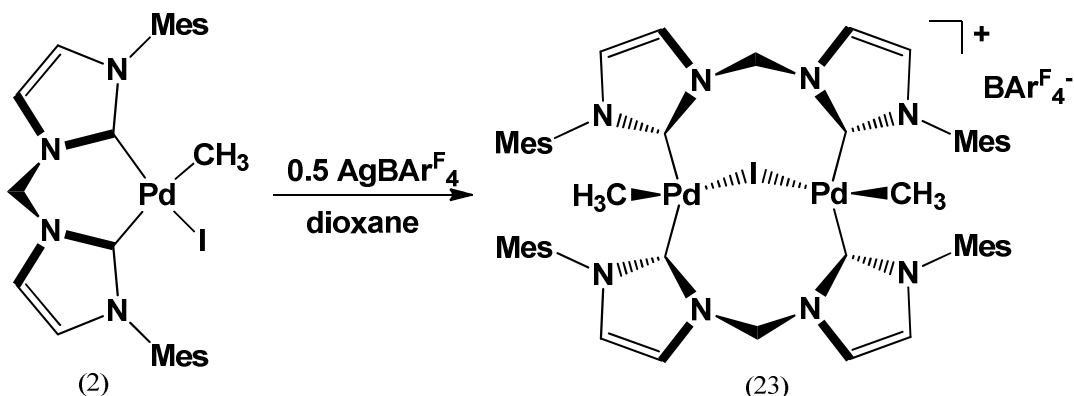
Complex **21** was soluble in most polar solvents such as dimethyl sulfoxide, acetonitrile, and dichloromethane. The ¹H NMR spectrum is similar to that of **20**, but sharper peaks were observed, and a downfield carbene carbon resonance appeared at 147.48 ppm. It was thought that replacing one acetonitrile molecule in complex **21** could produce a cationic methylpalladium complex analogous to complexes **3**, **10**, and **11**. However, the methylating reagents Sn(CH₃)₄, CH₃MgBr, and Al(CH₃)₃ did not produce any isolable product. Reaction of complex **21** with Sn(CH₃)₄ in CD₂Cl₂ was monitored by ¹H NMR spectroscopy at room temperature. A new set of peaks started to appear in the spectrum, which could be identified as the resonances from complex **22** ([Pd(1,1'-bis(2,4,6-trimethylbenzyl)-3,3'-(1,2-phenylene)diimidazol-2,2'-

diylidene)(CH₃CN)(CH₃)] [BF₄]). However, even after 20 days only ~5 % of the product was produced.

Synthesis of bridging bis(NHC) dimethylpalladium complex (23)

Complex **23** was produced in the attempted synthesis of a cationic methylpalladium DIMes^{Me} complex analogous to complex **3** with the larger anion BAr₄^{F-}. It was later found that less AgBAr₄^{F-} than required (one molar equivalent) was used due to weighing errors. The complex was again synthesized from the reaction between complex **2** and one half molar equivalents of AgBAr₄^{F-} in dioxane. Both reactants were placed in a flask under inert atmosphere. Dioxane was added as a solvent, and the mixture was stirred for 4 hours. The precipitate was removed by filtration through celite, volatiles were removed under vacuum, and the residue was dried for an additional two hours. The solid was then dissolved in diethyl ether, and the mixture was filtered through celite to remove residual AgI. The filtrate was concentrated, mixed with hexanes, and kept at -35 °C in the glove freezer for a couple of days, which produced pale yellow crystals. The X-ray crystal structure showed two palladiums bridged by two bis(NHC) ligands and one iodo ligand, with one methyl group bound to each palladium atom. ¹H NMR spectra in different solvents showed a more upfield Pd-CH₃ signal (0.16 ppm in CD₂Cl₂ and 0.24 ppm in C₆D₆) than all other investigated bis(NHC) methylpalladium complexes. An AB pattern was observed for the methylene protons, indicating a rigid backbone in solution. Two doublets and singlets each were observed for the imidazole and mesityl aromatic protons, respectively. Two singlets with an 8:4 integration ratio were observed for the BAr₄^{F-} anion. The same synthetic procedure was repeated using

one molar equivalent of complex **2** and one half molar equivalent of $\text{AgBAR}_4^{\text{F}}$ in dioxane. The product has the ^1H NMR resonance same as previous product, indicating approximately one half molar equivalent of $\text{AgBAR}_4^{\text{F}}$ had been used previously.



Scheme 2.9. Synthesis of bridging bis(NHC) dimethylpalladium complex **23**

Summary and Conclusion

Several stable *cis*-dimethyl palladium and cationic monomethyl palladium bis(NHC) complexes were synthesized. The stabilities of these methylpalladium complexes decreased with increasing ring size of the chelating bis(NHC). The stability of large chelate ring size bis(NHC)-containing cationic methylpalladium complexes can be increased by using the large, non-coordinating anion $\text{BAR}_4^{\text{F}-}$. A stable methylpalladium carbonyl intermediate with a bis(NHC) ligand was synthesized for the first time. This complex undergoes clean carbonylation to an acyl complex without any reductive elimination of imidazolium salts, modeling a necessary step in CO / alkene copolymerization. The rate of methyl migration is substantially lower than the most active bis(phosphine) complex. This study showed that methyl migration rate can be increased by increasing the chelate ring size. Therefore, a cationic methylpalladium

species with a larger chelating ring size bis(NHC), in combination with the $\text{BAr}_4^{\text{F}-}$ anion, is a potential pathway to create highly active catalysts for CO / alkene copolymerization.

Experimental

General Considerations. All manipulations were carried out under air unless otherwise noted. Diethyl ether (Acros), *n*-hexane (Acros), THF (Pharmco) and hexanes (Pharmco) were purified by distillation from sodium benzophenone ketyl. Dichloromethane (Pharmco) was washed with a sequence of concentrated H_2SO_4 , de-ionized water, 5% Na_2CO_3 and de-ionized water, followed by pre drying over anhydrous CaCl_2 , then refluxed over and distilled from P_2O_5 under nitrogen. Acetonitrile (Pharmco) was pre-dried over anhydrous CaCl_2 and refluxed over and distilled from CaH_2 under nitrogen. NMR solvents were purchased from Cambridge Isotopes Laboratories. $\text{DMSO}-d_6$ and $\text{CD}_3\text{CN}-d_3$ were dried over activated 4 Å molecular sieves followed by vacuum distillation at room temperature. CD_2Cl_2 was dried over activated 4 Å molecular sieves and stored over P_2O_5 before distillation at room temperature for use. All other reagents were purchased from Acros, Aldrich or Strem and used as received. $[\text{Pd}(\text{TMEDA})(\text{CH}_3)_2]$,³⁹ $[\text{Pd}(\text{bipy})(\text{CH}_3)_2]$,³⁹ 1,1'-dimesityl-3,3'-methylene-diimidazolium dibromide,¹² 1-(bromomethyl)-2,4,6-trimethylbenzene,⁴⁴ 1,1'- (1,2-phenylene)bis(imidazole),⁴⁵ $\text{AgBAr}_4^{\text{F}}$,⁴⁶ $\text{NaBAr}_4^{\text{F}}$,⁴⁷ $\text{H}(\text{Et}_2\text{O})_2\text{BAr}_4^{\text{F}}$,⁴⁷ 1,1'-dimesityl-3,3'-ethylene-diimidazolium dibromide,⁴⁸ and 1,1'-dimesityl-3,3'-propylene-diimidazolium dibromide⁴⁹ were prepared by literature procedures. NMR spectra were recorded on Varian GEMINI 2000 (300 MHz) and Varian Unity INOVA (400 and 600 MHz) spectrometers. Reported chemical shifts are referenced to residual solvent peaks (^{13}C ,

¹H). For low temperature studies, the NMR probe temperature was calibrated within 2 days of the experiment using a methanol standard. IR spectra were acquired from Nujol mulls on a Nicolet Protégé 460 FT-IR spectrometer. Elemental analyses were performed by Midwest Microlab, Indianapolis, Indiana. X-ray diffraction data were collected on a Bruker SMART APEX II diffractometer with a CCD detector using a combination of φ and ω scans. The crystal to detector distance was 6.0 cm. A Bruker Kryoflex liquid nitrogen cooling device was used for low-temperature data collections. Data integration employed the Bruker Apex2 software package.⁵⁰ Data collection employed SAINT.⁵¹ Multiscan absorption corrections were implemented using SADABS.⁵² All X-ray diffraction experiments employed graphite-monochromated Mo K α radiation ($\lambda=0.71073$ Å). Structures were solved by direct methods and refined by full-matrix least-squares on *F*² using the SHELXTL software suite.⁵³ Non-hydrogen atoms were assigned anisotropic temperature factors, with hydrogen atoms included in calculated positions (riding model).

Pd(1,1'-dimesityl-3,3'-methylenediimidazol-2,2'-diylidene)(CH₃)₂ (1)

To a solid mixture of 1,1'-dimesityl-3,3'-methylenediimidazolium dibromide (300 mg, 0.546 mmol) and potassium *tert*-butoxide (125 mg, 1.093 mmol) was added THF (40 mL) at -78 °C, and the mixture was stirred for 45 minutes at -78 °C to give a cloudy, light pink solution. This reaction mixture was transferred onto a solution of Pd(CH₃)₂(TMEDA) (138 mg, 0.546 mmol) in THF (15 mL) at -78 °C via cannula, and the resultant reaction mixture was stirred for another 45 minutes at -78 °C. The volatiles were removed under vacuum, the residue was extracted with methylene chloride, and diethyl ether was added to obtain colorless crystals, which were isolated by filtration.

Yield: 133 mg, 58.5 %. ^1H NMR (400 MHz, DMSO- d_6): δ 7.57 (2H, d, $^3J_{\text{HH}} = 2$ Hz, *imid.*), 7.04 (2H, d, $^3J_{\text{HH}} = 2$ Hz, *imid.*), 6.90 (4H, s, *m-CH* (mes.)), 6.19 (2H, s, CH_2), 2.51 (6H, s, *p-CH}_3*), 1.96 (12H, s, *o-CH}_3*), -1.11 (6H, s, Pd- CH_3). ^{13}C NMR (101.5 MHz, DMSO- d_6): δ 189.14 (carbene), 136.9 (*o-C*(mes.)), 136.83 (*p-C*(mes.)), 134.62 (*ipso-C*(mes.)), 128.12 (*m-C*(mes.)), 121.68 (*imid.-C*), 119.94 (*imid.-C*), 62.52 (CH_2), 20.59 (*p-CH}_3*(mes.)), 18.05 (*o-CH}_3*(mes.)), -5.38 (Pd- CH_3). Anal. Calculated for: $\text{C}_{27}\text{H}_{34}\text{N}_4\text{Pd}$: C, 62.24; H, 6.58; N, 10.76 %. Found: C, 62.16; H, 6.65; N, 10.57 %.

Pd(1,1'-dimesityl-3,3'-methylenediimidazol-2,2'-diylidene)(CH_3)(I) (2)

Methyl iodide (39 μg , 0.614 mmol) was added to a solution of Pd(1,1'-dimesityl-3,3'-methylenediimidazol-2,2'-diylidene)(CH_3) $_2$ (100 mg, 0.192 mmol) in THF (30 mL) at -78 $^\circ\text{C}$. The reaction mixture was warmed to 0 $^\circ\text{C}$ and stirred for one hour to give a bright white precipitate. The solid was isolated by filtration, followed by washing with diethyl ether. Yield: 87 mg, 71.9 %. ^1H NMR (400 MHz, DMSO- d_6): δ 7.80 (1H, s, *imid.*), 7.71 (1H, s, *imid.*), 7.35 (1H, s, *imid.*), 7.20 (1H, s, *imid.*), 6.98 (2H, s, *m-CH*(mes.)), 6.96 (2H, s, *m-CH*(mes.)), 6.40 (2H, s, CH_2), 2.27 (6H, s, *p-CH}_3*), 2.03 (6H, s, *o-CH}_3*), 2.03 (6H, bs, *o-CH}_3*), -0.54 (3H, s, Pd- CH_3). Anal. Calculated for: $\text{C}_{26}\text{H}_{31}\text{N}_4\text{IPd}$: C, 49.34; H, 4.94; N, 8.96 %. Found: C, 47.97; H, 4.77; N, 8.44 %.

[Pd (1,1'-dimesityl-3,3'-methylenediimidazol-2,2'-diylidene) (CH₃) (CH₃CN)] [BF₄]

(3)

AgBF₄ (31 mg, 0.158 mmol) was added a solution of Pd(1,1'-dimesityl-3,3'-methylene-diimidazol-2,2'-diylidene)(CH₃)(I) (100 mg, 0.158 mmol) in CH₃CN (10 mL) at 25 °C. The reaction mixture was stirred for one hour to give an ash brown precipitate. The precipitate was removed by filtration through celite, volatiles were stripped under vacuum, and the residue was dried for an additional 2 hours. The solid was redissolved in CH₃CN and filtered through celite to remove residual AgI. The solution was then concentrated, and diethyl ether was added to obtain white crystals, which were isolated by filtration. Yield: 74 mg, 74.0 %. ¹H NMR (400 MHz, CD₃CN-d₃): δ 7.53 (1H, d, ³J_{HH} = 2 Hz, *imid.*), 7.51 (1H, d, ³J_{HH} = 2 Hz, *imid.*), 7.05 (2H, s, *m-CH(mes.)*), 7.03 (1H, d, ³J_{HH} = 2 Hz, *imid.*), 7.02 (1H, d, ³J_{HH} = 2 Hz, *imid.*), 6.97 (2H, d, ³J_{HH} = 0.8 Hz, *m-CH(mes.)*), 6.19 (2H, s, CH₂), 2.32 (3H, s, *p-CH₃*), 2.29 (3H, s, *p-CH₃*), 2.04 (6H, s, *o-CH₃*), 1.97 (6H, s, *o-CH₃*), 1.95 (3H, s, CH₃CN), -0.65 (3H, s, Pd-CH₃). ¹H NMR (400 MHz, CD₂Cl₂-d₂): δ 7.75 (1H, d, ³J_{HH} = 2 Hz, *imid.*), 7.72 (1H, d, ³J_{HH} = 2 Hz, *imid.*), 7.01 (2H, s, *m-CH(mes.)*), 6.94 (2H, s, *m-CH(mes.)*), 6.86 (1H, d, ³J_{HH} = 2 Hz, *imid.*), 6.85 (1H, d, ³J_{HH} = 2 Hz, *imid.*), 6.40 (2H, bs, CH₂), 2.34 (3H, s, *p-CH₃*), 2.31 (3H, s, *p-CH₃*), 2.08 (6H, s, *o-CH₃*), 2.01 (6H, s, *o-CH₃*), 1.84 (3H, s, CH₃CN), -0.59 (3H, s, Pd-CH₃). ¹³C NMR (101.5 MHz, CD₃CN-d₃): δ 182.48 (carbene), 167.85 (carbene), 140.35 (*p-C(mes.)*), 140.16 (*p-C(mes.)*), 136.69 (*ipso-C(mes.)*), 136.42 (*ipso-C(mes.)*), 136.38 (*o-C(mes.)*), 135.89 (*o-C(mes.)*), 129.71 (*m-C(mes.)*), 129.62 (*m-C(mes.)*), 124.55 (*imid.-C*), 123.29 (*imid.-C*), 122.72 (*imid.-C*), 121.98 (*imid.-C*), 64.08 (CH₂), 27.02 (*p-CH₃*), 21.06 (*p-CH₃*), 18.83 (*o-CH₃*), 17.89 (*o-CH₃*), -8.26 (Pd-CH₃). ¹³C NMR (101.5

MHz, CD₂Cl₂-d₂): δ 182.04 (carbene), 167.31 (carbene) 139.49 (*p*-C(mes.)), 139.46 (*p*-C(mes.)), 135.93 (*ipso*-C(mes.)), 135.87 (*ipso*-C(mes.)), 135.84 (*o*-C(mes.)), 135.15 (*o*-C(mes.)), 129.11 (2 x *m*-C(mes.)), 123.64 (*imid.*-C), 122.37 (*imid.*-C), 122.31 (*imid.*-C), 121.73 (*imid.*-C), 120.64 (CN), 63.19 (CH₂), 21.10 (*p*-CH₃), 21.07 (*p*-CH₃), 18.76 (*o*-CH₃), 17.92 (*o*-CH₃), 3.26 (CNCH₃), -8.46 (Pd-CH₃). Anal. Calculated for: C₂₈H₃₄BF₄N₅Pd: C, 53.06; H, 5.41; N, 11.05 %. Found: C, 52.78; H, 5.33; N, 10.91 %.

[Pd (1,1'-dimesityl-3,3'-methylenediimidazol-2,2'-diylidene) (CH₃) (CO)] [BF₄] (4)

100 mg (0.158 mmol) of [Pd (1,1'-dimesityl-3,3'-methylenediimidazol-2,2'-diylidene) (CH₃) (CH₃CN)] [BF₄] was dissolved in 5 mL of CH₂Cl₂ in a sealable reaction vessel, and 1 atm of CO was admitted. The solution was stirred for 15 minutes, volatiles were removed, and the resulting solid was dried under vacuum overnight. The residue was dissolved in CH₂Cl₂, and the solution was filtered through celite. Diethyl ether and hexanes were added, forming white crystals that were collected by filtration. Yield: 75 mg, 76.9 %. ¹H NMR (400 MHz, CD₂Cl₂-d₂): δ 7.92 (1H, d, ³J_{HH} = 2 Hz, *imid.*), 7.90 (1H, d, ³J_{HH} = 2 Hz, *imid.*), 7.03 (2H, s, *m*-CH(mes.)), 7.03 (1H, d, ³J_{HH} = 2 Hz, *imid.*), 6.98 (1H, d, ³J_{HH} = 2 Hz, *imid.*), 6.96 (2H, s, *m*-CH(mes.)), 6.50 (2H, s, CH₂), 2.34 (3H, s, *p*-CH₃), 2.32 (3H, s, *p*-CH₃), 2.01 (6H, s, *o*-CH₃), 1.96 (6H, s, *o*-CH₃), -0.29 (3H, s, Pd-CH₃). ¹³C NMR (101.5 MHz, CD₂Cl₂-d₂): δ 183.01 (CO) 178.30 (carbene), 169.94 (carbene) 140.75 (*p*-C(mes.)), 140.05 (*p*-C(mes.)), 135.56 (*o*-C(mes.)), 135.38 (*ipso*-C(mes.)), 135.27 (*ipso*-C(mes.)), 135.02 (*o*-C(mes.)), 129.71 (*m*-C(mes.)), 129.40 (*m*-C(mes.)), 124.32 (*imid.*-C), 123.24 (*imid.*-C), 123.01 (*imid.*-C), 122.65 (*imid.*-C), 63.23 (CH₂), 21.16 (*p*-CH₃), 21.12 (*p*-CH₃), 18.50 (*o*-CH₃), 17.79 (*o*-CH₃), -13.16 (Pd-

CH₃). Anal. Calculated for: C₂₇H₃₁OBF₄N₄Pd: C, 52.24; H, 5.03; N, 9.03 %. Found: C, 52.29; H, 5.27; N, 8.88 %.

[Pd (1,1'-dimesityl-3,3'-methylenediimidazol-2,2'-diylidene) (CO) (C(O)CH₃)] [BF₄]
(5)

[Pd (1,1'-dimesityl-3,3'-methylenediimidazol-2,2'-diylidene) (CH₃) (CO)] [BF₄] (40 mg, 0.064 mmol) was dissolved in 2 mL of CH₂Cl₂ in a sealable vessel, and 1 atm of CO was admitted. The solution was stirred for 1 hour at 25 °C, and volatiles were removed under vacuum. The solid was slurried in hexanes and collected by filtration. Yield: 35 mg, 84.0 %. ¹H NMR analysis in CD₂Cl₂ showed product to be mixture of **5** (95%) and **4** (5%). NMR data were collected for a sample of this mixture placed under 1 atm CO, which resulted in quantitative conversion to **5** in solution. ¹H NMR (400 MHz, CD₂Cl₂-d₂): δ 7.94 (1H, d, ³J_{HH} = 2 Hz, *imid.*), 7.92 (1H, d, ³J_{HH} = 2 Hz, *imid.*), 7.05 (2H, s, *m-CH*(mes.)), 7.04 (1H, d, ³J_{HH} = 2 Hz, *imid.*), 6.98 (2H, s, *m-CH*(mes.)), 6.91 (1H, d, ³J_{HH} = 2 Hz, *imid.*), 6.55 (2H, s, CH₂), 2.35 (3H, s, *p-CH*₃), 2.32 (3H, s, *p-CH*₃), 1.99 (6H, s, *o-CH*₃), 1.94 (6H, s, *o-CH*₃), 1.29 (3H, s, C(O)CH₃). ¹³C NMR (101.5 MHz, CD₂Cl₂-d₂): δ 234.52 (C(O)CH₃) 178.07 (carbene), 168.16 (carbene) 140.92 (*p-C*(mes.)), 140.83 (*p-C*(mes.)), 135.68 (*o-C*(mes.)), 135.48 (*o-C*(mes.)), 135.06 (*ipso-C*(mes.)), 134.63 (*ipso-C*(mes.)), 129.80 (*m-C*(mes.)), 129.77 (*m-C*(mes.)), 123.66 (2 x *imid.-C*), 123.44 (*imid.-C*), 123.20 (*imid.-C*), 63.07 (CH₂), 44.30 (C(O)CH₃), 21.17 (*p-CH*₃), 21.11 (*p-CH*₃), 18.20 (*o-CH*₃), 17.84 (*o-CH*₃).

Pd(1,1'-dimesityl-3,3'-ethylenediimidazol-2,2'-diylidene)(CH₃)₂ (6)

To a solid mixture of 1,1'-dimesityl-3,3'-ethylenediimidazolium dibromide (250 mg, 0.446 mmol) and potassium *tert*-butoxide (100 mg, 0.892 mmol) was added THF (40 mL) at -78 °C, and the mixture was stirred for 3 hours at -78 °C to give a cloudy, light pink solution. This reaction mixture was transferred onto a solution of Pd(CH₃)₂(TMEDA) (113 mg, 0.446 mmol) in THF (15 mL) at -78 °C via cannula, and the resultant reaction mixture was stirred for another 3 hours at -78 °C. The volatiles were removed under vacuum, and the residue was extracted with THF. Diethyl ether and hexanes were added to obtain colorless crystals, which were isolated by filtration. Yield: 184 mg, 75 %. ¹H NMR (400 MHz, DMSO-d₆): δ 7.36 (2H, d, ³J_{HH} = 1.6 Hz, *imid.*), 6.97 (2H, d, ³J_{HH} = 1.6 Hz, *imid.*), 6.81 (4H, s, *m*-CH(*mes.*)), 5.80-4.20 (4H, bs, CH₂), 2.20 (6H, s, *p*-CH₃), 1.85 (12H, s, *o*-CH₃), -1.15 (6H, s, Pd-CH₃). ¹³C NMR (101.53 MHz, DMSO-d₆): δ 189.72 (carbene), 137.31 (*o*-C(*mes.*)), 136.64 (*p*-C(*mes.*)), 135.14 (*ipso*-C(*mes.*)), 128.03 (*m*-C(*mes.*)), 122.63 (*imid.*-C), 120.75 (*imid.*-C), 48.55 (CH₂), 20.56 (*p*-CH₃(*mes.*)), 18.60 (*o*-CH₃(*mes.*)), -4.65 (Pd-CH₃).

Pd(1,1'-dimesityl-3,3'-propylenediimidazol-2,2'-diylidene)(CH₃)₂ (7)

To a solid mixture of 1,1'-dimesityl-3,3'-propylenediimidazolium dibromide (400 mg, 0.696 mmol) and potassium *tert*-butoxide (156 mg, 1.393 mmol) was added THF (40 mL) at -78 °C, and the mixture was stirred for 4 hours at -78 °C to give a cloudy, light pink solution. This reaction mixture was transferred onto a solution of Pd(CH₃)₂(TMEDA) (176 mg, 0.696 mmol) in THF (15 mL) at -78 °C via cannula, and the resultant reaction mixture was stirred for another 3 hours at -78 °C. The volatiles were

removed under vacuum, and the residue was extracted with THF. Diethyl ether and hexanes were added to obtain colorless crystals, which were isolated by filtration. Yield: 174 mg, 47.7 %. ^1H NMR (400 MHz, DMSO- d_6): δ 7.34 (2H, d, $^3J_{\text{HH}} = 1.6$ Hz, *imid.*), 7.01 (2H, d, $^3J_{\text{HH}} = 1.6$ Hz, *imid.*), 6.82 (4H, s, *m-CH(mes.)*), 4.12 (4H, t, $^3J_{\text{HH}} = 6.2$ Hz, *CH*₂), 2.85 (2H, t, $^3J_{\text{HH}} = 6.2$ Hz, *CH*₂), 2.24 (6H, s, *p-CH*₃), 1.85 (12H, s, *o-CH*₃), -1.18 (6H, s, Pd-*CH*₃).

Pd(1,1'-dimesityl-3,3'-ethylenediimidazol-2,2'-diylidene)(CH₃)(I) (8)

Methyl iodide (39 μg , 0.614 mmol) was added to a solution of Pd(1,1'-dimesityl-3,3'-ethylenediimidazol-2,2'-diylidene)(CH₃)₂ (100 mg, 0.192 mmol) in THF (30 mL) at -78 °C. The reaction mixture was warmed to 0 °C and stirred for one hour to give a bright white precipitate. The solid was isolated by filtration, followed by washing with diethyl ether. Yield: 87 mg, 71.9 %. ^1H NMR (400 MHz, DMSO- d_6): δ 7.75 (1H, bs, *imid.*), 7.58 (1H, s, *imid.*), 7.39 (2H, bs, *imid.*), 6.96 (4H, sb, *m-CH(mes.)*), 5.70 (1H, bs, *CH*₂), 5.02 (1H, bs, *CH*₂), 4.69 (1H, bs, *CH*₂), 4.54 (1H, bs, *CH*₂), 2.64 (6H, s, *mes-CH*₃), 1.98 (6H, broad unresolved peak, *mes-CH*₃), 1.75 (3H, bs, *mes-CH*₃), 1.63 (3H, bs, *mes-CH*₃), -0.55 (3H, s, Pd-*CH*₃).

[Pd (1,1'-dimesityl-3,3'-ethylenediimidazol-2,2'-diylidene) (CH₃) (CH₃CN)] [BF₄] (10)

Cooled CH₃CN (10 mL) at -35 °C was added to AgBF₄ (31 mg, 0.158 mmol) and Pd(1,1'-dimesityl-3,3'-ethylenediimidazol-2,2'-diylidene)(CH₃)(I) (100 mg, 0.158 mmol) in a flask under inert atmosphere. The reaction mixture was stirred for one hour at

– 35 °C to give an ash brown precipitate. The precipitate was removed by filtration through celite, ~ 2-3 mL of diethyl ether was added to precipitate AgI, and the mixture was again filtered through celite to remove residual AgI. The solution was then concentrated, cooled diethyl ether at – 35 °C was added, and the solution was kept in the glove box freezer to obtain white crystals, which were isolated by filtration. Yield: 59 mg, 58 %. ¹H NMR (400 MHz, CD₃CN-d₃): δ 7.74 (1H, d, ³J_{HH} = 1.6 Hz, *imid.*), 7.54 (1H, d, ³J_{HH} = 1.6 Hz, *imid.*), 7.37 (1H, d, ³J_{HH} = 1.6 Hz, *imid.*), 7.34 (1H, s, *imid.*), 6.93-6.89 (4H, b, *m-CH(mes.)*), 5.69 (1H, b s, *CH*₂), 4.97 (1H, b s, *CH*₂), 4.71 (1H, b s, *CH*₂), 4.94 (1H, b s, *CH*₂), 2.24 (3H, s, *mes-CH*₃), 2.22 (3H, s, *mes-CH*₃), 1.96 (3H, s, *mes-CH*₃), 1.94 (3H, s, *mes-CH*₃), 1.84 (3H, s, *mes-CH*₃), 1.55 (3H, s, *p-CH*₃), -0.59 (3H, s, Pd-*CH*₃).

[Pd (1,1'-dimesityl-3,3'-ethylenediimidazol-2,2'-diylidene) (CO) (COCH₃)] [BF₄]

(12a) crude product

[(DIMEs^{Et})Pd(CH₃)(CH₃CN)][BF₄] was dissolved in CD₂Cl₂ in a J-Young NMR tube, and the solution was cooled to – 84 °C using an ethyl acetate slush bath. CO (1 atm) was added to the NMR tube while the liquid was held at -84 °C. The solution temperature was increased to room temperature, solvents were evaporated under vacuum, and the residue was dried for one hour. CD₂Cl₂ distilled into NMR tube and the crude product ¹H NMR spectrum was recorded. ¹H NMR (400 MHz, CD₂Cl₂-d₂): δ 7.65 (1H, d, ³J_{HH} = 2.4 Hz, *imid.*), 7.36 (1H, d, ³J_{HH} = 2.8 Hz, *imid.*), 7.09 (1H, d, ³J_{HH} = 2.4 Hz, *imid.*), 7.02 (2H, s, *m-CH(mes.)*), 6.96 (2H, s, *m-CH(mes.)*), 6.92 (1H, d, ³J_{HH} = 2.8 Hz, *imid.*),

4.68 (4H,t, $^3J_{\text{HH}} = 6.4$ Hz, CH_2), 2.35 (3H, s, *mes-CH*₃), 2.33 (3H, s, *mes-CH*₃), 2.04 (3H, s, *mes-CH*₃), 1.98 (3H, s, *mes-CH*₃), 1.78 (6H, s, *mes-CH*₃), 1.64 (3H, s, *acyl-CH*₃).

**[Pd (1,1'-dimesityl-3,3'-ethylenediimidazol-2,2'-diylidene) (CH₃) (CH₃CN)] [BAr^F₄]
(13)**

AgBAr^F₄ (75 mg, 0.077 mmol) was added to a solution of Pd(1,1'-dimesityl-3,3'-methylenediimidazolin-2,2'-diylidene)(CH₃)(I) (50 mg, 0.077 mmol) in CH₃CN (10 mL) at 25 °C. The reaction mixture was stirred for one hour to give an ash brown precipitate. The precipitate was removed by filtration through celite, volatiles were stripped under vacuum, and the residue was dried for an additional 2 hours. Solid was redissolved in CH₃CN, and the solution was filtered through celite to remove residual AgI. The solution was then concentrated, and diethyl ether was added to obtain white crystals, which were isolated by filtration. Yield: 48 mg, 44 %. ¹H NMR (400 MHz, CD₃CN-d₃): δ 7.72 (8H, s, *o*-H(BAr^F₄)), 7.66 (4H, s, *p*-H(BAr^F₄)), 7.42 (1H, d, $^3J_{\text{HH}} = 2.4$ Hz, *imid.*), 7.20 (1H, d, $^3J_{\text{HH}} = 2.8$ Hz, *imid.*), 7.03 (1H, d, $^3J_{\text{HH}} = 2.8$ Hz, *imid.*), 6.99 (1H, d, $^3J_{\text{HH}} = 2.4$ Hz, *imid.*), 6.96 (4H, bs, *m-CH*(*mes.*)), 5.91 (1H, bt, CH_2), 4.54-4.20 (3H, bm, CH_2), 2.29 (3H, s, *mes-CH*₃), 2.26 (3H, s, *mes-CH*₃), 2.17 (3H, bs, *mes-CH*₃), 2.07 (3H, bs, *mes-CH*₃), 1.82 (3H, bs, *mes-CH*₃), 1.58 (3H, bs, *p-CH*₃), -0.41 (3H, bs, Pd- CH_3).

[Ag₂ (DIMes^{Pr}) Br₂] (14)

DIMes^{Pr} Br₂ (500 mg, 0.871 mmol) and Ag₂O (202 mg, 0.871 mmol) were suspended in 80 mL of acetonitrile. The reaction mixture was stirred for 20 hours at room temperature under exclusion of light. The solution was then filtered through celite

and concentrated. Addition of hexanes produced white crystals, which were isolated by filtration. Yield: 612 mg, 89.2 %. ^1H NMR (400 MHz, $\text{CD}_2\text{Cl}_2-d_2$): δ 7.64(2H, bs, *imid.*), 6.97 (2H, bs, *imid.*), 6.94 (4H, s, *m-CH(mes.)*), 4.44 (4H, t, $^3J_{\text{HH}} = 10.2$ Hz, CH_2), 2.63 (2H, p, $^3J_{\text{HH}} = 10.2$ Hz, CH_2), 2.37 (6H, s, *p-CH}_3*), 1.86 (12H, s, *o-CH}_3*). ^1H NMR (400 MHz, $\text{DMSO}-d_6$): δ 7.76 (2H, s, *imid.*), 7.49 (2H, s, *imid.*), 6.99 (4H, s, *m-CH(mes.)*), 4.29 (4H, t, $^3J_{\text{HH}} = 8.8$ Hz, CH_2), 2.42 (2H, bp, CH_2), 2.35 (6H, s, *p-CH}_3*), 1.72 (12H, s, *o-CH}_3*).

[Ag₂ (DIMes^{Bu}) Cl₂] (15a)

DIMes^{Bu} Cl₂ (300 mg, 0.600 mmol) and Ag₂O (139 mg, 0.600 mmol) was suspended in 60 mL of acetonitrile. The reaction mixture was stirred for 20 hours at room temperature under exclusion of light. Then solution was filtered through celite and concentrated. Addition of hexanes produced white crystals, which were isolated by filtration. Yield: 343 mg, 80 %. ^1H NMR (400 MHz, $\text{DMSO}-d_6$): δ 7.72 (2H, s, *imid.*), 7.48 (2H, s, *imid.*), 7.05 (4H, s, *m-CH(mes.)*), 4.21 (4H, s, CH_2), 2.33 (6H, s, *p-CH}_3*), 1.90-1.78(16H, m, overlapping CH_2 (4H) and *o-CH}_3* (12H)).

[Ag₂ (DIMes^{Bu}) Br₂] (15b)

DIMes^{Bu} Br₂ (300 mg, 0.51 mmol) and Ag₂O (118 mg, 0.51 mmol) were suspended in 60 mL of acetonitrile. The reaction mixture was stirred for 18 hours at room temperature under exclusion of light. The solution was then filtered through celite and concentrated. Addition of hexanes produced white crystals, which were isolated by filtration. Yield: 335 mg, 81.9 %. ^1H NMR (400 MHz, $\text{DMSO}-d_6$): δ 7.71 (2H, s, *imid.*), 7.45 (2H, s, *imid.*), 7.02 (4H, s, *m-CH(mes.)*), 4.20 (4H, s, CH_2), 2.35 (6H, s, *p-CH}_3*), 1.79

(4H, s, CH_2), 1.74 (12H, $o-CH_3$). ^{13}C NMR (101.53 MHz, DMSO- d_6): δ 180.11 (carbene), 138.48 ($o-C$ (mes.)), 135.47 ($p-C$ (mes.)), 134.25 ($ipso-C$ (mes.)), 128.85 ($m-C$ (mes.)), 123.29 ($imid.-C$), 122.29 ($imid.-C$), 50.21 (N- CH_2), 28.10 (N- CH_2), 20.56 ($p-CH_3$ (mes.)), 17.10 ($o-CH_3$ (mes.)).

[Pd (DIMes^{Bu}) Cl₂] (16)

Ag₂(DIMesBu)Cl₂ (300 mg, 0.419 mmol) and PdCl₂ (111 mg, 0.419 mmol) were suspended in 80 mL of dichloromethane. The reaction mixture was stirred for 24 hours at room temperature under exclusion of light. The solution was then filtered through celite and concentrated. Layering diethyl ether onto the solution produced yellow crystals, which were isolated by filtration. Yield: 97 mg, 38.3 %. 1H NMR (400 MHz, DMSO- d_6): δ 7.01 (2H, d, $^3J_{HH} = 2$ Hz, $imid.$), 6.88 (4H, s, $m-CH$ (mes.)), 6.72 (2H, d, $^3J_{HH} = 2$ Hz, $imid.$), 4.74 (4H, t, CH_2), 2.48 (6H, s, $p-CH_3$), 2.42 (4H, m, CH_2), 1.90 (12H, $o-CH_3$).

(1,1'-Bis(2,4,6-trimethylbenzyl)-3,3'-(1,2-phenylene)diimidazolium dibromide (17)

A mixture of 1,1'-(1,2-phenylene)bis(imidazole) (500mg, 2.38 mmol) and 1-(bromomethyl)-2,4,6-trimethylbenzene (558 mg, 2.62 mmol) was suspended in toluene (25 mL), and the mixture was heated at 100 °C for 24 hours. Solids were collected by filtration and washed with THF. Isolated product was recrystallized using CH₂Cl₂ as solvent, and the solid was dried in vacuum for 12 h. Yield: 890 mg, 75 %. 1H NMR (400 MHz, DMSO- d_6): δ 9.19 (2H, s, $imid.$), 7.89 (4H, s, $imid.$) 7.78 (2H, d, $^3J_{HH} = 1.6$ Hz, $ph.$), 7.76 (2H, d, $^3J_{HH} = 1.6$ Hz, $ph.$), 6.98 (4H, s, $m-CH$ (mes.)), 5.40 (4H, s, CH_2), 2.27 (6H, s, $p-CH_3$), 2.22 (12H, $o-CH_3$). ^{13}C NMR (101.53 MHz, DMSO- d_6): 138.74 ($Ar-C$),

138.23 (*Ar-C*), 137.39 (*Ar-C*), 131.92 (*Ar-C*), 129.92 (*Ar-C*), 129.36 (*Ar-C*), 128.35 (*Ar-C*), 126.03 (*Ar-C*), 123.65 (*imid.-C*), 122.82 (*imid.-C*), 47.59 (*N-CH₂*), 20.56 (*p-CH₃(mes.)*), 19.39 (*o-CH₃(mes.)*). Anal. Calculated for: C₃₂H₃₆Br₂N₄: C, 60.39; H, 5.70; N, 8.81 %. Found: C, 57.92; H, 5.76; N, 8.57 %.

1,1'-Bis(2,4,6-trimethylbenzyl)-3,3'-(1,2-phenylene)diimidazol-2,2'-diylidene (18)

One molar equiv of **17** (300 mg, 0.471 mmol) and two molar equiv of K⁺O⁻tBu (106 mg, 0.943 mmol) were placed in a round bottom flask fitted to a swivel frit. THF was distilled into the flask at -78 °C, and the mixture was stirred at the same temperature for 4 hours. It was then allowed to warm up to room temperature, which resulted in a cloudy yellow solution. The reaction mixture was filtered to remove KBr byproduct, volatiles were stripped under vacuum, and the residue was dried for an additional two hours. The solid was extracted with hexanes, and the extract was concentrated. The concentrated solution was kept at -35°C for a couple of days to produce yellow crystals, which were isolated by filtration. Yield: 94 mg, 42 %. ¹H NMR (400 MHz, THF-d₆): δ 7.44 (1H, d, ³J_{HH} = 1.2 Hz, *imid.*), δ 7.17 (1H, d, ³J_{HH} = 1.2 Hz, *imid.*), 6.91-6.73(5H, m, overlapping *mes.*(2H) and *ph*(3H)), 6.42 (1H, t, ³J_{HH} = 8.0 Hz, *ph.*), 6.26 (2H, s, *m-CH(mes.)*), 6.23 (1H, d, ³J_{HH} = 2.4 Hz, *imid.*), 5.40 (1H, d, ³J_{HH} = 2.8 Hz, *imid.*), 5.24-4.69 (2H, AB, *CH₂*), 3.77-3.43 (2H, AB, *CH₂*), 2.41 (6H, s, *p-CH₃*), 2.25 (6H, s, *o-CH₃*), 1.90 (6H, s, *o-CH₃*).

(1,1'-Bis(2,4,6-trimethylbenzyl)-3,3'-(1,2-phenylene)diimidazol-2,2'-diylidene) Pd Br₂ (20)

A mixture of Pd(OAc)₂ (176mg, 0.786 mmol) and (1,1'-bis(2,4,6-trimethylbenzyl)-3,3'-(1,2-phenylene)diimidazolium dibromide (500 mg, 0.786 mmol) was dissolved in DMSO (10 mL) and heated at 50 °C for 2 hours, followed by heating at 110 °C for 3 hours. CH₂Cl₂ was added to the reaction mixture to obtain pale yellow crystals. The product was isolated by filtration and dried in vacuo for 12 h. Yield: 303 mg, 52 %. ¹H NMR (400 MHz, DMSO-*d*₆): δ 7.88-7.86 (2H, m, *ph.*), 7.79-7.71 (2H, m, *ph.*), 7.71 (2H, s, *imid.*), 7.00 (4H, s, *m-CH(mes.)*), 6.53 (2H, s, *imid.*), 6.05-5.41 (4H, AB pattern, *CH*₂), 2.27 (6H, s, *p-CH*₃), 2.23 (12H, *o-CH*₃). Anal. Calculated for: C₃₂H₃₄Br₂N₄Pd: C, 51.06; H, 4.63; N, 7.56 %. Found: C, 51.06; H, 4.55; N, 7.22 %.

[Pd (1,1'-bis(2,4,6-trimethylbenzyl)-3,3'-(1,2-phenylene)diimidazol-2,2'-diylidene) (CH₃CN)₂][BF₄]₂ (21)

A mixture of (1,1'-bis(2,4,6-trimethylbenzyl)-3,3'-(1,2-phenylene)diimidazolium dibromide (150 mg, 0.202 mmol), AgBF₄ (79 mg, 0.404 mmol), and anhydrous acetonitrile (15 mL) was placed in a sealed ampule under nitrogen. The reaction mixture was heated at 60 °C for 4h with stirring. The mixture was then filtered through celite, the solvent was removed under vacuum, and the residue was dried in vacuum for 3 h. The product was again dissolved in acetonitrile (5 mL), the solution was filtered through celite, solvent was evaporated, and the residue was dried in vacuum for 3 h. This sequence was repeated one more time. In the final sequence, diethyl ether was added to the filtrate to obtain product as white crystals. Product was isolated by filtration and dried

in vacuo for 12 h. Yield: 139 mg, 82%. ^1H NMR (400 MHz, DMSO- d_6): δ 7.95-7.91(4H, m, overlapping *imid.*(2H) and *ph*(2H)), 7.88-7.85 (2H, m, *ph.*), 7.03 (4H, s, *m-CH*(mes.)), 6.89 (2H, d, $^3J_{\text{HH}} = 2$ Hz, *imid.*), 5.68-5.24 (4H, AB, CH_2), 2.28 (6H, s, *p-CH}_3*), 2.08 (12H, s, *o-CH}_3*). ^{13}C NMR (101.53 MHz, CD_2Cl_2 - d_2): δ 147.48 (carbene), 140.60 (*Ar-C*), 138.41 (*Ar-C*), 131.58 (*Ar-C*), 131.35 (*Ar-C*), 130.31 (*Ar-C*), 127.48 (*Ar-C*), 125.70 (*Ar-C*), 124.86 (*imid.-C*), 122.95 (*imid.-C*), 49.94 (N- CH_2), 21.17 (*p-CH}_3*(mes.)), 19.92 (*o-CH}_3*(mes.)), 3.47(CH_3CN).

$[\text{Pd}_2(\mu^2\text{-DIMes}^{\text{Me}})_2(\text{I})(\text{CH}_3)_2][\text{BAr}^{\text{F}}_4]$ (23)

$\text{AgBAr}^{\text{F}}_4$ (77 mg, 0.079 mmol) was added to a solution of $\text{Pd}(1,1'\text{-dimesityl-3,3'-methylene-diimidazol-2,2'-diylidene})(\text{CH}_3)(\text{I})$ (100 mg, 0.158 mmol) in dioxane (10 mL) at 25 °C. The reaction mixture was stirred for 4 hours to give an ash brown precipitate. The precipitate was removed by filtration through celite, volatiles were stripped under vacuum, and the residue was dried for an additional 2 hours. Solid was dissolved in Et_2O and filtered through celite to remove residual AgI. The solution was then concentrated, hexanes was added, and the solution was kept at -35 °C for a couple of days to obtain pale yellow crystals, which were isolated by filtration. Yield: 84 mg, 54%. ^1H NMR (400 MHz, CD_2Cl_2 - d_2): δ 7.72 (8H, s, *o-H*(BAr^{F}_4)), 7.56 (4H, s, *p-H*(BAr^{F}_4)), 7.37(2H, d, $^3J_{\text{HH}} = 2$ Hz, *imid.*), 6.84 (2H, d, $^3J_{\text{HH}} = 2$ Hz, *imid.*), 6.79 (2H, s, *m-CH*(mes.)), 6.73 (2H, s, *m-CH*(mes.)), 8.03-6.03 (2H, AB, CH_2), 2.43 (6H, s, *p-CH}_3*), 1.79 (6H, s, *o-CH}_3*), 1.77 (6H, s, *o-CH}_3*), -1.16 (3H, s, Pd- CH_3). ^1H NMR (400 MHz, C_6D_6 - d_6): δ 8.41 (8H, s, *o-H*(BAr^{F}_4)), 7.67 (4H, s, *p-H*(BAr^{F}_4)), 6.61 (2H, s, *m-CH*(mes.)), 6.53 (2H, s, *m-CH*(mes.)), 6.24(2H, d, $^3J_{\text{HH}} = 2.4$ Hz, *imid.*), 5.83 (2H, d, $^3J_{\text{HH}} = 2.8$ Hz, *imid.*), 7.96-4.91 (2H, AB,

CH₂), 2.23 (6H, s, *p*-CH₃), 1.75 (6H, s, *o*-CH₃), 1.68 (6H, s, *o*-CH₃), 0.24 (3H, s, Pd-CH₃).

References

- (1) Herrmann, W. A. *Angewandte Chemie-International Edition* **2002**, *41*, 1290.
- (2) Peris, E.; Crabtree, R. H. *Coord. Chem. Rev.* **2004**, *248*, 2239.
- (3) Green, J. C.; Scurr, R. G.; Arnold, P. L.; Cloke, F. G. N. *Chemical Communications* **1997**, 1963.
- (4) Hahn, F. E. *Angewandte Chemie-International Edition* **2006**, *45*, 1348.
- (5) Scott, N. M.; Nolan, S. P. *European Journal of Inorganic Chemistry* **2005**, 1815.
- (6) Huang, J. K.; Stevens, E. D.; Nolan, S. P.; Petersen, J. L. *J. Am. Chem. Soc.* **1999**, *121*, 2674.
- (7) Diez-Gonzalez, S.; Nolan, S. P. *Coord. Chem. Rev.* **2007**, *251*, 874.
- (8) Hillier, A. C.; Grasa, G. A.; Viciu, M. S.; Lee, H. M.; Yang, C. L.; Nolan, S. P. *Journal of Organometallic Chemistry* **2002**, *653*, 69.
- (9) Ozdemir, I.; Demir, S.; Sahin, O.; Buyukgungor, O.; Cetinkaya, B. *Journal of Organometallic Chemistry* **2010**, *695*, 1555.
- (10) Stewart, I. C.; Benitez, D.; O'Leary, D. J.; Tkatchouk, E.; Day, M. W.; Goddard, W. A.; Grubbs, R. H. *J. Am. Chem. Soc.* **2009**, *131*, 1931.
- (11) Buscemi, G.; Biffis, A.; Tubaro, C.; Basato, M.; Graiff, C.; Tiripicchio, A. *Applied Organometallic Chemistry* **2010**, *24*, 285.

- (12) Gardiner, M. G.; Herrmann, W. A.; Reisinger, C. P.; Schwarz, J.; Spiegler, M. *Journal of Organometallic Chemistry* **1999**, 572, 239.
- (13) Bianchini, C.; Meli, A. *Coord. Chem. Rev.* **2002**, 225, 35.
- (14) Drent, E.; Budzelaar, P. H. M. *Chem. Rev.* **1996**, 96, 663.
- (15) Sen, A. *Accounts Chem. Res.* **1993**, 26, 303.
- (16) Pascu, S. I. *Rev. Roum. Chim.* **2009**, 54, 477.
- (17) Cavinato, G.; Toniolo, L.; Vavasori, A. In *Catalytic Carbonylation Reactions*; Springer-Verlag Berlin: Berlin, 2006; Vol. 18, p 125.
- (18) Drent, E.; Vanbroekhoven, J. A. M.; Doyle, M. J. *Journal of Organometallic Chemistry* **1991**, 417, 235.
- (19) McGuinness, D. S.; Saendig, N.; Yates, B. F.; Cavell, K. J. *J. Am. Chem. Soc.* **2001**, 123, 4029.
- (20) Tsoureas, N.; Danopoulos, A. A.; Tulloch, A. A. D.; Light, M. E. *Organometallics* **2003**, 22, 4750.
- (21) Chen, J. C. C.; Lin, I. J. B. *Organometallics* **2000**, 19, 5113.
- (22) McGuinness, D. S.; Green, M. J.; Cavell, K. J.; Skelton, B. W.; White, A. H. *Journal of Organometallic Chemistry* **1998**, 565, 165.
- (23) McGuinness, D. S.; Cavell, K. J. *Organometallics* **2000**, 19, 4918.
- (24) Mata, J. A.; Poyatos, M.; Peris, E. *Coord. Chem. Rev.* **2007**, 251, 841.
- (25) Pugh, D.; Danopoulos, A. A. *Coord. Chem. Rev.* **2007**, 251, 610.
- (26) Magill, A. M.; McGuinness, D. S.; Cavell, K. J.; Britovsek, G. J. P.; Gibson, V. C.; White, A. J. P.; Williams, D. J.; White, A. H.; Skelton, B. W. *Journal of Organometallic Chemistry* **2001**, 617, 546.

- (27) Nielsen, D. J.; Magill, A. M.; Yates, B. F.; Cavell, K. J.; Skelton, B. W.; White, A. H. *Chemical Communications* **2002**, 2500.
- (28) Nielsen, D. J.; Cavell, K. J.; Skelton, B. W.; White, A. H. *Inorg. Chim. Acta* **2006**, 359, 1855.
- (29) Danopoulos, A. A.; Tsoureas, N.; Macgregor, S. A.; Smith, C. *Organometallics* **2007**, 26, 253.
- (30) Douthwaite, R. E.; Green, M. L. H.; Silcock, P. J.; Gomes, P. T. *Journal of the Chemical Society-Dalton Transactions* **2002**, 1386.
- (31) Rix, F. C.; Brookhart, M.; White, P. S. *J. Am. Chem. Soc.* **1996**, 118, 4746.
- (32) Rix, F. C.; Brookhart, M. *J. Am. Chem. Soc.* **1995**, 117, 1137.
- (33) Rulke, R. E.; Delis, J. G. P.; Groot, A. M.; Elsevier, C. J.; vanLeeuwen, P.; Vrieze, K.; Goubitz, K.; Schenk, H. *Journal of Organometallic Chemistry* **1996**, 508, 109.
- (34) Dekker, G.; Elsevier, C. J.; Vrieze, K.; Vanleeuwen, P. *Organometallics* **1992**, 11, 1598.
- (35) Mul, W. P.; Oosterbeek, H.; Beitel, G. A.; Kramer, G. J.; Drent, E. *Angewandte Chemie-International Edition* **2000**, 39, 1848.
- (36) Toth, I.; Elsevier, C. J. *J. Am. Chem. Soc.* **1993**, 115, 10388.
- (37) Shultz, C. S.; Ledford, J.; DeSimone, J. M.; Brookhart, M. *J. Am. Chem. Soc.* **2000**, 122, 6351.
- (38) Ledford, J.; Shultz, C. S.; Gates, D. P.; White, P. S.; DeSimone, J. M.; Brookhart, M. *Organometallics* **2001**, 20, 5266.

- (39) Degraaf, W.; Boersma, J.; Smeets, W. J. J.; Spek, A. L.; Vankoten, G.
Organometallics **1989**, *8*, 2907.
- (40) Douthwaite, R. E.; Green, M. L. H.; Silcock, P. J.; Gomes, P. T. *Journal of the Chemical Society-Dalton Transactions* **2002**, 1386.
- (41) Chapter 3, complex **3a**
- (42) Bryndza, W. A. *Organometallics* **1985**, *4*, 1686.
- (43) Ahrens, S.; Zeller, A.; Taige, M.; Strassner, T. *Organometallics* **2006**, *25*, 5409.
- (44) Niehues, M.; Kehr, G.; Erker, G.; Wibbeling, B.; Frohlich, R.; Blacque, O.; Berke, H. *Journal of Organometallic Chemistry* **2002**, *663*, 192.
- (45) So, Y. H. *Macromolecules* **1992**, *25*, 516.
- (46) Miller, K. J.; Kitagawa, T. T.; Abu-Omar, M. M. *Organometallics* **2001**, *20*, 4403.
- (47) Brookhart, M.; Grant, B.; Volpe, A. F. *Organometallics* **1992**, *11*, 3920.
- (48) Lee, H. M.; Lu, C. Y.; Chen, C. Y.; Chen, W. L.; Lin, H. C.; Chiu, P. L.; Cheng, P. Y. *Tetrahedron* **2004**, *60*, 5807.
- (49) Song, L. C.; Luo, X.; Wang, Y. Z.; Gai, B.; Hu, Q. M. *Journal of Organometallic Chemistry* **2009**, *694*, 103.
- (50) APEX2, (2006) Bruker AXS, Madison, WI, USA.
- (51) SAINT, (2001) Bruker AXS, Madison, WI, USA.
- (52) Sheldrick, G. M. SADABS, (2000) Bruker AXS Inc., Madison, WI, USA.
- (53) Sheldrick, G. M. SHELXTL, (2000) Bruker AXS Inc., Madison, WI, USA.

CHAPTER III

SYNTHESIS AND CHARACTERIZATION OF DICATIONIC BIS(METHYLISOCYANIDE) ADDUCTS OF PALLADIUM(II) BIS(CARBENE) AND BIS(PHOSPHINE) COMPLEXES

Introduction

Since the isolation and characterization of the free first N-heterocyclic carbenes (NHCs) by Arduengo et al. in 1991,^{1,2} NHCs have become widely used ligands in transition metal catalyzed reactions such as cross-coupling reactions,³⁻¹⁵ olefin metathesis,¹⁶⁻²⁷ hydrosilylation,^{28,29} hydroformylation,³⁰ hydroamination³¹ and C-H activation.³²⁻³⁴ Initially it was believed that NHCs are electronic mimics and alternatives to phosphines.^{35,36} There is increasing experimental evidence that NHCs are superior to phosphine counterparts in both catalytic activity and scope.³⁷⁻³⁹ NHCs have several advantages over phosphines, such as reduced need for excess ligand in catalytic reactions due to the stronger metal-NHC bonding. They also have improved air and moisture stability, because of the tendency for the phosphine to oxidize in air, whereas NHCs are oxidation resistance. The superior activity of NHCs in catalysis arises from the combination of strong σ -donor, poor π -acceptor, and unique steric properties of NHCs.⁴⁰ The stronger σ -donation from NHCs to metal than from phosphines was supported by calorimetric studies,⁴¹ CO stretching frequencies⁴²⁻⁴⁴ and theoretical pK_a values.⁴⁵ The stretching frequency of CO (ν CO) in various transition metal-carbonyl complexes is the most widely used method for comparing the electronic properties of NHC and phosphine ligands. Initially, this method used the average infrared frequency of CO in Ni(CO)₃L complexes, known as the Tolman electronic parameter (TEP) as developed by Tolman.⁴⁶ This electronic parameter has been used to quantify the electron donor ability of phosphines and more recently has been used to study the electronic properties of NHCs using different metal complexes such as Ni(CO)₃(NHC),⁴² Rh(CO)₂X(NHC),^{47,48} Ir(CO)₂X(NHC) (X = halide),^{47,48} Fe(Cp)(CO)₂L⁴⁹ and M(CO)₅L (M = Cr, Mo, W).⁵⁰

Almost all of these IR frequency studies focused on the monodentate NHCs, and several these studies indicate a narrow range of donor ability in the commonly used NHCs.^{42,49,51} Changing the N-substituent⁴² or backbone saturation⁴⁵ has very little effect on variation of donor ability, but there are a few examples of NHCs with tunable donicity such as Bertand's borazine-derived NHCs⁵² and NHCs bearing electron withdrawing aryl groups.⁵³ Another way to tune the donicity is to use chelating bis(NHCs), where the donicity can be altered by variation of bite angle via changing chelating ring size. Another advantage of chelating bis(NHCs) is that they are expected to be more stable than monodentate NHCs because of the chelate effect.⁵⁴ In the current study, various alkane-bridged chelating bis(NHC) ligands were prepared to assess their donicity as a function of different structural parameters. Chelating bis(NHCs) offer a way to study the effects of ligand anisotropy on the reactivity of NHC-metal complexes.

Another similar type of carbenes, acyclic diaminocarbenes (ADCs), have electronic stabilization similar to that of NHCs.^{46,55,56} However, the increased reactivity of the free carbenes^{57,58} has limited the development of their coordination chemistry.^{50,59,60} There are a few reports suggesting that ADCs are stronger donors than the corresponding NHCs.⁴⁵ ADC donicity can be easily tunable compare to NHCs.⁶¹ In past few years, ADCs have been used as ligands in several metal-catalyzed reactions, in some cases with activities comparable to those of NHCs.⁶²⁻⁶⁵

Comparisons of σ -donicity of bis(NHCs) with bis(ADCs) and the more commonly used bis(phosphine) ligands will give an understanding of how changing the bite angle (via chelate ring size) will affect the donicity within the homologous ligand series and between different ligand series with the same ring size. Even though CO is the

most widely used ligand in IR probe studies, this method has the disadvantage of not separating σ -donor and π -acceptor effects. Isoelectronic alkyl isocyanides are stronger σ -donor and weaker π -acceptor ligands than CO.⁶⁶ Therefore, replacing CO with isoelectronic methyl isocyanide will provide a more useful assessment of relative σ -donor strength of ligands *trans* to it. Upon binding to a metal complex in a higher oxidation state ($\geq +2$), the stretching frequency of methyl isocyanide ($\nu \text{C}\equiv\text{N}$) will increase compared to the stretching frequency of free methyl isocyanide ($\nu \text{C}\equiv\text{N}$) due to electron donation from the weakly σ^* HOMO (antibonding orbital) to the metal center, with no significant contribution from metal-to-ligand π -backbonding. A larger change in $\Delta\nu$ (change in stretching frequency compared to free isocyanide) indicates stronger σ -donation from methyl isocyanide, arising from a lower *trans* influence and thus lower σ -donation from the ligand bound *trans* to methyl isocyanide. One study based on methyl isocyanide as a *trans* IR probe ligand in palladium(II) complexes,⁶⁷ shows that that common bis(phosphine) DPPE is a stronger σ -donor than a common bis(NHC) derived from mesityl imidazole, which contradicts previous studies identifying NHCs as stronger donors than phosphines. However, it is not clear how much this reflects on the intrinsic donicity of the ligands, as these ligands have different chelate ring size.

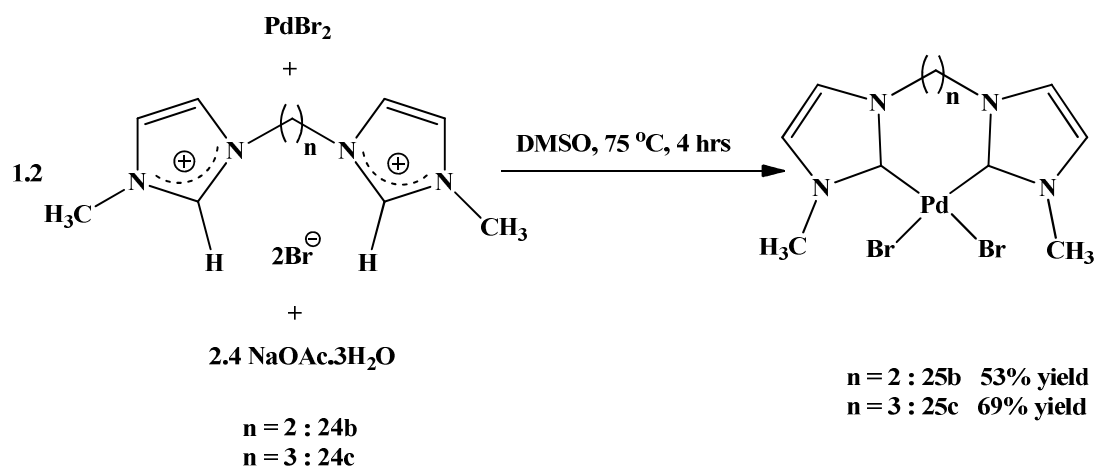
In the current investigation, the σ -donicities of several bis(NHC), bis(phosphine) and bis(ADC) ligands were investigated using methyl isocyanide as an IR probe ligand in cationic (chelate) $\text{Pd}(\text{CNCH}_3)_2^{2+}$ complexes. Comparison of donicity was performed by attaching various chelating ring size bis(NHC), bis(phosphine) and bis(ADC) ligands to cationic bis(methyl isocyanide) palladium(II) complexes.

Results and Discussion

Synthesis and characterization of imidazole-based bis(NHC) palladium(II) dihalide complexes (**25a-25d**)

Bis(imidazolium) salts with different alkane linkage lengths connecting two N-methyl imidazole rings, specifically 1,1'-dimethyl-3,3'-methylene-diimidazolium dibromide, 1,1'-dimethyl-3,3'-ethylene-diimidazolium dibromide, 1,1'-dimethyl-3,3'-propylene-diimidazolium dibromide and 1,1'-dimethyl-3,3'-butylene-diimidazolium dichloride were synthesized according to procedures published by Herrmann et al.,⁶⁸ Lee et al.,⁶⁹ Vitz et al.,⁷⁰ and Ahrens et al.⁵⁴ Methylene and butylene linked imidazole derived bis(NHC) palladium complexes, (1,1'-dimethyl-3,3'-methylenediimidazol-2,2-diylidene) palladium(II) dibromide (**25a**) and (1,1'-dimethyl-3,3'-butylenediimidazol-2,2-diylidene) palladium(II) dichloride (**25d**), were synthesized using the corresponding bis imidazolium salts according to procedures published by Herrmann et al.,⁷¹ and Ahrens et al.⁵⁴ Attempted syntheses of ethylene (**25b**) and propylene (**25c**) linked bis-imidazole derived bis(NHC) palladium dibromide complexes using procedures for similar complexes^{54,70,72} failed or did not provide significant yields. Screening of different palladium sources and bases revealed that palladium (II) bromide together with sodium acetate trihydrate and bis-imidazolium salt in wet dimethyl sulfoxide produced the expected results. Wet dimethyl sulfoxide was important for the reaction. When dry dimethyl sulfoxide was used for the reaction, it did not show any progress. Water in wet dimethyl sulfoxide may facilitate the interaction of the sodium acetate base with other reactants by bringing it into the solution phase.

The synthesis begins by treating one molar equivalent of palladium (II) bromide with 1.2 molar equivalents of 1,1'-dimethyl-3,3'-ethylene-diimidazolium dibromide (**24c**) or 1,1'-dimethyl-3,3'-propylene-diimidazolium dibromide (**24d**) and 2.4 molar equivalents of sodium acetate trihydrate in a thick walled glass vessel in wet dimethyl sulfoxide. The reaction mixture, which is bright orange in color, was stirred at 75 °C for three hours using a constant temperature oil bath. After completion of the reaction, which is indicated by significant lightening of color, solvent volume was reduced under vacuum. Deionized water was added to the remaining reaction mixture to increase solid formation. Products were isolated by filtration and were washed with deionized water to remove unreacted bis-imidazolium salts and sodium acetate. The light yellow ethylene linked (**25b**) and light green propylene linked (**2c**) bis(NHC) palladium dibromide complexes were isolated and dried under vacuum.



Scheme 3.1. Formation of bis(NHC) palladium (II) dibromide complexes **25b** and **25c**.

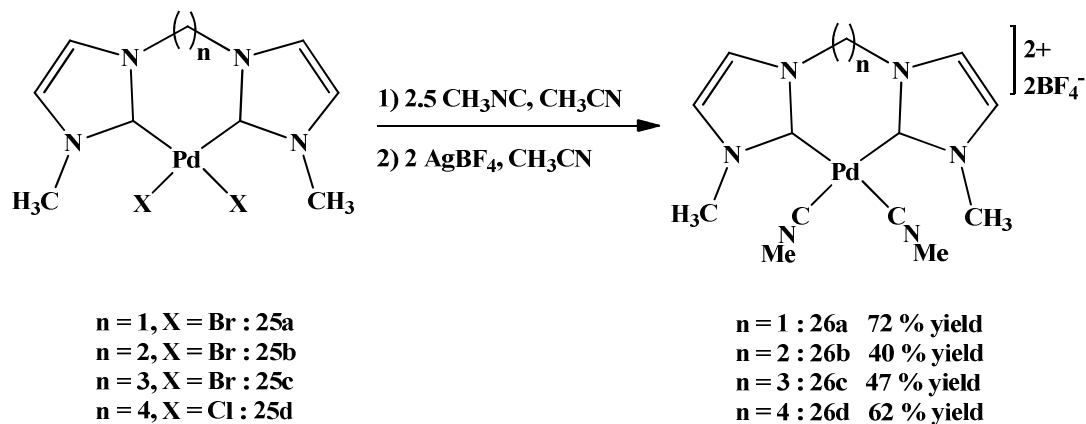
According to the ^1H NMR spectrum of the ethylene linked complex (**25b**) in DMSO-d_6 , two singlets were observed for imidazole protons at 7.35 ppm and 7.29 ppm.

The ethylene protons appeared as two sets of peaks with a 1:1 integration ratio at 5.20 ppm as a broad singlet and at 4.49 ppm as a broad doublet. Two N-methyl groups appeared at 3.86 ppm as a singlet. The ^1H NMR spectrum of the propylene linked complex (**25c**) also showed two singlets for imidazole protons at 7.33 ppm and 7.27 ppm. The propylene protons appeared as four sets of peaks at 4.84 ppm (triplet), 4.37-4.32 ppm (doublet of doublets), 2.34-2.30 ppm (multiplet) and 1.78-1.68 ppm (multiplet) with a 2:2:1:1 integration ratio. The N-methyl protons appeared as a singlet slightly more downfield than the ethylene analogue **25b** at 3.91 ppm.

Synthesis and characterization of imidazole derived bis(NHC) bis(methylisocyanide) palladium(II) tetrafluoroborate complexes (26a-26d)

A general synthetic procedure was adopted to synthesize a series of bis(NHC) bis(methylisocyanide) palladium (II) complexes with different linkage sizes. Two and a half molar equivalents of methylisocyanide was added to a suspension of bis(NHC) palladium dihalide in dry acetonitrile. The reaction mixture was stirred for two hours, during which time the reaction mixture became clear. Then two molar equivalents of silver tetrafluoroborate in dry acetonitrile was added to the reaction mixture to replace the outer sphere chloride anion with tetrafluoroborate anion. After addition of silver tetrafluoroborate, silver halide immediately started to precipitate, and the mixture was stirred for two hours to complete the precipitation. The resultant reaction mixture was filtered through celite to remove silver salts. The solvent was removed from the filtrate under vacuum and dried under vacuum for two hours. The resultant solid was redissolved in acetonitrile and filtered through celite, then stripped of solvent and dried under

vacuum. This sequence was repeated one more time. This sequence is very important to remove all the silver salts present in the product. Finally, white crystalline products were isolated by layering ether on the solution in acetonitrile.

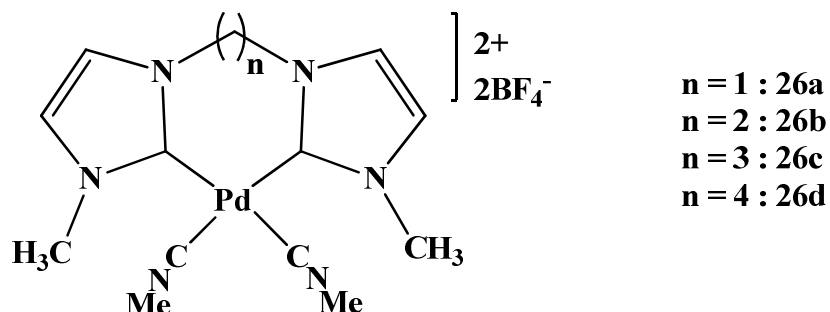


Scheme 3.2. Formation of bis(NHC) bis(methylisocyanide) palladium (II) complexes **26a-26d**.

These complexes were synthesized in yields ranging between 40 – 72 %. All of the bis(NHC) bis(methylisocyanide) palladium complexes **26a-26d** were stable under air at room temperature. These complexes were soluble in acetonitrile and dimethyl sulfoxide and partially soluble in chlorinated solvents. Table 3.1 summarizes the ^1H NMR data for bis(NHC) bis(methylisocyanide) palladium complexes **26a-26d**. All of these complexes show two sets of doublets for the imidazole protons between 7.16 – 7.77 ppm. Average chemical shifts values for imidazole protons shift upfield from the methylene linkage complex **26a** to propylene linkage complex **26c**, but these values decreases slightly from the propylene linkage complex **26c** to the butylene linkage complex **26d**. Linkage protons were also observed, the methylene in **26a** as a broad

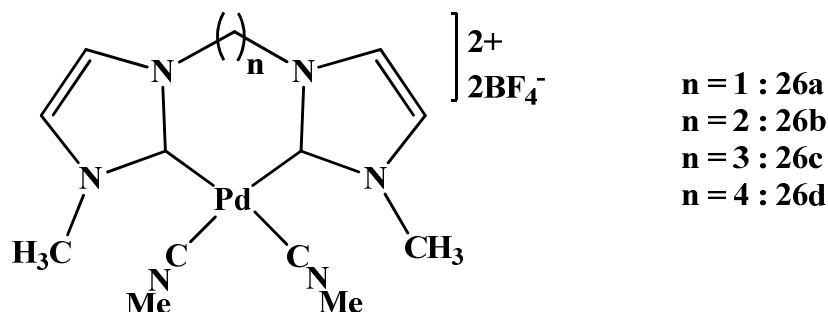
singlet, the ethylene in **26b** as two multiplets, the propylene in **26c** as four sets of multiplets, and the butylene in **26d** as four sets of broad singlets, with chemical shifts ranging from 1.52 – 6.35 ppm. These indicate alkylene linkages in the chelating rings were rigid in solution. The methyl protons of the two methyl isocyanides show one singlet around 3.8 ppm, but the imidazole methyl proton chemical shifts move upfield from the methylene linkage complex to the butylene linkage complex, with values changing from 3.71 to 3.44 ppm.

Table 3.1. ^1H NMR spectral data for bis(NHC) bis(methylisocyanide) palladium(II) complexes (chemical shifts in ppm).



Complex	Imidazole <i>H</i>	Linkage CH_2	$\text{C}\equiv\text{N}-\text{CH}_3$	$\text{N}-\text{CH}_3$
3a (n=1)	7.74(d, 2H, $^3J_{\text{HH}} = 2$ Hz)	6.35(bs, 2H)	3.86(s, 6H)	3.71(s, 6H)
	7.57(d, 2H, $^3J_{\text{HH}} = 2$ Hz)			
3b (n=2)	7.27(d, 2H, $^3J_{\text{HH}} = 2$ Hz)	4.95-4.87(m, 2H)	3.78(s, 6H)	3.50(s, 6H)
	7.22(d, 2H, $^3J_{\text{HH}} = 2$ Hz)	4.54-4.46(m, 2H)		
3c (n=3)	7.20(d, 2H, $^3J_{\text{HH}} = 2$ Hz)	4.61-4.55(m, 2H)	3.82(s, 6H)	3.46(s, 6H)
	7.16(d, 2H, $^3J_{\text{HH}} = 2$ Hz)	4.38-4.33(m, 2H)		
		2.33-2.26(m, 1H)		
		1.98-1.88(m, 1H)		
3d (n=4)	7.24(d, 2H, $^3J_{\text{HH}} = 2$ Hz)	4.50(br s, 2H)	3.82(s, 6H)	3.44(s, 6H)
		4.21(br s, 2H)		
		2.01(br s, 2H)		
		1.52(br s, 2H)		

Table 3.2. ^{13}C NMR spectral data for bis(NHC) bis(methylisocyanide) palladium(II) complexes (chemical shifts in ppm).



Complex	Carbene	Imidazole C	Linkage CH_2	N- CH_3	$\text{C}\equiv\text{N}-\text{CH}_3$
3a (n=1)	155.56	124.07	62.38	38.24	30.40
		123.02			
3b (n=2)	153.96	125.77	48.18	39.28	30.99
		125.04			
3c (n=3)	155.74	125.69	52.99	38.82	30.89
		125.45			
3d (n=4)	154.64	126.66	47.12	38.87	30.96
		123.97			

The ^{13}C NMR chemical shift values in acetonitrile- d_3 for complexes **26a** – **26d** are given in Table 3.2. All of these complexes showed only one signal for the carbene carbons in each complex, indicating symmetric molecules, and these values range from 154 to 156 ppm. The imidazole carbons showed two distinct carbon signals in the range of 123 – 127 ppm. Methyl carbons of methyl isocyanide appeared between 30 – 31 ppm,

but no signals were observed for isocyanide carbons. N-methyl carbons of imidazole showed only one singlet for each complex, with values ranging from 37 to 39 ppm. One carbon signal each was observed for the methylene carbon of complex **26a** and the ethylene carbons of complex **26b**, and two carbon signals were observed for the propylene carbons of complex **26c** and the butylene carbons of complex **26d**. Both ^1H NMR and ^{13}C NMR data indicate two-fold symmetric molecules in solution.

Crystals of complexes **3a-3d** were grown by the slow diffusion of diethyl ether into acetonitrile solutions of the complexes. These crystals grew as colorless blocks. X-ray crystal structures display C_s , C_1 , C_s and C_1 symmetry respectively in complexes **26a**, **26b**, **26c** and **26d**. One molecule of acetonitrile (solvent) was found in the unit cell of complex **26a** only. Complex **26a** crystals formed in the orthorhombic $P 2_1 2_1 2_1$ space group. The other three complexes did not show any solvent molecules in the crystal structure. Complexes **26b** and **26c** crystallize in the triclinic $P\bar{1}$ space group and complex **26d** in the monoclinic $P2_1/c$ space group. Bond lengths from the carbene carbon atoms C(1) and C(2) to adjacent nitrogen atoms N(1), N(2), N(3) and N(4) were similar, ranging from 1.341 – 1.354 Å in all complexes. These values are larger than the average value for Csp^2 -N double bond distances (1.28 Å)⁷³ due to aromatic delocalization in the imidazole rings. The N-C_{carbene}-N bond angles in the imidazole rings for complexes **26a-26d** were within the range of 105.47-106.14°, which is comparable to known Pd-NHC complexes.⁵⁴ Pd-C_{carbene} bond lengths range from 1.9947 to 2.022 Å, which is slightly longer than those in reported bis(NHC) palladium dihalide complexes.⁵⁴ The isocyanide N≡C bonds were consistent with triple bonds, falling in the range of 1.131-1.141 Å.⁶⁷ The summation of bond angles around the palladium centres for complexes **26a-26d** was

around 360° , indicating square planar geometry around the palladium centres. The $C_{\text{carbene}}\text{-Pd-}C_{\text{carbene}}$ angles (bite angles) increase with increasing chelating ring size except for complex **26b**. The $C_{\text{carbene}}\text{-Pd-}C_{\text{carbene}}$ angles were 84.03° , 83.90° and 85.26° for complexes **26a**, **26b**, and **26c**, respectively, which is less than the ideal bond angle of 90° in square planar complexes. However for complex **26d**, the $C_{\text{carbene}}\text{-Pd-}C_{\text{carbene}}$ bond angle was 89.80° , which is very close to the ideal bond angle of 90° in square planar complexes. This may be due to the increase in the chelating ring size from 6 to 9 for complexes **26a-26d**. The $C_{\text{isocyanide}}\text{-Pd-}C_{\text{isocyanide}}$ angles for complexes **26a-26c** ($91\text{-}92^\circ$) did not change much, but for complex **26d** it decreased to 88.79° . The increases in chelating ring size made the plane of the imidazole rings in a ligand become less V-shaped and flip away from the square plane of the complex. This structural variation can be measured as dihedral angle. The lowest dihedral angle was observed for complex **26a** (42.3°) and the value increases with increasing chelate ring size. However, the value for complex **26d** (79.6°) decreases slightly from the value for complex **26c** (80.7°), even though complex **26d** has the largest chelate ring (Figure 3.5). Complex **26a** showed the largest distances between the imidazole ring nitrogens, N1-N4 and N2-N4, and this distance decreases with increase in chelating ring size. The alkylene linkages in complexes **26b-26c** were slightly twisted to accommodate the larger ring sizes. These structural changes indicate growing steric demand with larger ring size (Figures 3.1-3.4 and Tables 3.3-3.10).

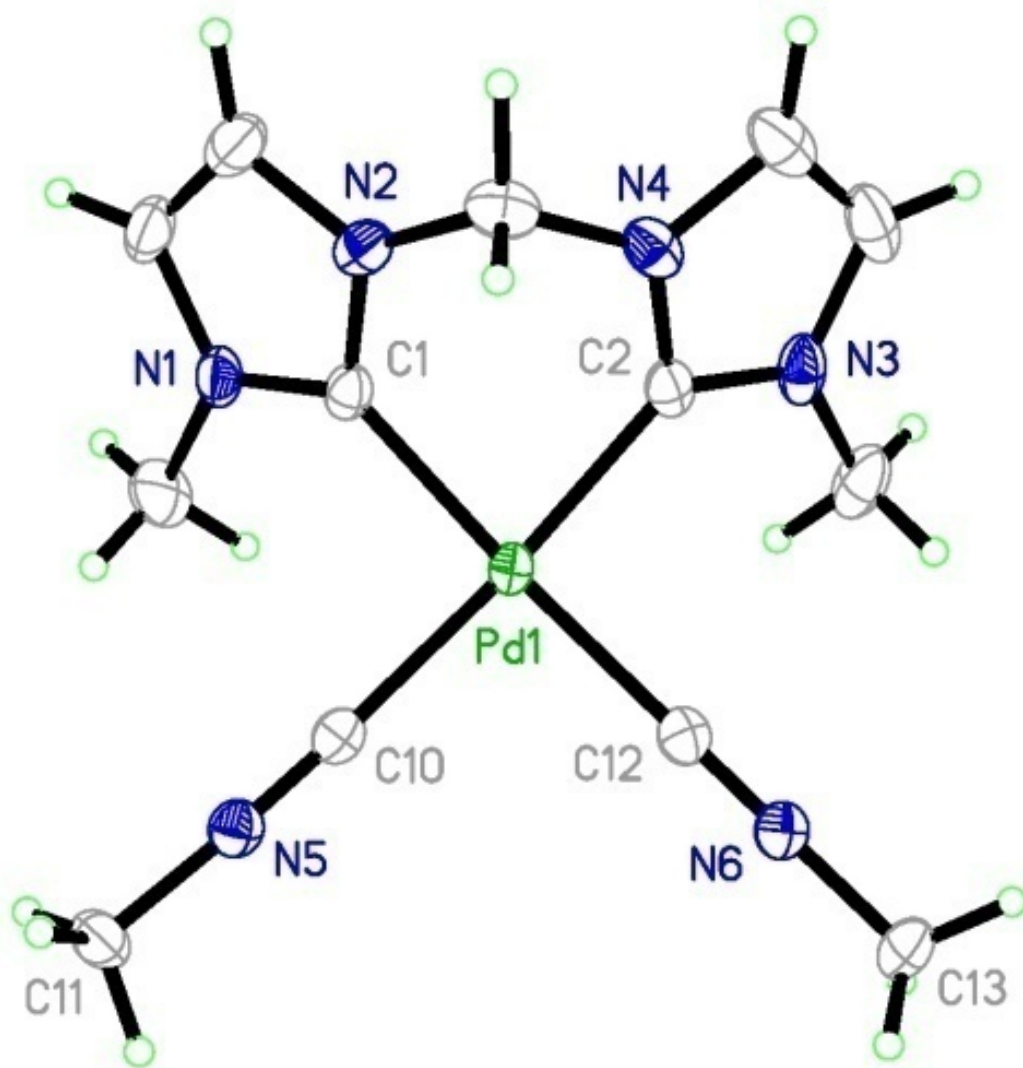


Figure 3.1. Molecular structure of complex **26a** with 50% probability ellipsoids. Tetrafluoroborate counter ions and acetonitrile solvent molecule are omitted for clarity.

Table 3.3. Selected bond lengths (Å) and bond angles (°) of complex **26a**

	Bond Lengths (Å)
Pd(1)-C(1)	2.0075(18)
Pd(1)-C(2)	2.0083(19)
Pd(1)-C(10)	2.002(2)
P(1)-C(12)	2.0102(19)
C(1)-N(1)	1.344(2)
C(1)-N(2)	1.348(2)
C(2)-N(3)	1.341(3)
C(2)-N(4)	1.345(3)
C(10)-N(5)	1.139(3)
C(12)-N(6)	1.138(2)
	Bond angles (°)
C(1)-Pd(1)-C(2)	84.03(8)
C(10)-Pd(1)-C(12)	91.89(8)
C(1)-Pd(1)-C(10)	91.49(7)
C(2)-Pd(1)-C(12)	92.56(8)
C(1)-Pd(1)-C(12)	176.59(8)
C(2)-Pd(1)-C(10)	173.36(8)
N(1)-C(1)-N(2)	105.47(16)
N(3)-C(2)-N(4)	105.52(17)

Table 3.4. Crystal data and structure refinement details for complex **26a**

Empirical formula	C ₁₅ H ₂₁ B ₂ F ₈ N ₇ Pd
Formula weight	579.41
Crystal system	Orthorhombic
Space group	P2 ₁ 2 ₁ 2 ₁
Unit cell dimensions	a = 11.08150(10) Å α = 90 ° b = 12.33220(10) Å β = 90 ° c = 16.5078 (2) Å γ = 90 °
Volume	2255.94(4) Å ³
Z	4
Density (calculated)	1.706 Mg/m ³
Absorption coefficient	0.906 mm ⁻¹
Crystal size	0.22 x 0.20 x 0.18 mm
θ range for data collection	2.06 – 29.12 °
Index range	-15 ≤ h ≤ 15 -16 ≤ k ≤ 16 -19 ≤ l ≤ 22
Temperature	115(2) K
Wave length	0.71073 Å
Reflections collected	28542
Independent reflections	5954 (R _{int} = 0.0279)
Final R indices [I > 2σ(I)]	R1 = 0.0205 wR2 = 0.0481
R indices (all data)	R1 = 0.0219 wR2 = 0.0487
Goodness-of-fit on F ²	1.040

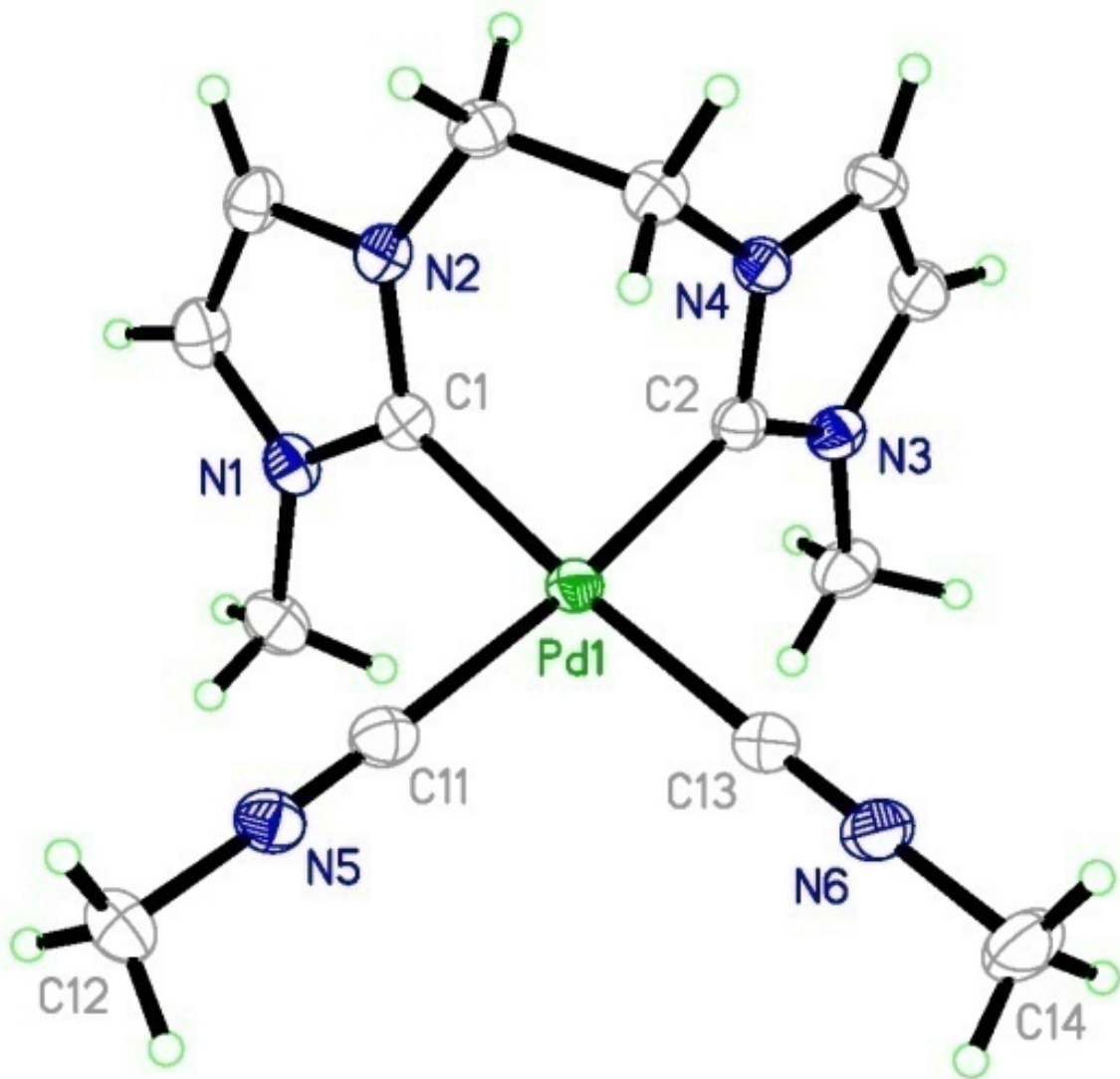


Figure 3.2. Molecular structure of complex **26b** with 50% probability ellipsoids.

Tetrafluoroborate counter ions are omitted for clarity.

Table 3.5. Selected bond lengths (Å) and bond angles (°) of complex **26b**

	Bond Lengths (Å)
Pd(1)-C(1)	2.0107(16)
Pd(1)-C(2)	1.9947(16)
Pd(1)-C(11)	2.0149(18)
P(1)-C(13)	2.0101(18)
C(1)-N(1)	1.347(2)
C(1)-N(2)	1.354(2)
C(2)-N(3)	1.339(2)
C(2)-N(4)	1.345(2)
C(11)-N(5)	1.137(2)
C(13)-N(6)	1.133(2)
	Bond angles (°)
C(1)-Pd(1)-C(2)	83.90(6)
C(11)-Pd(1)-C(13)	91.69(7)
C(1)-Pd(1)-C(11)	91.80(7)
C(2)-Pd(1)-C(13)	92.43(7)
C(1)-Pd(1)-C(13)	175.63(8)
C(2)-Pd(1)-C(11)	174.15(6)
N(1)-C(1)-N(2)	105.71(14)
N(3)-C(2)-N(4)	106.14(14)

Table 3.6. Crystal data and structure refinement details for complex **26b**

Empirical formula	C ₁₄ H ₂₀ B ₂ F ₈ N ₆ Pd
Formula weight	552.38
Crystal system	Triclinic
Space group	P $\bar{1}$
Unit cell dimensions	a = 10.2044(1) Å α = 95.467(1) ° b = 10.3560(1) Å β = 113.629 ° c = 12.0415(2) Å γ = 110.055(1) °
Volume	1054.33(3) Å ³
Z	2
Density (calculated)	1.740 Mg/m ³
Absorption coefficient	0.963 mm ⁻¹
Crystal size	0.38 x 0.38 x 0.13 mm
θ range for data collection	1.92 – 28.28 °
Index range	-13 ≤ h ≤ 13 -13 ≤ k ≤ 13 -15 ≤ l ≤ 16
Temperature	150(2) K
Wave length	0.71073 Å
Reflections collected	22255
Independent reflections	5201 (R _{int} = 0.0250)
Final R indices [I > 2σ(I)]	R1 = 0.0222 wR2 = 0.0579
R indices (all data)	R1 = 0.0233 wR2 = 0.0586
Goodness-of-fit on F ²	1.049

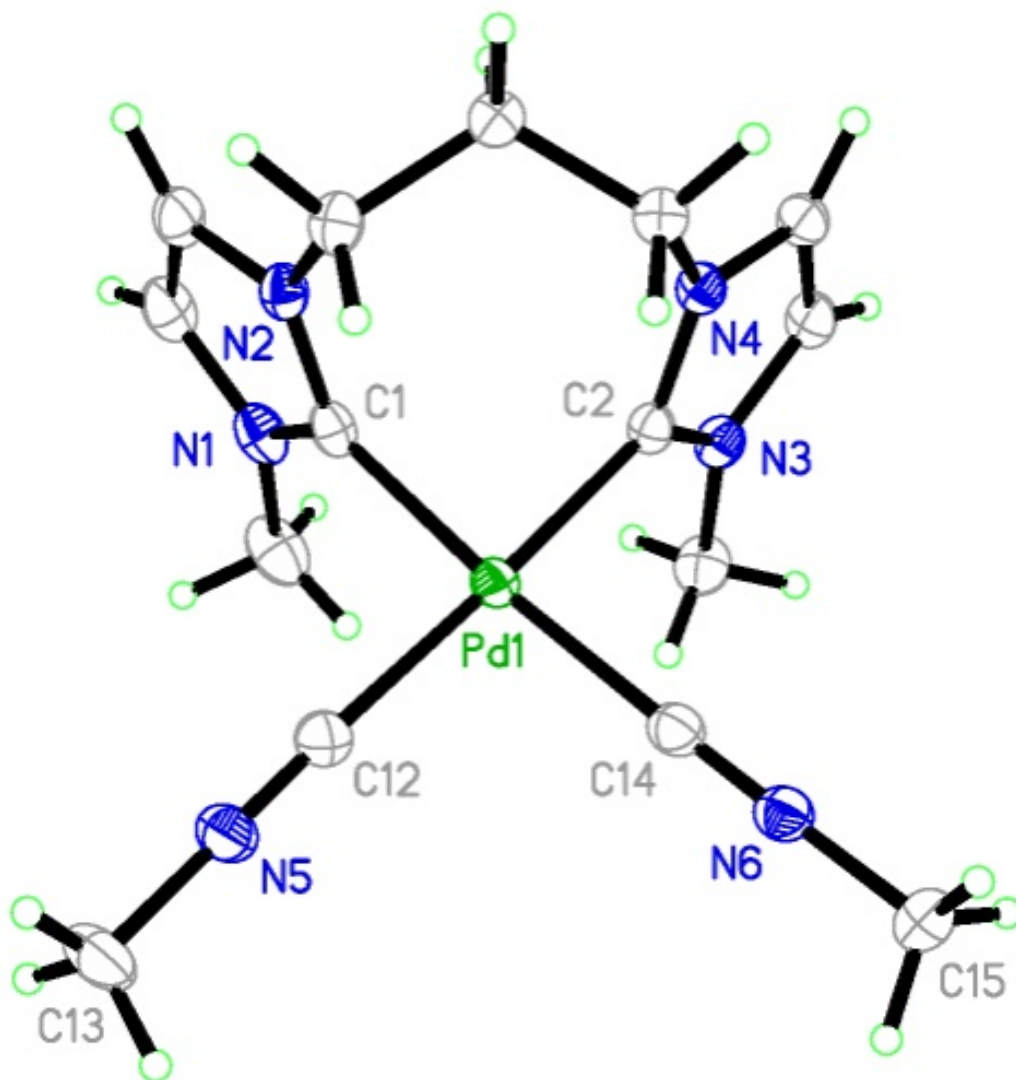


Figure 3.3. Molecular structure of complex **26c** with 50% probability ellipsoids.

Tetrafluoroborate counter ions are omitted for clarity.

Table 3.7. Selected bond lengths (Å) and bond angles (°) of complex **26c**

	Bond Lengths (Å)
Pd(1)-C(1)	2.0117(15)
Pd(1)-C(2)	2.0073(14)
Pd(1)-C(12)	2.0111(16)
P(1)-C(14)	2.0077(16)
C(1)-N(1)	1.3450(19)
C(1)-N(2)	1.345(2)
C(2)-N(3)	1.3438(18)
C(2)-N(4)	1.3469(19)
C(12)-N(5)	1.135(2)
C(14)-N(6)	1.141(2)
	Bond angles (°)
C(1)-Pd(1)-C(2)	85.26(6)
C(12)-Pd(1)-C(14)	91.26(6)
C(1)-Pd(1)-C(12)	92.65(6)
C(2)-Pd(1)-C(12)	90.81(6)
C(1)-Pd(1)-C(14)	175.78(6)
C(2)-Pd(1)-C(12)	177.84(6)
N(1)-C(1)-N(2)	105.53(13)
N(3)-C(2)-N(4)	106.11(12)

Table 3.8. Crystal data and structure refinement details for complex **26c**

Empirical formula	C ₁₅ H ₂₂ B ₂ F ₈ N ₆ Pd
Formula weight	566.41
Crystal system	Triclinic
Space group	P $\bar{1}$
Unit cell dimensions	a = 10.6194(1) Å α = 110.535 ° b = 10.8662(1) Å β = 95.983(1) ° c = 11.6646(2) Å γ = 114.757 °
Volume	1093.58(3) Å ³
Z	2
Density (calculated)	1.720 Mg/m ³
Absorption coefficient	0.931 mm ⁻¹
Crystal size	0.32 x 0.27 x 0.25 mm
θ range for data collection	1.95 – 29.57 °
Index range	-14 ≤ h ≤ 14 -14 ≤ k ≤ 15 -16 ≤ l ≤ 26
Temperature	115(2) K
Wave length	0.71073 Å
Reflections collected	28899
Independent reflections	6082 (R _{int} = 0.0251)
Final R indices [I > 2σ(I)]	R1 = 0.0222 wR2 = 0.0557
R indices (all data)	R1 = 0.0233 wR2 = 0.0563
Goodness-of-fit on F ²	1.053

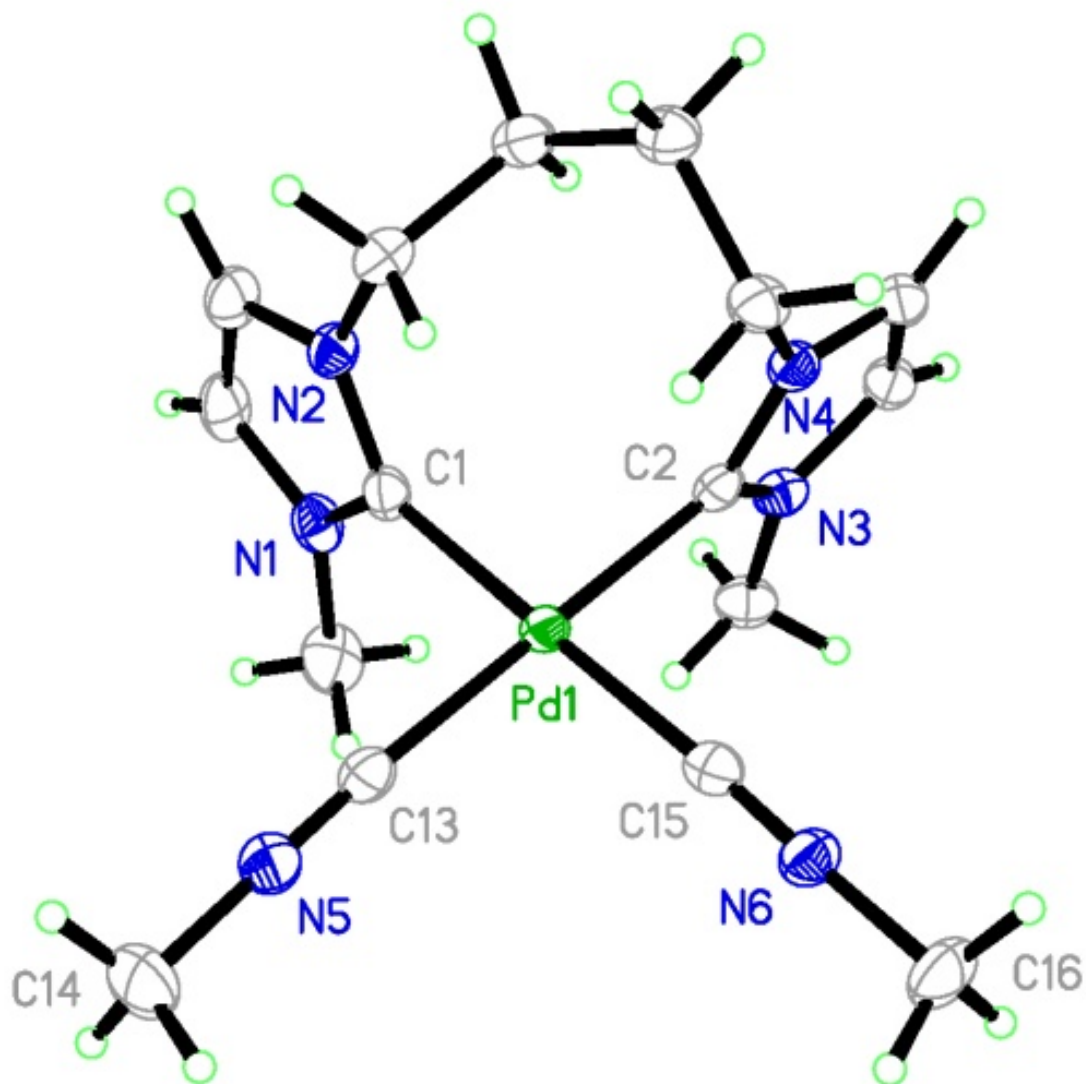


Figure 3.4. Molecular structure of complex **26d** with 50% probability ellipsoids.

Tetrafluoroborate counter ions are omitted for clarity.

Table 3.9. Selected bond lengths (Å) and bond angles (°) of complex **26d**

	Bond Lengths (Å)
Pd(1)-C(1)	2.022(2)
Pd(1)-C(2)	2.022(2)
Pd(1)-C(13)	2.005(2)
P(1)-C(15)	1.999(2)
C(1)-N(1)	1.349(3)
C(1)-N(2)	1.347(3)
C(2)-N(3)	1.341(3)
C(2)-N(4)	1.349(3)
C(13)-N(5)	1.131(3)
C(15)-N(6)	1.132(3)
	Bond angles (°)
C(1)-Pd(1)-C(2)	89.80(9)
C(13)-Pd(1)-C(15)	88.79(9)
C(1)-Pd(1)-C(13)	91.72(9)
C(2)-Pd(1)-C(15)	89.65(9)
C(1)-Pd(1)-C(15)	178.82(10)
C(2)-Pd(1)-C(13)	177.39(10)
N(1)-C(1)-N(2)	105.6(2)
N(3)-C(2)-N(4)	105.7(2)

Table 3.10. Crystal data and structure refinement details for complex **26d**

Empirical formula	C ₁₆ H ₂₄ B ₂ F ₈ N ₆ Pd
Formula weight	580.43
Crystal system	Monoclinic
Space group	P2 ₁ /c
Unit cell dimensions	a = 11.9318(3) Å α = 90 ° b = 12.5178(3) Å β = 93.4020 ° c = 15.4105 (4) Å γ = 90 °
Volume	2297.65(10) Å ³
Z	4
Density (calculated)	1.678 Mg/m ³
Absorption coefficient	0.888 mm ⁻¹
Crystal size	0.22 x 0.15 x 0.04 mm
θ range for data collection	1.71 – 27.48 °
Index range	-14 ≤ h ≤ 15 -16 ≤ k ≤ 15 -20 ≤ l ≤ 19
Temperature	115(2) K
Wave length	0.71073 Å
Reflections collected	23224
Independent reflections	5269 (R _{int} = 0.0349)
Final R indices [I > 2σ(I)]	R1 = 0.0296 wR2 = 0.0639
R indices (all data)	R1 = 0.0412 wR2 = 0.0693
Goodness-of-fit on F ²	1.042

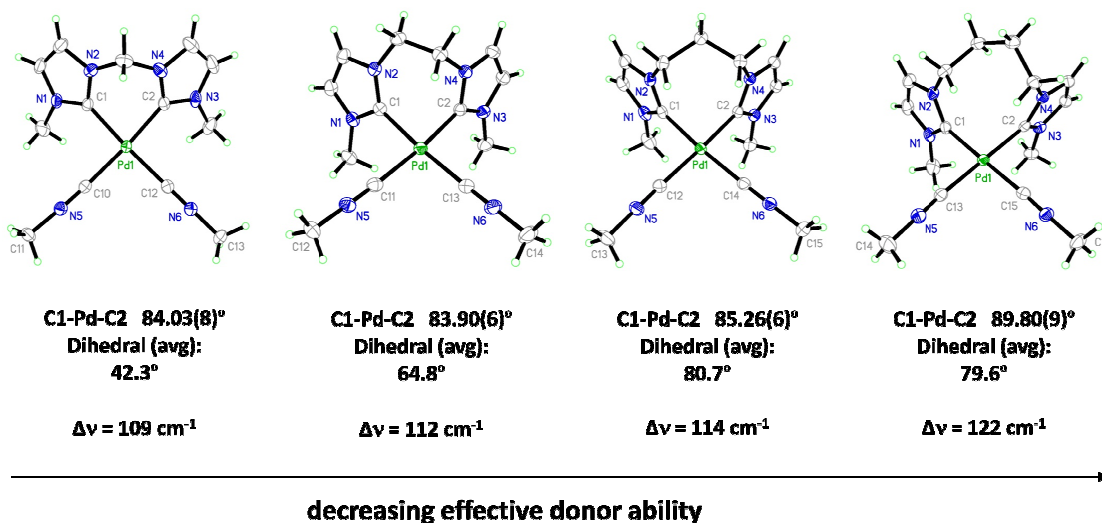


Figure 3.5. Variaton of donicity with dihedral angle and bite angle for complexes **26a-d**.

The IR stretching frequencies for complexes **26a-26d** are shown in Table 3.11. IR spectra of these complexes show two overlapping peaks for stretching of $\text{C}\equiv\text{N}$, and average values are shown in the table. The IR stretching frequencies of these complexes were greater than the stretching frequencies of free methyl isocyanide (2160 cm^{-1}) by about $\sim 100\text{ cm}^{-1}$. These high $\Delta\nu$ values indicate strong σ -donation from the methylisocyanide σ^* orbital (HOMO) to empty metal d-orbitals, with very weak or no π -backbonding from filled metal orbitals to the empty π antibonding orbitals of the isocyanides. The average IR stretching frequencies increased with in increasing chelating ring size, which indicates a decrease in of σ -donation from carbene to palladium with increasing chelating ring size. Therefore, the methylene linkage bis(NHC) ligand, which formed a six membered ring with palladium, was the strongest donor ligand, and the

butylene linkage bis(NHC) ligand, which formed a nine membered ring with palladium, was the weakest effective donor ligand based on *trans*-ligand IR probe studies.

Table 3.11. Infrared spectral data for bis(NHC) palladium bis(methylisocyanide) complexes

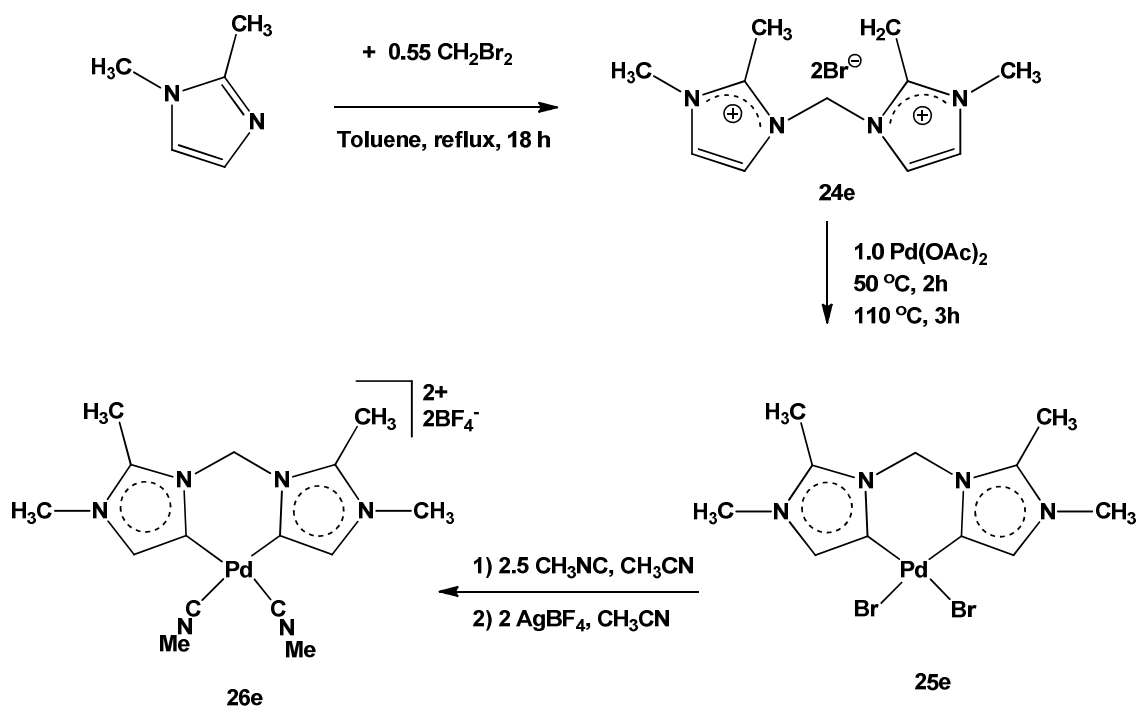
Complex	Linkage	Ring Size	$\nu_{\text{ave}} \text{N}\equiv\text{C}$ (cm^{-1})	$\Delta\nu_{\text{ave}} \text{N}\equiv\text{C}$ (cm^{-1})
-	Free CH_3NC	-	2160	-
3a	Methylene	6	2269	109
3b	Ethylene	7	2272	112
3c	Propylene	8	2274	114
3d	Butylene	9	2282	122

Synthesis and characterization of “abnormal” C4-bound bis(NHC)

bis(methylisocyanide) palladium (II) tetrafluoroborate complex (26e)

1,1',2,2'-Tetramethyl-3,3'-methylenediimidazolium dibromide (**24e**) and (1,1',2,2'-tetramethyl-3,3'-methylenediimidazol-2,2'-diylidene) palladium(II) dibromide (**25e**) were synthesized using published procedures similar to the diiodide analogues.⁷⁴ One molar equivalent of 1,2-dimethyl disubstituted imidazole and 0.55 mol equivalent of dibromoethane were mixed with toluene in a thick-walled glass vessel. The reaction mixture was stirred at reflux temperature for 18 h. The formed precipitate was filtered off and washed with toluene and Et_2O to isolate the bis(imidazolium) salt. Then, equal molar

equivalents of this bis(imidazolium) salt and palladium(II) acetate were mixed in wet dimethyl sulfoxide in a thick-walled glass vessel. The reaction mixture was stirred at 50 °C for 2 hours, followed by 110 °C for 3 hours. After cooling to room temperature, dichloromethane and diethyl ether were added to the reaction mixture to increase the precipitate formation. “Abnormal” C4-bound bis(NHC) palladium(II) dibromide (**25e**) was isolated as a pale yellow solid by filtration. Two and a half molar equivalents of methylisocyanide were added to the suspension of “abnormal” C4-bound bis(NHC) palladium(II) dibromide (**25e**) in dry acetonitrile. The reaction mixture was stirred for two hours, during which time the reaction mixture became clear. A solution of two molar equivalents of silver tetrafluoroborate in dry acetonitrile was then added to the reaction mixture, which immediately started to form a precipitate and was stirred for two hours. The resultant solution was filtered through celite to remove silver salts. The solvent was removed from the filtrate under vacuum, and the residue was dried under vacuum for two hours. The resultant solid was redissolved in acetonitrile, the mixture was filtered through celite, solvent was stripped and the residue was dried under vacuum. This sequence was repeated one more time to remove silver salts. Finally, white crystalline product of “abnormal” C4-bound bis(NHCs) bis(methylisocyanide) palladium(II) complex (**26e**) was isolated by layering diethyl ether on the acetonitrile solution (Scheme 3.3).



Scheme 3.3. Formation of “abnormal” C4-bound bis(NHC) bis(methylisocyanide) palladium(II) complex **26e**

One singlet each was observed for protons of the imidazole, the methylene linkage, the isocyanide methyl, the imidazole N-bound methyl, and the imidazole C2-bound methyl at 6.98, 5.86, 3.67, 3.53 and 2.60 ppm respectively in the ^1H NMR spectrum recorded in acetonitrile- d_3 . These values are slightly upfield compared to the analogous C2-bound methylene linkage bis(NHC) bis(methylisocyanide) palladium(II) (**26a**) complex. The ^{13}C NMR spectrum in acetonitrile- d_3 showed one carbene carbon signal at 144.87 ppm, which is the lowest carbene carbon value among all investigated bis(NHC) bis(methylisocyanide) palladium(II) complexes. The imidazole backbone carbons were observed at more downfield (133.56 and 128.94 ppm) values than the analogous C2-bound bis(NHC) bis(methylisocyanide) palladium(II) complexes (**26a**-

26d), but the N-bound methyl carbon was observed slightly upfield (35.23 ppm) compared to its analogues. The methyl carbon of methylisocyanide did not show much shift (30.72 ppm) compared to the other complexes (**26a-26d**). Two distinct peaks were observed for the stretching of the N≡C group of methylisocyanide in the IR spectrum. The average value for IR stretching frequencies of this complex was 2251 cm⁻¹ ($\Delta\nu = 91$ cm⁻¹), the lowest stretching frequency for the N≡C group in methylisocyanide for all investigated bis(methylisocyanide)palladium(II) complexes, indicating stronger σ -donation from the “abnormal” bound bis(NHC) ligand to palladium.

Crystals of complex **26e** were grown by the slow diffusion of diethyl ether into an acetonitrile solution. These crystals grew as colorless blocks and displayed C_S symmetry in the crystal structure. The structure belongs to the monoclinic P2₁/c space group. Bond lengths from carbene carbon atoms C(1) and C(2) to the adjacent nitrogen atoms N(2) and N(4) were 1.3972 and 1.4008 Å. These values are larger than the values for other bis(NHC) bis(methylisocyanide) palladium complexes (**26a-26d**). The imidazole C-C bond lengths, C(1)-C(3) and C(2)-(4), were 1.3674 and 1.3714 Å which is slightly shorter than the values for complexes **26a-26d**, indicating the presence of a conjugated double bond. The Pd-C_{carbene} bond lengths, 2.0058 and 2.0109 Å, were longer than those of reported “abnormal” C4-bound bis(NHC) palladium complexes.^{74,75} However, values were similar to the bis(NHC) bis(methylisocyanide) palladium complexes **26a-26c**. The N-C_{carbene}-C bond angles in the imidazole ring were 103.67° and 103.63°. The C_{carbene}-Pd-C_{carbene} angle was 88.96°, which is larger than the bite angles in complexes **26a-26c** but comparable to that in complex **26d**. The summation of bond angles around the palladium

centre for complex **26e** was around 360° , indicating disturbed square planar geometry around the palladium centre.

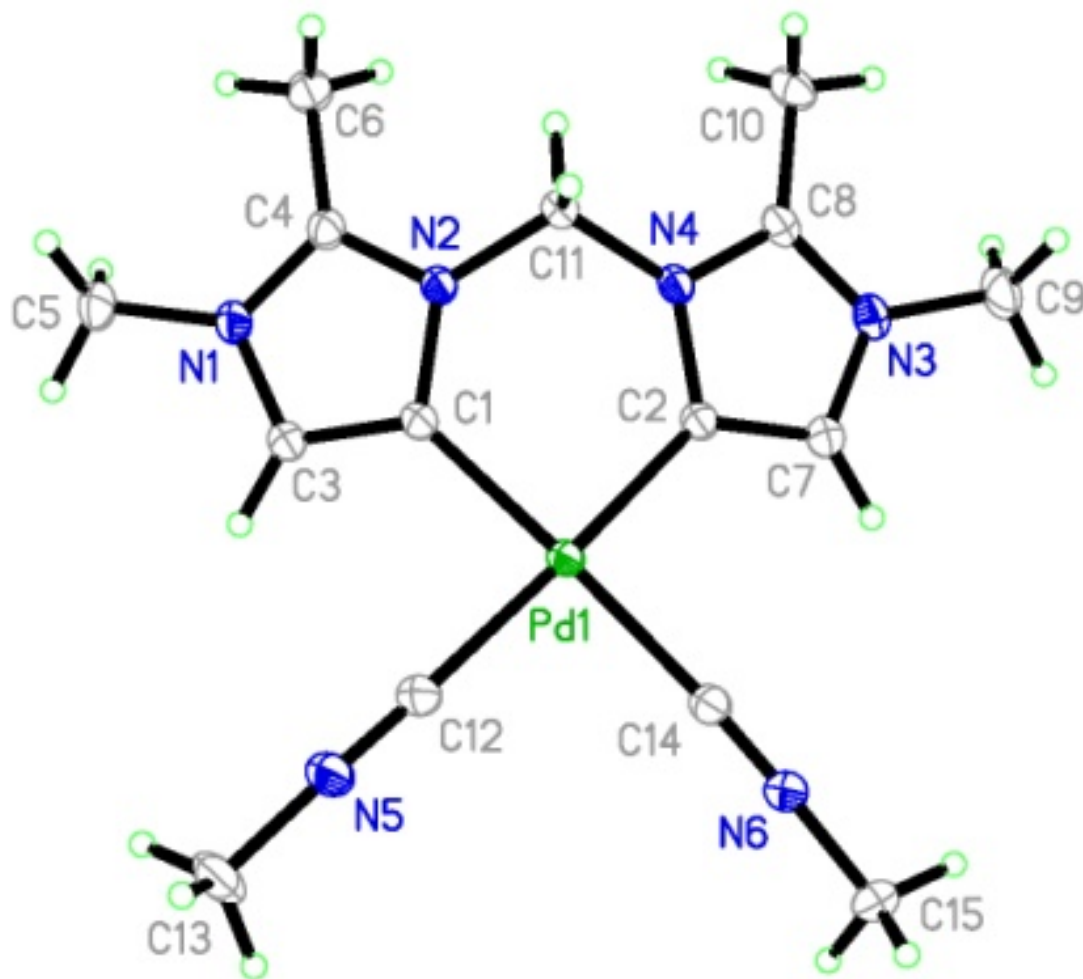


Figure 3.6. Molecular structure of complex **26e** with 50% probability ellipsoids. Tetrafluoroborate counter ions are omitted for clarity.

Table 3.12. Selected bond lengths (Å) and bond angles (°) of complex **26e**

	Bond Lengths (Å)
Pd(1)-C(1)	2.0058(10)
Pd(1)-C(2)	2.0109(10)
Pd(1)-C(12)	2.0108(11)
P(1)-C(14)	2.0200(11)
C(1)-N(2)	1.3972(13)
C(1)-C(3)	1.3674(14)
C(2)-N(4)	1.4008(13)
C(2)-C(7)	1.3714(14)
C(12)-N(5)	1.1437(14)
C(14)-N(6)	1.1460(14)
	Bond angles (°)
C(1)-Pd(1)-C(2)	88.96(4)
C(12)-Pd(1)-C(14)	91.58(4)
C(1)-Pd(1)-C(12)	88.48(4)
C(2)-Pd(1)-C(14)	90.85(4)
C(1)-Pd(1)-C(14)	171.67(4)
C(2)-Pd(1)-C(12)	177.32(4)
C(3)-C(1)-N(2)	103.67(9)
C(7)-C(2)-N(4)	103.63(9)

Table 3.13. Crystal data and structure refinement details for complex **26e**

Empirical formula	C ₁₅ H ₂₂ B ₂ F ₈ N ₆ Pd
Formula weight	566.41
Crystal system	Monoclinic
Space group	P2 ₁ /c
Unit cell dimensions	a = 12.0190(2) Å α = 90 ° b = 12.5150(2) Å β = 106.477(1) ° c = 14.8437(2) Å γ = 90 °
Volume	2141.06(6) Å ³
Z	4
Density (calculated)	1.757 Mg/m ³
Absorption coefficient	0.951 mm ⁻¹
Crystal size	0.50 x 0.40 x 0.30 mm
θ range for data collection	1.77 – 34.97 °
Index range	-19 ≤ h ≤ 19 -20 ≤ k ≤ 20 -23 ≤ l ≤ 23
Temperature	115(2) K
Wave length	0.71073 Å
Reflections collected	78577
Independent reflections	9390 (R _{int} = 0.0272)
Final R indices [I > 2σ(I)]	R1 = 0.0224 wR2 = 0.0569
R indices (all data)	R1 = 0.0254 wR2 = 0.0586
Goodness-of-fit on F ²	1.040

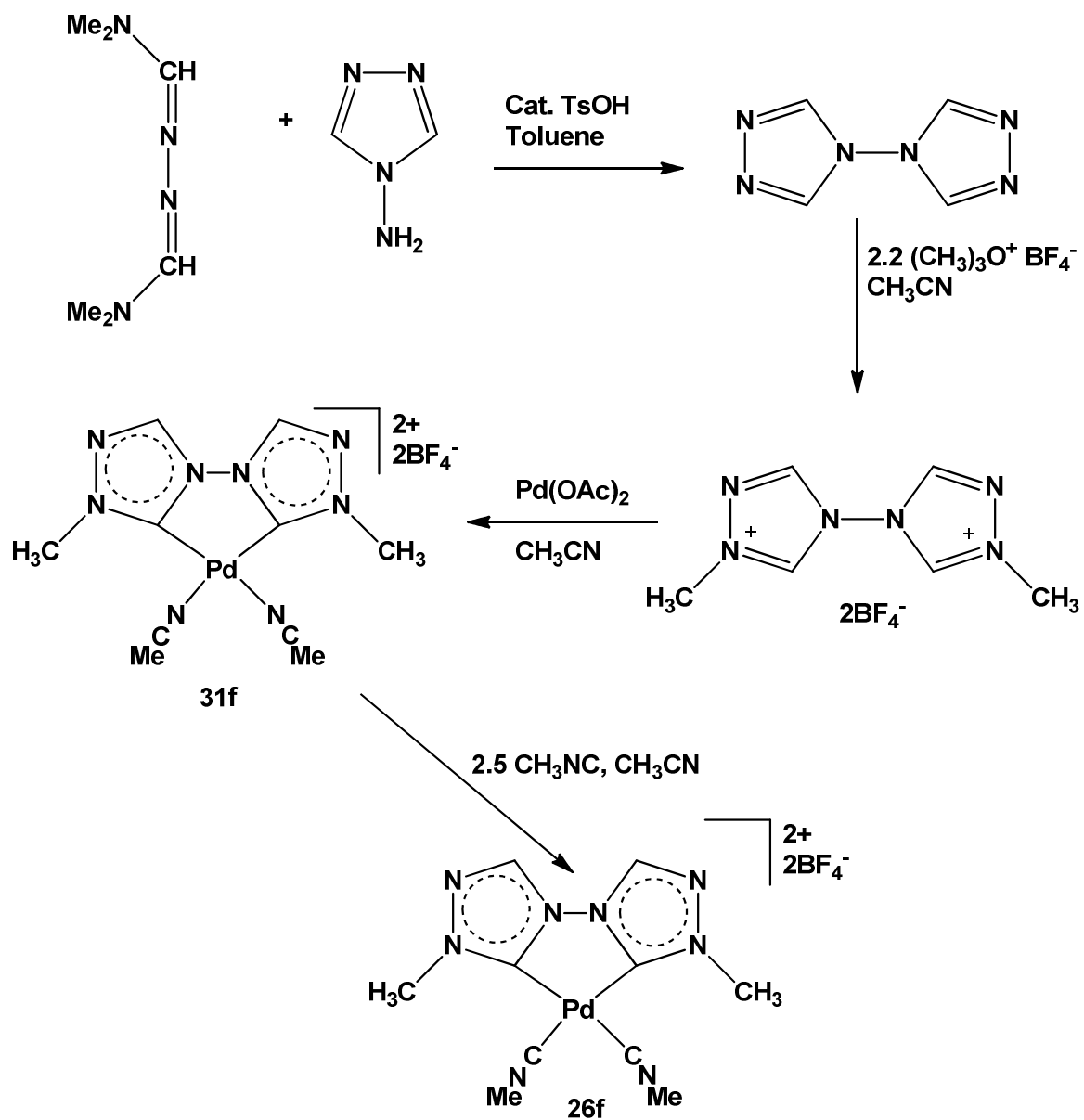
Synthesis and characterization of bitriazole derived bis(NHC) bis(methylisocyanide) palladium(II) bis(tetrafluoroborate) complex (26f)

The acetonitrile adduct of “bitriazole” bis(NHC) palladium (II) tetrafluoroborate was synthesized according to a procedure published by Crabtree et al. in 2008.⁷⁶ This acetonitrile adduct was treated with 2.5 molar equivalent of methylisocyanide in acetonitrile. The reaction mixture was stirred at room temperature for two hours, and then volatiles were evaporated under vacuum. The resultant solid was recrystallized using acetonitrile and diethyl ether.

The ¹H NMR spectrum showed a downfield signal for the triazole protons at 9.20 ppm. The methyl protons of the triazole ring showed a singlet at 4.21 ppm, which is downfield compared to the methyl protons of other bis(NHC) bis(methylisocyanide) palladium complexes (**26a-26e**). The methyl protons of the methylisocyanide appeared at 3.71 ppm, which is comparable to other investigated complexes. In the ¹³C NMR spectrum, the carbene carbon signal appeared at 159.87 ppm, the highest carbene carbon value among all investigated bis(NHC) bis(methylisocyanide) palladium complexes (**26a-26f**). The triazole ring carbon signal appeared at 135.66 ppm, similar to the “abnormal” bis(NHC)Palladium bis(isocyanide) complex (**26e**) but much more downfield than other bis(NHC)palladium bis(isocyanide) complexes (**26a-26d**). The triazole and methylisocyanide methyl carbon atoms showed peaks at 42.12 and 31.88 ppm, slightly downfield compared with other complexes (**26a-26e**).

The IR spectrum showed two overlapping peaks for methylisocyanide N≡C stretching frequencies, and the average value was 2279 cm⁻¹ ($\Delta\nu = 119 \text{ cm}^{-1}$). This value was only lower than the butylene linkage bis(NHC) palladium bis(methylisocyanide)

complex **26d**, indicating weaker donation from the triazole bis(NHC) ligand to palladium.



Scheme 3.4. Formation of “bitriazole” C3-bound bis(NHC) palladium(II) bis(methylisocyanide) complex **26f**

Crystals of complex **26f** were grown by the slow diffusion of diethyl ether into an acetonitrile solution. These crystals grew as colorless blocks. The X-ray crystal structure displays C_{2v} symmetry in the complex. The average bond length from the carbene carbon atoms C(1) and C(2) to adjacent nitrogen atoms N(1), N(2), N(3) and N(4) was 1.3477 Å. These values are close to the average value of 1.337 Å reported for the triazole derived bis(NHC) bis(acetonitrile) palladium tetrafluoroborate complex by Crabtree.⁷⁶ The Pd- C_{carbene} bond lengths, 2.0231 and 2.0235 Å, were slightly longer than the reported values of 1.979 and 1.986 Å for Crabtree's complex⁷⁶ but within the range of values for other investigated bis(NHC) palladium bis(methylisocyanide) complexes, thus indicating a slightly weaker bond between palladium and the carbene carbon in this bis(NHC) palladium bis(methylisocyanide) complex. This is likely due to the strong *trans*-influence of methylisocyanide compared to acetonitrile. The N- C_{carbene} -N bond angles in the triazole rings were 102.49 and 102.21°, similar to values reported for Crabtree's complex (103.1 and 102.2 Å).⁷⁶ The C_{carbene} -Pd- C_{carbene} angle was 79.50°, which is the smallest among all investigated bis(NHC) bis(methylisocyanide) palladium bis(methylisocyanide) complexes. This was the only complex with a five membered chelating ring size; therefore it had the smallest bite angle (C_{carbene} -Pd- C_{carbene} angle). The summation of bond angles around the palladium centre for complex **26f** was around 360°, indicating a distorted square planar geometry around the palladium centre.

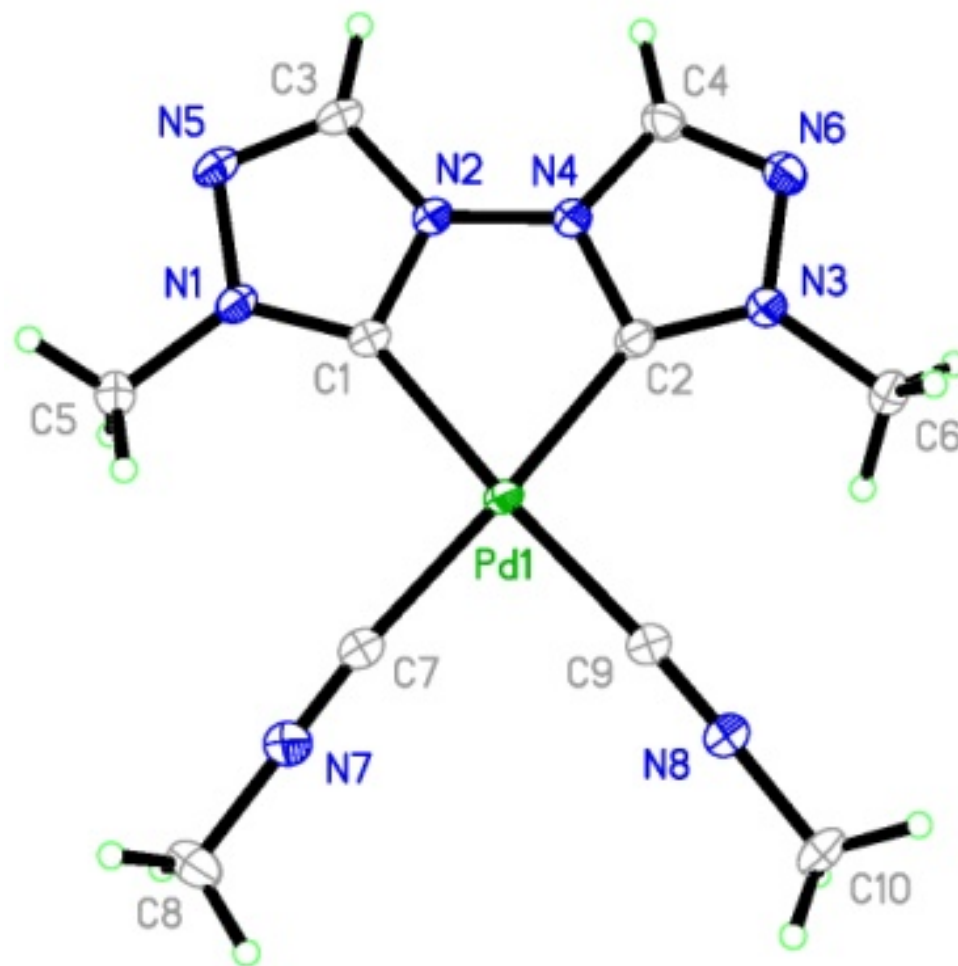


Figure 3.7. Molecular structure of complex **26f** with 50% probability ellipsoids.

Tetrafluoroborate counter ions are omitted for clarity.

Table 3.14. Selected bond lengths (Å) and bond angles (°) of complex **26f**

	Bond Lengths (Å)
Pd(1)-C(1)	2.0231(10)
Pd(1)-C(2)	2.0235(10)
Pd(1)-C(7)	1.9958(11)
P(1)-C(9)	1.9858(11)
C(1)-N(1)	1.3269(13)
C(1)-N(2)	1.3604(13)
C(2)-N(3)	1.3285(13)
C(2)-N(4)	1.3589(13)
C(7)-N(7)	1.1387(15)
C(9)-N(8)	1.1406(14)
	Bond angles (°)
C(1)-Pd(1)-C(2)	79.50(4)
C(7)-Pd(1)-C(9)	87.23(4)
C(1)-Pd(1)-C(7)	97.14(4)
C(2)-Pd(1)-C(9)	96.11(4)
C(1)-Pd(1)-C(9)	175.59(4)
C(2)-Pd(1)-C(7)	176.22(4)
N(1)-C(1)-N(2)	102.49(8)
N(3)-C(2)-N(4)	102.21(9)

Table 3.15. Crystal data and structure refinement details for complex **26f**

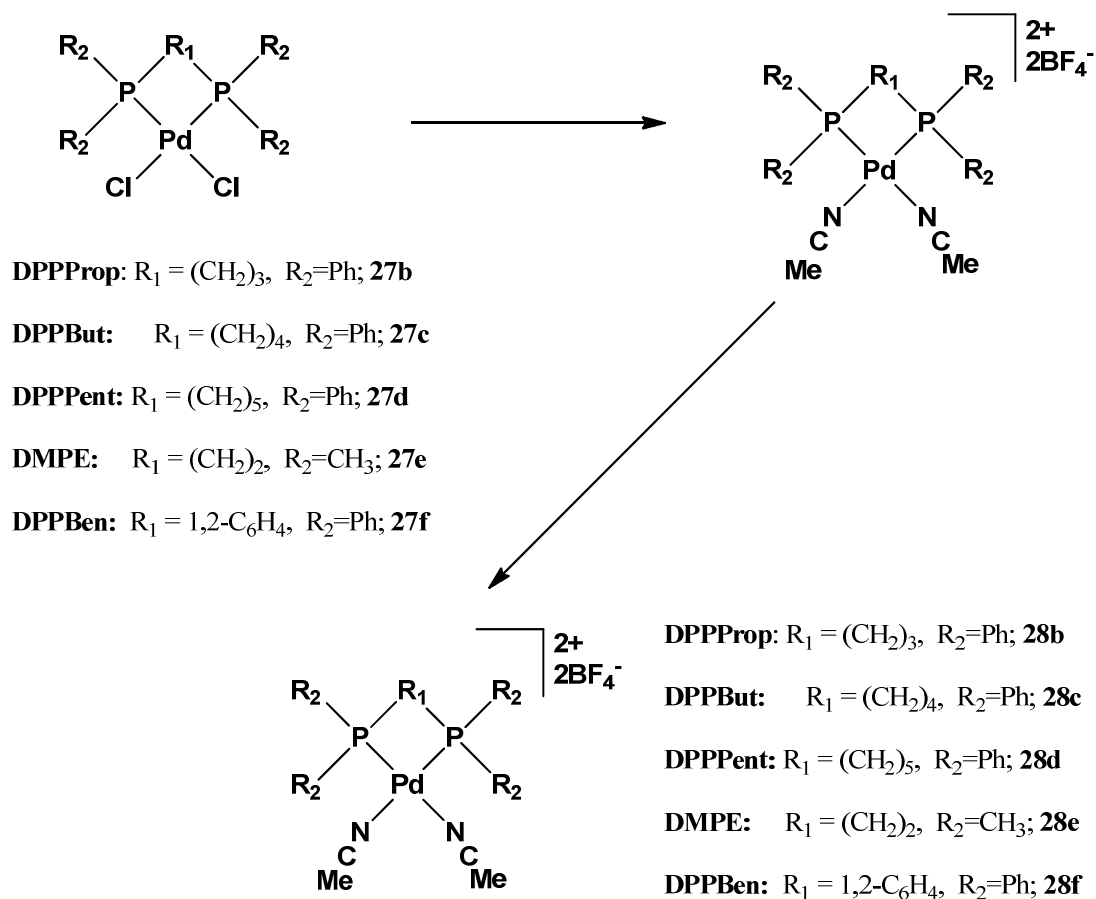
Empirical formula	C ₁₀ H ₂₄ B ₂ F ₈ N ₈ Pd
Formula weight	526.31
Crystal system	Monoclinic
Space group	P2 ₁ /c
Unit cell dimensions	a = 11.8269(2) Å α = 90 ° b = 10.3522(2) Å β = 103.3410(10) ° c = 16.0081(2) Å γ = 90 °
Volume	1907.05(6) Å ³
Z	4
Density (calculated)	1.833 Mg/m ³
Absorption coefficient	1.063 mm ⁻¹
Crystal size	0.45 x 0.38 x 0.32 mm
θ range for data collection	2.36 – 33.11 °
Index range	-18 ≤ h ≤ 18 -15 ≤ k ≤ 15 -24 ≤ l ≤ 24
Temperature	115(2) K
Wave length	0.71073 Å
Reflections collected	59789
Independent reflections	7230 (R _{int} = 0.0244)
Final R indices [I > 2σ(I)]	R1 = 0.0190 wR2 = 0.0484
R indices (all data)	R1 = 0.0209 wR2 = 0.0495
Goodness-of-fit on F ²	1.058

Synthesis and characterization of bis(phosphine) bis(methylisocyanide) palladium(II) tetrafluoroborate complexes (28b-28d)

Several bis(phosphine) palladium(II) bis(methylisocyanide) tetrafluoroborate complexes were synthesized using a common procedure (Scheme 3.7) similar to the synthesis of bis(diphenylphosphino)ethane palladium bis(methylisocyanide) tetraphenyl borate **28a** developed by Wanniarachchi et al.⁶⁷ The synthesis was started by placing the corresponding bis(phosphine) palladium dichloride, 2.2 molar equivalent of silver tetrafluoroborate and dry acetonitrile in a thick walled glass vessel under nitrogen. The reaction mixture was heated at 60 °C for two hours to substitute the chloride ligand with acetonitrile. The formed silver chloride precipitates were removed by filtration through celite. The volatiles in the filtrate were removed under vacuum, and the solid was dried for 3 hours to remove trace amount of acetonitrile. The remaining solids were then dissolved in distilled dichloromethane and filtered through celite to remove any silver salt present. The filtrate was treated with 2.2 molar equivalents of methylisocyanide and stirred for two hours. The solvent volume was reduced under reduced pressure, and addition of distilled diethyl ether or layering of ether on the solution produced crystalline product.

This common procedure was used to attached various bis(phosphine) ligands, 1,3-bis(diphenylphosphino)propane (**DPPPprop**), 1,4-bis(diphenylphosphino)Butane (**DPPBut**), 1,5-bis(diphenylphosphino)pentane (**DPPPent**), 1,2-bis(dimethylphosphino)ethane (**DMPE**), and 1,2-bis(diphenylphosphino)benzene (**DPPBen**) to bis(methylisocyanide) palladium(II) tetrafluoroborate complexes (**28b-28f**). These synthesized bis(phosphine) complexes and previously reported 1,2-

bis(diphenylphosphino)ethane (**DPPE**) bis(methylisocyanide) palladium(II) complex **28a** were used for IR probe studies.



Scheme 3.5. Synthesis of bis(phosphine) bis(methylisocyanide) palladium bis(tetrafluoroborate) complexes (**28b-28f**).

{1,2-Bis(diphenylphosphino)propane} palladium (II) bis(methylisocyanide) bis(tetrafluoroborate) or [(DPPProp) Pd(II) (CNCH₃)₂] [BF₄]₂ complex **28b**

Complex **28b** was isolated as a pale yellow crystalline solid in 67% yield. The ¹H NMR spectrum showed aromatic protons as a multiplet ranging from 7.54-7.63 ppm. The methyl protons of methylisocyanide appear as a singlet at 3.10 ppm. The linkage propylene protons showed two sets of broad singlets and a broad triplet at 3.00 and 2.04

ppm, respectively, with a four to two integration ratio. In the ^{13}C NMR spectrum aromatic carbons appeared between 127.41-132.72 ppm. The methyl carbon signal appeared at 29.54 ppm. The propylene linkage carbons showed two peaks at 20.26 (triplet) and 17.62 (singlet) ppm. The ^{31}P NMR spectrum showed a singlet at 2.62 ppm for the two phosphorus atoms, indicating two chemically equivalent phosphorus groups. The IR spectrum showed two overlapping peaks for the methyloisocyanide stretching frequency ($\nu \text{N}\equiv\text{C}$), and the average value was 2268 cm^{-1} ($\Delta\nu = 108 \text{ cm}^{-1}$). This value was lower than the values for the C2-bound imidazole based and triazole based bis(NHC) bis(methyloisocyanide) palladium complexes (**26a-26d** and **26f**), indicating stronger donation from the DPPProp ligand compare to these bis(NHC) carbene ligands. However the methyloisocyanide stretching frequency value was higher than the previously reported value for the analogous five membered chelate complex, 1,2-bis(diphenylphosphino)ethane bis(methyloisocyanide) palladium(II) tetraphenylborate (2262 cm^{-1}).⁶⁷ Therefore, the DPPProp ligand is a weaker donor ligand than DPPE ligand, suggesting that an increase in chelating ring size will decrease the effective donation from ligand to metal. This trend was also observed among C2-bound imidazole-based bis(NHC) ligands.

Crystals of complex **28b** were grown by the slow diffusion of diethyl ether into a dichloromethane solution. These crystals were grown as pale yellow rods. The X-ray structure displayed a near C_s symmetry. The bond lengths between palladium and the two phosphorus atoms were 2.3269 and 2.3471 Å, close to the value reported for palladium bis(phosphines) complexes.⁶⁷ The P-Pd-P bite angle of 89.06° was larger than the reported value of 84.08° for the similar five-membered chelate

[(DPPE)Pd(CNCH₃)₂][BF₄]₂ complex **28a**.⁶⁷ The Pd-C_{isocyanide} bond lengths of 2.048 and 2.072 Å are similar to a previously reported similar five membered DPPE complex.⁶⁷

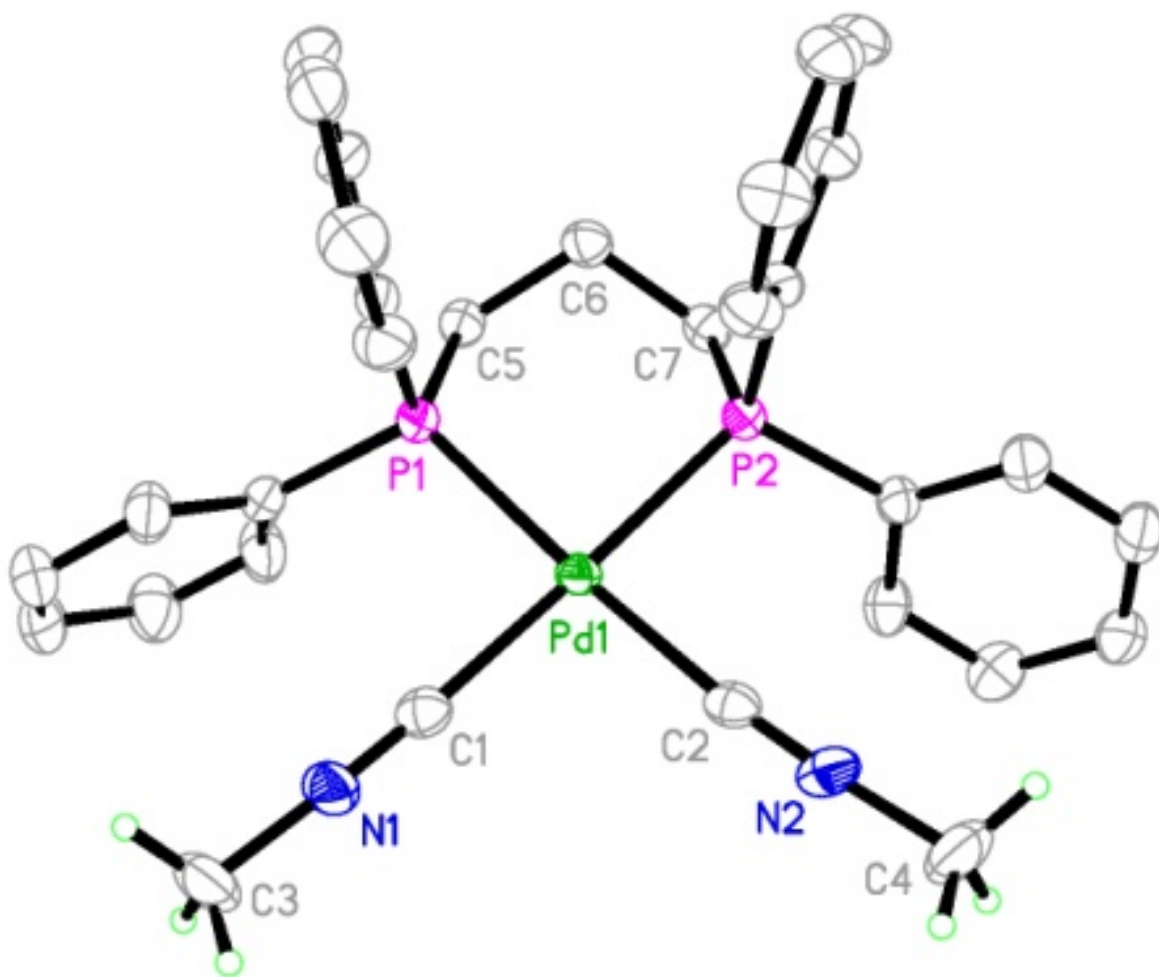


Figure 3.8. Molecular structure of complex **28b** with 50% probability ellipsoids.

Tetrafluoroborate counter ions are omitted for clarity.

Table 3.16. Selected bond lengths (Å) and bond angles (°) of complex **28b**

	Bond Lengths (Å)
Pd(1)-C(1)	2.072(3)
Pd(1)-C(2)	2.048(3)
Pd(1)-P(1)	2.3269(7)
P(1)-P(2)	2.3471(7)
C(1)-N(1)	1.161(3)
C(2)-N(2)	1.144(3)

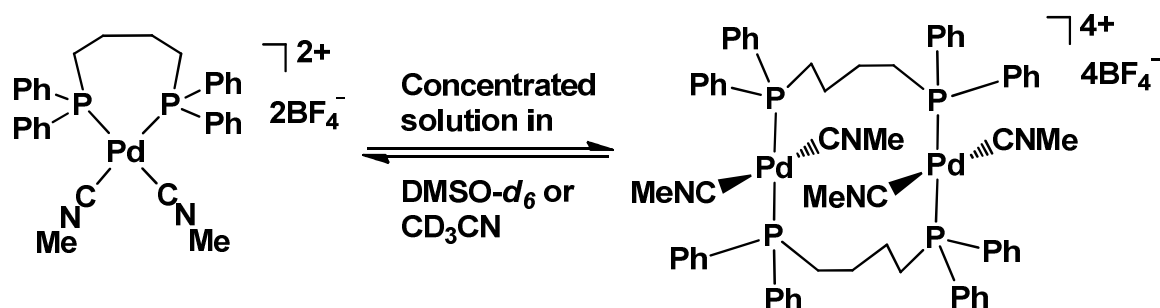
	Bond angles (°)
C(1)-Pd(1)-C(2)	92.38(10)
P(1)-Pd(1)-P(2)	89.06(2)
C(1)-Pd(1)-P(1)	89.92(7)
C(2)-Pd(1)-P(2)	88.48(8)
C(1)-Pd(1)-P(2)	177.53(8)
C(2)-Pd(1)-P(1)	175.40(8)
Pd(1)-C(1)-N(1)	177.5(2)
Pd(1)-C(2)-N(2)	174.8(2)

Table 3.17. Crystal data and structure refinement details for complex **28b**

Empirical formula	C ₃₁ H ₃₂ B ₂ F ₈ N ₂ P ₂ Pd
Formula weight	774.55
Crystal system	Monoclinic
Space group	P2 ₁ /c
Unit cell dimensions	a = 21.7551(2) Å α = 90 ° b = 16.34010(10) Å β = 93.5680(10) ° c = 20.4829(2) Å γ = 90 °
Volume	7267.16(11) Å ³
Z	8
Density (calculated)	1.416 Mg/m ³
Absorption coefficient	0.663 mm ⁻¹
Crystal size	0.29 x 0.23 x 0.18 mm
θ range for data collection	1.56 – 26.18 °
Index range	-26 ≤ h ≤ 26 -19 ≤ k ≤ 19 -25 ≤ l ≤ 25
Temperature	115(2) K
Wave length	0.71073 Å
Reflections collected	61393
Independent reflections	14166 (R _{int} = 0.0287)
Final R indices [I > 2σ(I)]	R1 = 0.0337 wR2 = 0.0798
R indices (all data)	R1 = 0.0535 wR2 = 0.0863
Goodness-of-fit on F ²	1.123

Bis{1,2-bis(diphenylphosphino)butane} tetrakis(methylisocyanide) dipalladium(II) tetrafluoroborate or [(DPPBut)₂ Pd₂ (CNCH₃)₄] [BF₄]₄ complex **28c**

Complex **28c** was isolated as a pale yellow crystalline solid in 77% yield. The dilute solution of the compound in DMSO-*d*₆ (2-3 mg / 0.6 mL) showed aromatic protons as a multiplet ranging from 7.54-7.63 ppm in the ¹H NMR spectrum. The methyl protons of methylisocyanide showed a singlet at 3.21 ppm, slightly downfield compared to the analogous DPPProp complex **28b**. Linkage butylene protons showed two sets of broad peaks at 2.90 ppm (singlet) and 1.78 ppm (doublet) with a 4:4 integration ratio. However when the complex **28c** concentration was increased (> 5mg / 0.6 mL) in the NMR solution, another set of peaks started to show up in ¹H NMR spectrum, and these disappeared upon dilution of the same solution. This new set of peaks corresponded to butylene and aromatic protons and appeared slightly downfield compare to the original peaks, but no change in the methyl protons of methylisocyanide was observed. This new set of peaks was identified as a dimeric palladium complex (Scheme 3.6). The same change was observed in acetonitrile-*d*₃ NMR solvent as well.



Scheme 3.6. Monomer-dimer equilibrium of complex **28c** in concentrated DMSO-*d*₆ or CD₃CN solutions.

The ^{13}C NMR spectrum showed aromatic carbon signals from 128.49 to 132.88 ppm. The monomer and dimer equilibrium prevented the assignment of all aromatic carbon signals. However, only one signal was observed for the methyl carbon of the methyl isocyanides at 29.74 ppm. Butylene carbons showed two signals at 24.75 and 29.78 ppm. The IR spectrum showed a single peak at 2272 cm^{-1} for $\text{N}\equiv\text{C}$ stretching. This value was greater than the $\text{N}\equiv\text{C}$ stretching value for complex **28b** and the previously reported DPPE complex **28a**.

Crystals of complex **28c** were grown by the slow diffusion of diethyl ether into an acetonitrile solution. These crystals were grown as pale yellow cubes. The X-ray structure displayed a dimeric palladium complex with C_i symmetry. The ligand arrangement around the palladium centre showed *trans* geometry, with two palladium atoms bridging by two DPPBut ligands, and two methylisocyanide ligands bound to each palladium in *trans* orientation. Therefore, this complex was not suitable for *trans*-ligand IR probe studies.

In the crystal structure, the average palladium-phosphorous bond length was 2.3518 \AA , which is slightly shorter than that in complex **28b**. The average $\text{Pd}-\text{C}_{\text{isocyanide}}$ bond length was 1.972 \AA , which is shorter than that in complex **5b**. This difference is due to lesser *trans*-influence from isocyanide compared to an alkyl diphenyl phosphine ligand. Because of this *trans* arrangement of ligands, the average $\text{P}-\text{Pd}-\text{P}$ and $\text{C}_{\text{isocyanide}}-\text{Pd}-\text{C}_{\text{isocyanide}}$ bond angles were 176.46° and 170.17° , respectively. Because of these structural characteristics, specifically the *trans* arrangement of the methyl isocyanides, complex **28c** cannot be used in IR probe studies to access the effective donor ability of the chelating ligand DPPBut.

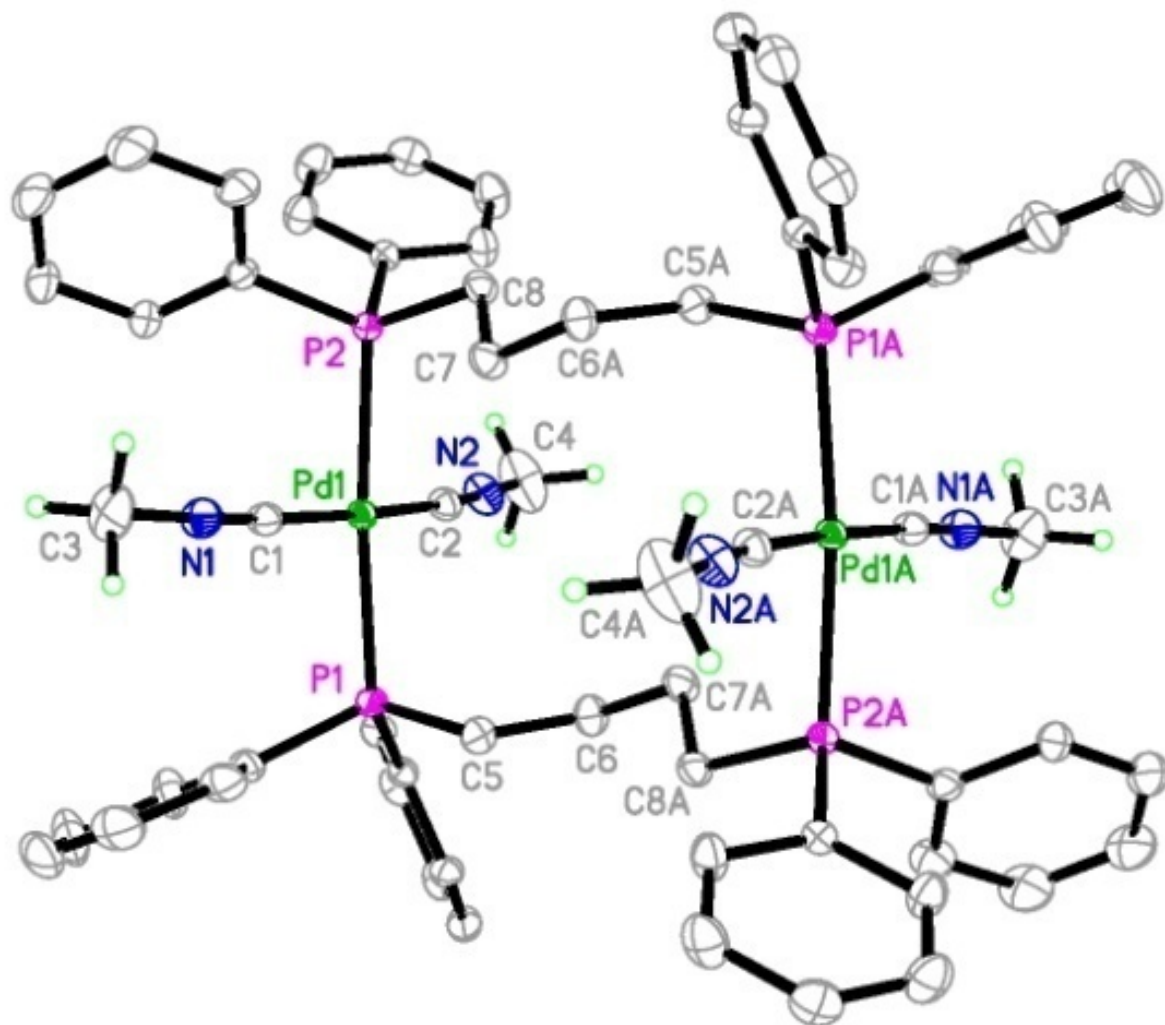


Figure 3.9. Molecular structure of complex **28c** with 50% probability ellipsoids.

Tetrafluoroborate counter ions are omitted for clarity.

Table 3.18. Selected bond lengths (Å) and bond angles (°) of complex **28c**

	Bond Lengths (Å)
Pd(1)-C(1)	1.9787(15)
Pd(1)-C(2)	1.9657(15)
Pd(1)-P(1)	2.3516(4)
P(1)-P(2)	2.3520(4)
C(1)-N(1)	1.1410(19)
C(2)-N(2)	1.142(2)

	Bond angles (°)
C(1)-Pd(1)-C(2)	176.46(6)
P(1)-Pd(1)-P(2)	170.167(13)
C(1)-Pd(1)-P(1)	87.77(4)
C(2)-Pd(1)-P(2)	89.99(4)
C(1)-Pd(1)-P(2)	87.94(4)
C(2)-Pd(1)-P(1)	94.71(4)
Pd(1)-C(1)-N(1)	175.68(14)
Pd(1)-C(2)-N(2)	174.00(15)

Table 3.19. Crystal data and structure refinement details for complex **28c**

Empirical formula	$C_{68}H_{74}B_4F_{16}N_4P_4Pd_2$
Formula weight	1659.25
Crystal system	Monoclinic
Space group	$P2_1/n$
Unit cell dimensions	$a = 12.12580(10) \text{ \AA}$ $\alpha = 90^\circ$ $b = 16.4862(2) \text{ \AA}$ $\beta = 105.3180(10)^\circ$ $c = 18.9291(2) \text{ \AA}$ $\gamma = 90^\circ$
Volume	$3649.65(7) \text{ \AA}^3$
Z	2
Density (calculated)	1.510 Mg/m^3
Absorption coefficient	0.666 mm^{-1}
Crystal size	0.50x 0.50 x 0.48 mm
θ range for data collection	$1.66 - 36.15^\circ$
Index range	$-20 \leq h \leq 20$ $-27 \leq k \leq 26$ $-29 \leq l \leq 31$
Temperature	115(2) K
Wave length	0.71073 \AA
Reflections collected	84982
Independent reflections	17425 ($R_{\text{int}} = 0.0302$)
Final R indices [$I > 2\sigma(I)$]	$R1 = 0.0350$ $wR2 = 0.0934$
R indices (all data)	$R1 = 0.0446$ $wR2 = 0.1003$
Goodness-of-fit on F^2	1.029

Bis(1,5-bis(diphenylphosphino)pentane) bis(methylisocyanide) palladium(II) tetrafluoroborate or [(DPPent) Pd (CNCH₃)₂] [BF₄]₂ complex **28d**

Complex **28d** was synthesized in 77% yield as a pale yellow solid. The ¹H NMR in DMSO-*d*₆ showed two sets of signals for the aromatic protons at 7.83 and 7.63 ppm with an 8:12 integration ratio. The linkage pentylene protons showed three sets of broad singlets with a 4:2:4 integration ratio. The methyl protons of the isocyanides gave a singlet at 2.90 ppm, which was upfield compare to analogous complexes with shorter linkages. Increasing the concentration of complex **28d** in the NMR solvent did not change the peak appearance as it did for complex **28c**. The ¹³C NMR spectrum showed aromatic carbon signals between 132.38-124.42 ppm. The methyl carbon of methylisocyanide appeared at 29.79 ppm. Linkage pentalyene carbons showed three signals at 32.90, 26.03 and 25.42 ppm. The IR spectrum showed a single stretching frequency value for N≡C at 2268 cm⁻¹, which is similar to the value for complex **28b** but lower than complex **28c** and indicated a *trans* orientation of ligands. Identification of the geometry around the palladium centre is important to compare these values. However, attempts to grow crystals failed due to poor stability of the complex in solution. Reported complexes with the DPPent complexes mostly were dimeric or bridging complexes. According to ¹H NMR observation and based on complex **28c** and literature examples, complex **28d** most likely a *trans* bridging complex.

Bis(1,2-bis(dimethylphosphino)ethane) bis(methylisocyanide) palladium(II) tetrafluoroborate or [(DMPE) Pd (CNCH₃)₂] [BF₄]₂ complex **28e**

Complex **28e** was air sensitive and therefore needed to be handled under inert conditions. Layering diethyl ether on the solution of **28e** in acetonitrile to allow slow diffusion gave transparent crystals in a 56% yield. This step is important to isolate the complex in pure form, because other techniques produced impure, oily products. The ¹H NMR showed that one molecule of acetonitrile was trapped in the crystals per molecule of complex **28e**, and this was confirmed by elemental analysis and the X-ray crystal structure. The methyl protons of methylisocyanide appeared downfield compare to other complexes (**28a-28d**) at 3.56 ppm. The linkage ethylene protons showed a multiplet from 2.37 to 2.22 ppm, and the DMPE methyl protons appeared at 1.86 ppm as a doublet. The methylisocyanide N≡C carbon and the methyl carbon showed a broad signal at 127.69 ppm and a triplet at 31.28 ppm, respectively. The linkage ethylene carbons showed a doublet of doublets at 28.26 ppm, and the DMPE methyl carbon showed a doublet at 13.48 ppm. A single peak was observed for phosphorous atoms in the ³¹P NMR spectrum at 60.11 ppm, indicating a similar chemical environment for both phosphorous atoms. The IR spectrum showed two overlapping peaks at 2268 cm⁻¹.

Crystals of complex **28e** were grown by slow diffusion of diethyl ether into an acetonitrile solution. These crystals were grown as transparent rods. The X-ray structure displayed a C₂ symmetry. One acetonitrile molecule was found per molecule of complex **28e** in the X-ray structure. The average bond length between palladium and phosphorous was 2.274 Å, which is slightly shorter than complex **28b**. The average Pd-C_{isocyanide} bond length was 2.0312 Å, which is greater than complex **28b**. This difference is due to the

higher donor ability of DMPE compared to other examined bis(phosphine) ligands. The P-Pd-P bond angle was 84.01° , lower than the other investigated *cis* bis(phosphine) complexes. The $C_{\text{isocyanide}}\text{-Pd-}C_{\text{isocyanide}}$ bond angle or bite angle was 92.00° , greater than those for complexes **28a-28d**.

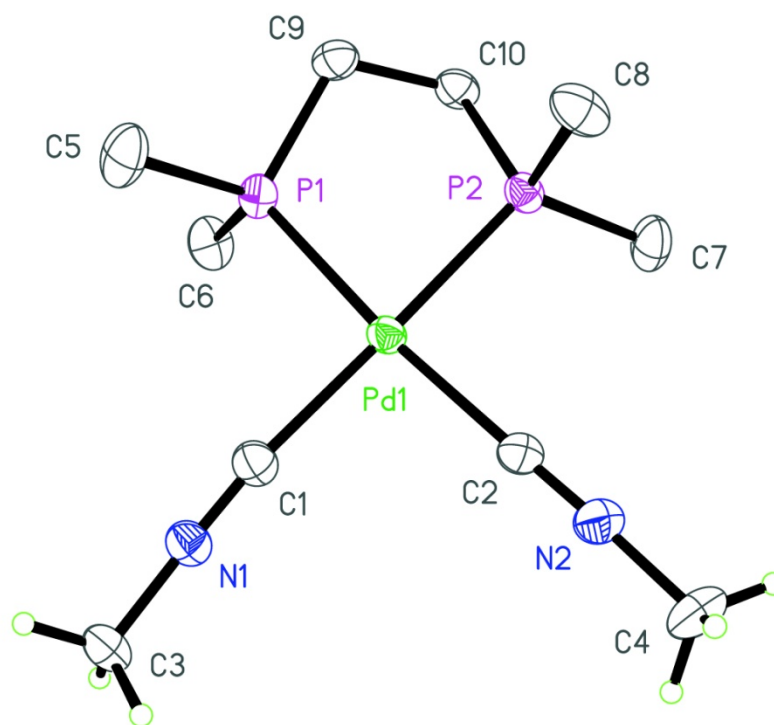


Figure 3.10. Molecular structure of complex **28e** with 50% probability ellipsoids. Tetrafluoroborate counter ions are omitted for clarity.

Table 3.20. Selected bond lengths (Å) and bond angles (°) of complex **28e**

	Bond Lengths (Å)
Pd(1)-C(1)	2.0409(16)
Pd(1)-C(2)	2.0216(17)
Pd(1)-P(1)	2.2805(4)
P(1)-P(2)	2.2674(4)
C(1)-N(1)	1.137(2)
C(2)-N(2)	1.137(2)

	Bond angles (°)
C(1)-Pd(1)-C(2)	92.00(7)
P(1)-Pd(1)-P(2)	84.009(16)
C(1)-Pd(1)-P(1)	93.70(5)
C(2)-Pd(1)-P(2)	90.19(5)
C(1)-Pd(1)-P(2)	176.81(5)
C(2)-Pd(1)-P(1)	173.71(5)
Pd(1)-C(1)-N(1)	174.03(15)
Pd(1)-C(2)-N(2)	179.19(17)

Table 3.21. Crystal data and structure refinement details for complex **28e**

Empirical formula	C ₁₂ H ₂₅ B ₂ F ₈ N ₃ P ₂ Pd
Formula weight	553.31
Crystal system	Orthorhombic
Space group	P 2 ₁ 2 ₁ 2 ₁
Unit cell dimensions	a = 9.82260(10) Å α = 90 ° b = 14.1041(2) Å β = 90 ° c = 16.4346(2) Å γ = 90 °
Volume	2276.83(5) Å ³
Z	4
Density (calculated)	1.614 Mg/m ³
Absorption coefficient	1.022 mm ⁻¹
Crystal size	0.40 x 0.25 x 0.25 mm
θ range for data collection	1.90 – 30.51 °
Index range	-14 ≤ h ≤ 13 -20 ≤ k ≤ 20 -23 ≤ l ≤ 23
Temperature	115(2) K
Wave length	0.71073 Å
Reflections collected	39078
Independent reflections	6947 (R _{int} = 0.0265)
Final R indices [I > 2σ(I)]	R1 = 0.0189 wR2 = 0.0463
R indices (all data)	R1 = 0.0197 wR2 = 0.0470
Goodness-of-fit on F ²	1.029

(1,2-Bis(diphenylphosphino)benzene) bis(methylisocyanide) palladium(II) tetrafluoroborate or [(DPPBen) Pd (CNCH₃)₂] [BF₄]₂ complex **28f**

Complex **28f** was isolated in 56% yield. The ¹H NMR spectrum showed proton signals for aromatic protons between 7.94-7.56 ppm. The methyl protons of methylisocyanide appeared at 3.33 ppm, which is slightly upfield compared to complex **28e** and downfield compared to complexes **28b-28d**. In the ¹³C NMR spectrum, aromatic carbons appeared between 137.55-126.62 ppm. The methyl carbon signal appeared at 31.15 ppm. The ³¹P NMR spectrum showed a singlet at 63.69 ppm for the two phosphorus atoms, indicating two chemically equivalent phosphorus groups.

The IR spectrum shows two overlapping peaks for the methylisocyanide stretching frequencies (ν C \equiv N), with an average value of 2272 cm⁻¹ ($\Delta\nu = 112$ cm⁻¹). This value was lower than the values for the triazole-based five-membered chelate bis(NHC) bis(methylisocyanide) palladium complex and greater than the values for five membered chelate (DPPE) bis(methylisocyanide) palladium and (DMPE) bis(methylisocyanide) palladium complexes, indicating moderate effective donor ability among five membered chelate complexes.

Crystals of complex **28f** were grown by the slow diffusion of diethyl ether into an acetonitrile solution. These crystals were grown as pale yellow blocks. The X-ray structure displayed C₁ symmetry. The average bond length between palladium and phosphorous was 2.275 Å, and the average bond length between Pd-C_{isocyanide} was 2.034 Å. Bond angles of P-Pd-P and C_{isocyanide}-Pd-C_{isocyanide} were 84.83 and 89.12°. Most of these structural parameters are very much similar to the parameters of complex **28a**, but the bite angle was slightly larger in value.

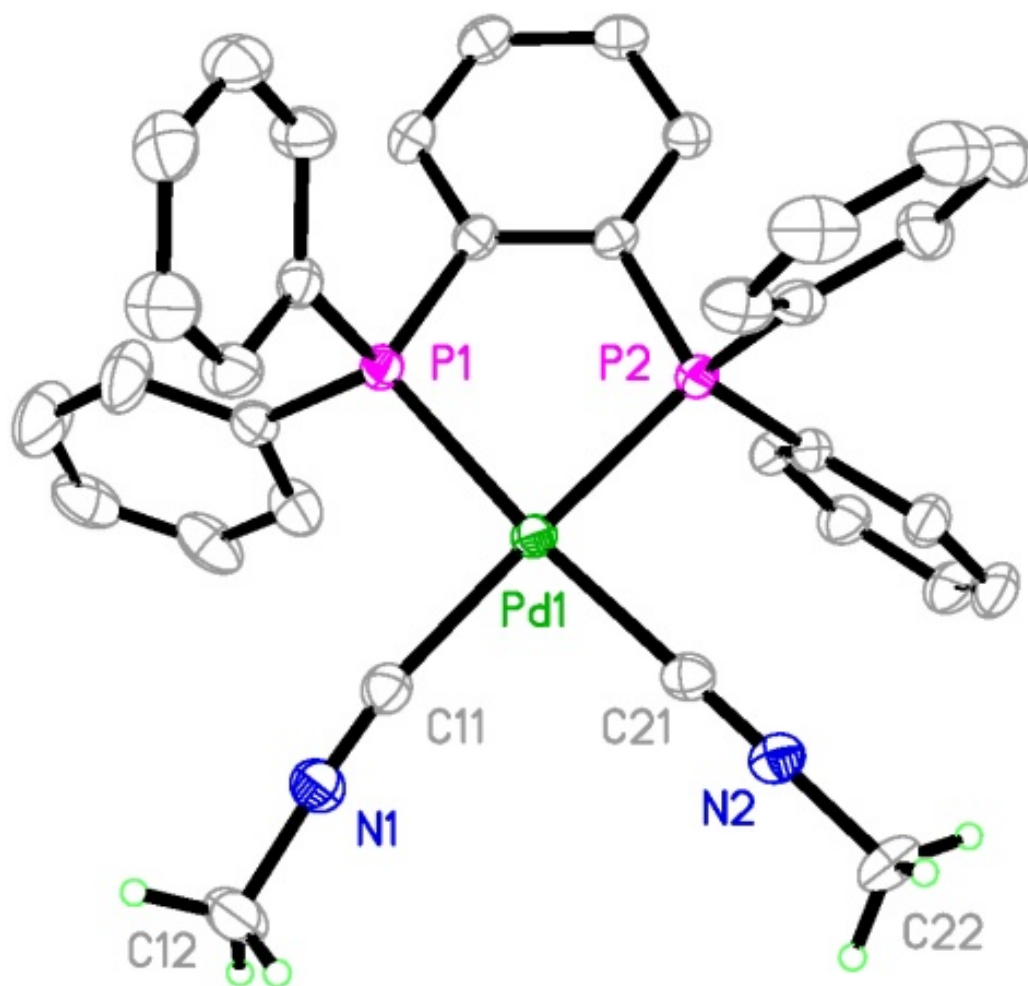


Figure 3.11. Molecular structure of complex **28f** with 50% probability ellipsoids. Tetrafluoroborate counter ions are omitted for clarity.

Table 3.22. Selected bond lengths (Å) and bond angles (°) of complex **28f**

	Bond Lengths (Å)
Pd(1)-C(1)	2.040(2)
Pd(1)-C(2)	2.028(2)
Pd(1)-P(1)	2.2798(5)
P(1)-P(2)	2.2709(5)
C(1)-N(1)	1.133(3)
C(2)-N(2)	1.137(3)

	Bond angles (°)
C(1)-Pd(1)-C(2)	89.12(8)
P(1)-Pd(1)-P(2)	84.832(18)
C(1)-Pd(1)-P(1)	96.14(6)
C(2)-Pd(1)-P(2)	89.98(6)
C(1)-Pd(1)-P(2)	177.02(6)
C(2)-Pd(1)-P(1)	174.58(6)
Pd(1)-C(1)-N(1)	171.01(19)
Pd(1)-C(2)-N(2)	177.86(18)

Table 3.23. Crystal data and structure refinement details for complex **28f**

Empirical formula	C ₃₄ H ₃₀ B ₂ F ₈ N ₂ P ₂ Pd
Formula weight	808.56
Crystal system	Monoclinic
Space group	P2 ₁ /c
Unit cell dimensions	a = 9.0787(2) Å α = 90 ° b = 24.5423(4) Å β = 98.4870(10) ° c = 15.5711(3) Å γ = 90 °
Volume	3431.44(11) Å ³
Z	4
Density (calculated)	1.565 Mg/m ³
Absorption coefficient	0.706 mm ⁻¹
Crystal size	0.40 x 0.37 x 0.25 mm
θ range for data collection	1.56 – 26.21 °
Index range	-12 ≤ h ≤ 12 -29 ≤ k ≤ 32 -20 ≤ l ≤ 20
Temperature	115(2) K
Wave length	0.71073 Å
Reflections collected	38319
Independent reflections	8437 (R _{int} = 0.0253)
Final R indices [I > 2σ(I)]	R1 = 0.0302 wR2 = 0.0743
R indices (all data)	R1 = 0.0343 wR2 = 0.0767
Goodness-of-fit on F ²	1.024

Synthesis and characterization of bis(ADC) bis(methylisocyanide) palladium(II) bis(tetrafluoroborate) complexes (30a-30c)

Comparison of the σ -donor abilities of the bis(ADC) ligands with bis(NHC) and bis(phosphine) ligands was performed by synthesizing a new eight membered chelate bis(ADC) palladium(II) bis(methylisocyanide) complex **30a** and determining the X-ray crystal structure of a previously reported five membered chugaev type bis(ADC) palladium(II) bis(methylisocyanide) complex **30b**⁷⁷. Along with these complexes, the known seven-membered chelate bis(ADC) palladium(II) bis(methylisocyanide) complex **30c**,⁶⁷ derived from (*rac*) N,N'-dimethyl-1,2-diaminocyclohexane, was examined for comparison.

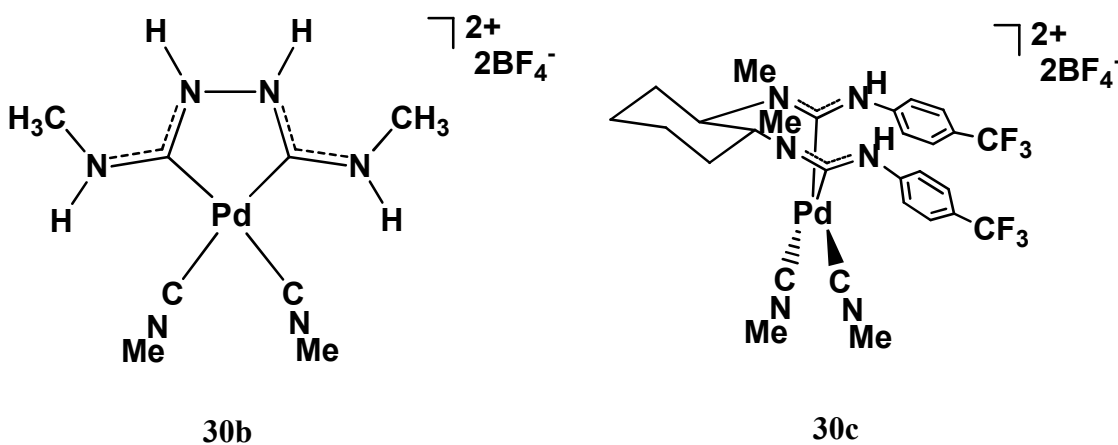


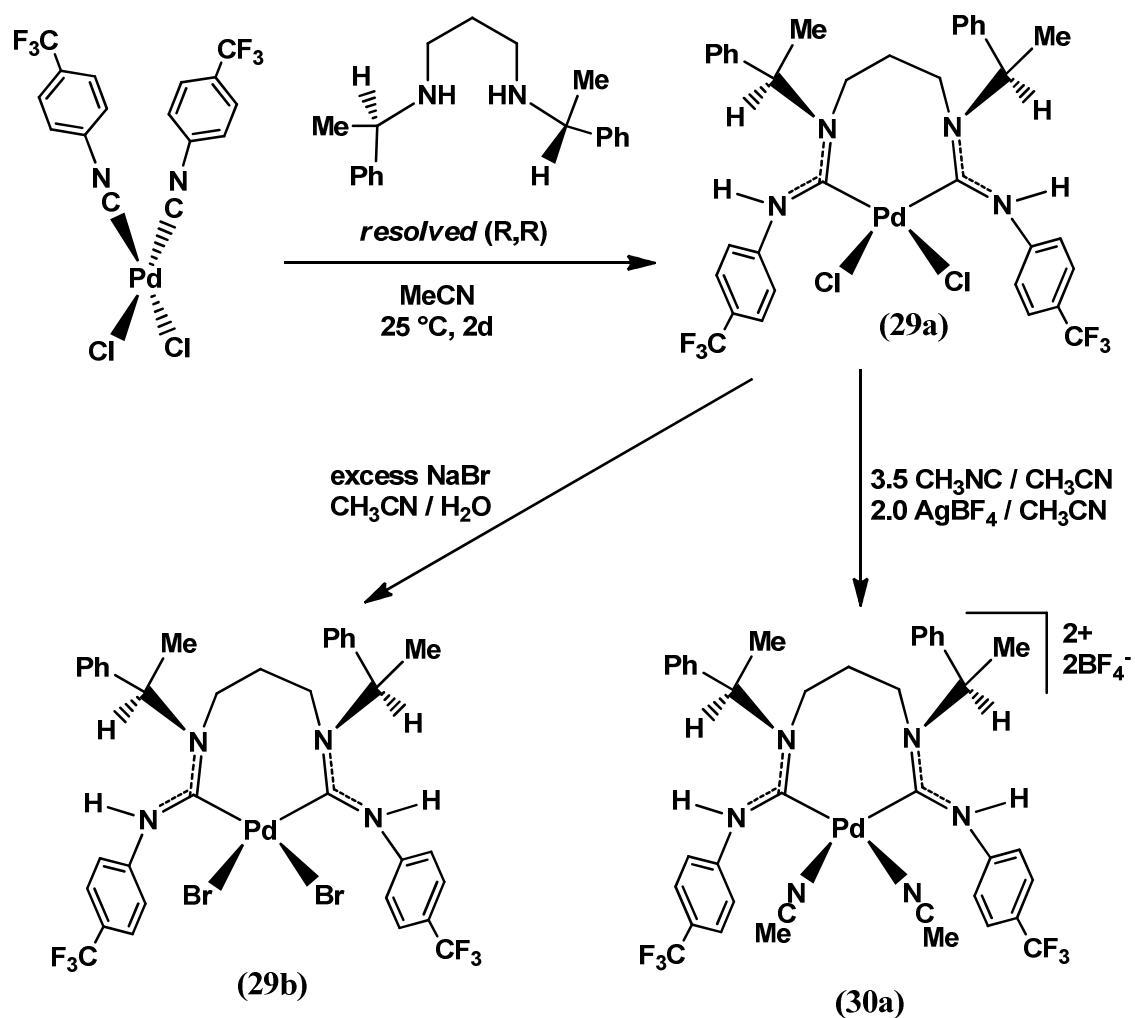
Figure 3.12 . Structure of five and seven membered chelate bis(ADC) palladium(II) bis(methylisocyanide) complexes. Adapted from References from 67 and 77.

**N,N'-Bis[(R)-1-phenylethyl]-bis(ADC) bis(methylisocyanide) palladium
bis(tetrafluoroborate) complex 30a**

Reaction of *cis* bis(*p*-trifluoromethylphenylisocyanide) palladium(II) dichloride with N,N'-bis[(*R*)-1-phenylethyl]-1,3-diaminopropane in dichloromethane for 2 days produced a white microcrystalline eight membered-chelate bis(acyclic diaminocarbene) PdCl₂ complex **29a**.⁷⁸ The dichloride complex **29a** was treated with excess methylisocyanide in acetonitrile. This mixture was stirred at room temperature for 2 hours to produce the acetonitrile adduct. The chloride anions in the bis(ADC) palladium acetonitrile adduct were replaced with tetrafluoroborate anions by treatment with silver tetrafluoroborate in acetonitrile. Immediately after the addition of AgBF₄, the reaction mixture started to precipitate silver chloride, and it was stirred for two hours to complete the reaction. The reaction mixture was filtered through celite to remove the silver chloride. The product was isolated by layering diethyl ether onto the concentrated solution in acetonitrile.

The ¹H NMR spectrum of complex **30a** in DMSO-d₆ displayed two inequivalent NH signals at 10.43 and 10.25 ppm, two inequivalent Ph(CH₃)CH broad signals at 5.92 and 5.83 ppm, and a pair of Ph(CH₃)CH doublets at 1.57 and 1.41 ppm. In addition, each of the six protons on the propylene linker gives rise to a unique multiplet, with chemical shifts ranging from 4.35 to 0.56 ppm. This suggests that the propylene backbone of the chelate ring is conformationally rigid in solution. The two nitrogen-bound methyl groups showed two singlets at 3.68 and 3.64 ppm. These data are consistent with a reported chelating bis(ADC) bis(methylisocyanide) palladium complex possessing C₁ symmetry,⁶⁷ with the two chiral N-substituents occupying stereochemically distinct

environments. The ^{13}C NMR in $\text{DMSO-}d_6$ showed two signals for carbene carbons at 188.69 and 187.32 ppm. All methyl, methylene and methine carbons showed one signal each for each carbon. These ^{13}C NMR data confirm the C1 symmetry in the complex. The IR spectrum showed two overlapping peaks for the methylisocyanide stretching frequency ($\nu \text{C}\equiv\text{N}$), and the average value was 2270 cm^{-1} ($\Delta\nu = 110 \text{ cm}^{-1}$).



Scheme 3.7. Formation of eight membered chelate bis(ADC) complexes **29a**, **29b** and **30a**

All attempts to grow X-ray quality crystals of complexes **29a** and **30a** were unsuccessful. Bis(ADC)PdCl₂ **29a** was not sufficiently soluble in any solvent, and it was converted to the more soluble bis(ADC)PdBr₂ analogue **29b** by treatment with excess NaBr in aqueous CH₃CN. The ¹³C NMR spectrum of **29b** revealed two inequivalent carbene resonances at 193.6 and 191.6 ppm, slightly downfield compared to the analogous bis(methylisocyanide) bis(ADC) complex (**30a**).

Crystals of complex **29b** were grown by slow evaporation of an acetonitrile solution of the complex. These crystals were grown as transparent rods, and X-ray structure confirmed a C₁-symmetric conformation of the chiral bis(ADC) ligand. The complex crystallized in the chiral orthorhombic space group P2₁2₁2₁, and X-ray anomalous dispersion effects substantiated the (R,R) stereochemistry of the ligand. The two (R)-1-phenylethyl N-substituents show the same orientation relative to the nitrogen to which they are attached. They adopt this orientation to minimize steric interactions with each other and the propylene linkage, resulting in the two phenyl groups pointing toward different sides of the molecule. The propylene linkage is folded away from the palladium atom and forms an eight-membered chelating ring with a chair-like geometry.

In the structure, strain in the bis(ADC) ligand is visible, caused by the steric influence of the N-substituent. The hydrogens of the propylene carbons C3 and C5 are very close to neighboring NH hydrogens (1.86 and 1.85 Å) to minimize the steric interaction between the chiral groups and the propylene linker. In addition, the substituents on the carbene nitrogen are twisted away from the NCN planes to avoid steric interactions, but this also disrupts favorable π -electron conjugation in the carbene units.

This strain is evident in the torsion angles between the NCN planes and the carbons of the chiral N-substituents: the N1–C1–N3–C3 torsion angle is 14.1(5)°, and the N2–C2–N4–C5 torsion angle is 9.0(5)°. The N2–C2–N4–C8 torsion angle of 174.0(3)° also indicates a substantial deviation from co-planarity at the end of the propylene linker that is closest to a phenyl ring of the N-substituents, suggesting that steric repulsions are occurring. The Pd-C_{carbene} distances of 1.981(4) and 2.012(3) Å are similar to values observed in the related 7-membered chelate bis(ADC) complexes.⁶⁷

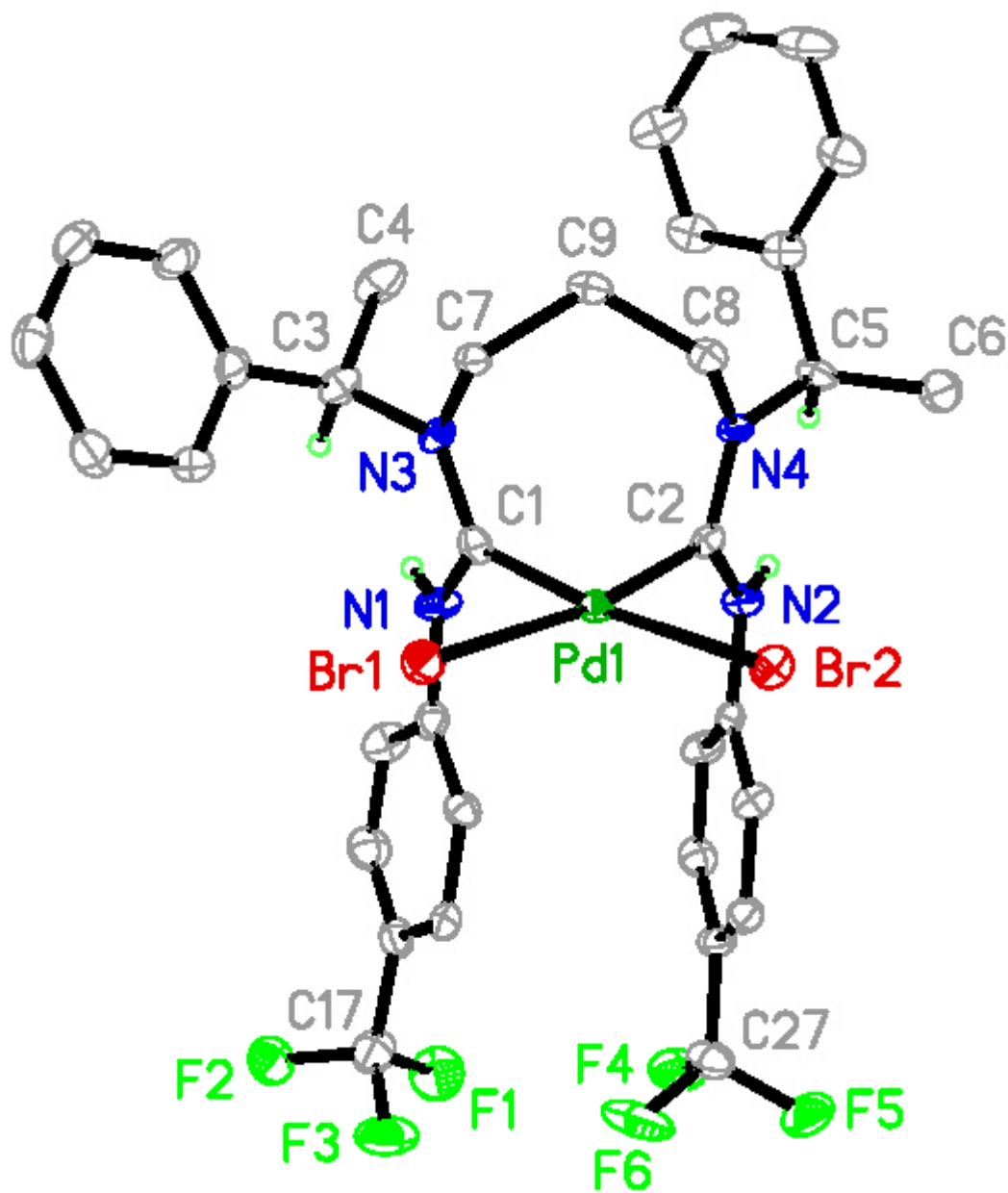


Figure 3.13. Molecular structure of complex **29b** with 50% probability ellipsoids.

Tetrafluoroborate counter ions are omitted for clarity.

Table 3.24. Selected bond lengths (Å) and bond angles (°) of complex **29b**

	Bond Lengths (Å)
Pd(1)-C(1)	1.981(4)
Pd(1)-C(2)	2.012(3)
Pd(1)-Br(1)	2.5207(4)
P(1)-Br(2)	2.5302(4)
C(1)-N(1)	1.347(4)
C(1)-N(3)	1.335(4)
C(2)-N(2)	1.338(4)
C(2)-N(4)	1.330(4)

	Bond angles (°)
C(1)-Pd(1)-C(2)	84.06(13)
Br(1)-Pd(1)-Br(2)	94.991(13)
C(1)-Pd(1)-Br(1)	88.68(10)
C(2)-Pd(1)-Br(2)	91.74(9)
C(1)-Pd(1)-Br(2)	173.78(10)
C(2)-Pd(1)-Br(1)	170.64(9)
N(1)-C(1)-N(3)	116.6(3)
N(2)-C(2)-N(4)	118.9(3)

Table 3.25. Crystal data and structure refinement details for complex **29b**

Empirical formula	C ₃₅ H ₃₄ Br ₂ F ₆ N ₄ Pd
Formula weight	890.88
Crystal system	Orthorhombic
Space group	P 2 ₁ 2 ₁ 2 ₁
Unit cell dimensions	a = 7.31230(10) Å α = 90 ° b = 17.5737(2) Å β = 90 ° c = 26.6940(3) Å γ = 90 °
Volume	3430.29(7) Å ³
Z	4
Density (calculated)	1.725 Mg/m ³
Absorption coefficient	2.935 mm ⁻¹
Crystal size	0.33 x 0.07 x 0.04 mm
θ range for data collection	1.53 – 25.63 °
Index range	-8 ≤ h ≤ 8 -21 ≤ k ≤ 21 -32 ≤ l ≤ 32
Temperature	115(2) K
Wave length	0.71073 Å
Reflections collected	26414
Independent reflections	6452 (R _{int} = 0.0483)
Final R indices [I > 2σ(I)]	R1 = 0.0265 wR2 = 0.0538
R indices (all data)	R1 = 0.0323 wR2 = 0.0557
Goodness-of-fit on F ²	1.016

Five membered chelate Chugaev-type bis(ADC) palladium(II) bis(methylisocyanide) complex 30b

Complex **30b** was synthesized using a reported procedure.⁷⁹ Transparent, needle-shaped crystals were grown by the slow diffusion of diethyl ether into an acetonitrile solution. The X-ray crystal structure displayed C_{2v} symmetry. The Pd-C_{carbene} bond lengths, 2.012 and 2.004 Å, were slightly longer than those in previously reported analogous dichloride complex.⁸⁰ Bond lengths from the carbene carbon atoms C(1) and C(2) to adjacent nitrogen atoms N(1), N(2), N(3) and N(4) were very close due to delocalized π electrons among these atoms. The average bond length was 1.319 Å, and this was longer than the reported double bond distance for Csp^2 -N (1.28 Å) due to the π electron delocalization. The C_{carbene}-Pd-C_{carbene} (79.69°) angle and the N-C_{carbene}-N (avg: 118.3°) angles were similar to the analogous dichloride complex. The only significant structural difference between these two complexes was the shorter palladium carbene bond length in the dichloride complex. The IR spectrum shows two overlapping peaks for the methylisocyanide stretching frequency (ν C \equiv N), and the average value was 2268 cm⁻¹ ($\Delta\nu = 108$ cm⁻¹).

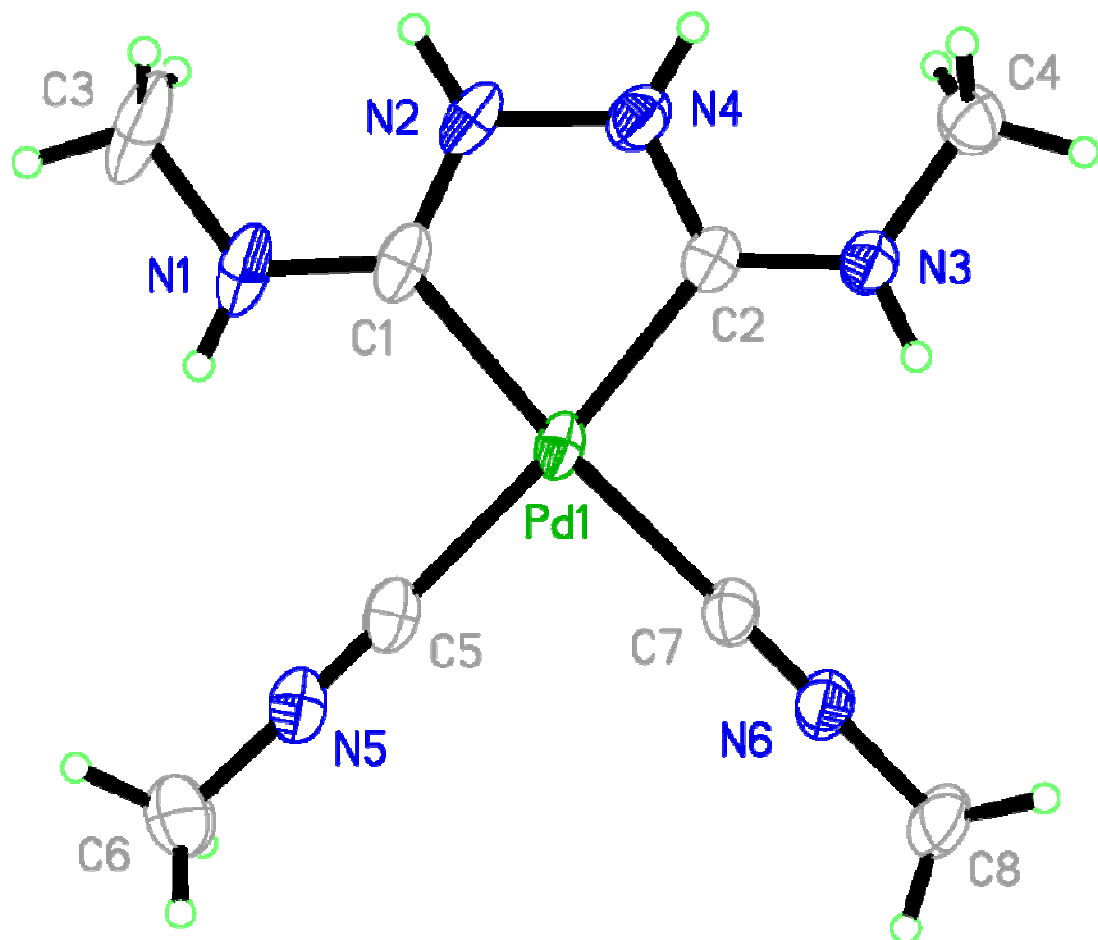


Figure 3.14. Molecular structure of complex **30b** with 50% probability ellipsoids.

Tetrafluoroborate counter ions are omitted for clarity.

Table 3.26. Selected bond lengths (Å) and bond angles (°) of complex **30b**

	Bond Lengths (Å)
Pd(1)-C(1)	2.0117(19)
Pd(1)-C(2)	2.004(2)
Pd(1)-C(5)	2.019(2)
P(1)-C(15)	2.0198(19)
C(1)-N(1)	1.316(3)
C(1)-N(2)	1.321(3)
C(2)-N(3)	1.312(3)
C(2)-N(4)	1.327(3)
C(5)-N(5)	1.135(3)
C(7)-N(6)	1.131(3)
	Bond angles (°)
C(1)-Pd(1)-C(2)	79.69(8)
C(5)-Pd(1)-C(7)	90.35(8)
C(1)-Pd(1)-C(5)	94.80(9)
C(2)-Pd(1)-C(7)	95.03(8)
C(1)-Pd(1)-C(7)	174.40(9)
C(2)-Pd(1)-C(5)	173.43(8)
N(1)-C(1)-N(2)	118.3(2)
N(3)-C(2)-N(4)	118.21(19)

Table 3.27. Crystal data and structure refinement details for complex **30b**

Empirical formula	C ₉ H _{19.89} B ₂ F ₈ N ₇ O _{2.45} Pd
Formula weight	545.43
Crystal system	Monoclinic
Space group	C2/c
Unit cell dimensions	a = 27.0958(3) Å α = 90 ° b = 7.796400(10) Å β = 122.2540(10) ° c = 22.5804(3) Å γ = 90 °
Volume	4034.03(9) Å ³
Z	8
Density (calculated)	1.796 Mg/m ³
Absorption coefficient	1.015 mm ⁻¹
Crystal size	0.45 x 0.19 x 0.13 mm
θ range for data collection	1.78 – 30.53 °
Index range	-37 ≤ h ≤ 35 -10 ≤ k ≤ 10 -32 ≤ l ≤ 28
Temperature	115(2) K
Wave length	0.71073 Å
Reflections collected	33776
Independent reflections	5992 (R _{int} = 0.0252)
Final R indices [I > 2σ(I)]	R1 = 0.0282 wR2 = 0.0685
R indices (all data)	R1 = 0.0342 wR2 = 0.0731
Goodness-of-fit on F ²	1.051

Comparison of σ -donor abilities and structural features of bis(carbene) and bis(phosphine) ligands

Figure 3.15 summarizes the data for σ -donicity and structural features for all newly synthesized complexes, together with two previously investigated complexes **28a** and **30c**. Complex **26d** showed the highest stretching frequency at 2282 cm^{-1} ($\Delta\nu = 122\text{ cm}^{-1}$), indicating the weakest effective σ -donor ability from the imidazole-based butylene linkage bis(NHC) ligand. The next weakest effective σ -donor ligand was the triazole-derived bis(NHC), with its palladium complex **26f** showing second highest stretching frequency at 2279 cm^{-1} ($\Delta\nu = 119\text{ cm}^{-1}$). This is followed by another imidazole based bis(NHC) ligands with a propylene linker (**26c**, $\Delta\nu = 114\text{ cm}^{-1}$), the seven-membered chelate bis(ADC) ligand (**30c**, $\Delta\nu = 113\text{ cm}^{-1}$), and the imidazole-based bis(NHC) ligand with an ethylene linkage (**26b**, $\Delta\nu = 112\text{ cm}^{-1}$). The DPPBen palladium complex **28f** showed similar donation to the bis(NHC) complex **26b**. The bite angles for complexes **26b**, 83.90° , and **28f**, 84.80° , were very close, but the chelating ring size was one atom larger for **26b** (seven membered chelating ring). DPPBen was the weakest σ -donor ligand among all investigated bis(phosphine) ligands. Another bis(phosphine) complex **28c**, containing DPPB, also showed the same stretching frequency as **26b** and **28f** (2272 cm^{-1}), but it cannot be used in this IR probe study. Because of the *trans* orientation of the chelate ligand in complex **28c**, the methylisocyanide ligands are not properly oriented to assess the donation from the phosphine ligand.

Figure 3.15. Donor scale versus ligand structure for bis(carbene) and bis(phosphine) ligands

Weaker effective donor		Weaker effective donor	
	$\nu(\text{CN})_{\text{avg}} = 2282 \text{ cm}^{-1}$ $\Delta\nu = 122$ Bite angle = 89.80°		$\nu(\text{CN})_{\text{avg}} = 2270 \text{ cm}^{-1}$ $\Delta\nu = 110$ Bite angle = 84.06°
	$\nu(\text{CN})_{\text{avg}} = 2279 \text{ cm}^{-1}$ $\Delta\nu = 119$ Bite angle = 79.5°		$\nu(\text{CN})_{\text{avg}} = 2269 \text{ cm}^{-1}$ $\Delta\nu = 109$ Bite angle = 84.03°
	$\nu(\text{CN})_{\text{avg}} = 2274 \text{ cm}^{-1}$ $\Delta\nu = 114$ Bite angle = 85.26°		$\nu(\text{CN})_{\text{avg}} = 2268 \text{ cm}^{-1}$ $\Delta\nu = 108$ Bite angle = 79.69°
	$\nu(\text{CN})_{\text{avg}} = 2273 \text{ cm}^{-1}$ $\Delta\nu = 113$ Bite angle = 82.76°		$\nu(\text{CN})_{\text{avg}} = 2268 \text{ cm}^{-1}$ $\Delta\nu = 108$ Bite angle = 89.02°
	$\nu(\text{CN})_{\text{avg}} = 2272 \text{ cm}^{-1}$ $\Delta\nu = 112$ Bite angle = 83.90°		$\nu(\text{CN})_{\text{avg}} = 2268 \text{ cm}^{-1}$ $\Delta\nu = 108$ Bite angle = 84.08°
	$\nu(\text{CN})_{\text{avg}} = 2272 \text{ cm}^{-1}$ $\Delta\nu = 112$ Bite angle = 84.80°		$\nu(\text{CN})_{\text{avg}} = 2262 \text{ cm}^{-1}$ $\Delta\nu = 102$ Bite angle = 79.50°
	$\nu(\text{CN})_{\text{avg}} = 2272 \text{ cm}^{-1}$ $\Delta\nu = 112$ Bite angle = 170.17°		$\nu(\text{CN})_{\text{avg}} = 2251 \text{ cm}^{-1}$ $\Delta\nu = 91$ Bite angle = 88.96°
Stronger donor		Stronger donor	

The lowest stretching frequency, 2251 cm^{-1} ($\Delta\nu = 91\text{ cm}^{-1}$), was found in the ‘abnormal’ C4-bound bis(NHC) complex **26e**. Therefore, this is the strongest donating ligand among all investigated. The bite angle for complex **26e** is 88.96° , very close to the ideal value in square planar complexes. Complex **28a** with the DPPE ligand showed the next lowest stretching frequency, 2262 cm^{-1} ($\Delta\nu = 102\text{ cm}^{-1}$), followed by two more complexes of bis(phosphine) ligands (**28e** and **28b**) and a bis(ADC) complex **30b** at the same value, 2268 cm^{-1} . These results suggest that most of the bis(phosphine) ligands are stronger donor ligands than bis(NHC) except for the abnormal bis(NHC), in this type of dicationic Pd(II) complexes, which contradicts previous studies on NHC versus phosphine ligands.⁴¹⁻⁴⁵ Those studies suggest that NHCs are stronger donor ligands than phosphines, but almost all of these studies were done on monodentate ligands. Only one previous studies done in our lab⁶⁷ indicates that bis(phosphines) are stronger donor than bis(NHCs), but here ligands with two different chelating ring size were used. All phosphine ligands with five-membered chelating ring sizes (**28a**, **28e** and **28f**) were stronger donor ligands than the bis(NHC) five membered chelate complex **5f**. Six membered chelate complexes also showed the same trend where bis(phosphine) DPPProp (in complex **28b**) was a stronger donor than the methylene linkage bis(NHC) ligand (in complex **26a**). No seven membered chelate bis(phosphine) complex was synthesized, as synthetic attempts produced dimeric complex **28c** with the DPPBut ligand.

Bis(ADC) ligands showed intermediate donor ability compared to bis(phosphine) and bis(NHC) ligands. Within five membered chelating ring ligands, bis(ADC) complex **30b** was a stronger donor than the bis(NHC) ligand of **26f** and a weaker effective donor than the bis(phosphine) ligands DPPE and DMPE in complexes **28a** and **28e**. However,

another five-membered bis(phosphine) complex **28f** showed weaker donation than the Chugaev complex **30b**. Therefore, based on these studies, ‘abnormal’ C4-bound bis(NHC) ligands are the strongest donor ligands, bis(phosphine) ligands are the next strongest donor ligands, and C2-bound bis(NHC) ligands are the weakest effective donor ligands. The bis(ADC) ligands fall in between bis(phosphine) and bis(NHC) in ligand donor ability.

A trend can be observed within homologous ligand series. The σ -donation from the bis(ligand) decreases with increasing chelating ring size, while other parameters such as substituent and backbone are kept constant. For the imidazole-derived C2-bound bis(NHC) series, σ -donation decreased from **26a** to **26d** ($\Delta\nu$: $109\text{ cm}^{-1} \rightarrow 122\text{ cm}^{-1}$) as chelating ring size increased (6 \rightarrow 9). In addition, both bite angle and dihedral angle also increased from **26a** to **26d**, except for bite angle from **26a** to **26b** and dihedral angle from **26c** to **26d**. Similarly, the five membered chelating ring DPPE ligand of **28a** ($\Delta\nu = 102\text{ cm}^{-1}$) showed stronger donation than DPPProp, which forms the six membered chelate complex **28b** ($\Delta\nu = 102\text{ cm}^{-1}$).

Summary and Conclusion

A series of bis(NHC), bis(phosphine) and bis(ADC) palladium(II) bis(methylisocyanide) tetrafluoroborate complexes were synthesized and fully characterized. For all of these complexes except complex **28d**, X-ray crystal structures were determined. Changes in stretching frequencies of methylisocyanide in the palladium complexes reflect the amount of σ -donation from the ligand *trans* to methylisocyanide. All of the complexes with X-ray crystal structure except complex **28c** showed *cis*

orientations of the two methylisocyanide ligands, which is essential to assess the σ -donation from the ligand *trans* to methylisocyanide. According to methylisocyanide stretching frequencies, the imidazole-derived 'abnormal' C4-bound bis(NHC) ligand was the strongest donor ligand among all investigated chelate ligands. Generally, imidazole derived C2-bound or triazole-derived C3-bound bis(NHC) ligands are the weakest effective donor ligands, followed by bis(ADC). Identification of stronger donation from bis(phosphine) ligands than from bis(carbenes) contradicts most previous studies.⁴¹⁻⁴⁵ This may arise from the use of cationic Pd(II) complexes, whereas other studies used neutral complexes. Donicity decreases with increasing chelating ring size within a homologous ligand series, with other structural and electronic parameters kept constant.

Experimental

General Considerations. All manipulations were carried out under air unless otherwise noted. Diethyl ether (Acros) and hexanes (Pharmco) were purified by distillation from sodium benzophenone ketyl. Dichloromethane (Pharmco) was washed with a sequence of concentrated H₂SO₄, de-ionized water, 5% Na₂CO₃ and de-ionized water, followed by pre drying over anhydrous CaCl₂, then refluxing over and distillation from P₂O₅ under nitrogen. Acetonitrile (Pharmco) was pre-dried over anhydrous CaCl₂ and then refluxed over and distilled from CaH₂ under nitrogen. Water was purified by an E-pure system (Barnstead) and had a resistivity of >17.6 M Ω cm. NMR solvents were purchased from Cambridge Isotope Laboratories. DMSO-*d*₆ and CD₃CN-*d*₃ were dried over activated 4 Å molecular sieves followed by vacuum distillation at room temperature. CD₂Cl₂ was dried over activated 4 Å molecular sieves and stored over P₂O₅ before

distillation at room temperature for use. All other reagents were purchased from Acros, Aldrich, or Strem and used as received. *p*-Trifluoromethyl isocyanide⁸¹ methylisocyanide,⁸² (COD)PdCl₂,⁸³ [(DPPE)Pd(CH₃CN)₂][BF₄]₂ **5a**,⁶⁷ (DPPPprop)PdCl₂ **4b**,⁸⁴ (DPPBut)PdCl₂ **4c**,⁸⁵ (DPPPEn)PdCl₂ **4d**,⁸⁶ (DMPE)PdCl₂ **4e**,⁸⁷ and (DPPBen)PdCl₂ **4f**⁸⁸ were prepared by published procedures. NMR spectra were acquired on Varian GEMINI 2000 (300 MHz) and Unity INOVA (400 MHz) spectrometers. Reported NMR shifts were referenced to residual solvent peaks (¹H, ¹³C) or to a calibrated external standard (³¹P). IR spectra were acquired from Nujol mulls on a Nicolet Protégé 460 FT-IR or Perkin Elmer system 2000 FT-IR spectrometer using 0.5 cm⁻¹ resolution. Elemental analyses were performed by Midwest Microlab, LLC, Indianapolis. X-ray diffraction data were collected on a Bruker SMART APEX II diffractometer with a CCD detector using a combination of φ and ω scans. A Bruker Kryoflex liquid nitrogen cooling device was used for low-temperature data collections. Data integration employed the Bruker SAINT software package.⁸⁹ All X-ray diffraction experiments employed graphite-monochromated Mo K α radiation ($\lambda=0.71073$ Å). Structures were solved by direct methods and refined by full-matrix least-squares on *F*² using the SHELXTL software suite.⁹⁰ Non-hydrogen atoms were assigned anisotropic temperature factors, with hydrogen atoms included in calculated positions (riding model).

1,1',2,2'-Tetramethyl-3,3'-methylenediimidazolium dibromide (24e)

A mixture of 1,2-dimethylimidazole (1000 mg, 10.40 mmol) and dibromomethane (439 μ L, 6.24 mmol) was mixed with toluene (15 ml) in a thick-walled glass vessel. The reaction mixture was stirred at reflux temperature for 12 hours. The

formed precipitate was filtered off and washed with toluene and Et₂O to isolate the bis(imidazolium) salt. Yield: 1040 mg, 69 %. ¹H NMR (400 MHz, DMSO-d₆): δ 7.99 (d, 4H, ³J_{HH} = 2 Hz, *imidazole*), 7.79 (d, 2H, ³J_{HH} = 2 Hz, *imidazole*), 6.77 (s, 2H, CH₂), 3.79 (s, N-CH₃), 2.77 (s, 6H, C-CH₃). ¹³C NMR (100 MHz, DMSO-d₆): δ 146.53 (imid. N-C-N), 123.05 (imid. C), 120.97 (imid. C), 56.74 (N-CH₂), 35.13 (imid.N-CH₃), 10.44 (imid.C-CH₃).

(1,1'-Dimethyl-3,3'-ethylenediimidazol-2,2-diylidene) palladium(II) dibromide (25b)

A mixture of PdBr₂ (200 mg, 0.751 mmol), sodium acetate trihydrate (245 mg, 1.803 mmol) and 1,1'-dimethyl-3,3'-ethylenediimidazolium dibromide (317 mg, 0.905 mmol) were dissolved in wet DMSO (10 mL), and the mixture was heated at 75 °C for 3 h. The mixture was cooled to room temperature, solvent volume was reduced under vacuum, and water was added to get product as pale yellow crystals. Product was isolated by filtration and was dried in vacuo for 12 h. Yield: 185 mg, 53 %. ¹H NMR (400 MHz, DMSO-d₆): δ 7.32 (d, 4H, ³J_{HH} = 13.2 Hz, *imidazole*), 5.20 (br s, 2H, CH₂), 4.49 (br d, 2H, ³J_{HH} = 7.2 Hz, CH₂), 3.86 (s, 6H, N-CH₃). ¹³C NMR (100 MHz, DMSO-d₆): δ 156.86 (carbene), 123.73 (imid. C), 122.60 (imid. C), 46.68 (N-CH₂), 38.26 (imid. N-CH₃), 38.24 (imid.N-CH₃). Anal. Calculated for: C₁₀H₁₄ Br₂N₄Pd: C, 26.31; H, 3.09; N, 12.28 %. Found: C, 26.52; H, 3.14; N, 12.03 %.

(1,1'-Dimethyl-3,3'-propylenediimidazol-2,2-diylidene) palladium(II) dibromide (25c)

A mixture of PdBr₂ (250 mg, 0.939 mmol), sodium acetate trihydrate (307 mg, 2.253 mmol) and 1,1'-dimethyl-3,3'-propylenediimidazolium dibromide (413 mg, 1.127 mmol) were dissolved in wet DMSO (10 mL) and heated at 75 °C for 3 h. The mixture was cooled to room temperature, solvent volume was reduced under vacuum, and water was added to get product as pale yellow crystals. Product was isolated by filtration and dried in vacuo for 12 h. Yield: 307 mg, 69 %. ¹H NMR (400 MHz, DMSO-d₆): δ 7.30 (d, 4H, ³J_{HH} = 16.8 Hz, *imidazole*), 4.84 (t, 2H, ³J_{HH} = 12.8 Hz, CH₂), 4.37-4.32 (dd, 2H, ³J_{HH} = 14.2, 5.6 Hz, CH₂), 3.91 (s, 6H, N-CH₃), 2.34-2.30 (m, 1H, CH₂), 1.78-1.68 (m, 1H, CH₂). ¹³C NMR (100 MHz, DMSO-d₆): δ 1160.29 (carbene), 123.07 (imid. C), 122.96 (imid. C), 51.33 (N-CH₂), 37.58 (C-CH₂), 31.28 (imid.N-CH₃). Anal. Calculated for: C₁₁H₁₆ Br₂N₄Pd: C, 28.08; H, 3.43; N, 11.91 %. Found: C, 27.95; H, 3.28; N, 11.76 %.

(1,1',2,2'-Tetramethyl-3,3'-methylenediimidazol-2,2'-diylidene) palladium(II) dibromide (25e)

A mixture of Pd(OAc)₂ (100 mg, 0.445 mmol) and 1,1',2,2'-tetramethyl-3,3'-methylenediimidazolium dibromide (163 mg, 0.445 mmol) were dissolved in DMSO (5 mL), and the mixture was heated at 50 °C for 2 hours followed by 110 °C for 3 hours. CH₂Cl₂ was added to the reaction mixture to get pale yellow crystals. Product was isolated by filtration and was dried in vacuo for 12 h. Yield: 165 mg, 75 %. ¹H NMR (400 MHz, DMSO-d₆): δ 7.03 (s, 2H, *imidazole*), 6.06 (s, 2H, CH₂), 3.67 (s, 6H, N-

CH_3), 2.65 (s, 6H, C- CH_3), Anal. Calculated for: $C_{11}H_{16}Br_2N_4Pd$: C, 28.08; H, 3.43; N, 11.91 %. Found: C, 27.56; H, 3.35; N, 11.26 %.

**[(1,1'-Dimethyl-3,3'-methylenediimidazol-2,2'-diylidene) palladium(II) (CNCH₃)₂]
[BF₄]₂ (26a)**

Methyl isocyanide (16 μ L, 0.283 mmol) was added to a stirred solution of (1,1'-dimethyl-3,3'-methylenediimidazol-2,2'-diylidene)palladium(II) dibromide (50 mg, 0.113 mmol) in acetonitrile (10 mL,) and the mixture was stirred for 1 h. Then $AgBF_4$ (44 mg, 0.226 mmol) was added, and the reaction mixture was stirred for 2 h. The mixture was filtered through celite, solvent was evaporated, and the solid was dried in vacuum for 12 h. The product was again dissolved in acetonitrile (5 mL), it was filtered through celite, solvent was evaporated, and the solid was dried in vacuum for 12 h. This sequence was repeated one more time. In the final sequence, diethyl ether was added to the filtrate to obtain product as white crystals. The product was isolated by filtration and dried in vacuo for 12 h. Yield: 48 mg, 72 %. 1H NMR (300 MHz, DMSO- d_6): δ 7.74(d, 2H, $^3J_{HH} = 2$ Hz, imidazole), δ 7.57(d, 2H, $^3J_{HH} = 2$ Hz, imidazole), δ 6.35 (br s, 2H, CH_2), 3.86 (s, 6H, CN- CH_3), 3.71 (s, 6H, imid.N- CH_3). ^{13}C NMR (100 MHz, CD_3CN-d_3): δ 155.56 (carbene), 124.07 (imid. C), 123.02(imid. C), 62.38(N- CH_2), 38.24 (imid. N- CH_3), 30.40 (CN- CH_3). IR (Nujol, cm^{-1}): 2269 v(m). Anal. Calculated for $C_{13}H_{18}B_2F_8N_6Pd.0.22CH_2Cl_2$: C, 28.36; H, 3.33; N, 14.93 %. Found: C, 28.26; H, 3.15; N, 14.71 %.

**[(1,1'-Dimethyl-3,3'-ethylenediimidazol-2,2'-diylidene)palladium(II) (CNCH₃)₂]
[BF₄]₂ (26b)**

Methyl isocyanide (31 μ L, 0.548 mmol) was added to a stirred solution of {1,1'-dimethyl-3,3'-ethylenediimidazol-2,2'-diylidene}palladium(II) dibromide (100 mg, 0.219 mmol) in acetonitrile (10 mL) and the solution was stirred for 1 h. Then AgBF₄ (85 mg, 0.438 mmol) was added and the reaction mixture was stirred for 2 h. The mixture was filtered through celite, solvent was evaporated, and product was dried in vacuum for 12 h. The product was again dissolved in acetonitrile (5 mL), it was filtered through celite, solvent was evaporated, and product was dried in vacuum for 12 h. This sequence was repeated 2 more times. In the final sequence, diethyl ether was added to the filtrate to obtain product as white crystals. Product was isolated by filtration and was dried in vacuum for 12 h. Yield: 48 mg, 40 %. ¹H NMR (400 MHz, CD₃CN-d₃): δ 7.27 (d, 2H, ³J_{HH} = 2 Hz, *imidazole*), 7.22 (d, 2H, ³J_{HH} = 2 Hz, *imidazole*), 4.95-4.87 (m, 2H, CH₂), 4.54-4.46 (m, 2H, CH₂), 3.78 (s, 6H, CN-CH₃), 3.50 (s, 6H, imid.N-CH₃). ¹³C NMR (100 MHz, CD₃CN-d₃): δ 153.96 (carbene), 125.77 (imid. C), 125.04 (imid. C), 48.18 (N-CH₂), 39.28 (imid.N-CH₃), 30.99 (t, ³J_{HH} = 7.4 Hz, CN-CH₃). IR (Nujol, cm⁻¹): 2272 v(m). Anal. Calculated for C₁₄H₂₀ B₂F₈N₆Pd: C, 30.44; H, 3.65; N, 15.22 %. Found: C, 30.66; H, 3.65; N, 15.21 %.

**[(1,1'-Dimethyl-3,3'-propylenediimidazol-2,2'-diylidene) palladium(II) (CNCH₃)₂]
[BF₄]₂ (26c)**

Methyl isocyanide (30 μ L, 0.531 mmol) was added to a stirred solution of {1,1'-dimethyl-3,3'-propylenediimidazol-2,2'-diylidene}palladium(II) dibromide (100 mg,

0.213 mmol) in acetonitrile (10 mL), and it was stirred for 1 h. Then AgBF₄ (83 mg, 0.425 mmol) was added to the reaction mixture, and it was stirred for 2 h. The mixture was filtered through celite, solvent was evaporated, and product was dried in vacuum for 12 h. The solid was again dissolved in acetonitrile (5 mL), it was filtered through celite, solvent was evaporated, and product was dried in vacuum for 12 h. This sequence was repeated 2 more times. In the final sequence, diethyl ether was added to the filtrate to obtain product as white crystals. Product was isolated by filtration and dried in vacuo for 12 h. Yield: 56 mg, 47 %. ¹H NMR (400 MHz, CD₃CN-d₃): δ 7.20 (d, 2H, ³J_{HH} = 2 Hz, *imidazole*), 7.16 (d, 2H, ³J_{HH} = 1.6 Hz, *imidazole*), 4.61-4.55 (dd, 2H, ³J_{HH} = 14.8 & 11.2 Hz, CH₂), 4.38-4.33 (m, 2H, ³J_{HH} = 15 & 5.8 Hz, CH₂), 3.82 (s, 6H, CN-CH₃), 3.46 (s, 6H, imid.N-CH₃), 2.33-2.26(m, 1H, CH₂), 1.98-1.88(m, 1H, CH₂). ¹³C NMR (100 MHz, CD₃CN-d₃): δ 155.74 (carbene), 125.69 (imid. C), 125.45 (imid. C), 52.99 (N-CH₂), 38.82 (imid. N-CH₃), 31.67 (C-CH₂), 30.89 (t, CN-CH₃). IR (Nujol, cm⁻¹): 2274 v(m). Anal. Calculated for C₁₅H₂₂ B₂F₈N₆Pd: C, 31.81; H, 3.92; N, 14.84 %. Found: C, 31.83; H, 3.84; N, 14.64 %.

**[(1,1'-Dimethyl-3,3'-butylenediimidazol-2,2'-diylidene) palladium(II) (CNCH₃)₂]
[BF₄]₂ (26d)**

Methyl isocyanide (27 μL, 0.474 mmol) was added to a stirred solution of {1,1'-dimethyl-4,4'-butylenediimidazol-2,2'-diylidene}palladium(II) chloride (75 mg, 0.189 mmol) in acetonitrile (10 mL), and it was stirred for 1 h. Then AgBF₄ (74 mg, 0.379 mmol) was added to the reaction mixture, and it was stirred for 2 h. The mixture was filtered through celite, solvent was evaporated, and the product was dried in vacuum for

12 h. The solid was again dissolved in acetonitrile (5 mL), it was filtered through celite, solvent was evaporated, and product was dried in vacuum for 12 h. This sequence was repeated 2 more times. In the final sequence, diethyl ether was added to the filtrate to obtain product as white crystals. Product was isolated by filtration and dried in vacuo for 12 h. Yield: 68 mg, 62 %. ^1H NMR (400 MHz, $\text{CD}_3\text{CN-d}_3$): δ 7.24 (s, 4H, *imidazole*), 4.50 (br s, 2H, CH_2), 4.21 (br s, 2H, CH_2), 3.82 (s, 6H, CN-CH_3), 3.44 (s, 6H, imid.N- CH_3), 2.01 (br s, 2H, CH_2), 1.52 (br s, 2H, CH_2), ^{13}C NMR (100 MHz, $\text{CD}_3\text{CN-d}_3$): δ 154.64 (carbene), 126.66 (imid. C), 123.97 (imid. C), 47.12 (N- CH_2), 38.87 (imid. N- CH_3), 30.96 (t, CN-CH_3), 26.00 (C- CH_2). IR (Nujol, cm^{-1}): 2282 v(m). Anal. Calculated for $\text{C}_{16}\text{H}_{24}\text{B}_2\text{F}_8\text{N}_6\text{Pd}$: C, 33.11; H, 4.17; N, 14.48 %. Found: C, 33.35; H, 4.25; N, 14.40 %.

[(1,1',2,2'-Tetramethyl-3,3'-methylenediimidazol-4,4'-diylidene) palladium(II) (CNCH_3) $_2$] [BF_4] $_2$ (26e)

Methyl isocyanide (18 μL , 0.319 mmol) was added to a stirred solution of {1,1',2,2'-tetramethyl-3,3'-methylenediimidazol-2,2'-diylidene }palladium(II) dibromide (60 mg, 0.128 mmol) in acetonitrile (10 mL), and the solution was stirred for 1 h. Then AgBF_4 (50 mg, 0.255 mmol) was added, and the reaction mixture was stirred for 2 h. The mixture was filtered through celite, solvent was evaporated, and product was dried in vacuum for 12 h. The product was again dissolved in acetonitrile (5 mL), it was filtered through celite, solvent was evaporated, and it was dried in vacuum for 12 h. This sequence was repeated 2 more times. In the final sequence, diethyl ether was added to the filtrate to obtain product as white crystals. Product was isolated by filtration and was

dried in vacuo for 12 h. Yield: 53 mg, 74 %. ^1H NMR (400 MHz, $\text{CD}_3\text{CN-d}_3$): δ 6.98 (s, 2H, *imidazole*), 5.86 (s, 2H, CH_2), 3.67 (s, 6H, CN-CH_3), 3.53 (s, 6H, *imid.N-CH}_3*), 2.60 (s, 6H, *imid.C-CH}_3*). ^{13}C NMR (100 MHz, $\text{CD}_3\text{CN-d}_3$): δ 144.87(carbene), 133.56 (*imid.C-CH}_3*), 131.93 (t, CN-CH_3), 128.94 (*imid. CH*), 60.87 (N-CH_2), 35.23 (*imid. N-CH}_3*), 30.72 (t, CN-CH_3), 10.52 (*imid. C-CH}_3*). IR (Nujol, cm^{-1}): 2251 v(m). Anal. Calculated for $\text{C}_{15}\text{H}_{22}\text{B}_2\text{F}_8\text{N}_6\text{Pd}$: C, 31.81; H, 3.92; N, 14.84 %. Found: C, 32.08; H, 3.92; N, 14.94 %.

[1,1'-dimethyl-4,4'-bi-1,2,4-triazol-3,3'-diylidene) palladium(II) (CNCH_3) $_2$] [BF_4] $_2$ (26f)

Methyl isocyanide (27 μL , 0.475 mmol) was added to a stirred solution of [{1,1'-dimethyl-4,4'-bi-1,2,4-triazol-3,3'-diylidene}palladium(II) (NCCH_3) $_2$] $[\text{BF}_4]$ $_2$ (100 mg, 0.190 mmol) in acetonitrile (10 mL), and the solution was stirred for 2 h. Then AgBF_4 (83 mg, 0.425 mmol) was added to the reaction mixture, and it was stirred for 2 h. Solvent volume was reduced, and diethyl ether was added to the filtrate to obtain product as white crystals. Product was isolated by filtration and was dried in vacuo for 12 h. Yield: 83 mg, 83 %. ^1H NMR (400 MHz, $\text{CD}_3\text{CN-d}_3$): δ 9.20 (s, 2H, *imidazole*), 4.21 (s, 6H, CN-CH_3), 3.71 (s, 6H, *triazol.N-CH}_3*). ^{13}C NMR (100 MHz, $\text{CD}_3\text{CN-d}_3$): δ 159.87 (carbene), 135.66 (*triazol. C*), 120.82 (t, CN-CH_3), 42.12 (*triazol. N-CH}_3*), 31.88 (t, CN-CH_3). IR (Nujol, cm^{-1}): 2279 v(m). Anal. Calculated for $\text{C}_{10}\text{H}_{14}\text{B}_2\text{F}_8\text{N}_6\text{Pd}$: C, 22.82; H, 2.68; N, 21.30 %. Found: C, 22.84; H, 2.67; N, 21.30 %.

[(1,3-Bis(diphenylphosphino)propane) palladium(II) (CNCH₃)₂][BF₄]₂ (28b)

A mixture of (DPPPpropane)PdCl₂ (100 mg, 0.170 mmol), AgBF₄ (66 mg, 0.339 mmol), and anhydrous acetonitrile (10 mL) was placed in a sealed ampule under nitrogen. The reaction mixture was heated at 60 °C for 1 h with stirring. The mixture was then filtered through celite, the solvent was removed under vacuum, and the residue was dried in vacuum for 3 h. Dichloromethane (10 mL) was added, and the mixture was again filtered through celite. The filtrate was treated with methylisocyanide (24 μL, 0.424 mmol) and stirred at room temperature for 2 h. The solvent volume was reduced under reduced pressure, and diethyl ether was added to obtain product as yellow crystals. The product was isolated by filtration and dried in vacuo. Yield: 89 mg, 67%. ¹H NMR (400 MHz, DMSO-d₆), δ 7.63-7.54(m, 20H, Ph), 3.10 (s, 6H, CNCH₃), 3.00 (br s, 4H, P-CH₂), δ 2.04(br t, 2H, ³J_{HH} = 1.6 Hz, C-CH₂). ¹³C NMR (100 MHz, DMSO-d₆): δ 132.72 (dd, ²J_{PC} = 5.5 Hz, *ortho*-PPh₂), 132.55 (s, *para*-PPh₂), 129.43 (dd, ³J_{PC} = 5.5 Hz, *meta*-PPh₂), 127.41 (dd, ¹J_{PC} = 62.6, ³J_{PC} = 5.9 Hz, *ipso*-PPh₂), 29.54 (CN-CH₃), 20.26 (t, ³J_{PH} = 21.8 Hz, P-CH₂), 17.62(C-CH₂). ³¹P NMR (162 MHz DMSO-d₆): δ 2.62 (s). IR (Nujol, cm⁻¹): 2268 v(m). Anal. Calculated for C₃₁H₃₂B₂F₈N₂P₂Pd: C, 48.07; H, 4.16; N, 3.62 %. Found: C, 48.18; H, 4.32; N, 3.62 %.

[(1,4-Bis(diphenylphosphino)butane)palladium(II)-bis(methylisocyanide)][BF₄]₂ (28c)

A mixture of (DPPButane)PdCl₂ (100 mg, 0.166 mmol), AgBF₄ (65 mg, 0.331 mmol), and anhydrous acetonitrile (10 mL) was placed in a sealed ampule under nitrogen. The reaction mixture was heated at 60 °C for 2 h with stirring. The mixture was

then filtered through celite, the solvent was removed under vacuum, and the residue was dried in vacuum for 3 h. Dichloromethane (10 mL) was added and the mixture was again filtered through celite. The filtrate was treated with methylisocyanide (23 μ L, 0.414 mmol), product started to precipitate as pale yellow crystals, and the mixture was stirred at room temperature for 2 h to complete the reaction. The product was isolated by filtration and dried in vacuo. Yield: 87 mg, 77 %. ^1H NMR (400 MHz, DMSO- d_6): δ 7.74-7.61 (m, 20H, Ph), 3.21 (s, 6H, CNCH₃), 2.90 (br s, 4H, CH₂), 1.83-1.78 (br d, $^3J_{\text{CH}} = 24.4$ Hz, 4H, CH₂). ^{13}C NMR (100 MHz, DMSO- d_6): δ 132.88 (t, $^3J_{\text{PC}} = 5.5$ Hz, Ar-C), 132.17 (s, Ar-C), 131.96 (s, Ar-C), 129.53 (t, $^3J_{\text{PC}} = 5.5$ Hz, Ar-C), 129.26 (Ar-C), 129.06 (Ar-C), 128.49 (Ar-C), 29.78 (CN-CH₃), 24.75 (t, P-CH₂), 22.63 (C-CH₂). ^{31}P NMR (162 MHz DMSO- d_6): δ 23.97 (s). IR (Nujol, cm^{-1}): 2273 v(m). Anal. Calculated for C₃₂H₃₄B₂F₈N₂P₂Pd: C, 45.39-48.74; H, 4.16-4.35; N, 3.21-3.55 %. Found: C, 47.42; H, 4.59; N, 3.45 % (1 mole CH₂Cl₂ trapped in compound).

[(1,5-Bis(diphenylphosphino)pentane)palladium(II)-bis(methylisocyanide)][BF₄]₂ (28d)

A mixture of (DPPPentane)PdCl₂ (100 mg, 0.162 mmol), AgBF₄ (63 mg, 0.323 mmol), and anhydrous acetonitrile (10 mL) was placed in a sealed ampule under nitrogen. The reaction mixture was heated at 60 °C for 2h with stirring. The mixture was then filtered through celite, the solvent was removed under vacuum, and the residue was dried in vacuum for 3 h. Dichloromethane (10 mL) was added and the mixture was again filtered through celite. The filtrate was treated with methylisocyanide (23 μ L, 0.405 mmol) and stirred at room temperature for 2 h. The solvent volume was reduced under

reduced pressure, and diethyl ether was added to obtain product as yellow crystals. The product was isolated by filtration and dried in vacuo. Yield: 91 mg, 71%. ^1H NMR (400 MHz, DMSO- d_6), δ 7.83 (br m, 8H, Ph), 7.65 (br m, 12H, Ph), 3.12 (br s, 4H, CH_2), 2.90 (s, 6H, CNCH_3), 1.83 (br s, 2H, CH_2), 1.65 (br s, 4H, CH_2). ^{13}C NMR (100 MHz, DMSO- d_6): δ 132.38 (t, $^3J_{\text{PC}} = 5.8$ Hz, Ar-C), 129.36 (t, $^3J_{\text{PC}} = 5.5$ Hz, Ar-C), 129.07 (Ar-C), 128.80 (Ar-C), 124.42 (Ar-C), 32.90 (br s, P- CH_2), 29.79 (CN- CH_3), 26.03 (C- CH_2), 25.42 (C- CH_2). ^{31}P NMR (162 MHz DMSO- d_6): δ 20.24 (s). IR (Nujol, cm^{-1}): 2268 $\nu(\text{m})$. Anal. Calculated for $\text{C}_{33}\text{H}_{36}\text{B}_2\text{F}_8\text{N}_2\text{P}_2\text{Pd}$: C, 49.38; H, 4.52; N, 3.49 %. Found: C, 49.20; H, 4.60; N, 3.52 %.

[(1,2-Bis(dimethylphosphino)ethane)palladium(II) (CH_3NC) $_2$][BF_4] $_2$ (28e)

A mixture of (DMPE) PdCl_2 (150 mg, 0.458 mmol), AgBF_4 (178 mg, 0.916 mmol), and anhydrous acetonitrile (10 mL) was placed in a sealed ampule under nitrogen. The reaction mixture was heated at 60 $^\circ\text{C}$ for 1 h with stirring. The mixture was then filtered through celite, the solvent was removed under vacuum, and the residue was dried in vacuum for 3 h. Anhydrous acetonitrile (10 mL) was added, and the mixture was again filtered through celite. The filtrate was treated with methylisocyanide (64 μL , 1.145 mmol) and stirred at room temperature for 2 h. The solvent volume was reduced under vacuum, and diethyl ether was layered over it to get white crystals. The product was isolated by filtration and dried in vacuo. Yield: 131 mg, 56%. ^1H NMR (400 MHz, $\text{CD}_3\text{CN-}d_3$): δ 3.56 (s, 6H, CNCH_3), 2.37-2.22 (m, 4H, P- CH_2), 1.86 (d, 12H, $^2J_{\text{PH}} = 12.8$ Hz, P- CH_3). ^{13}C NMR (100 MHz, $\text{CD}_3\text{CN-}d_3$): δ 127.69 (b s, CN- CH_3), 31.28 (t, CN- CH_3), 28.26 (dd, $^1J_{\text{PC}} = 36.7$ Hz, $^2J_{\text{PC}} = 10.3$ Hz, P- CH_2) 13.48 (d, $^1J_{\text{PC}} = 33.7$ Hz, P-

CH₃) ³¹P NMR (162 MHz CD₃CN-d₆): δ 60.11 (s). IR (Nujol, cm⁻¹): 2270 v(m). Anal. Calculated for C₁₀H₂₂B₂F₈N₂P₂Pd.CH₃CN: C, 26.04; H, 4.55; N, 7.59 %. Found: C, 26.17; H, 4.48; N, 7.60 %.

[(1,2-Bis(diphenylphosphino)benzene)palladium(II) (CH₃NC)₂][BF₄]₂ (28f)

A mixture of (DPPBenzene)PdCl₂ (150 mg, 0.241 mmol), AgBF₄ (94 mg, 0.481 mmol), and anhydrous acetonitrile (10 mL) was placed in a sealed ampule under nitrogen. The reaction mixture was heated at 60 °C for 2 h with stirring. The mixture was then filtered through celite, the solvent was removed under vacuum, and the residue was dried in vacuum for 3 h. Dichloromethane (10 mL) was added, and the mixture was again filtered through celite. The filtrate was treated with methylisocyanide (23 μL, 0.405 mmol) and stirred at room temperature for 2 h. The solvent was removed under vacuum, the residue was dissolved in acetonitrile, and diethyl ether was layered over the solution to get pale yellow crystals. The product was isolated by filtration and dried in vacuo.

Yield: 113 mg, 65%. ¹H NMR (400 MHz, CD₃CN-d₃): δ 7.94-7.56 (m, 24H, Ph), 3.33 (s, 6H, CNCH₃). ¹³C NMR (100 MHz, CD₃CN-d₃): δ 137.55 (dd, ¹J_{PC} = 60.1 Hz, ²J_{PC} = 34.4 Hz, ipso-PPhP), 136.12 (dd, ³J_{PC} = 8.1 Hz, ⁴J_{PC} = 2.2 Hz, meta/para-PPhP), 135.44 (dd, ²J_{PC} = 18.7 Hz, ³J_{PC} = 4 Hz, ortho/meta-PPhP), 134.77 (d, ⁴J_{PC} = 2.9 Hz, para-PPh₂), 134.61 (d, ²J_{PC} = 12.4 Hz, ortho-PPh₂), 130.97 (d, ³J_{PC} = 12.4 Hz, meta-PPh₂), 126.62 (d, ¹J_{PC} = 59.3 Hz, ipso-PPh₂) δ 31.15 (CN-CH₃). ³¹P NMR (162 MHz CD₃CN-d₆): δ 63.49 (s). IR (Nujol, cm⁻¹): 2272 v(m). Anal. Calculated for: C₃₄H₃₀B₂F₈N₂P₂Pd: C, 50.50; H, 3.74; N, 3.46 %. Found: C, 50.77; H, 3.87; N, 3.51 %.

N,N'-Bis[(R)-1-phenylethyl]-bis(ADC) palladium dibromide complex (29b)

Bis(ADC)PdCl₂ complex **29a** (95 mg, 0.12 mmol) was suspended in acetonitrile (60 mL) in a round bottomed flask. NaBr (512 mg, 5 mmol) and 2.0 mL of deionized water were added. The flask was sealed with a polyethylene stopper, and the mixture was stirred for 12 h at 25 °C. The resultant turbid solution was filtered through a sintered glass frit, and the filtrate was concentrated to 2 mL under reduced pressure without applying heat. Deionized water (10 mL) was added, resulting in formation of a grey precipitate that floated on the liquid surface. The solid was collected by suction filtration, washed with deionized water (20 mL) and diethyl ether (5 mL), and dried in vacuo overnight. Yield: 85 mg (0.095 mmol), 80%. ¹H NMR (400 MHz, DMSO-d₆): δ d 9.64 (s, 1 H, NH), 9.58 (s, 1 H, NH), 8.23 (d, ³J_{HH} = 8.0 Hz, 2 H, CF₃-Ph), 8.05 (d, ³J_{HH} = 8.0 Hz, 2 H, CF₃-Ph), 7.65-7.43 (m, 6 H, Ar), 7.35-7.13 (m, 8 H, Ar), 5.92 (q, ³J_{HH} = 6.4 Hz, 1 H, PhCH), 5.74 (q, ³J_{HH} = 6.4 Hz, 1 H, PhCH), 5.64 (m, 1 H, CH₂), 5.49 (m, 1 H, CH₂), 3.82 (m, 1 H, CH₂), 3.28 (m, 1 H, CH₂), 1.54 (m, 1 H, CH₂), 1.43 (2d unresolved, 6 H, CH₃), 0.76 (m, 1 H, CH₂). ¹³C NMR (101 MHz, DMSO-d₆): δ 193.6 (carbene), 191.6 (carbene), 143.8 (CF₃-Ph *ipso*), 143.7 (CF₃-Ph *ipso*), 138.4 (Ph *ipso*), 137.8 (Ph *ipso*), 128.9 (Ph), 128.7 (Ph), 128.6 (Ph), 128.4 (Ph), 127.4 (Ph), 126.5 (Ph), 124.9 (CF₃-Ph *meta*), 124.8 (CF₃-Ph *meta*), 124.1 (2 q overlapped, ²J_{C,F} = 30 Hz, CF₃-Ph *para*), 124.1 (2 q overlapped, ¹J_{C,F} = 272 Hz, CF₃), 122.3 (CF₃-Ph *ortho*), 121.7 (CF₃-Ph *ortho*), 56.6 (NCMe), 55.8 (NCMe), 54.3 (NCH₂), 53.5 (NCH₂), 29.2 (NCH₂CH₂), 18.0 (CH₃), 15.4 (CH₃). Anal. Calculation for C₃₅H₃₄Br₂F₆N₄Pd: C, 47.19; H, 3.85; N, 6.29. Found: C, 47.20; H, 3.90; N, 6.40%.

{[N,N'-Bis[(R)-1-phenylethyl]-bis(ADC)] palladium(II) (CNCH₃)₂} {BF₄}₂ (30a)

Methyl isocyanide (18 μ L, 0.31 mmol) was added to a stirred solution of bis(ACD) palladium dichloride complex **6a** (100 mg, 0.125 mmol) in acetonitrile (10 mL), and it was stirred for 2 h. Then AgBF₄ (49 mg, 0.25 mmol) was added to the reaction mixture, and it was stirred for 2 h. The mixture was filtered through celite, solvent was evaporated, and product was dried in vacuum for 12 h. The solid was again dissolved in acetonitrile (5 mL), the solution was filtered through celite, solvent was evaporated, and the solid was dried in vacuum for 12 h. This sequence was repeated 2 more times. In the final sequence, diethyl ether was added to the filtrate to obtain product as white crystals. Product was isolated by filtration and dried in vacuo for 12 h. Yield: 73 mg, 60 %. ¹H NMR (400 MHz, DMSO-d₆): δ d 10.43 (s, 1 H, NH), 10.25 (s, 1 H, NH), 7.62-7.51 (m, 5 H, CF₃-Ph), 7.44-7.36 (m, 9 H, Ar), 7.31 (d, ³J_{HH} = 8.0 Hz, 2 H, CF₃-Ph), 7.10 (d, ³J_{HH} = 8.0 Hz, 2 H, CF₃-Ph), 5.92 (q, ³J_{HH} = 6.8 Hz, 1 H, PhCH), 5.74 (q, ³J_{HH} = 6.4 Hz, 1 H, PhCH), 4.35-2.20 (m, 2 H, CH₂), 4.08-4.05 (m, 1 H, CH₂), 3.69 (s, 3H, CNCH₃), 3.64 (s, 3H, CNCH₃), 3.50-2.35 (m, 1 H, CH₂), 1.52 (2d, ³J_{HH} = 6.4, 3 H, CH₃), 1.50-1.45 (m, 1 H, CH₂), 1.41 (2d, ³J_{HH} = 6.4, 3 H, CH₃), 0.59-0.53 (m, 1 H, CH₂). ¹³C NMR (101 MHz, DMSO-d₆): δ 188.69 (carbene), 187.32 (carbene), 143.01 (CF₃-Ph ipso), 142.96 (CF₃-Ph ipso), 138.92 (Ph ipso), 137.65 (Ph ipso), 130.32 (Ph), 130.27 (Ph), 130.13 (Ph), 130.09 (Ph), 129.51 (Ph), 127.48 (Ph), 127.44 (Ph), 127.20 (Ph), 127.19 (Ph), 127.44 (CF₃-Ph *meta*), 124.8 (CF₃-Ph *meta*), 128.09 (q, ²J_{C,F} = 88 Hz, CF₃-Ph *para*), 128.03 (q, ²J_{C,F} = 88 Hz, CF₃-Ph *para*), 124.43 (q, ¹J_{C,F} = 720 Hz, CF₃), 124.93 (q, ¹J_{C,F} = 720 Hz, CF₃), 123.21 (CF₃-Ph *ortho*), 122.73 (CF₃-Ph *ortho*), 60.10 (NCMe), 59.04 (NCMe), 56.87 (NCH₂), 56.73 (NCH₂), 31.30 (CNCH₃), 29.78 (NCH₂CH₂), 18.17

(CH₃), 16.28 (CH₃). IR (Nujol, cm⁻¹): 2270 v(m). Anal. Calculated for C₃₉H₄₀N₄F₁₄B₂Pd: C, 47.47; H, 4.09; N, 8.51. Found: C, 44.38; H, 4.23; N, 8.51%.

References

- (1) Arduengo, A. J.; Harlow, R. L.; Kline, M. *J. Am. Chem. Soc.* **1991**, *113*, 361
- (2) Dixon, D. A.; Arduengo, A. J. *J. Phys. Chem.* **1991**, *95*, 4180.
- (3) Weskamp, T.; Bohm, V. P. W.; Herrmann, W. A. *Journal of Organometallic Chemistry* **1999**, *585*, 348
- (4) Mankad, N. P.; Toste, F. D. *J. Am. Chem. Soc.* **2010**, *132*, 12859
- (5) Liu, Z.; Shi, M. *Tetrahedron* **2010**, *66*, 2619
- (6) Peh, G. R.; Kantchev, E. A. B.; Er, J. C.; Ying, J. Y. *Chemistry-a European Journal* **2010**, *16*, 4010
- (7) Jiang, L.; Li, Z. N.; Zhao, D. F. *Chinese Journal of Organic Chemistry* **2010**, *30*, 200
- (8) Kim, C. B.; Jo, H.; Ahn, B. K.; Kim, C. K.; Park, K. *Journal of Organic Chemistry* **2009**, *74*, 9566
- (9) Lundgren, R. J.; Sappong-Kumankumah, A.; Stradiotto, M. *Chemistry-a European Journal* **2010**, *16*, 1983
- (10) Miyazaki, S.; Koga, Y.; Matsumoto, T.; Matsubara, K. *Chemical Communications* **2010**, *46*, 1932
- (11) Hillier, A. C.; Grasa, G. A.; Viciu, M. S.; Lee, H. M.; Yang, C. L.; Nolan, S. P. *Journal of Organometallic Chemistry* **2002**, *653*, 69

- (12) Ellul, C. E.; Reed, G.; Mahon, M. F.; Pascu, S. I.; Whittlesey, M. K.
Organometallics **2010**, *29*, 4097
- (13) Dash, C.; Shaikh, M. M.; Ghosh, P. *European Journal of Inorganic Chemistry*
2009, 1608
- (14) Li, F. W.; Hor, T. S. A. *Adv. Synth. Catal.* **2008**, *350*, 2391
- (15) Xi, Z.; Liu, B.; Chen, W. *Journal of Organic Chemistry* **2008**, *73*, 3954.
- (16) Weskamp, T.; Kohl, F. J.; Hieringer, W.; Gleich, D.; Herrmann, W. A.
Angewandte Chemie-International Edition **1999**, *38*, 2416
- (17) Herrmann, W. A.; Weskamp, T. *Abstracts of Papers of the American Chemical Society* **1999**, *217*, 022
- (18) Frenzel, U.; Weskamp, T.; Kohl, F. J.; Schattenman, W. C.; Nuyken, O.;
Herrmann, W. A. *Journal of Organometallic Chemistry* **1999**, *586*, 263
- (19) Frenzel, U.; Nuyken, O.; Kohl, F. J.; Schattenmann, W. C.; Weskamp, T.;
Herrmann, W. A. *Abstracts of Papers of the American Chemical Society* **1999**,
217, 197
- (20) Alonso-Villanueva, J.; Rodriguez, M.; Vilas, J. L.; Laza, J. M.; Leon, L. M.
Journal of Macromolecular Science Part a-Pure and Applied Chemistry **2010**, *47*,
1130
- (21) Kadyrov, R.; Wolf, D.; Azap, C.; Ostgard, D. J. *Topics in Catalysis* **2010**, *53*,
1066
- (22) Kabro, A.; Roisnel, T.; Fischmeister, C.; Bruneau, C. *Chemistry-a European Journal* **2010**, *16*, 12255
- (23) Stewart, I. C.; Douglas, C. J.; Grubbs, R. H. *Organic Letters* **2008**, *10*, 441

- (24) Stewart, I. C.; Benitez, D.; O'Leary, D. J.; Tkatchouk, E.; Day, M. W.; Goddard, W. A.; Grubbs, R. H. *J. Am. Chem. Soc.* **2009**, *131*, 1931
- (25) Kuhn, K. M.; Bourg, J. B.; Chung, C. K.; Virgil, S. C.; Grubbs, R. H. *J. Am. Chem. Soc.* **2009**, *131*, 5313
- (26) Chung, C. K.; Grubbs, R. H. *Organic Letters* **2008**, *10*, 2693
- (27) Boydston, A. J.; Xia, Y.; Kornfield, J. A.; Gorodetskaya, I. A.; Grubbs, R. H. *J. Am. Chem. Soc.* **2008**, *130*, 12775.
- (28) Diez-Gonzalez, S.; Stevens, E. D.; Scott, N. M.; Petersen, J. L.; Nolan, S. P. *Chemistry-a European Journal* **2008**, *14*, 158
- (29) Chen, T.; Liu, X. G.; Shi, M. *Tetrahedron* **2007**, *63*, 4874.
- (30) Gil, W.; Trzeciak, A. M.; Ziolkowski, J. J. *Organometallics* **2008**, *27*, 4131.
- (31) Ozdemir, I.; Demir, S.; Sahin, O.; Buyukgungor, O.; Cetinkaya, B. *Journal of Organometallic Chemistry* **2010**, *695*, 1555.
- (32) Yu, D. Y.; Zhang, Y. G. *Proceedings of the National Academy of Sciences of the United States of America* **2010**, *107*, 20184
- (33) Davies, C. J. E.; Page, M. J.; Ellul, C. E.; Mahon, M. F.; Whittlesey, M. K. *Chem Commun (Camb)* **2010**, *46*, 5151
- (34) Buscemi, G.; Biffis, A.; Tubaro, C.; Basato, M.; Graiff, C.; Tiripicchio, A. *Applied Organometallic Chemistry* **2010**, *24*, 285.
- (35) Peris, E.; Crabtree, R. H. *Coord. Chem. Rev.* **2004**, *248*, 2239
- (36) Green, J. C.; Scurr, R. G.; Arnold, P. L.; Cloke, F. G. N. *Chemical Communications* **1997**, 1963.
- (37) Hahn, F. E. *Angewandte Chemie-International Edition* **2006**, *45*, 1348

- (38) Scott, N. M.; Nolan, S. P. *European Journal of Inorganic Chemistry* **2005**, 1815
- (39) Herrmann, W. A. *Angewandte Chemie-International Edition* **2002**, *41*, 1290.
- (40) Kelly, R. A.; Clavier, H.; Giudice, S.; Scott, N. M.; Stevens, E. D.; Bordner, J.; Samardjiev, I.; Hoff, C. D.; Cavallo, L.; Nolan, S. P. *Organometallics* **2008**, *27*, 202.
- (41) Huang, J. K.; Schanz, H. J.; Stevens, E. D.; Nolan, S. P. *Organometallics* **1999**, *18*, 2370.
- (42) Dorta, R.; Stevens, E. D.; Scott, N. M.; Costabile, C.; Cavallo, L.; Hoff, C. D.; Nolan, S. P. *J. Am. Chem. Soc.* **2005**, *127*, 2485
- (43) Dorta, R.; Stevens, E. D.; Hoff, C. D.; Nolan, S. P. *J. Am. Chem. Soc.* **2003**, *125*, 10490
- (44) Chianese, A. R.; Li, X. W.; Janzen, M. C.; Faller, J. W.; Crabtree, R. H. *Organometallics* **2003**, *22*, 1663.
- (45) Magill, A. M.; Cavell, K. J.; Yates, B. F. *J. Am. Chem. Soc.* **2004**, *126*, 8717.
- (46) Tolman, C. A. *Chem. Rev.* **1977**, *77*, 313.
- (47) Wolf, S.; Plenio, H. *Journal of Organometallic Chemistry* **2009**, *694*, 1487
- (48) Song, G. Y.; Zhang, Y.; Li, X. W. *Organometallics* **2008**, *27*, 1936.
- (49) Mercs, L.; Labat, G.; Neels, A.; Ehlers, A.; Albrecht, M. *Organometallics* **2006**, *25*, 5648.
- (50) Frey, G. D.; Herdtweck, E.; Herrmann, W. A. *Journal of Organometallic Chemistry* **2006**, *691*, 2465.
- (51) Diez-Gonzalez, S.; Nolan, S. P. *Coord. Chem. Rev.* **2007**, *251*, 874.
- (52) Prasang, C.; Donnadiou, B.; Bertrand, G. *J. Am. Chem. Soc.* **2005**, *127*, 10182.

- (53) Leuthausser, S.; Schwarz, D.; Plenio, H. *Chemistry-a European Journal* **2007**, *13*, 7195.
- (54) Ahrens, S.; Zeller, A.; Taige, M.; Strassner, T. *Organometallics* **2006**, *25*, 5409.
- (55) Alder, R. W.; Blake, M. E. *Chemical Communications* **1997**, 1513
- (56) Alder, R. W.; Allen, P. R.; Murray, M.; Orpen, A. G. *Angewandte Chemie-International Edition* **1996**, *35*, 1121.
- (57) Alder, R. W.; Blake, M. E.; Chaker, L.; Harvey, J. N.; Paolini, F.; Schutz, J. *Angewandte Chemie-International Edition* **2004**, *43*, 5896
- (58) Otto, M.; Conejero, S.; Canac, Y.; Romanenko, V. D.; Rudzevitch, V.; Bertrand, G. *J. Am. Chem. Soc.* **2004**, *126*, 1016.
- (59) Herrmann, W. A.; Ofele, K.; von Preysing, D.; Herdtweck, E. *Journal of Organometallic Chemistry* **2003**, *684*, 235
- (60) Herrmann, W. A.; Schutz, J.; Frey, G. D.; Herdtweck, E. *Organometallics* **2006**, *25*, 2437.
- (61) Collins, M. S.; Rosen, E. L.; Lynch, V. M.; Bielawski, C. W. *Organometallics* **2010**, *29*, 3047.
- (62) Seo, H.; Roberts, B. P.; Abboud, K. A.; Merz, K. M.; Hong, S. W. *Organic Letters* **2010**, *12*, 4860
- (63) Rosen, E. L.; Sung, D. H.; Chen, Z.; Lynch, V. M.; Bielawski, C. W. *Organometallics* **2010**, *29*, 250
- (64) Yu, I.; Wallis, C. J.; Patrick, B. O.; Diaconescu, P. L.; Mehrkhodavandi, P. *Organometallics* **2010**, *29*, 6065

- (65) Hashmi, A. S. K.; Hengst, T.; Lothschutz, C.; Rominger, F. *Adv. Synth. Catal.* **2010**, *352*, 1315.
- (66) Treichel, P. M.; Wagner, K. P. *Journal of Organometallic Chemistry* **1973**, *61*, 415.
- (67) Wanniarachchi, Y. A.; Kogiso, Y.; Slaughter, L. M. *Organometallics* **2008**, *27*, 21.
- (68) Muehlhofer, M.; Strassner, T.; Herdtweck, E.; Herrmann, W. A. *Journal of Organometallic Chemistry* **2002**, *660*, 121.
- (69) Lee, H. M.; Lu, C. Y.; Chen, C. Y.; Chen, W. L.; Lin, H. C.; Chiu, P. L.; Cheng, P. Y. *Tetrahedron* **2004**, *60*, 5807.
- (70) Vitz, J.; Mac, D. H.; Legoupy, S. *Green Chemistry* **2007**, *9*, 431.
- (71) Herrmann, W. A.; Schwarz, J.; Gardiner, M. G.; Spiegler, M. *Journal of Organometallic Chemistry* **1999**, *575*, 80.
- (72) Gardiner, M. G.; Herrmann, W. A.; Reisinger, C. P.; Schwarz, J.; Spiegler, M. *Journal of Organometallic Chemistry* **1999**, *572*, 239.
- (73) Smith, M. B.; March, J. *MARCH'S Advanced Organic Chemistry: Reactions, Mechanisms, and Structure*; John Wiley & Sons: New York, 2001; pp.20.
- (74) Heckenroth, M.; Kluser, E.; Neels, A.; Albrecht, M. *Dalton Transactions* **2008**, 6242.
- (75) Heckenroth, M.; Kluser, E.; Neels, A.; Albrecht, M. *Angewandte Chemie-International Edition* **2007**, *46*, 6293.
- (76) Poyatos, M.; McNamara, W.; Incarvito, C.; Clot, E.; Peris, E.; Crabtree, R. H. *Organometallics* **2008**, *27*, 2128.

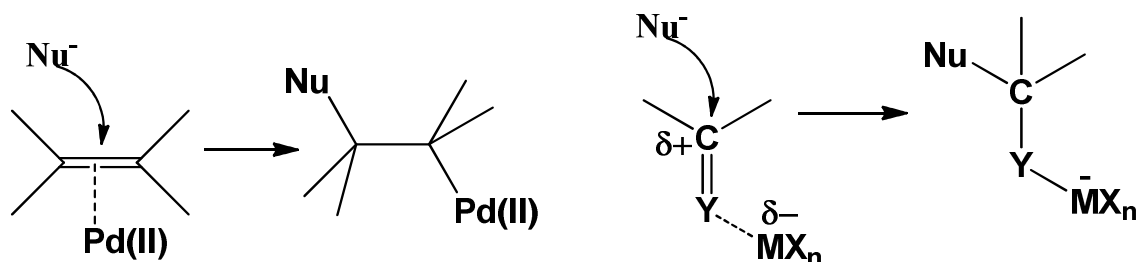
- (77) Butler, W. M.; Enemark, J. H.; Parks, J.; Balch, A. L. *Inorganic Chemistry* **1973**, *12*, 451.
- (78) Wanniarachchi, Y. A. Ph.D. Thesis, Oklahoma State University, 2005.
- (79) Burke, A.; Balch, A. L.; Enemark, J. H. *J. Am. Chem. Soc.* **1970**, *92*, 2555.
- (80) Butler, W. M.; Enemark, J. H. *Inorganic Chemistry* **1971**, *10*, 2416.
- (81) Wanniarachchi, Y. A.; Slaughter, L. M. *Chemical Communications* **2007**, 3294.
- (82) Schuster, R. E.; Scott, J. E.; Casanova, J. *Org. Synth.* **1966**, *46*, 75.
- (83) Drew, D.; Doyle, J. R.; Shaver, A. G. *Inorg. Synth.* **1972**, *13*, 52.
- (84) Steffen, W. L.; Palenik, G. J. *Inorganic Chemistry* **1976**, *15*, 2432.
- (85) Gavagnin, R.; Cataldo, M.; Pinna, F.; Strukul, G. *Organometallics* **1998**, *17*, 661.
- (86) Neo, K. E.; Neo, Y. C.; Chien, S. W.; Tan, G. K.; Wilkins, A. L.; Henderson, W.; Hor, T. S. A. *Dalton Transactions* **2004**, 2281.
- (87) Gray, L. R.; Gulliver, D. J.; Levason, W.; Webster, M. *Journal of the Chemical Society-Dalton Transactions* **1983**, 133.
- (88) Kobayashi, T. A.; Abe, F.; Tanaka, M. *Journal of Molecular Catalysis* **1988**, *45*, 91.
- (89) Bruker, *SAINT-plus*, Version 6.29, Bruker AXS, Madison, WI, USA. 2001.
- (90) Sheldrick, G. M. *SHELXTL*, Version 6.14; Bruker AXS: Madison, WI, USA, 2000.

CHAPTER IV

CORELATION OF LIGAND DONICITY WITH CATALYTIC ACTIVITY FOR ELECTROPHILIC CATIONIC BIS(CARBENE) PALLADIUM (II) CATALYSTS

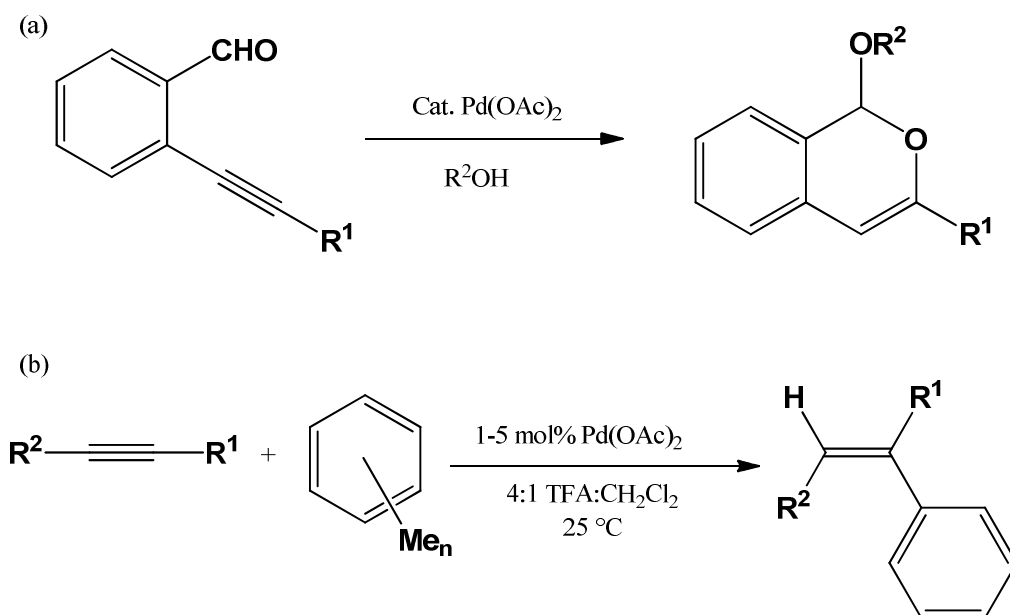
Introduction

In organic synthesis, palladium is more versatile than the other group 10 metals nickel and platinum.^{1,2} The reason for the greater usefulness of palladium compared to the other two metals is not straightforward. Palladium has both adequate stability and suitable activity for a variety of catalytic reactions, arising from an intermediate nature between nickel and platinum. Palladium catalysts can serve as typical late transition metal catalysts^{3,4} and as Lewis acid catalysts,^{5,6} both types of catalytic activity being important in organic reactions. Late transition metal catalysis is usually based on the Pd(0)-Pd(II) redox cycle. Another role of late transition metal catalysts of Pd(II) is the activation of alkenes or alkynes towards attack of a nucleophile by the formation of a complex with π -electrons of alkene or alkyne double bonds. A typical role of a Lewis acid catalyst is enhancing the reactivity of a substrate by forming a complex with lone pairs (C=Y; Y = O, NR, etc.) and activating the positively polarized carbon centre toward attack of a nucleophile. Despite palladium being a soft metal, the presence of an empty orbital in the coordinatively unsaturated 16-electron Pd(II) species is important for this Lewis acidity. In certain transformations, the presence of both late transition metal and Lewis acid catalysis is important.^{7,8}



Scheme 4.1. Role of Pd(II) as a late transition metal and a Lewis acid catalyst (adapted from Reference 1).

Palladium catalyzed reactions are regulated by the amount of σ -donation from the ligands attached to the metal center. Strong σ -donating ligands on Pd(0) increase the electron density around the metal center, promoting reactions in which the metal becomes oxidized or acts as a nucleophile. Conversely, weakly σ -donating ligands on Pd(II) facilitate electrophilic reactions at the metal center (as a Lewis acid). The IR probe studies in Chapter III gave a comparison of the donor abilities of bidentate ligands using cationic palladium(II) complexes. This chapter is focused on the correlation of these ligands' donor abilities with the catalytic activities of cationic palladium(II) complexes in electrophilic organic reactions. For this purpose, two catalytic reactions were selected: the cyclization of acetylinic aldehydes reported by Yamamoto et al. in 2002,⁹ and the hydroarylation of aromatic C-H bonds with alkynes reported by Fujiwara et al. in 2000.¹⁰



Scheme 4.2. Test reactions for Pd(II) electrophilicity: (a) cyclization of acetylinic aldehydes⁹ and (b) hydroarylation of aromatic C-H bonds with alkynes.¹⁰

Cyclic alkenyl ethers are useful compounds with significant biological importance, which can be prepared by the cyclization of acetylinic aldehydes. Electrophilic activation of alkynes toward different heteronucleophiles is useful for preparation of heterocyclic compounds such as indoles,¹¹ isoquinolines,¹² benzofurans,¹³ and isocoumarins.¹⁴ In these studies, hydroxyl and amine functionalities have been used as nucleophiles.

Catalytic activation of C-H bonds in arenes and formation of new C-C bonds is useful in organic synthesis from an economical and environmental standpoint. Fujiwara reported hydroarylation reactions¹⁰ using simple palladium complexes such as Pd(OAc)₂ as catalysts in an acidic medium to promote coupling reactions of arenes with alkynes. This involves cheap and commercially available reagents. Other metals such as platinum(II)¹⁵ and gold(III)¹⁶ have shown catalytic activity but with lesser efficiency. Biffis and coworker have shown that using a bis(NHC) as a ligand in these complexes can improve the stability and the activity of the palladium complexes.¹⁷⁻¹⁹

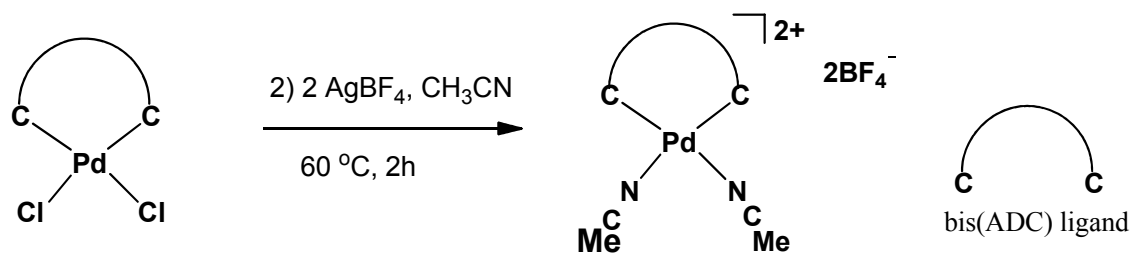
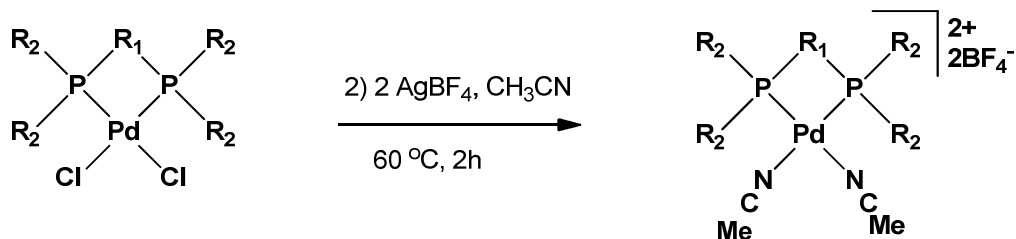
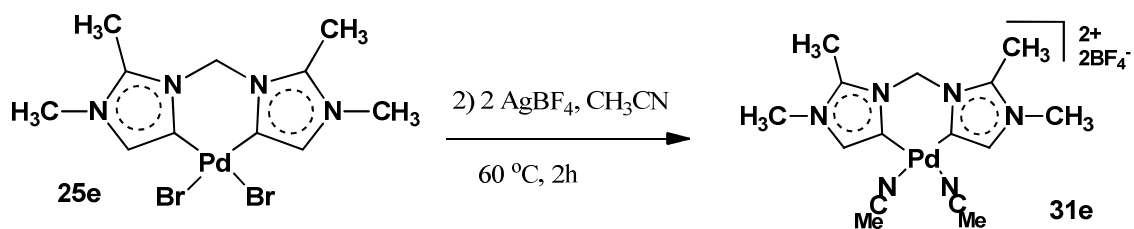
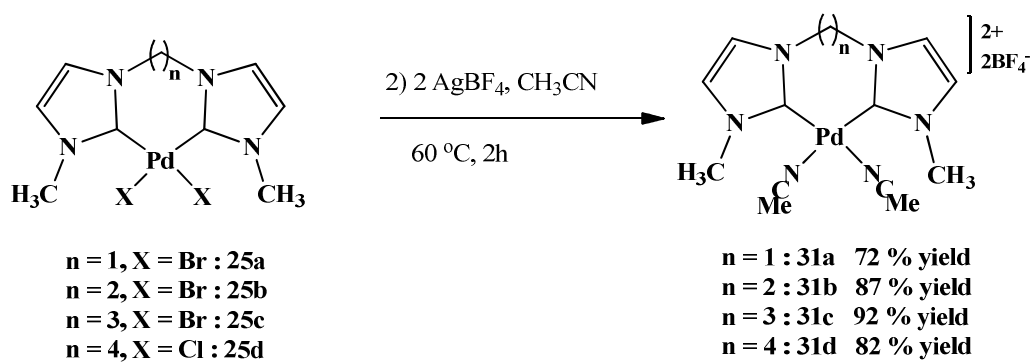
Results and Discussion

Synthesis and characterization of cationic (chelate)palladium(II) bis(acetonitrile) complexes for catalytic studies.

Bis(acetonitrile) adducts of palladium complexes with ‘normal’ and ‘abnormal’ bis(NHCs) (**31a-31e**) were synthesized by reacting palladium dihalide complexes with silver tetrafluoroborate in acetonitrile. The synthesis was started by placing one molar equivalent of bis(NHC) palladium dihalide complex and two molar equivalents of silver tetrafluoroborate in a sealable thick-walled glass vessel. After addition of acetonitrile, the

reaction mixture was heated at 60 °C for a couple of hours (depending on the type of carbene) to complete precipitation of silver halide. The resultant reaction mixture, after cooling to room temperature, was filtered through celite to remove silver salts. The solvent was removed from the filtrate under vacuum, and the solid was dried for an additional couple of hours under vacuum. The resultant solid was redissolved in acetonitrile, the solution was filtered through celite, the solvent was removed, and the solid was dried under vacuum. This sequence was repeated one more time. This sequence is very important to remove all the silver salts present in the product. Finally, white crystalline products were isolated by layering ether on the solution in acetonitrile. The synthetic procedure for the bis(acetonitrile) adduct of the palladium complex with the 'triazole' bis(NHC) (**31f**) was discussed in Chapter 3 (Scheme 3.4).

Oily products were isolated in the syntheses of bis(acetonitrile) adducts of palladium with bis(phosphine) ligands, except for the DPPBen complex, when the synthetic route followed for bis(NHC) complexes was used. Therefore, for catalytic reactions, one molar equivalent of bis(phosphine) palladium dichloride (**27a-27f**), two molar equivalents of AgBF₄, and acetonitrile were mixed in a sealable glass vessel and heated at 60 °C for 2 hours. The resultant reaction mixture was filtered through celite to remove silver salts. The solvent was removed from the filtrate under vacuum, and the residue was dried under vacuum for two hours. The resultant solid was redissolved in acetonitrile and filtered through celite, the solvent was removed, and the product was dried under vacuum. This product was dissolved in a known volume of solvent to be used in the catalytic study. The required volume was then withdrawn and placed in the reaction mixture.



29a = 8 membered bis(ADC)
 33a = Chugaev bis(ADC)
 33b = 7 membered bis(ADC)

34a = 8 membered bis(ADC)
 34b = Chugaev bis(ADC)
 34c = 7 membered bis(ADC)

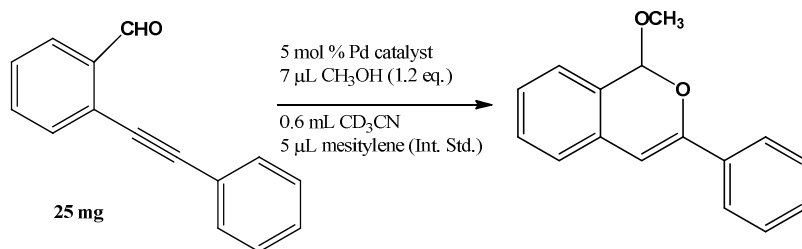
Scheme 4.3. Synthesis of bis(acetonitrile) adducts of palladium(II) complexes.

Bis(ADC) complexes **34a** and **34c** were synthesized as white crystals using a procedure similar to that used for the bis(NHC) complexes. However, the Chugaev type five-membered chelate bis(ADC) complex (**34b**) was prepared similarly to the bis(phosphine) complexes, because of the instability of the isolated bis(acetonitrile) adduct.

Cyclization of acetylinic aldehydes to cyclic alkenyl ethers:

Initial catalytic studies

The substrate for the test catalytic reaction, 2-(phenylethynyl)benzaldehyde (**S1**), was synthesized using a published procedure.²⁰ Initial studies were carried out as NMR scale reactions using J-Young NMR tubes. Mesitylene was selected as an internal standard for the catalytic reaction. Substrate (**S1**) and the internal standard, mesitylene, were mixed with 5% Pd catalyst in 0.6 mL of CD₃CN. Then 1.2 equiv of CH₃OH was added to the NMR tube, and the reaction was monitored by ¹H NMR spectroscopy at room temperature. A relaxation delay of d1=5 was used during the acquisition of spectra. Integration ratios of the aldehyde proton of the substrate (**S1**), the methine proton of the product (**P1**), and the aromatic protons of mesitylene were used to determine the concentrations of substrate and product at a given time in the reaction mixture. Results are summarized in Table 4.1.



Scheme 4.4. NMR scale catalytic cyclization of 2-(phenylethynyl)benzaldehyde

Table 4.1. Summary of NMR scale catalytic cyclization of 2-(phenylethynyl)benzaldehyde with different catalysts

Pd catalyst	% yield By NMR	Time / h	Initial rate (mM/ min.)	
			Reactant disappearance	Product appearance
31a	76.70	11	0.39	0.37
	98.06	30		
31b	99.05	11	0.56	0.55
	100	21.5		
31c	87.85	11	0.50	0.46
	99.25	21.5		
31e	60.06	11	0.14	0.13
	100.0	25		
31f	51.5	11	0.26	0.23
	100.0	21.5		
32a	100.0	2	-	-
32b	84.83	9	1.24	1.40
32c	28.46	11	0.40	0.34
	28.76	20		
32d	5.0	75	-	-
34a	65.34	11	0.40	0.35

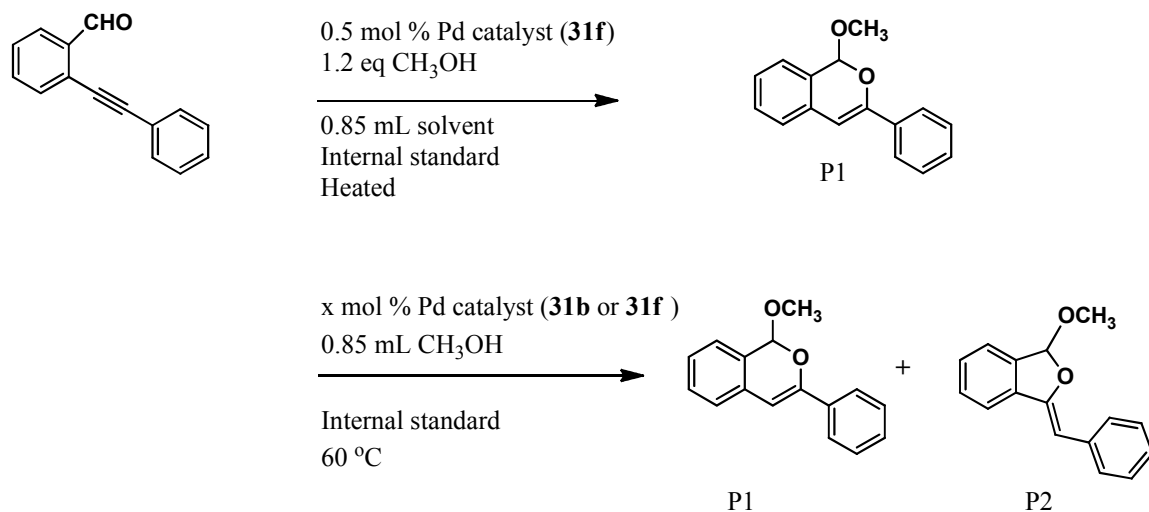
All tested bis(NHC) complexes gave excellent yields (>95%) within 24 hours. However, reactions catalyzed by two bis(phosphine) complexes **32a** (DPPE) and **32b** (DPPPro) were finished in a shorter time. An unidentified byproduct was detected in the reactions catalyzed by bis(phosphine) complexes **32b** and **32c** and bis(ADC) complex **34a**. Initial rates were calculated for 15-20% substrate consumption. All catalysts showed an induction period in the rate plots. Later it was found that acetonitrile is competing with substrate for binding to palladium. Therefore acetonitrile cannot use as solvent for this catalytic reaction when measuring initial rates.

Selection of suitable solvent and temperature

To identify a suitable solvent for the cyclization reaction, five different solvents, dichloromethane, toluene, chlorobenzene, THF and 1,4-dioxane were used in the catalytic reaction. Substrate **S1** was mixed with 0.5% Pd catalyst (**31f**) in the solvent, and then 1.2 equivalents of CH₃OH was added. The reaction mixture was heated at 60 °C for 3 hours, and percentage yield was determined by G.C. The reaction was monitored using 'triazole' based bis(NHC) complex **31f**. In dichloromethane solvent, the reaction temperature used in was 40 °C, and in other solvents it was 60 °C. Reactions in dichloromethane, toluene, chlorobenzene, and THF gave poor yields, but reactions in 1,4-dioxane solvent gave good yields. The best yields were observed when dichloroethane was used as solvent. Therefore, dichloroethane was the solvent of choice for this cyclization reaction.

Methanol was investigated as solvent and nucleophile for the cyclization reaction. This resulted in a mixture of *endo*-6-membered product **P1** and *exo*-5-membered product **P2** in various ratios with different catalysts and catalytic loadings. With catalyst **31b**, it

was found that larger catalytic loading favored the formation of the *exo*-5-membered ring product **P2**. Belmont in 2007 reported AgOTf catalyzed cyclization of **S1** to form a mixture of product **P1** and **P2** in a 5.1:1 ratio.²¹



Scheme 4.5. Solvent and temperature effect on cyclization reaction of **S1** relevant to Tables 4.2, 4.3 and 4.4.

Table 4.2. Solvent effect on the cyclization of **S1** with catalyst **31f**.

Solvent	Temperature/ °C	% yield (P1) by G.C.
CH ₂ Cl ₂	40	14
Toluene	60	16
Chlorobenzene	60	31
THF	60	32
1,4-dioxane	60	82
CH ₂ ClCH ₂ Cl	60	98

Table 4.3. Use of methanol as a solvent for cyclization of **S1** to produce **P1** and **P2**.

Pd catalyst	X mol % Pd	% P1^a	% P2^a	Reaction time (min.)
31f	5	43	56	20
	2.5	75	25	20
	1	80	20	20
31b	1	18	79	10

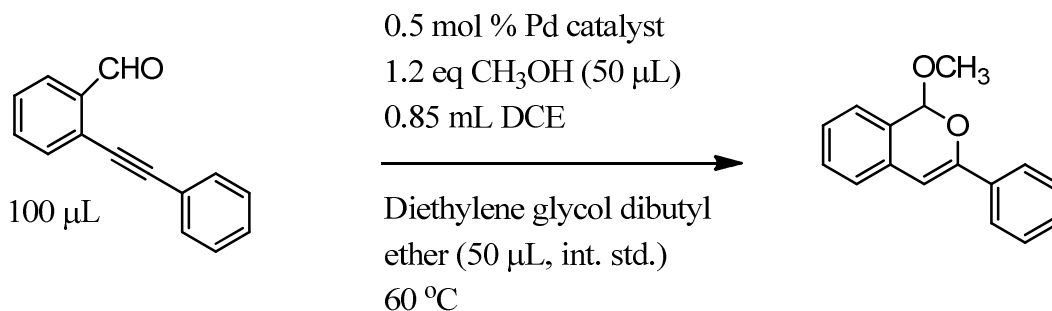
^a % Yield by GC analysis

Using DCE as a solvent, the reaction temperature was varied to identify the optimum reaction temperature. The reaction was monitored by G.C. in 20 minute time intervals. At 50 and 60 °C, maximum yield was observed, but shorter reaction times were required at 60 °C. When the reaction temperature was increased to 80 °C, yields dropped to 68%, and formation of palladium black in the reaction mixtures was observed.

Table 4.4. Temperature effect on the cyclization of **S1** with catalyst **31f** in DCE.

Temperature °C	Maximum % yield by GC	Time for maximum yield / min.
25	65	180
50	98	80
60	98	40
80	68	40

Therefore, the optimized reaction conditions were chosen to be one molar equivalent of **S1**, 1.2 equivalents of CH₃OH and 0.5% Pd catalyst in DCE at 60 °C. Diethylene glycol dibutyl ether was selected as a suitable internal standard for this cyclization reaction.



Scheme 4.6. Optimized reaction conditions for cyclization of **S1**.

The reaction conditions shown in Scheme 4.6 were used in the cyclization reaction with different catalysts. All reactants and solvent were put into a 4 mL reaction vial closed by a screw cap with a PTFE/silicon septum under inert atmosphere. The reaction mixture was heated at 60 °C for 5 minutes. Then methanol was injected into the vial, and measurement of reaction time started. Aliquots of reaction mixture were withdrawn via micro syringe at suitable time intervals. The catalyst in the withdrawn sample was quenched with excess methylisocyanide in hexanes. The precipitated palladium complex was filtered through glass fiber, and the filtrate was diluted to a known volume. These prepared samples were stored in a freezer at -4 °C until G.C. analysis. After G.C. analysis, concentrations of substrate (**S1**) and product (**P1**) were calculated using calibration curves. Before the initial rate studies, a trial experiment was

used to establish the time interval for sample collection. Initial rates for substrate disappearance ($-d[S1]/dt$) and product appearance ($d[P1]/dt$) and uncertainties were determined up to 15-20% substrate consumption. Initial rates were determined from linear least-squares regression analyses of the plots of **[S1]** and **[P1]** versus time. Uncertainties are reported at the 95% confidence level.

G.C. analyses were continued beyond 15-20% substrate consumption to identify the minimum time required to produce the maximum yield. Then separate vial reaction were set up as above, but without the internal standard, diethylene glycol dibutyl ether. The reaction mixture was heated at 60 °C to a time required to get the maximum yield identified by G.C. experiments. Products were isolated by flash chromatography using hexanes : ethyl acetate (9:1) as eluent. These results, together with IR stretching frequencies for methylisocyanide adducts of catalyst analogues, are shown in Table 4.5.

Table 4.5. Catalytic reaction data for cyclization of **S1** with various catalysts together with IR stretching frequencies for analogous methylisocyanide adducts

[(MeNC) ₂ Pd (L)] ²⁺	C≡N _{Δv} cm ⁻¹	[(MeNC) ₂ Pd (L)] ²⁺ catalyst	Initial rate mM/s		% Yield ^a	Time min.
			d[S1]/dt	d[P1]/dt		
26a	2269	31a	0.25(1)	0.21(1)	100 (95)	140
26b	2272	31b	0.74(9)	0.73(2)	100(98)	70
26c	2274	31c	1.24(14)	1.20(6)	100(97)	30
26d	2282	31d	3.29(7)	3.29(7)	100(96)	9
26e	2251	31e	0.018(1)	0.018(1)	96(96)	650
26f	2279	31f	1.20(7)	0.88(9)	98(95)	40
28a	2262	32a	9.47(75)	9.04(57)	97(94)	4
28b	2268	32b	3.09(16)	2.94(36)	96(93)	10
28c	2272	32c	4.62(62)	3.39(82)	72(50)	7
28e	2268	32e	0.56(4)	0.40(1)	97(95)	100
30a	2270	34a	0.068(3)	0.068(3)	85(83)	480
30b	2268	34b	0.20(2)	0.11(3)	68(60)	220
30c	2273	34c	1.13(3)	1.15(7)	98(95)	50

^a Isolated yield in parenthesis is after column chromatography

All bis(NHC) complexes (**31a-31f**) gave excellent yields (>95%) with various reaction times. Bis(phosphine) complexes **32a**, **32b** and **32e** also gave excellent yields, but the dimeric bis(phosphine) complex **32c** gave a moderate yield. Bis(ADC) complex **34c** gave an excellent yield but the other bis(ADC) complexes **34a** and **34b** produced

only moderate to good yields (68-85%). Most of the bis(phosphine) complexes (**32a-32c**) showed a very short reaction time (4-10 minutes), with **31d** being the only bis(NHC) complex to show a comparable reaction time (9 minutes). To correlate the catalytic activity with donor ability of ligands, a plot of initial cyclization rates versus Δv_{MeNC} for various catalysts is shown in Figure 4.1. Catalysts **32c**, **32e**, and **34a** were excluded from this comparison due to *trans*-dimeric nature of **32c** and the instability of **32e** and **34a** (formation of palladium black during initial rate studies and poor elemental analysis results).

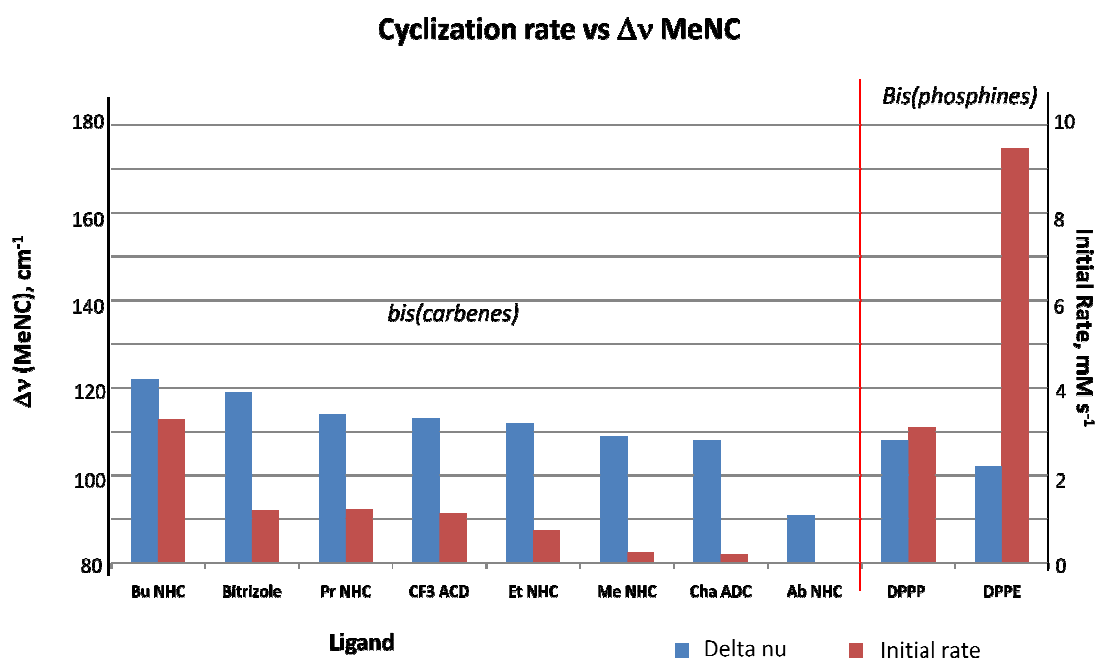
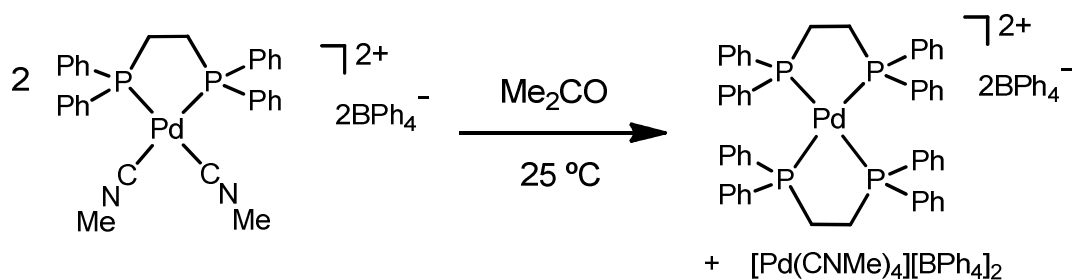


Figure 4.1. Cyclization rate of alkenylaldehyde versus Δv_{MeNC} for various (chelate) Pd^{2+} complexes.

According to Figure 4.1, all bis(carbene) complexes show a correlation between initial rate of cyclization and donor ability (Δv_{MeNC}), but no correlation was observed for

the bis(phosphine) complexes. Cyclization rate decreased with decreasing Δv_{MeNC} value (increasing donor ability). This is attributed to weaker donor ligands (larger Δv_{MeNC}) producing electron-poor Pd centers, thus increasing Lewis acidity. Therefore, higher cyclization rates were observed. Conversely, lower cyclization rates were observed for strong donor ligands (smaller Δv_{MeNC}) due to a reduction in Lewis acidity by electron-rich Pd centers. The unusual higher cyclization rate for bis(phosphine) complexes, despite their low Δv_{MeNC} values, is proposed to result from labile phosphine ligands. Two types of evidence for phosphine lability were found during this investigation.



Scheme 4.7. Evidence for phosphine lability during crystal growth of the DPPE complex.

Attempted synthesis of a larger chelate ring size bis(phosphine) complex with the DPPBut ligand revealed a monomer $[(\text{DPPBut}) \text{Pd}(\text{II}) (\text{CNCH}_3)_2] [\text{BF}_4]_2$ -dimer $[(\text{DPPBut})_2 \text{Pd}(\text{II})_2 (\text{CNCH}_3)_4] [\text{BF}_4]_4$ equilibrium in the NMR solution (Chapter III, Scheme 3.6). This is due to the labile DPPBut ligand. The second type of evidence was found during crystal growth of $[(\text{DPPE}) \text{Pd}(\text{II}) (\text{CNCH}_3)_2] [\text{BF}_4]_2$, when complex $[(\text{DPPE})_2 \text{Pd}(\text{II})] [\text{BF}_4]_2$ was isolated instead (Scheme 4.7). This happened due to exchange of DPPE from one complex with two methylisocyanides in another complex. This product's crystal structure was identified by X-ray crystallography.

Therefore, a rigid, non-labile bis(phosphine) ligand, DPPBen, was selected for this study. Its complex's Δv_{MeNC} value and cyclization rate are shown in Figure 4.2 together with the bis(carbene) complexes.

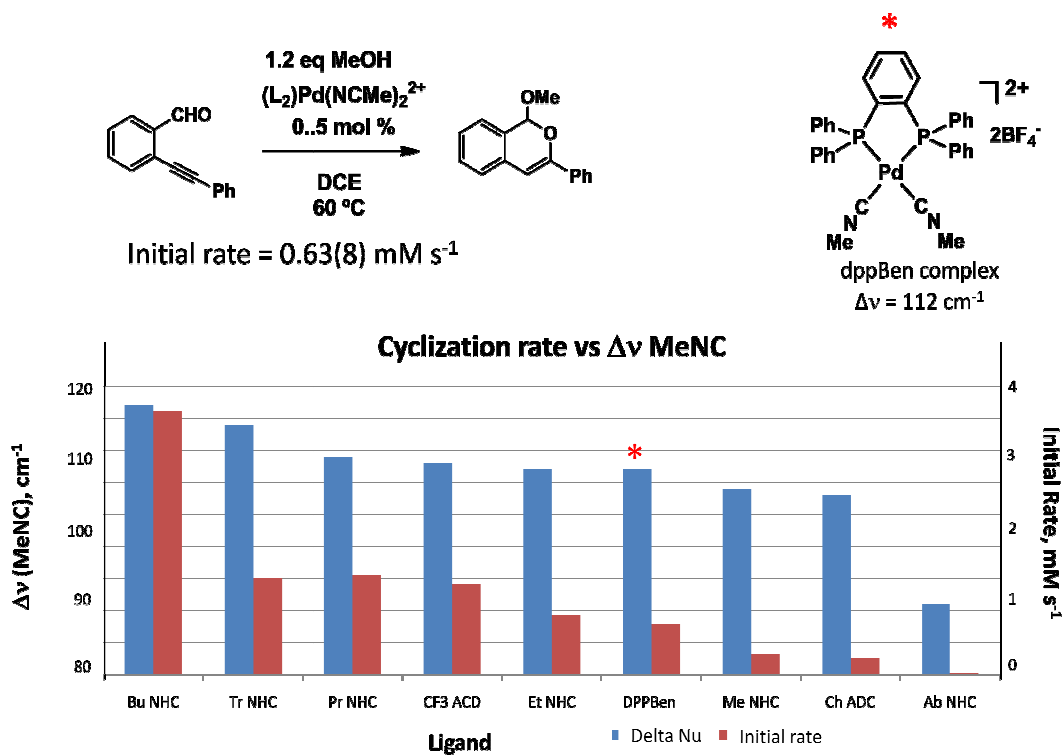


Figure 4.2. Cyclization rate of alkyne-aldehyde versus Δv_{MeNC} for the rigid, non-labile DPPBen complex and bis(carbene) complexes.

For the DPPBen complex, cyclization rate and Δv_{MeNC} value were in between those found for the ethylene and methylene linkage bis(NHC) complexes. According to Figure 4.2, the cyclization rate decreased with increasing ligand donor ability (decreasing Δv_{MeNC}). However, this is not a linear relationship. Electronic effects appear to be most important, but steric effects may also play a role. The highest initial rate was observed for

the weakest donor ligand, the butylene linkage bis(NHC) complex, and the lowest rate was observed for the strongest donor ligand, the 'abnormal' bis(NHC).

Density Functional Theoretical (DFT) calculations

Density Functional Theoretical (DFT) calculations were done using the Gaussian 03 software package to determine the frontier orbital energies for optimized (bisNHC)Pd²⁺ species. The B3LYP density functional with the CEP-31G(d) basis set was employed for these calculations. Calculated values together with experimental values are shown in Figure 4.3. The optimized (bisNHC)Pd²⁺ bite angles are similar to the values in the X-ray crystal structures of bis(methylisocyanide) adducts of (bisNHC)Pd²⁺ species **26a-26d**. Very small deviations were observed for **26a** and **26c** (< 2° %) but significant deviations were observed for **26b** and **26d** (5-8° %). LUMO energies increased from **26a** to **26d** (with increasing chelate ring size), with a similar increase in the HOMO energies, but the increase in the latter is slightly lower up to **26c**. The energy gap between the HOMO and LUMO stays relatively similar, but the lowest gap was observed for **26d**. Dihedral angle shows the best correlation with LUMO energy, with these two values increasing from **26a** to **26c** along with increasing chelate ring size, and then both values drop slightly for **26d** relative to **26c**. Generally, increases in bite angle, dihedral angle, σ -donation, reaction rate, and LUMO and HOMO energies are observed with increased chelate ring size, but this relationship is not linear and some deviation is observed. Based on these results, no clear correlation can be seen, and further DFT studies may be required.

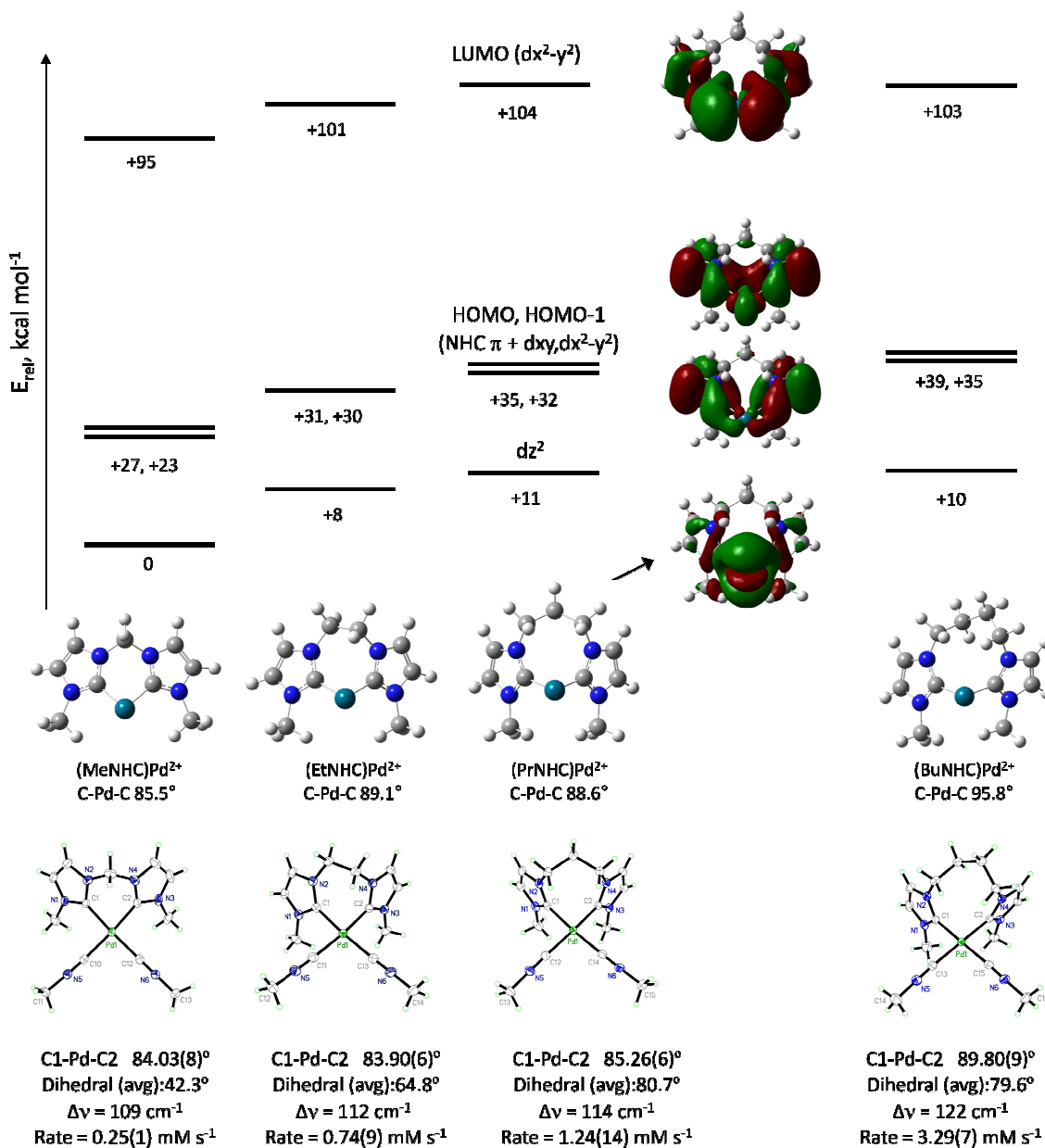


Figure 4.3. Virtual LUMO energies from optimized (bisNHC)Pd²⁺ (B3LYP/CEP-31G(d), Gaussian03) together with experimental and catalytic rate data.

Ligand steric effects versus cyclization rate

Tolman cone angle θ ,²² solid angles Ω , ligand repulsive energies E_R ,²³ Taft-Dubois E_s steric parameters,²⁴ and QALE^{25,26} are the most commonly used steric and

stereoelectronic parameters for studying ligand effects. Steric effects of chelates and non-symmetrical ligands are best modeled using solid angles.²⁷ Solid angles reflect the size, shape and conformation of the ligand, which is dependent on the coordination environment and other ligands present in the system. For steric effects, ‘*G*’ can be calculated using equation (1).²⁷

$$G = \frac{\Omega}{4\pi r} 100 = \frac{A}{4\pi r^2} 100 \quad (1)$$

Where, Ω = solid angle, A = shadow area and r = radius.

$G_{\text{Pd}}(\text{L})$ represents the percentage of the Pd coordination sphere shielded by ligand L (ligand shielding), and G_γ represent the percentage of Pd coordination sphere shielded by more than one ligand (ligand shadow overlap). These were calculated using single crystal X-ray structures of different complexes. These data, together with other previously determined stereoelectronic parameters, are shown in Figure 4.4. The lowest bis(NHC) ‘ligand shielding’ was observed in the methylene linkage complex **26a**, and shielding increases with increasing chelate ring size. The highest ‘ligand shielding’ was observed in the butylene linkage complex **26d**. This trend correlates with the reaction rate and Δv_{MeNC} , where both values increase with increasing chelate ring size.

More interestingly, the less sterically shielded ligand complex **26a** showed stronger donation compared to the more sterically shielded complex **26d**, which showed weaker donation. Nolan in 2003 reported the same type of trend in $\text{Cp}^*\text{Ru}(\text{NHC})\text{Cl}$ complexes, where bulkier NHCs bind more weakly to Ru than less bulky NHCs.²⁸ The larger $G_{\text{Pd}}(\text{L})$ may reflect a weaker Pd-carbene bond, thus reducing electron density

around Pd. Therefore, the Lewis acidity of Pd increases, leading to an increase in electrophilic cyclization rate.

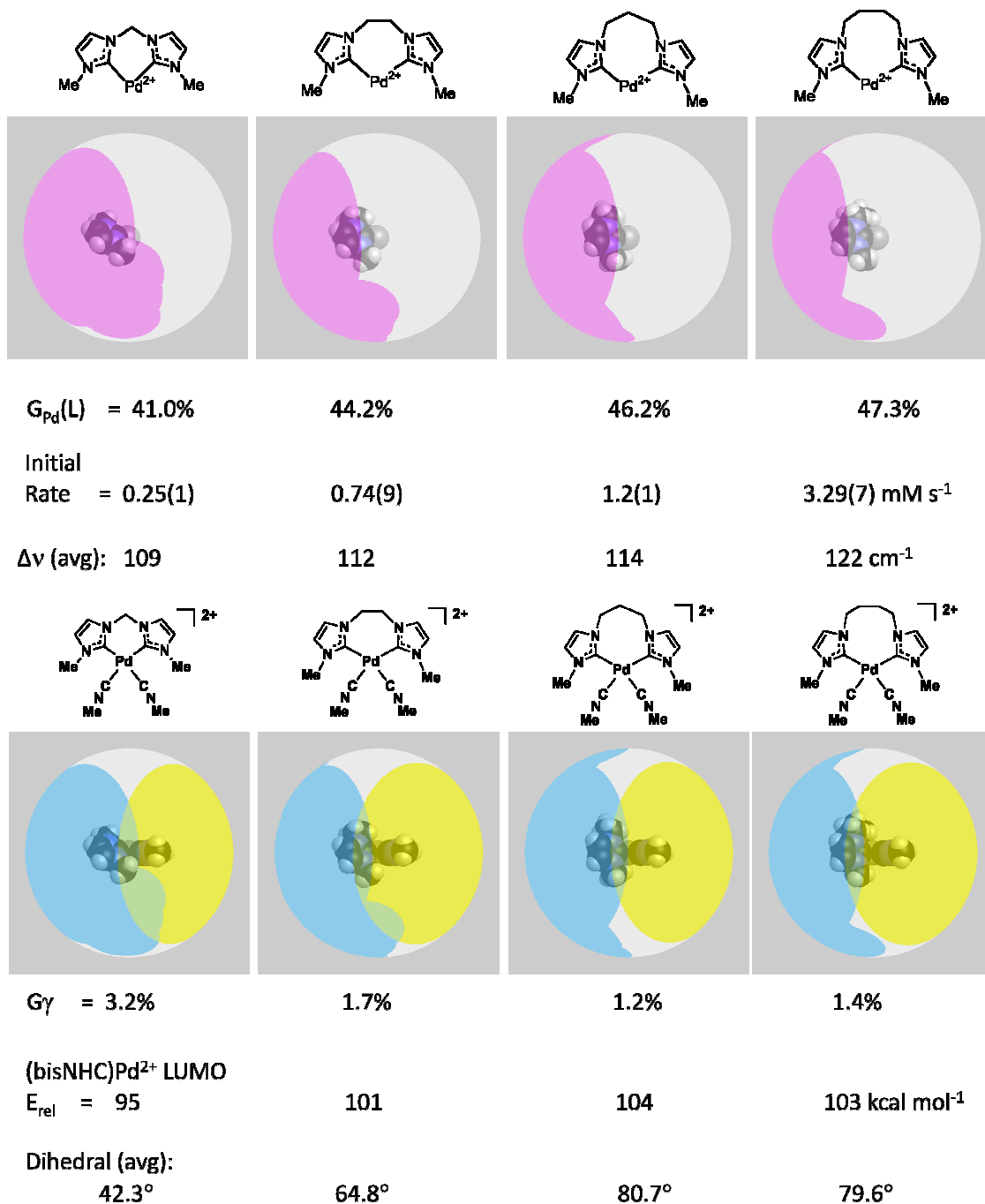


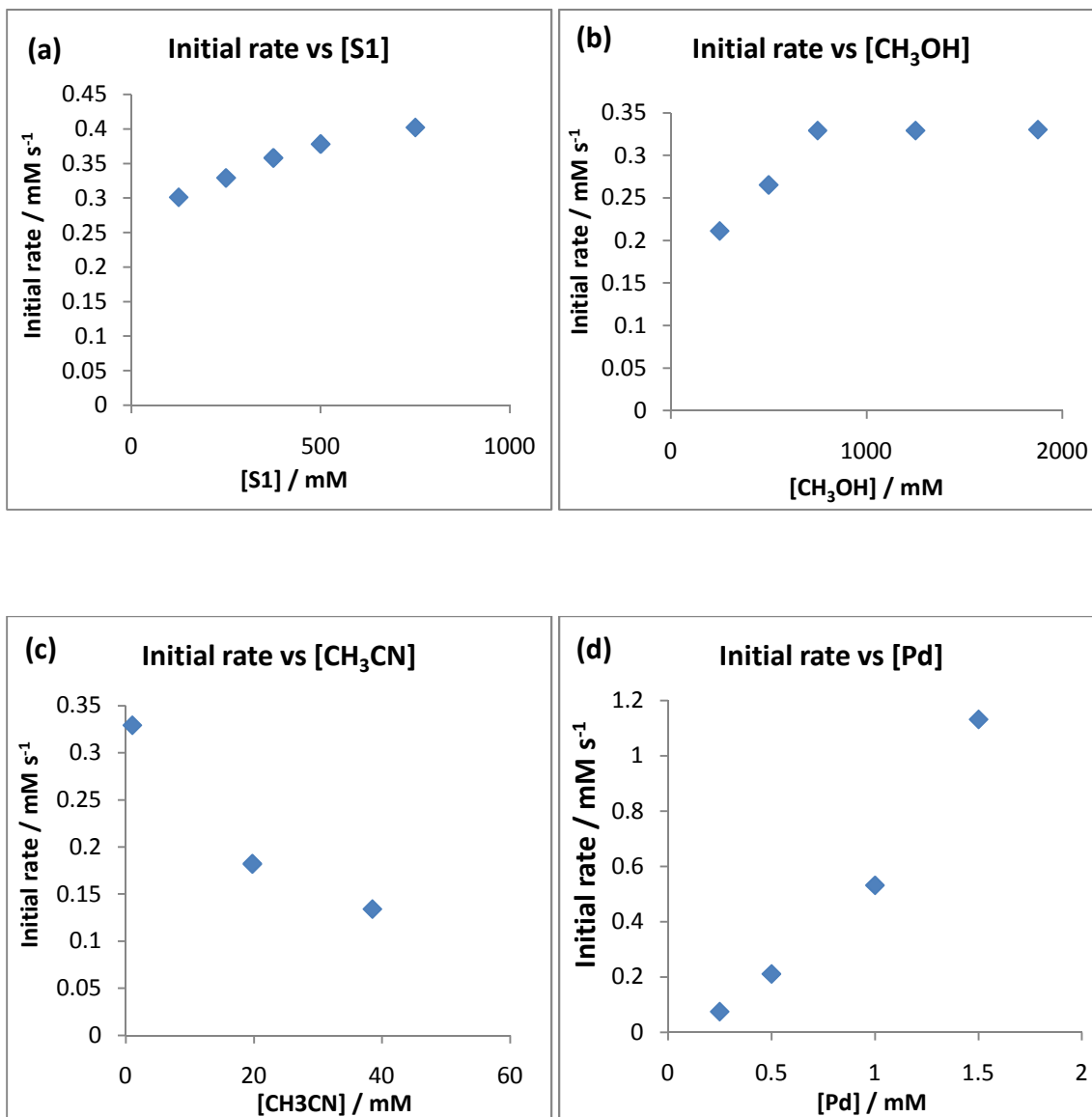
Figure 4.4. Calculated $G_{Pd(L)}$ and G_γ together with other stereoelectronic parameters

G_γ , representing the percentage of the Pd metal coordination sphere shielded by more than one ligand, shows the highest value for **26a**, decreases toward **26c**, and then shows a slightly increased value in **26d**. Dihedral angle inversely correlates with G_γ , with the lowest value observed for **26a**, an increase toward **26c**, and then a slightly decreased value in **26d**. The increase in dihedral angle moves the N-methyl groups away from the methylisocyanide ligand, making G_γ decreased. Large G_γ can reduce the catalytic activity because of steric interaction between bis(NHC) ligand and incoming substrate. Interestingly the relative LUMO energies of bis(NHC)Pd²⁺ also showed the same changes as G_γ . Therefore, a combination of steric and electronic parameters of the bis(NHC) ligands affects the catalytic activities of the complexes.

The reaction mechanism

The effects of changing concentrations of S1, Pd, methanol and acetonitrile on the rate of cyclization were measured by changing one variable and keeping the others constant. The rate is affected by all of these variables, as shown in Figure 4.5. Based on these results and previous studies,^{9,21} the reaction mechanism shown in Figure 4.6 can be proposed, with final protonation or attack of hemiacetal on alkyne or attack of methanol as the rate determining step. The rate is increased with increasing concentrations of S1, Pd, and methanol, while the rate decreased with increasing acetonitrile concentration, but these are not in linear relationships. The rate increases with increasing Pd concentration and did not fit simple first or second order kinetic plots. Acetonitrile inhibits the reaction, which is important, because the pre-catalyst contain two acetonitrile molecules. It showed

saturation kinetics at higher methanol concentration, this is may be due to changing the rate determined step to acetonitrile dissociation from pre-catalyst.



Reaction condition: (a) $[\text{Pd}] = 0.5 \text{ mM}$, $[\text{CH}_3\text{OH}] = 750 \text{ mM}$, $[\text{CH}_3\text{CN}] = 1 \text{ mM}$, (b) $[\text{Pd}] = 0.5 \text{ mM}$, $[\text{S1}] = 250 \text{ mM}$, $[\text{CH}_3\text{CN}] = 1 \text{ mM}$, (c) $[\text{S1}] = 0.5$, $[\text{Pd}] = 0.5 \text{ mM}$, $[\text{CH}_3\text{OH}] = 750 \text{ mM}$, (d) $[\text{S1}] = 250 \text{ mM}$, $[\text{CH}_3\text{OH}] = 250 \text{ mM}$, $[\text{CH}_3\text{CN}] = 1 \text{ mM}$ and diethyl glycol dibutyl ether as internal standard. Heated at 60°C and analyzed by G.C.

Figure 4.5. Effects on reaction rate of varying concentration of S1, CH₃CN, Pd catalyst, and CH₃OH.

In the proposed mechanism, dissociation of acetonitrile from the pre-catalyst **(i)** produces the active catalyst **(ii)**. The active catalyst **(ii)** forms a complex with the oxygen of the substrate aldehyde group **(iii)**. This makes the aldehyde susceptible to attack by methanol to produce a hemiacetal. The coordination of the alkyne of the substrate to Pd(L)^{2+} **(iv)** activates it towards nucleophilic attack of the hydroxyl moiety of the hemiacetal to produce the vinylpalladium intermediate **(v)**. This Pd(L)^{2+} can be either the previous Pd(L)^{2+} , which activated the aldehyde or a new Pd(L)^{2+} species. This explains why Pd did not show simple 1st or 2nd order kinetics. Finally, protonation of the vinylpalladium species produces cyclic alkenyl ether product (P1) and regenerates the active catalyst.

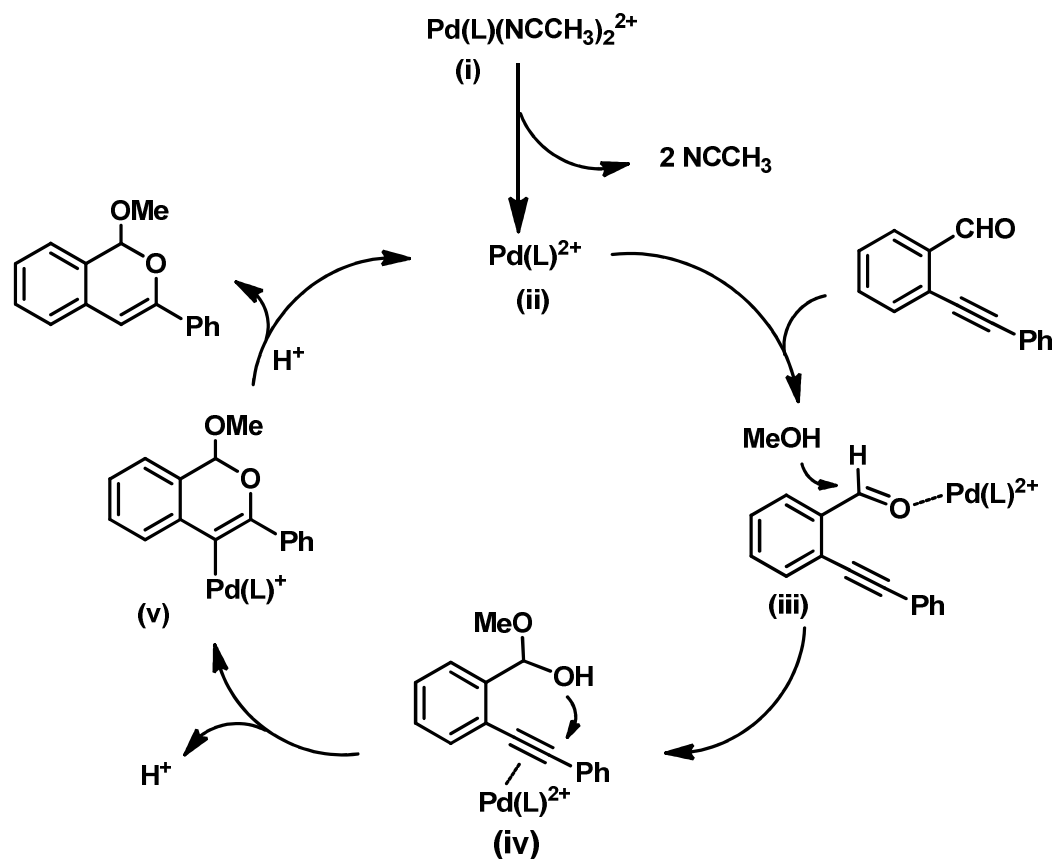
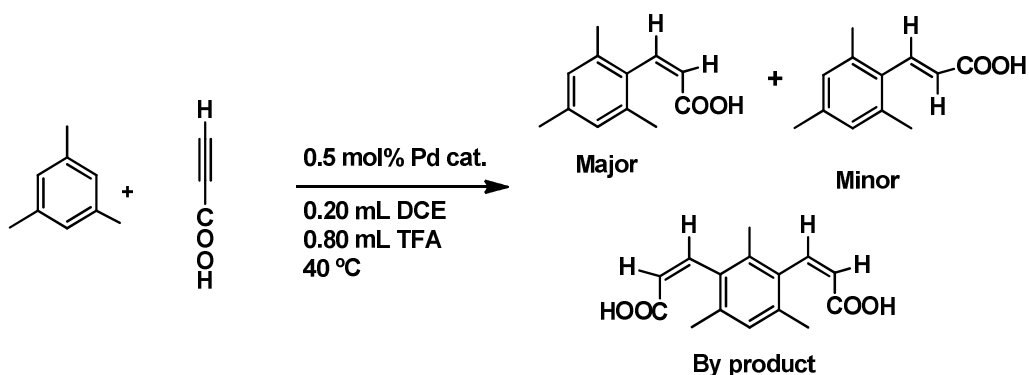


Figure 4.6. Reaction mechanism for cyclization of 2-(Phenylethynyl)benzaldehyde (S1)

Hydroarylation of aromatic C-H bonds with alkynes

A hydroarylation reaction was used to further assess the correlation between catalytic activity and donor ability. Mesitylene and propiolic acid were selected as arene and alkyne substrates, respectively. A slight modification of reaction conditions reported for Fujiwara was used for the reaction. Trifluoroacetic acid and dichloroethane were used as solvents in a 4:1 ratio. Excess propiolic acid was used for the reaction with a propiolic acid to mesitylene ratio of 1.4 : 1. Because of the acidic reaction conditions only bis(NHC) complexes were checked for catalytic activity. The reaction conditions are summarized in Scheme 4.8. Mesitylene, the palladium catalyst, and solvents (TFA and DCE) were placed in a 4 mL reaction vial closed by a screw cap with a PTFE/silicon septum. The reaction was initiated by injecting propiolic acid through the septum, and measurement of reaction time was started. Aliquots of the reaction mixture were withdrawn using a micro syringe at appropriate time intervals. Withdrawn samples were quenched by adding to CDCl_3-d_1 , and then analyzed by ^1H NMR. Dichloroethane present in the reaction mixture was used as an internal standard to calculate the concentrations of products. Results are summarized in Table 4.6.



Scheme 4.8. Hydroarylation reaction between mesitylene (1 equivalent) and propiolic acid (1.4 equivalents).

Table 4.6. Results for catalytic mesitylene (1 equivalent) addition to propiolic acid (1.4 equivalents).

Pd Catalyst	Mesitylene disappearance rate (mM /s)	% yield at 0.5 h (Z:E) ^a	% yield at 1 h (Z:E) ^a	% yield at 4 h (Z:E) ^a
8a	0.015(2)	37	50	85 (40:1)
8b	0.045(2)	53	69 (40:1)	82 (35:1)
8c	0.135(12)	77 (25:1)	-	-
8d	0.164(25)	74 (25:1)	-	-
8e	0.120(30)	30	61 (15:1)	72 (20:1)
8f	0.109(16)	61 (25:1)	71 (25:1)	74 (20:1)

^a Based on mesitylene using ¹H NMR

All bis(NHC) catalysts gave good yields (72 – 85 %). At the completion of the reaction all propiolic acid was consumed and some unreacted mesitylene was identified. Both Z and E isomers of the alkene product were identified, with Z as major product and E as the minor isomer. Trace amounts of the 1:2 arene/alkyne addition product were detected as a byproduct. Most transition metal catalysts undergo addition to C-C multiple bond in a *cis*-fashion, resulting in *trans*-products, but this reaction results in the *cis*-isomer (Z) as the major product. This is due to the reaction mechanism, where arene addition to the alkyne happens via electrophilic substitution.²⁹ These observations agreed with previously reported hydroarylation reactions.^{10,15-19,29,30} There were a few reports suggesting that excess of arene leads to the Z isomer excessively. Therefore, all of the

reactions were repeated using a 2:1 ratio of mesitylene to propiolic acid using same reaction conditions and method. The results are summarized in Table 4.7.

Table 4.7. Pd-catalyzed hydroarylation between mesitylene (2 equivalents) and propiolic acid (1 equivalent) correlated with IR stretching frequencies for analogous (ligand) Pd²⁺ methylisocyanide adducts.

Pd Catalyst	Mesitylene disappearance rate (mM /s)	% yield^a	[(MeNC)₂ Pd (L)]²⁺	Δν_{MeNC} cm⁻¹
31a	0.018(1)	94	26a	2269
31b	0.054(1)	92	26b	2272
31c	0.144(8)	98	26c	2274
31d	0.212(33)	94	26d	2282
31e	0.172(17)	92	26e	2251
31f	0.178(16)	96	26f	2279

^a Based on propiolic acid using ¹H NMR, E isomer is less than 3% of total product

All catalysts showed excellent yields (>92%) with excellent stereoselectivity (Z > 97%), and no double addition products were detected. Mesitylene concentrations were calculated from ¹H NMR integration ratios using dichloroethane as an internal standard. Initial rates for mesitylene disappearance (d[Mes]/dt) and uncertainties were determined up to 15-20% substrate consumption. Initial rates were determined from linear least-squares regression analyses of the plots of [Mes] versus time. Uncertainties are reported

at the 95% confidence level. To compare the catalytic activities with donor abilities of ligands, hydroarylation rate versus $\Delta\nu_{\text{MeNC}}$ with various catalysts are shown in Figure 4.3.

Figure 4.7 shows a correlation between hydroarylation rate and donor ability except for the ‘abnormal’ bis(NHC) complex (**26e** / **31e**). The highest hydroarylation rate was observed with the weakest donor ligand, the butylene linkage bis(NHC) of complex (**26d** / **31d**). The hydroarylation rate decreases with increasing donor ability until the methylene linkage bis(NHC) complex (**26a** / **31a**). However, an unusual increase in rate is observed for the strongest donor ligand, the ‘abnormal’ bis(NHC) complex (**26e** / **31e**). There were previous reports indicating the instability of ‘abnormal’ bis(NHC) metal complexes in acidic medium.³¹ Therefore, separate experiments were carried out to assess the stability of the ‘abnormal’ bis(NHC) metal complex **31e** and the butylene linkage bis(NHC) complex **31d**, the most active catalyst.

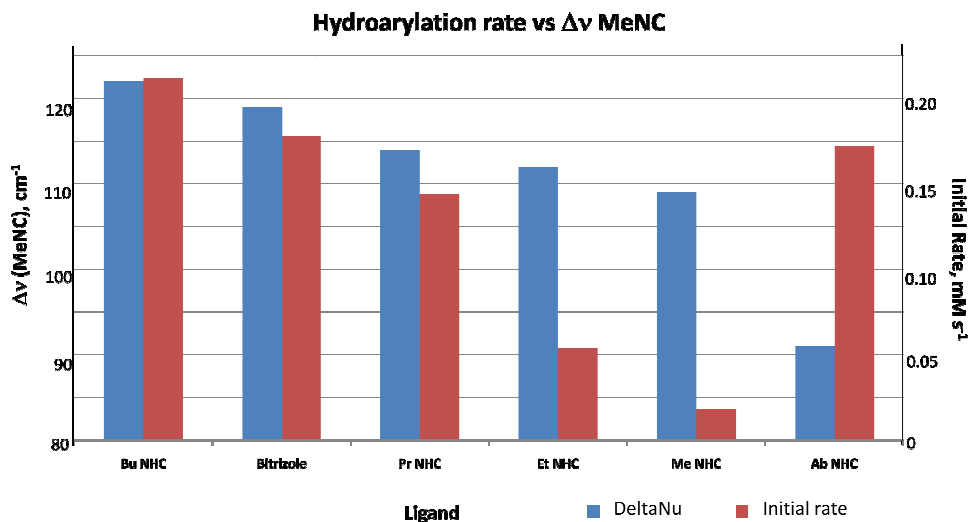
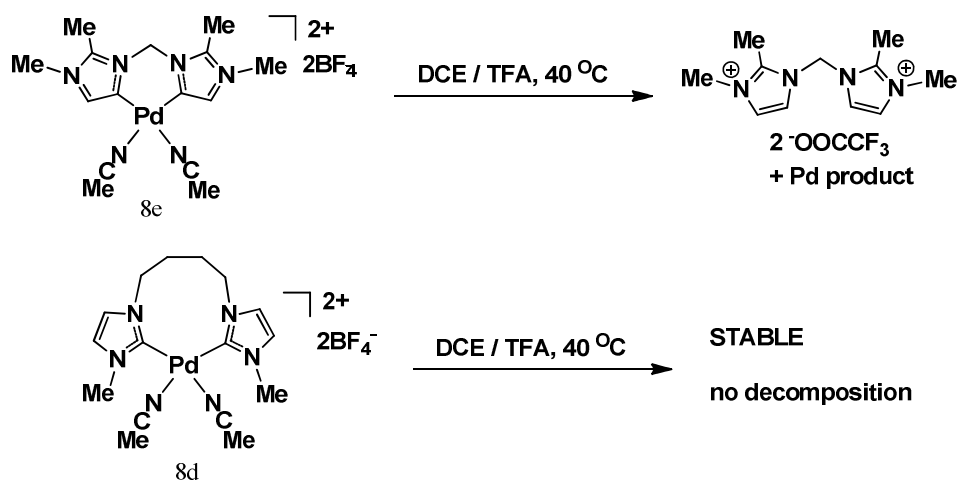


Figure 4.7. Hydroarylation rate versus $\Delta\nu_{\text{MeNC}}$ for bis(NHC) Pd^{2+} catalysts

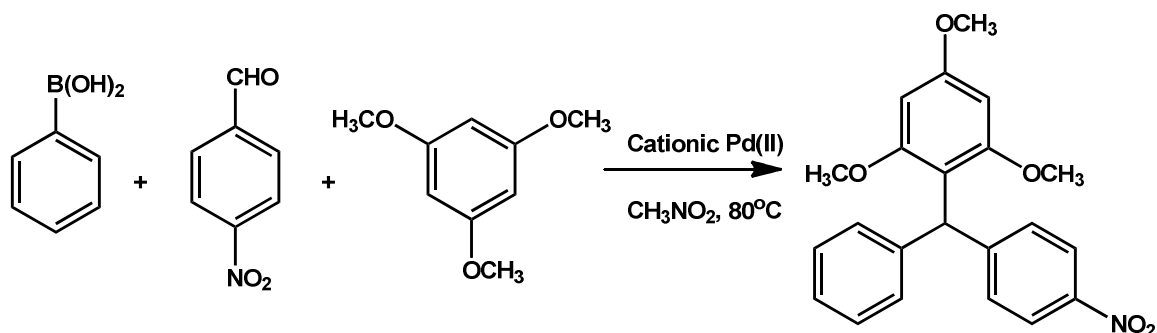
Palladium complexes **31d** and **31e** were dissolved in the solvent mixture (TFA : DCE 4:1) used for the hydroarylation reaction without substrates. The reaction mixtures were heated at 40°C for the time required to complete the reaction for the corresponding catalysts. The solutions were evaporated, then the residue was dried under vacuum, and ¹H NMR spectra were recorded. Complex **31d** did not show any decomposition, but complex **31e** did show significant decomposition (~75%) to a product that was identified as the corresponding imidazolium salt (Scheme 4.9). The ¹H NMR of the ‘abnormal’ bis imidazolium salt **24e** was checked in CF₃COOD-*d*₁. Resonances were similar to those found in the decomposed product of **31e**, thus indicating ‘abnormal’ bis(NHC) complex **31e** decomposed to imidazolium salt under acidic reaction condition for hydroarylation. No precipitate formation was observed during hydroarylation reactions of complex **31e**, but a bright pale orange color was observed, whereas other catalysts produced a light yellow/orange color. This suggests possible formation of naked palladium or nano particles, which leads to higher reaction rates than usual. These studies confirm the correlation between electrophilic catalytic activity and ligand donor ability, as observed in the catalytic cyclization of acetylinic aldehydes.



Scheme 4.9. Stability of bis(NHC) complexes **31d** and **31e** in acidic conditions

Other electrophilic catalytic reactions investigated

The one pot synthesis of asymmetric triarylmethanes from arylboronic acids, arylaldehydes and activated arylaldehydes with cationic Pd(II) was reported by Lu in 2007 (Scheme 4.10).³²



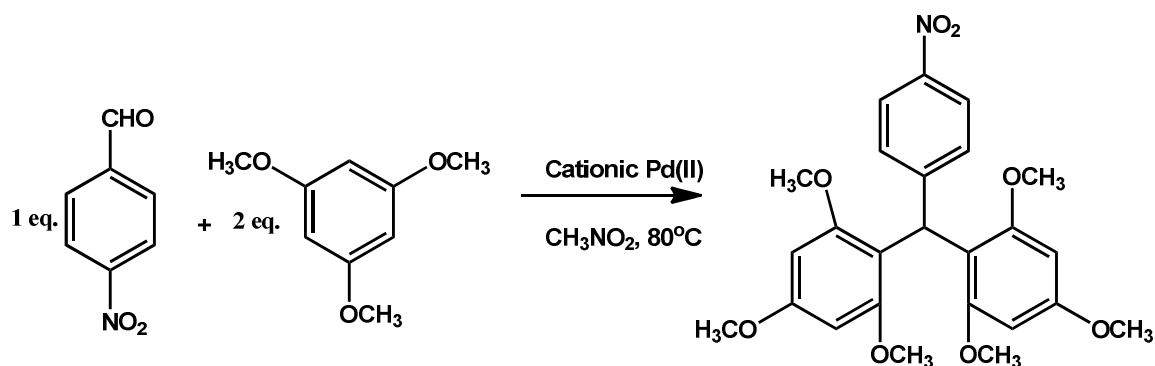
Scheme 4.10. One pot synthesis of asymmetrical triarylmethanes (adapted from reference 32)

The methylene linkage bis(NHC) Pd dibromide complex **25b** and bis(phosphine) complex (DPPB)PdCl₂ **27d** were used as palladium catalysts for initial studies. AgBF₄ was used to abstract halide and generate a cationic Pd(II) complex in-situ. The catalytic

study was started by placing 1.2 molar equivalents of phenylboronic acid, 1 molar equivalent of 4-nitrobenzaldehyde, 5 mol % Pd catalyst, 10 mol % AgBF₄, and CH₃NO₂ in a sealable thick-wall glass vessel. The reaction mixture was stirred and heated at 80 °C for 30 minutes, then 2 molar equivalents of 1,3,5-trimethoxybenzene was added, and the mixture was heated at 80 °C for another 12 hours. TLC analysis suggested significant amounts of unreacted phenylboronic acid. The resultant mixture was filtered through celite to remove palladium and silver salts, and the filtrate was concentrated. The residue was purified by flash chromatography (EtOAc : hexanes 1:9) and ~ 80 % unreacted phenylboronic acid was recovered. The expected triarylmethane was not detected but ~ 65 % of the double addition product ‘bis(2,4,6-trimethoxyphenyl)(*p*-nitrophenyl)methane’ was detected. The synthesis of this compound was previously reported with 1,3,5-trimethoxybenzene and 4-nitrobenzaldehyde using the AuCl₃/3AgOTf catalytic system.²⁶ The blank reaction, without palladium catalyst, also produced double addition product in excellent yield (> 90 %), suggesting silver salts also catalyze this double addition reaction.

Using the bis(acetonitrile) adduct of bis(NHC) complex **31a**, catalytic production of bis(2,4,6-trimethoxyphenyl)(*p*-nitrophenyl)methane was examined only using 1,3,5-trimethoxybenzene and 4-nitrobenzaldehyde. The synthesis was started by placing 1 molar equivalent of 4-nitrobenzaldehyde, 2 molar equivalents of 1,3,5-trimethoxybenzene, 5 mol % Pd catalyst, and CH₃NO₂ in a sealable thick-walled glass vessel. The reaction mixture was stirred and heated at 80 °C for 12 hours. The resultant mixture was concentrated, and the residue was purified by flash chromatography (EtOAc

: hexanes 1:9). Bis(2,4,6-trimethoxyphenyl)(*p*-nitrophenyl)methane was isolated in good yield (~ 80 %).



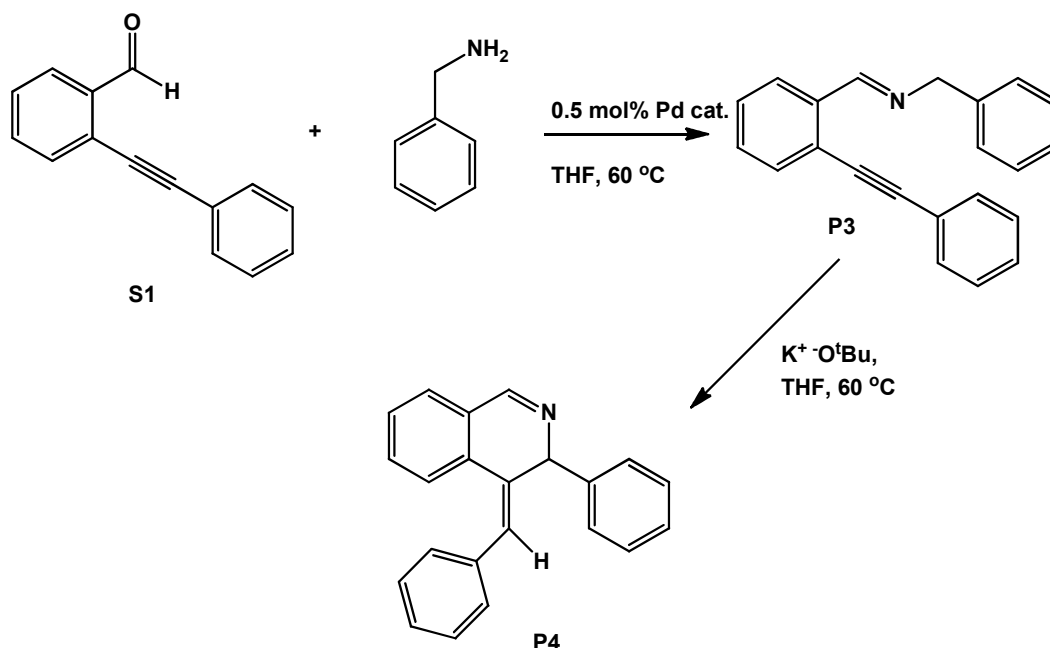
Scheme 4.11. Synthesis of bis(2,4,6-trimethoxyphenyl)(*p*-nitrophenyl)methane

These results suggests that during the triarylmethane synthesis, nucleophilic addition of phenylboronic acid to 4-nitrobenzaldehyde was not occurring. Reaction of phenylboronic acid and 4-nitrobenzaldehyde with 5% catalyst in CH₃NO₂ failed. During the time of this investigation, more electrophilic palladium catalysts were not synthesized, and modification of the reaction condition was not performed. Therefore using more electrophilic palladium catalysts like **31d** and optimizing reaction condition may produce asymmetric triarymethanes.

Cyclization of 2-(phenylethynyl)benzaldehyde using benzyl amine as a nucleophile

Dihydroisoquinoline derivatives have been synthesized using (phenylethynyl)benzaldehyde and amine together with another nucleophile or reducing agent like sodium borohydride.^{34,35} Ye reported very trace amounts of dihydroisoquinoline derivatives in the reaction of 2-(phenylethynyl)benzaldehyde **S1**,

benzylamine and ethynylbenzene.³⁵ Optimized reaction conditions for the cyclization of **S1** with methanol were used to set up a reaction between **S1** and benzylamine using bis(NHC) catalyst **31b**. No cyclization product was observed with elongated reaction times, but imine product **P3** was produced quantitatively within five minutes of reaction at 60 °C. The blank reaction revealed that Pd catalyst is necessary to obtain product **P3** at shorter reaction time. The solvent was changed to THF, and the reaction was set up in a 4 mL reaction vial closed by a screw cap with a PTFE/silicon septum. After complete consumption of **S1**, 1 molar equivalent of $K^+ ^-O^tBu$ in THF was injected, and the mixture was heated at 60 °C until the reaction was complete. Product was isolated using flash chromatography. The product was assigned as **P4** based on 1D-NMR data. More investigation is necessary to confirm the structure.



Scheme 4.12. Pd-catalyzed reaction between of 2-(phenylethynyl)benzaldehyde **S1**, benzylamine, and $K^+ ^-O^tBu$.

Summary and conclusion

The acetonitrile adducts of bis(NHC) palladium complexes showed excellent catalytic activities towards cyclization of 2-(phenylethynyl)benzaldehyde and hydroarylation of propiolic acid with mesitylene. The initial rates of these reactions with bis(carbene) complexes show a correlation with ligand donicity predicted by methylisocyanide IR probe studies in Chapter III. The highest initial rates for both catalytic reactions were observed for bis(NHC) complex **31d**, the complex with the weakest donor ligand. Complex **31e**, with the strongest donor 'abnormal' bis(NHC), shows the lowest initial rate for cyclization of 2-(phenylethynyl)benzaldehyde, but under acidic hydroarylation condition it decomposed to bis(imidazolium) salts. However, most of the bis(phosphine) ligands did not show this correlation because of their lability in palladium complexes. A non-labile, rigid bis(phosphine) complex **32f** shows the some correlation as bis(NHC) complexes. Therefore, the methylisocyanide IR probe study can be used to predict catalytic activity in electrophilic reactions.

Steric factors also show a correlation with catalytic activity and donor ability. Reaction rates increase with increasing percentage of the Pd metal coordination sphere shielded by ligand L (ligand shielding), $G_{Pd(L)}$. The bis(NHC) complex **31d**, showing the highest $G_{Pd(L)}$ value, also showed the highest initial rate. If a higher percentage of the Pd coordination sphere was overlapped by more than one ligand (G_γ), it also affected the reaction rate. This G_γ value showed a correlation with dihedral angle and LUMO energies of $(bisNHC)Pd^{2+}$.

Because of these correlations between stereoelectronic factors and donicity, it can be suggested that a proper balance between steric and electronic factors is necessary to

design highly active catalysts. The bis(NHC) complexes showed wide variations in catalytic activity and donicity. Therefore, bis(NHC) ligands can be tuned to support electrophilic catalysis by a metal, in contrast to the prevailing use of mono-NHCs to engender electron rich metal centers.

Experimental

General Considerations. All manipulations were carried out under air unless otherwise noted. Diethyl ether (Acros), *n*-hexane (Acros), THF (Pharmco), toluene, 1,4-dioxane and hexanes (Pharmco) were purified by distillation from sodium benzophenone ketyl. Dichloromethane (Pharmco) and dichloroethane were washed with a sequence of concentrated H₂SO₄, de-ionized water, 5% Na₂CO₃ and de-ionized water, followed by pre drying over anhydrous CaCl₂, then refluxing over and distillation from P₂O₅ under nitrogen. Acetonitrile (Pharmco) was pre-dried over anhydrous CaCl₂ and refluxed over and distilled from CaH₂ under nitrogen. NMR solvents were purchased from Cambridge Isotope Laboratories. DMSO-*d*₆ and CD₃CN-*d*₃ were dried over activated 4 Å molecular sieves followed by vacuum distillation at room temperature. CD₂Cl₂ was dried over activated 4 Å molecular sieves and stored over P₂O₅ before distillation at room temperature for use. All other reagents were purchased from Acros, Aldrich, or Strem and used as received. 2-(Phenylethynyl)benzaldehyde (**S1**)²⁰ was prepared by literature procedures. Products of 2-(phenylethynyl)benzaldehyde cyclization and hydroarylation reactions were identified by comparison with published data.^{21,30} NMR spectra were recorded on Varian GEMINI 2000 (300 MHz) and Varian Unity INOVA (400 and 600 MHz) spectrometers. Reported chemical shifts are referenced to residual solvent peaks

(13C, 1H). GC spectra were acquired from an Agilent 6850 series GC system with FID detectors using an HP-1 column (0.32 mm widebore, 0.25 μ m film and 30 m length).

Elemental analyses were performed by Midwest Microlab, Indianapolis, Indiana.

General procedures for catalytic reactions

Cyclization of 2-(Phenylethynyl)benzaldehyde (S1)

2-(Phenylethynyl)benzaldehyde (0.5 mmol, 100 μ L) and diethylene glycol dibutyl ether (50 μ L) were mixed with 0.5 mol % Pd catalyst in 0.85 mL of 1,2-dichloroethane, and the mixture was heated at 60 $^{\circ}$ C for 5 minutes. CH_3OH (0.6 mmol, 25 μ L) was then added to the reaction mixture, and the temperature was maintained at 60 $^{\circ}$ C. 10 μ L samples were withdrawn at appropriate time intervals and added to excess CH_3NC in hexanes to quench the reaction. The mixture was filtered through celite to remove catalyst, and the filtrate was diluted to a known volume and analyzed by G.C. In a separate experiment, product was isolated using flash chromatography.

Hydroarylation of propiolic acid with mesitylene

Mesitylene (2.0 mmol, 286 μ L), Pd catalyst (0.5 mol % based on propiolic acid), 0.20 mL dichloroethane and 0.80 mL trifluoroacetic acid were mixed in a 4 mL reaction vial under argon. The mixture was heated at 40 $^{\circ}$ C for 3 minutes, and then propiolic acid (1.0 mmol, 63 μ L) was added. 10 μ L samples were withdrawn at appropriate time intervals and added to CDCl_3 to quench the reaction. Samples were analyzed by ^1H NMR

using dichloroethane integration as an internal standard. Products were identified by comparison with reported NMR spectra of products.

Kinetic Studies

Experiments were set up as described above for general catalytic procedures. Reactant concentration was varied according to experiment. Concentrations of substrate and products at various time were determined using G.C. or ^1H NMR. The rates of reactions and uncertainties were determined from linear least-square regression analysis of plots of concentrations of substrate and product versus time. Uncertainties were reported at the 95% confidence level.

[[1,1'-Dimethyl-3,3'-ethylenediimidazol-2,2'-diylidene}palladium(II) (NCCH₃)₂][BF₄]₂ 31b

A mixture of (1,1'-dimethyl-3,3'-ethylenediimidazol-2,2'-diylidene)PdBr₂ (100 mg, 0.218 mmol), AgBF₄ (90 mg, 0.438 mmol), and anhydrous acetonitrile (10 mL) was placed in a sealed ampule under nitrogen. The reaction mixture was heated at 60 °C for 4 h with stirring. The mixture was then filtered through celite, the solvent was removed under vacuum, and the residue was dried in vacuum for 3 h. The product was again dissolved in acetonitrile (5 mL), it was filtered through celite, solvent was evaporated, and the residue was dried in vacuum for 3 h. This sequence was repeated one more time. In the final sequence, diethyl ether was added to the filtrate to obtain product as white crystals. The product was isolated by filtration and dried in vacuo for 12 h. Yield: 104 mg, 87%. ^1H NMR (400 MHz, DMSO-*d*₆): δ 7.51(d, 4H, $^3J_{\text{HH}} = 7.6$ Hz, *imidazole*), 5.31-

5.29 (m, 2H, CH₂), 4.60-4.54 (m, 2H, CH₂), 3.91 (s, 6H, imid.N-CH₃) 2.08 (s, 6H, CN-CH₃). ¹³C NMR (100 MHz, DMSO-d₆): δ 144.27 (carbene), 125.00 (imid. C), 124.03 (imid. C), 118.18 (NC-CH₃), 47.20 (N-CH₂), 37.48 (imid.N-CH₃), 1.18 (t, CH₃-CN).
Anal. Calculated for C₁₄H₂₀ B₂F₈N₆Pd: C, 30.44; H, 3.65; N, 15.22 %. Found: C, 30.80; H, 3.77; N, 15.21 %.

[[1,1'-Dimethyl-3,3'-propylenediimidazol-2,2'-diylidene]palladium(II) (NCCH₃)₂] [BF₄]₂ 31c

A mixture of (1,1'-dimethyl-3,3'-propylenediimidazol-2,2'-diylidene)PdBr₂ (60 mg, 0.128 mmol), AgBF₄ (50 mg, 0.255 mmol), and anhydrous acetonitrile (10 mL) was placed in a sealed ampule under nitrogen. The reaction mixture was heated at 60 °C for 4 h with stirring. The mixture was then filtered through celite, the solvent was removed under vacuum, and the residue was dried in vacuum for 3 h. The product was again dissolved in acetonitrile (5 mL), it was filtered through celite, the solvent was evaporated, and the product was dried in vacuum for 3 h. This sequence was repeated one more time. In the final sequence, diethyl ether was added to the filtrate to obtain product as white crystals. The product was isolated by filtration and dried in vacuo for 12 h. Yield: 67 mg, 92%. ¹H NMR (400 MHz, DMSO-d₆): δ 7.47(d, 2H, ³J_{HH} = 2 Hz, *imidazole*), 7.44(d, 2H, ³J_{HH} = 1.6 Hz, *imidazole*), 5.05 (br t, 2H, ³J_{HH} = 12.8, CH₂), 4.49-4.44 (dd, ³J_{HH} = 5.8, 14.2, 2H, CH₂), 4.07 (s, 6H, imid.N-CH₃), 2.38-2.34 (m, 1H, CH₂), 2.07 (s, 6H, CH₃-CN), 1.82-1.73 (m, 1H, CH₂). ¹³C NMR (100 MHz, DMSO-d₆): δ 147.24 (Carbene), 124.84 (imid. C), 124.60 (imid. C), 118.18 (NC-CH₃), 51.31 (N-CH₂), 37.62 (imid.N-CH₃), 30.97 (C-CH₂), 1.18 (t, CH₃-CN). Anal. Calculated for: C₁₅H₂₂ B₂F₈N₆Pd: C, 31.81; H, 3.92; N, 14.84 %. Found: C, 32.67; H, 4.09; N, 14.93 %.

**[{1,1'-Dimethyl-3,3'-butylenediimidazol-2,2'-diylidene}palladium(II) (NCCH₃)₂]
[BF₄]₂ 31d**

A mixture of (1,1'-dimethyl-3,3'-butylenediimidazol-2,2'-diylidene)PdCl₂ (178 mg, 0.449 mmol), AgBF₄ (175 mg, 0.897 mmol), and anhydrous acetonitrile (10 mL) was placed in a sealed ampule under nitrogen. The reaction mixture was heated at 60 °C for 4 h with stirring. The mixture was then filtered through celite, the solvent was removed under vacuum, and the residue was dried in vacuum for 3 h. The product was again dissolved in acetonitrile (5 mL), it was filtered through celite, the solvent was evaporated and the product was dried in vacuum for 3 h. This sequence was repeated one more time. In the final sequence, diethyl ether was layered over the filtrate to obtain product as white crystals. Product was isolated by filtration and dried in vacuo for 12 h. Yield: 137 mg, 54%. ¹H NMR (400 MHz, CD₃CN-d₃): δ 7.21 (s, 4H, *imidazole*), 4.89 (br m, 2H, CH₂), 4.24 (br m, 2H, CH₂), 3.98 (s, 6H, imid.N-CH₃), 2.05 (br s, 2H, CH₂), 1.96 (s, 6H, CN-CH₃), 1.50 (br s, 2H, CH₂), ¹³C NMR (100 MHz, CD₃CN-d₃): δ 146.23 (carbene), 126.57 (imid. C), 124.08 (imid. C), 47.19 (N-CH₂), 38.87 (imid.N-CH₃), 26.03 (C-CH₂), 1.78 (CH₃-CN). Anal. Calculated for C₁₆H₂₄ B₂F₈N₆Pd: C, 33.11; H, 4.17; N, 14.48 %. Found: C, 33.03; H, 4.16; N, 14.37 %.

**[(1,1',2,2'-Tetramethyl-3,3'-methylenediimidazol-2,2'-diylidene) palladium(II)
(NCCH₃)₂] [BF₄]₂ 31f**

A mixture of (1,1',2,2'-tetramethyl-3,3'-methylenediimidazol-2,2'-diylidene)PdBr₂ (100 mg, 0.212 mmol), AgBF₄ (98 mg, 0.426 mmol), and anhydrous acetonitrile (10 mL) was placed in a sealed ampule under nitrogen. The reaction mixture was heated at 60 °C for 4 h with stirring. The mixture was then filtered through celite, the solvent was

removed under vacuum, and the residue was dried in vacuum for 3 h. The product was again dissolved in acetonitrile (5 mL), it was filtered through celite, the solvent was evaporated and the product was dried in vacuum for 3 h. This sequence was repeated one more time. In the final sequence, diethyl ether was added to the filtrate to obtain product as white crystals. Product was isolated by filtration and dried in vacuo for 12 h. Yield: 98 mg, 82%. ^1H NMR (400 MHz, DMSO- d_6): δ 6.98 (s, 2H, *imidazole*), 6.05 (s, 2H, *CH*₂), 3.68 (s, 6H, *imid.N-CH*₃), 2.65 (s, 6H, *imid.C-CH*₃), 2.08 (s, 6H, *NC-CH*₃). ^{13}C NMR (100 MHz, DMSO- d_6): δ 143.17 (carbene), 126.16 (*imid.C-CH*₃), 123.59 (*CN-CH*₃), 118.21 (*imid.CH*), 59.77 (*N-CH*₂), 34.16 (*imid.N-CH*₃), 9.72 (*imid.C-CH*₃), 1.20 (*NC-CH*₃). Anal. Calculated for C₁₅H₂₂ B₂F₈N₆Pd: C, 31.81; H, 3.92; N, 14.84 %. Found: C, 31.90; H, 3.98; N, 14.82 %.

[(1,2-Bis(diphenylphosphino)benzene)palladium(II)(NCCH₃)₂][BF₄]₂

A mixture of (DPPBenzene)PdCl₂ (150 mg, 0.241 mmol), AgBF₄ (94 mg, 0.481 mmol), and anhydrous acetonitrile (10 mL) was placed in a sealed ampule under nitrogen. The reaction mixture was heated at 60 °C for 2 h with stirring. The mixture was then filtered through celite, the solvent was removed under vacuum, and the residue was dried in vacuum for 3 h. Dichloromethane (10 mL) was added, and the mixture was again filtered through celite. The solvent was removed under vacuum, the product was dissolved in acetonitrile, and diethyl ether was layered over the solution to get pale yellow crystals. Product was isolated by filtration and dried in vacuo for 12 h. Yield: 120 mg, 61%. ^1H NMR (400 MHz, CD₃CN- d_3): δ 7.92-7.59 (m, 24H, Ph), 1.96 (s, 6H, *NCCH*₃). ^{13}C NMR (100 MHz, CD₃CN- d_3): δ 136.60 (Ph), 135.24 (Ph), 135.12 (Ph),

135.01 (Ph), 134.94 (Ph), 134.80 (Ph), 134.73 (Ph), 134.68 (Ph), 131.00 (Ph), 130.93 (Ph), 130.87 (Ph), 126.02 (Ph), 1.76 (NC-CH₃). Anal. Calculated for: C₃₄H₃₀B₂F₈N₂P₂Pd: C, 50.50; H, 3.74; N, 3.46 %. Found: C, 50.19; H, 3.84; N, 3.54 %.

References

- (1) Tietze, L. F.; Ila, H.; Bell, H. P. *Chem. Rev.* **2004**, *104*, 3453.
- (2) Mikami, K.; Hatano, M.; Akiyama, K. *Scripta Materialia* **2011**, *64*, 161.
- (3) Yamamoto, H. *Lewis Acids in Organic Synthesis*; Wiley-VCH: Weinheim, **2000**, Vol. 1-2.
- (4) Yamamoto, H. *Lewis Acid Reagents* Oxford University Press: New York, **1999**.
- (5) Murahashi, S.-I., Davies, S. G. *Transition Metal Catalysed Reactions* Blackwell Science: Cambridge, MA, **1999**.
- (6) Tsuji, J. *Transition Metal Reagents and Catalysts: InnoVations in Organic Synthesis*; Wiley: New York, **2000**.
- (7) Sawamura, M.; Sudoh, M.; Ito, Y. *J. Am. Chem. Soc.* **1996**, *118*, 3309.
- (8) Ikeda, S.-i.; Mori, N.; Sato, Y. *J. Am. Chem. Soc.* **1997**, *119*, 4779.
- (9) Asao, N.; Nogami, T.; Takahashi, K.; Yamamoto, Y. *J. Am. Chem. Soc.* **2002**, *124*, 764.
- (10) Jia, C. G.; Piao, D. G.; Oyamada, J. Z.; Lu, W. J.; Kitamura, T.; Fujiwara, Y. *Science* **2000**, *287*, 1992.
- (11) Kamijo, S.; Yamamoto, Y. *Journal of Organic Chemistry* **2003**, *68*, 4764.
- (12) Ohtaka, M.; Nakamura, H.; Yamamoto, Y. *Tetrahedron Lett.* **2004**, *45*, 7339.

- (13) Bates, C. G.; Saejueng, P.; Murphy, J. M.; Venkataraman, D. *Organic Letters* **2002**, *4*, 4727.
- (14) Yao, T. L.; Larock, R. C. *Tetrahedron Lett.* **2002**, *43*, 7401.
- (15) Oyamada, J.; Kitamura, T. *Tetrahedron Lett.* **2005**, *46*, 3823.
- (16) Reetz, M. T.; Sommer, K. *Eur J Org Chem* **2003**, 3485.
- (17) Biffis, A.; Gazzola, L.; Gobbo, P.; Buscemi, G.; Tubaro, C.; Basato, M. *Eur J Org Chem* **2009**, 3189.
- (18) Buscemi, G.; Biffis, A.; Tubaro, C.; Basato, M.; Graiff, C.; Tiripicchio, A. *Applied Organometallic Chemistry* **2010**, *24*, 285.
- (19) Buscemi, G.; Biffis, A.; Tubaro, C.; Basato, M. *Catalysis Today* **2009**, *140*, 84.
- (20) Dyker, G.; Stirner, W.; Henkel, G. *Eur J Org Chem* **2000**, 1433.
- (21) Godet, T.; Vaxelaire, C.; Michel, C.; Milet, A.; Belmont, P. *Chemistry-a European Journal* **2007**, *13*, 5632.
- (22) Tolman, C. A. *Chem. Rev.* **1977**, *77*, 313.
- (23) Brown, T. L. *Inorganic Chemistry* **1992**, *31*, 1286.
- (24) Lomas, J. S.; Luong, P. K.; Dubois, J. E. *J. Am. Chem. Soc.* **1977**, *99*, 5478.
- (25) Fernandez, A.; Reyes, C.; Wilson, M. R.; Woska, D. C.; Prock, A.; Giering, M. P. *Organometallics* **1997**, *16*, 342.
- (26) Liu, H. Y.; Eriks, K.; Prock, A.; Giering, W. P. *Organometallics* **1990**, *9*, 1758.
- (27) Guzei, I. A.; Wendt, M. *Dalton Transactions* **2006**, 3991.
- (28) Hillier, A. C.; Sommer, W. J.; Yong, B. S.; Petersen, J. L.; Cavallo, L.; Nolan, S. P. *Organometallics* **2003**, *22*, 4322.
- (29) Tunge, J. A.; Foresee, L. N. *Organometallics* **2005**, *24*, 6440.

- (30) Oyamada, J.; Kitamura, T. *Tetrahedron* **2007**, *63*, 12754.
- (31) Heckenroth, M.; Kluser, E.; Neels, A.; Albrecht, M. *Angewandte Chemie-International Edition* **2007**, *46*, 6293.
- (32) Lin, S. H.; Lu, X. Y. *Journal of Organic Chemistry* **2007**, *72*, 9757.
- (33) Nair, V.; Abhilash, K. G.; Vidya, N. *Organic Letters* **2005**, *7*, 5857.
- (34) Ding, Q.; Yu, X.; Wu, J. *Tetrahedron Lett.* **2008**, *49*, 2752.
- (35) Ye, Y.; Ding, Q. P.; Wu, H. *Tetrahedron* **2008**, *64*, 1378.

CHAPTER V

POLARIZED NAZAROV CYCLIZATIONS CATALYZED BY CATIONIC BIS(CARBENE) PALLADIUM (II) COMPLEXES AND SILVER SALTS

Introduction

The presence of five membered carbocycles in natural products and bioactive compounds has driven interest in the development of successful methods for their synthesis. For the past few decades, the Nazarov cyclization reaction has shown tremendous growth in reaction scope and application. It has found application in key steps of the syntheses of natural products, drugs and other compounds.¹ The Nazarov cyclization reaction is a 4π electrocyclic reaction which creates a new carbon-carbon bond stereospecifically through orbital reorganization. The mechanism involves conversion of divinyl ketones **1** to cyclopentenones **5** through Lewis acid activation.²

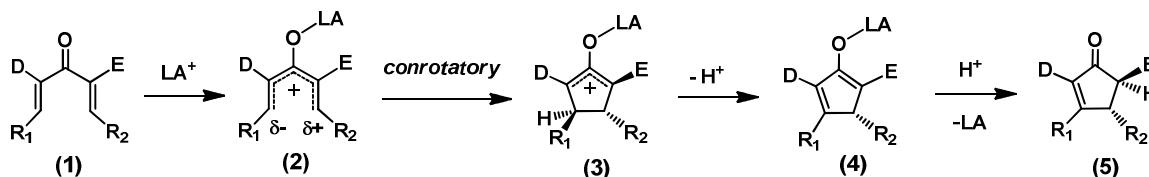


Figure 5.1. Nazarov cyclization mechanism

First, divinyl ketone **(1)** binds to a Lewis acid to give a pentadienyl cation **(2)**. Cyclization of **(2)** then produces an oxyallyl cation **(3)**. This cyclization must proceed with conservation of orbital symmetry, so disrotatory ring closure is electronically forbidden. Therefore, only the conrotatory ring closure pathway is followed, producing an anti configuration of R₁ and R₂ **(3)** and ensuring stereospecific bond formation. Finally, a proton shift from **(3)** produces cyclopentenones **(5)** through a Lewis acid-bound enolate **(4)**. This step produces a double bond normally in the thermodynamically more stable position, which is that with the highest degree of substitution.² Harsh reaction conditions affects the position of the double bond in the final product.

In early work, stoichiometric amounts of strong Lewis acids,³⁻⁵ often with a strong promoter⁶⁻⁹ such as BF₃, AlCl₃, SnCl₄ or TiCl₄, were used to get optimum yields in Nazarov cyclization reactions. The introduction of polarized vinyl ketones contributed to new developments in this field. These highly reactive vinyl ketones undergo catalytic cyclization by a number of mild Lewis acids and transition metal complexes.¹⁰

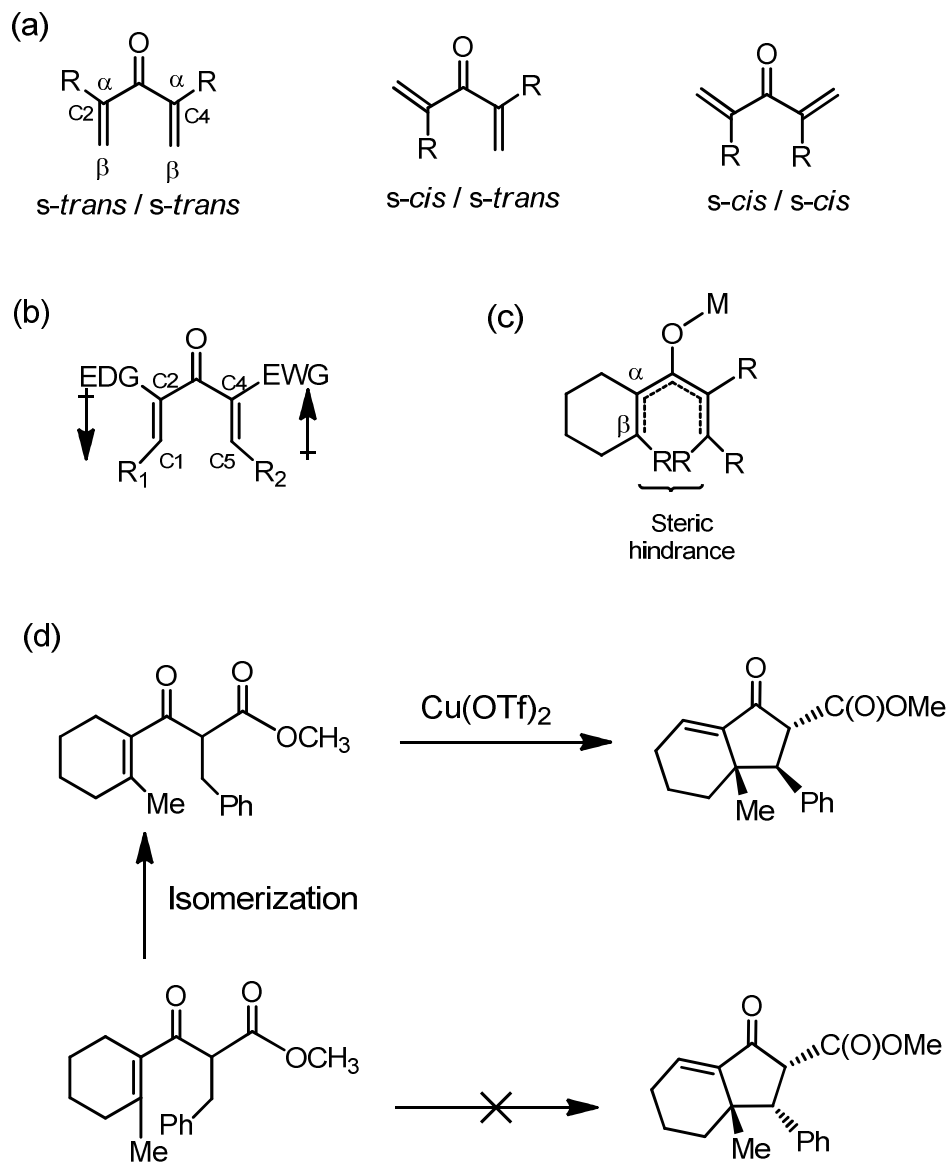


Figure 5.2. Effects of different substituent patterns on the catalytic activity.

Certain characteristics of the substrate will affect the catalytic activity, as shown in Figure 5.2. The α -substituents on C2 and C4 on the divinyl ketone improve the cyclization activity due to higher rates of cyclization, favoring the *s-trans* enone conformers.² Electron-donating groups at the C2 position and electron-withdrawing groups at the C4 position increase cyclization rates due to creation of a “polarized” divinyl ketone system.² Internal β -substituted substrates encounter steric hindrance due to the planar conformation adopted by the cation during electrocyclization. Denmark showed that tetrasubstituted alkenes cyclize slower than trisubstituted alkenes.¹¹ It is reported that isomers with *Z* geometry cyclize directly to give the product, while the *E* isomer undergoes isomerization prior to cyclization, resulting in only one diastereomer being observed in reactions of mixtures of isomers.¹²⁻¹⁴

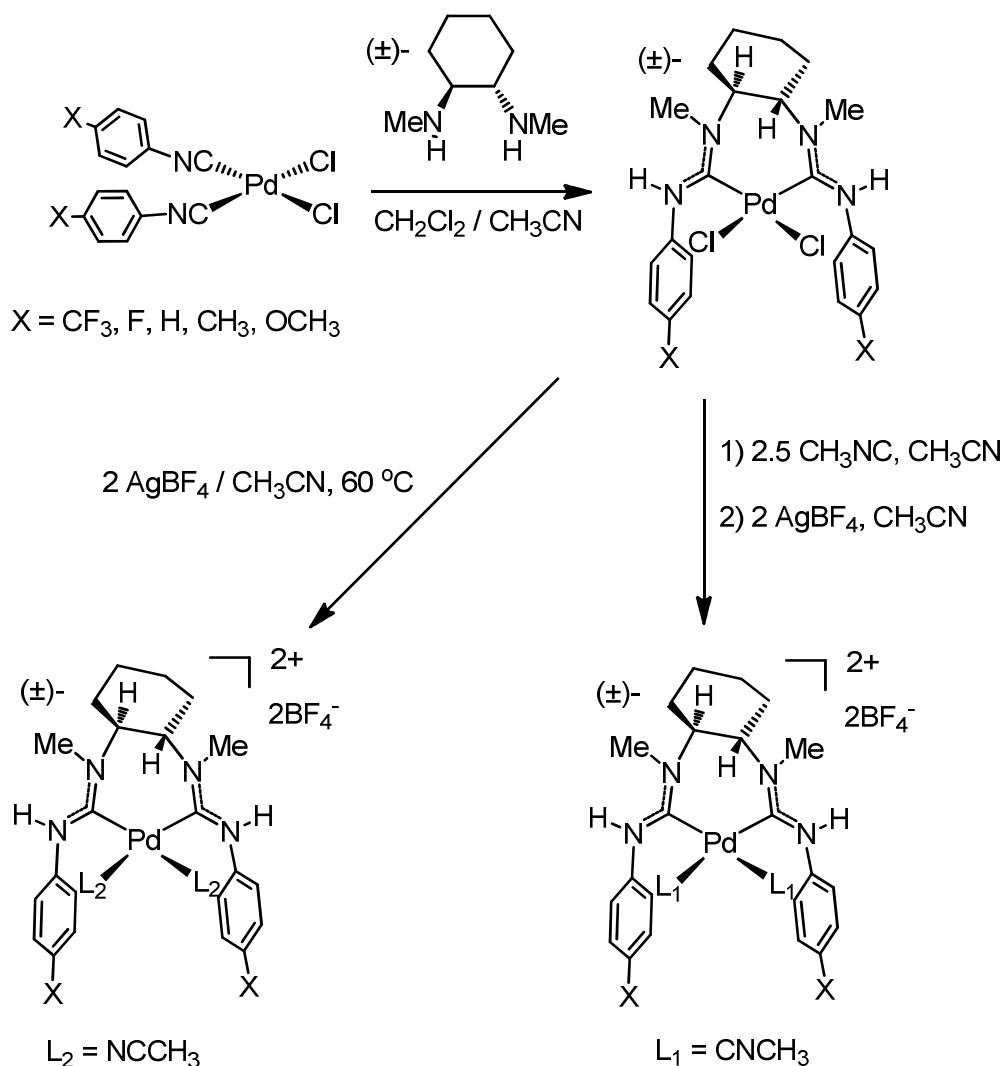
Substrates with an oxygen substituent at the C4 position of the dienone are cyclized efficiently under lower catalytic loading. Frontier et al. reported that cationic iridium(III)¹⁵ and palladium(II)¹⁶ complexes catalyzed cyclization of polarized vinyl β -keto esters. The availability of two adjacent *cis*-coordination sites is important for the catalytic activity. The presence of Na salts as an additive in the Nazarov cyclization promoted the intermediate oxyallyl cation to undergo a Wagner-Meerwein rearrangement to form spirocyclic cyclopentenones.^{15,16} Togni in 2004 reported a V(IV) salen dichloride complex with an AgSbF₆ additive to catalyze the Nazarov cyclization of polarized vinyl keto esters.¹⁷ Until now, there has not much been investigation done to identify the role of silver salts as a promoter in Nazarov cyclizations.

The current investigation focused on polarized Nazarov cyclization reactions catalyzed by cationic bis(ADC) palladium complexes.

Results and Discussion

Synthesis of bis(ADC) complexes

Wanniarachchi¹⁸ and Miranda¹⁹ in the Slaughter research group reported five different bis(ADC) palladium complexes with a cyclohexane diamine backbone. The only difference in these complexes is the phenyl *para* substituent. Five different *p*-substituents were used, from electron withdrawing CF₃ to electron donating OCH₃.



Scheme 5.1. Synthesis of bis(ADC) palladium complexes (adapted from references 16 and 17)

Bis(ADC) complexes were synthesized according to Wanniarachchi¹⁸ and Miranda's¹⁹ procedure as given in Scheme 5.1. The synthesis started by placing one equivalent of bis(isocyanide) palladium dichloride precursors and dry dichloromethane in a two neck round bottom flask fixed with a septum and a needle vial. One equivalent of (*rac*)-*N, N'*-dimethyl-1,2-diaminocyclohexane was added to the precursor via a syringe pump under argon, and the mixture was stirred for an additional two hours at room temperature. The solvent was then stripped under vacuum, the residue was dried, and dry acetonitrile was added. The resultant mixture was refluxed for two hours under argon, during which time a white precipitate began to form. The white solid, bis(ADC)PdCl₂ was isolated by filtration and dried under vacuum. In order to synthesize MeNC adducts for IR probe studies, the bis(ADC)PdCl₂ complexes were treated with excess methylisocyanide (2.5 equivalents) in dry acetonitrile. This mixture was stirred at room temperature for 2 hours to produce MeNC adducts. Chloride anions in the bis(ADC) palladium acetonitrile adducts were replaced with tetrafluoroborate anions by treatment with silver tetrafluoroborate in acetonitrile. Immediately after the addition of AgBF₄, the reaction mixture started to precipitate silver chloride, and the mixture was stirred for two hours to complete the reaction. The reaction mixture was filtered through celite to remove the silver chloride. The product was isolated by layering diethyl ether onto the concentrated solution in acetonitrile. IR stretching frequencies of N≡C in bis(methylisocyanide) adducts of bis(ADC) palladium complexes were recorded at high resolution (0.5 cm⁻¹). The *p*-CF₃ substituted ADC complex showed the highest stretching frequency, thus indicating lowest effective donicity. ADC complexes with *p*-CH₃ and *p*-

OCH₃ substituents showed the lowest stretching frequencies and highest effective donicity. These values correlated with Hammett constants (σ) as shown in Table 5.1.

Table 5.1. $\Delta\nu_{N\equiv C}$ values for bis(ADC) complexes with Hammett constant

Bis(ADC) complex (X)	$\nu_{ave} N\equiv C$ (cm⁻¹)	$\Delta\nu_{ave} N\equiv C$ (cm⁻¹)	Hammett constant^a (σ_p)
(CF ₃)	2273	113	0.53
(F)	2266	106	0.15
(H)	2261	101	0.00
(CH ₃)	2260	100	-0.14
(OCH ₃)	2260	100	-0.29 or -0.12

$${}^a \log K/K_0 = \sigma\rho$$

$${}^{**} \sigma_p = pK_a(\text{benzoic acid}) - pK_a(\text{substituted benzoic acid}) \text{ when } \rho=1$$

K = acid dissociation constant of substituted benzoic acid

K₀ = acid dissociation constant of benzoic acid

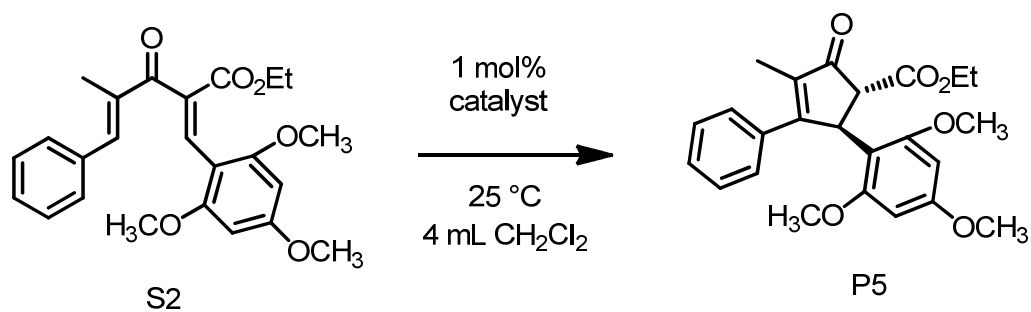
σ = substituent constant

ρ = sensitivity of the reaction to substituent effects

In order to synthesize acetonitrile adducts for catalytic studies, the bis(ADC)PdCl₂ complexes were treated with two molar equivalents of AgBF₄ in dry acetonitrile. This mixture was stirred at 60°C for 2 hours to produce acetonitrile adducts and to precipitate the AgCl. The reaction mixture was cooled and filtered through celite to remove the silver chloride. The product was isolated by layering diethyl ether onto the concentrated solution in acetonitrile.

Initial rate studies with Nazarov cyclization

Miranda reported¹⁹ that bis(acetonitrile) adducts of palladium bis(ADC) complexes catalyzed the cyclization of ethyl-4-methyl-3-oxo-5-phenyl-2-(2,4,6-trimethoxybenzylidene)pent-4-enoate (**S2**) in CH₂Cl₂.



Scheme 5.2. Reaction conditions for cyclization of **S2**

Initial rates for cyclization reactions with different bis(ADC) complexes were measured using the reaction conditions shown in Scheme 5.2. The catalyst, internal standard and CH₂Cl₂ were placed into a 4 mL reaction vial closed by a screw cap with a PTFE/silicon septum under inert atmosphere. A known amount of substrate in CH₂Cl₂ was then injected into the vial, and measurement of time started. Aliquots of the reaction mixture were withdrawn via micro syringe at suitable time intervals. The catalyst in the withdrawn sample was quenched with excess methylisocyanide in acetonitrile, and the sample was diluted to known volume. These prepared samples were stored in a freezer at -4 °C until analyzed by HPLC. After HPLC analysis, the concentrations of substrate (**S2**) and product (**P5**) were calculated using calibration curves. Before the initial rate studies, a trial experiment was used to establish time intervals for sample collection. Initial rates for substrate disappearance ($-d[\text{S2}]/dt$) and product appearance ($d[\text{P5}]/dt$) and uncertainties were determined up to 15-20% substrate consumption. Initial rates were

determined from linear least-squares regression analyses of the plots of [S2] and [P5] versus time. Uncertainties are reported at the 95% confidence level.

HPLC analyses were continued beyond the 15-20% substrate consumption to identify the minimum time required to produce maximum yield. Separate reactions were set up as above but without internal standard. These reaction mixtures were stirred for the time required to get maximum yield as identified by HPLC experiments. Products were isolated by flash chromatography using hexanes : ethyl acetate (9:1) as eluent. These results, together with IR stretching frequencies for methylisocyanide adducts of the catalysts, are shown in Table 5.2 and Figure 5.3.

Table 5.2. Catalytic reaction data for cyclization of S2 with different bis(ADC) palladium complexes together with IR stretching frequency for analogous methylisocyanide adducts

Bis(ADC) complex (X)	$\Delta\nu_{N\equiv C}$ cm ⁻¹	Initial rate mM/s		% Yield ^a	Time min.
		d[S1]/dt	d[P1]/dt		
(CF ₃)	113	7.47	7.01	97 (93)	25
(F)	106	3.36	3.23	98(94)	60
(H)	101	1.33	1.26	97(93)	180
(CH ₃)	100	1.24	1.19	96(95)	210
(OCH ₃)	100	1.21	1.13	98(96)	210

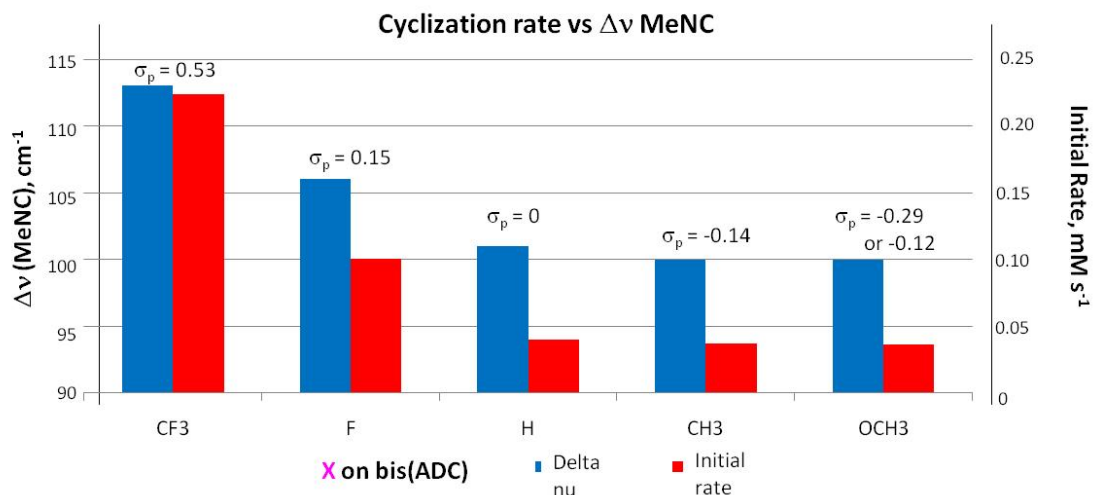


Figure 5.3. Nazarov cyclization rate versus $\Delta\nu_{\text{N}\equiv\text{C}}$ with bis(ADC) palladium catalysts

These results showed a correlation between cyclization rate and ligand donicity of the bis(ADC) complexes. The highest cyclization rate was observed for the weakest effective donor ligand, the *p*-CF₃ substituted bis(ADC) complex. The cyclization rate decreased with increasing donor ability. The lowest cyclization rate was observed for the strongest donor ligands, the *p*-CH₃ and *p*-OCH₃ substituted bis(ADC) complexes. All five bis(ADC) catalysts gave excellent yields (> 90%) but with different reaction rates. According to the reaction rate, the *p*-CF₃ substituted bis(ADC) complex was the most active catalyst. Using this most active catalyst, conditions were tested for the lowest catalytic loading. It was found that down to 0.1 mol% catalyst loading can be used while still achieving excellent yields (> 88%) at room temperature, as shown in Table 5.3.

Table 5.3. Lower catalytic loading with *p*-CF₃ bis(ADC) complex

mol % Pd	Time	HPLC (isolated) Yield
0.5	1 h	96 (92)
0.1	1	30
	3	63
	10	92 (88)
0.025	7	30

Catalytic activity with a dimeric version of the CF₃ bis(ADC) complex with bridging chlorides, shown in Figure 5.4, was also tested in this catalytic study. It showed the lowest initial cyclization rate for substrate disappearance (0.21 μM / s) and product appearance (0.20 μM / s). This catalyst has only one vacant site for substrate binding. These results agree with Frontier, who reported that the availability of *cis* vacant sites is necessary for higher activity.

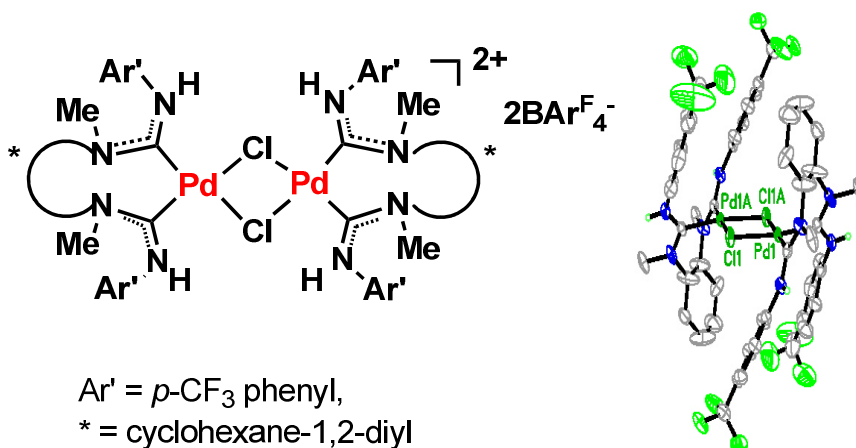


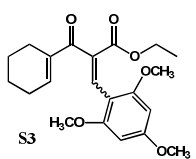
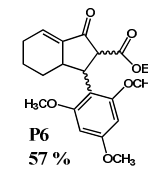
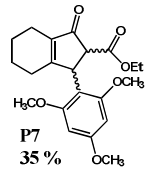
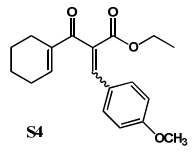
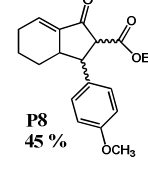
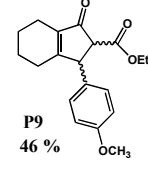
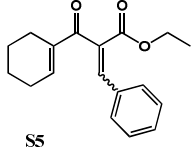
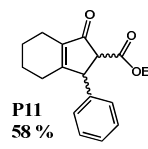
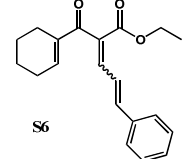
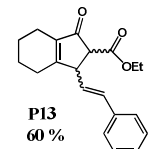
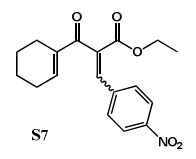
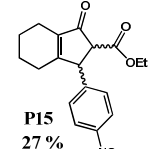
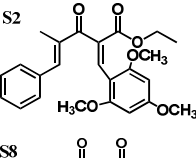
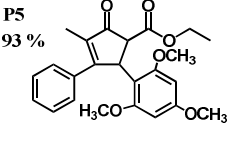
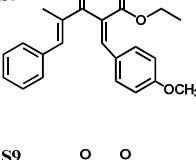
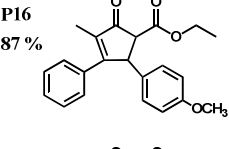
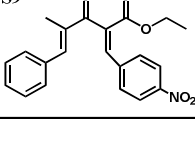
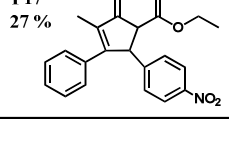
Figure 5.4. Dimeric analogue of *p*-CF₃ bis(ADC) complex with bridging chloride

Substrate scope for Nazarov cyclization

The most active catalyst, the *p*-CF₃ bis(ADC) complex, was tested with different substrates to determine the reaction scope as shown in Table 5.4. The Nazarov substrate **S3** was cyclized rapidly (< 30 min.) at room temperature using 1 mol % catalyst, leading to products **P6** and **P7**. Replacing trimethoxyphenyl at C5(vinyl) position with *p*-methoxyphenyl **S4** reduced the catalytic activity, so slightly harsh reaction conditions were needed (60 °C for 30 minutes). For substrates **S5** and **S6** with phenyl and cinnamyl at the C4 position, longer reaction times were needed, but moderate yields were obtained. These substrates produce only one type of products with the double bond located inside the cyclopentenone. Electron-withdrawing *p*-NO₂ phenyl groups at the C5 position, result in only 27 % yield after seven days of heating at 60 °C. These results indicate that an electron donating group at the C5 position accelerates the Nazarov cyclization. Another group of substrates also showed the same tendency (**S2**, **S7**, and **S8**).

Frontier and Eisenberg reported Nazarov cyclization catalyzed by Ir¹⁵ and Pd¹⁶ complexes for similar types of substrates, but with methyl esters and methyl substituted at 2nd position of cyclohexenyl ring. The *p*-CF₃ substituted bis(ADC) complex showed improved catalytic activity compare to those Pd catalysts, however similar or lesser catalytic activity compared to those Ir catalysts.

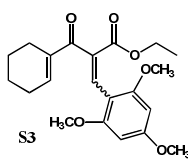
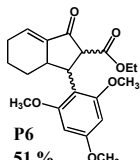
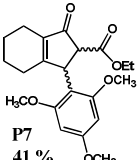
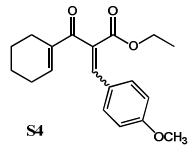
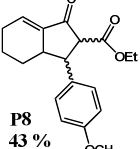
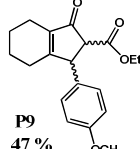
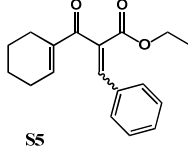
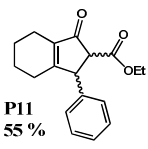
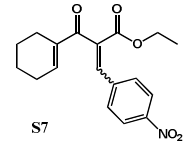
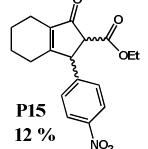
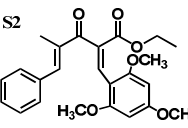
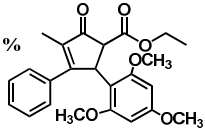
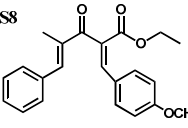
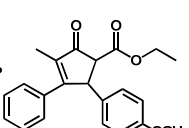
Table 5.4. Substrate scope with *p*-CF₃ bis(ADC) complex

Entry	Substrate	time	Solvent	Temp. / °C	% Yield ^a
1 ^b		0.5 h	CH ₂ Cl ₂	25	 P6 57 %  P7 35 %
2 ^c		0.5 h	CH ₂ ClCH ₂ Cl	60	 P8 45 %  P9 46 %
3 ^c		5 d	CH ₂ ClCH ₂ Cl	60	 P11 58 %
4 ^c		5 d	CH ₂ ClCH ₂ Cl	60	 P13 60 %
5 ^c		7 d	CH ₂ ClCH ₂ Cl	60	 P15 27 %
6 ^b		0.5 h	CH ₂ Cl ₂	25	 P5 93 %
7 ^c		1 h	CH ₂ ClCH ₂ Cl	60	 P16 87 %
8 ^c		5 d	CH ₂ ClCH ₂ Cl	60	 P17 27 %

Reaction conditions: substrate (61 mM) in 4 mL solvent. ^aIsolated yield. ^b1.0 mol % catalyst, ^c5.0 mol % catalyst

The least active monomeric catalyst, the *p*-OCH₃ substituted bis(ADC) complex, was also tested for its activity with different substrates. As shown in Table 5.5 its activity is lower than that of the *p*-CF₃ bis(ADC) complex with all substrates, but the same pattern of yields is observed.

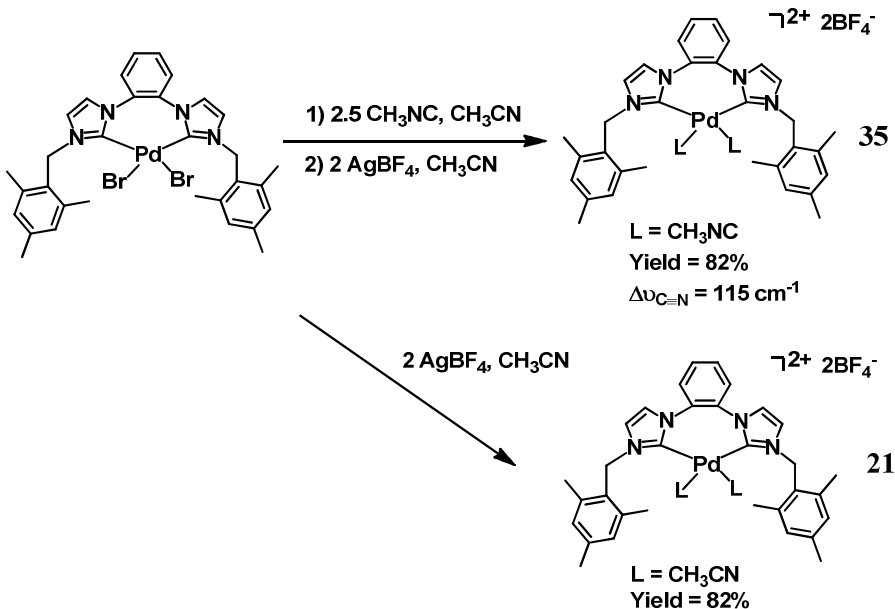
Table 5.5. Substrate scope with *p*-OCH₃ bis(ADC) complex

Entry	Substrate	time	Solvent	Temp. / °C	% Yield ^a
1 ^b		12 h	CH ₂ Cl ₂	25	 
2 ^c		5 h	CH ₂ ClCH ₂ Cl	60	 
3 ^c		5 d	CH ₂ ClCH ₂ Cl	60	
4 ^c		7 d	CH ₂ ClCH ₂ Cl	60	
5 ^b		3.5 h	CH ₂ Cl ₂	25	
6 ^c		4 h	CH ₂ ClCH ₂ Cl	60	

Reaction conditions: substrate (61 mM) in 4 mL solvent. ^aIsolated yield. ^b1.0 mol % catalyst, ^c5.0 mol % catalyst

Nazarov cyclization with a rigid bis(NHC) palladium complex

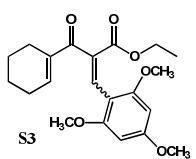
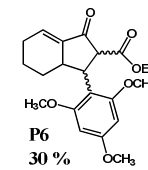
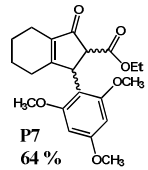
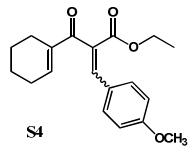
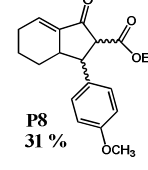
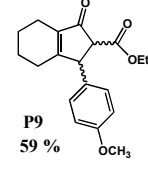
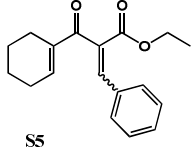
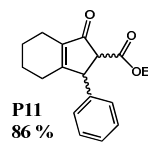
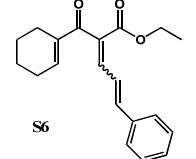
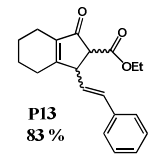
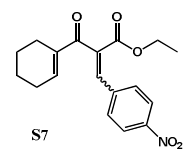
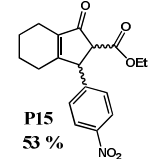
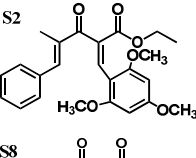
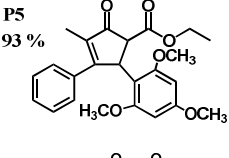
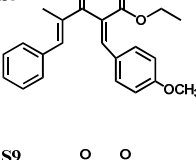
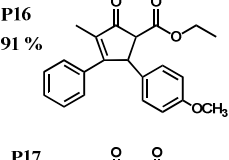
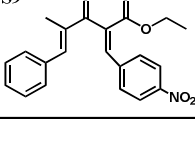
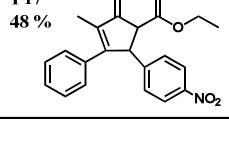
A cationic rigid bis(NHC) palladium complex with labile bis(acetonitrile) ligands synthesized in Chapter II was also tested as a catalyst for Nazarov substrates **S2-S9**. The bis(methylisocyanide) adduct **35** was synthesized by procedures similar to those given in Chapter III for comparison of ligand donicity.



Scheme 5.3. Synthesis of rigid bis(NHC) palladium complexes with bis(methylisocyanide) and bis(acetonitrile) coordination.

This bis(NHC) complex showed a higher $\Delta\nu_{N=C}$ than the *p*-CF₃ bis(ADC) complex, indicating weaker effective donicity. The catalytic activity with different substrates is summarized in Table 5.6. It showed slightly superior activity compared to the active *p*-CF₃ bis(ADC) complex, but the same substrate scope pattern, consistent with the donicity studies. For substrates **S5** and **S6** this catalyst produces good yield but, it is still unable to achieve good yields for substituents with electron withdrawing groups at the C5 position (**S7** and **S9**).

Table 5.6. Substrate scope with rigid bis(NHC) complex **21**

Entry	Substrate	time	Solvent	Temp. / °C	% Yield ^a
1 ^b		0.5 h	CH ₂ Cl ₂	25	 P6 30 %  P7 64 %
2 ^c		1 h	CH ₂ ClCH ₂ Cl	60	 P8 31 %  P9 59 %
3 ^c		40 h	CH ₂ ClCH ₂ Cl	60	 P11 86 %
4 ^c		40 h	CH ₂ ClCH ₂ Cl	60	 P13 83 %
5 ^c		5 d	CH ₂ ClCH ₂ Cl	60	 P15 53 %
6 ^b		0.25 h	CH ₂ Cl ₂	25	 P5 93 %
7 ^c		1 h	CH ₂ ClCH ₂ Cl	60	 P16 91 %
8 ^c		5 d	CH ₂ ClCH ₂ Cl	60	 P17 48 %

Reaction conditions: substrate (61 mM) in 4 mL solvent. ^aIsolated yield. ^b1.0 mol % catalyst, ^c5.0 mol % catalyst

Nazarov cyclization catalyzed by silver salts

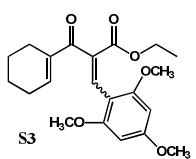
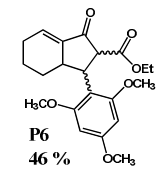
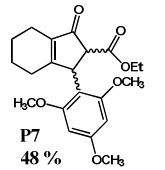
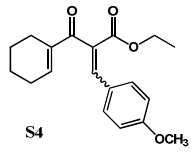
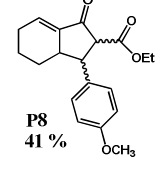
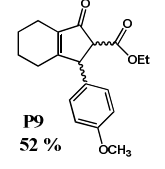
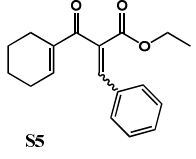
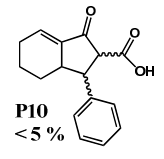
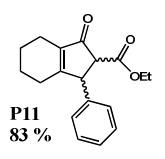
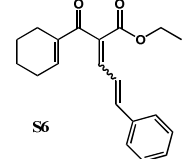
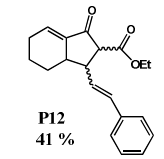
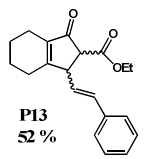
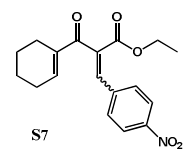
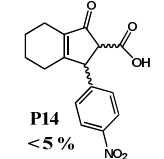
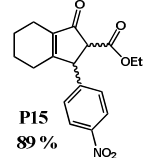
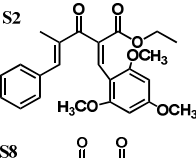
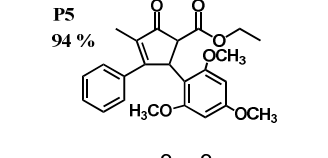
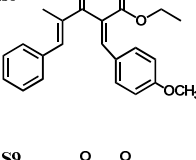
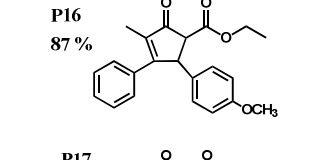
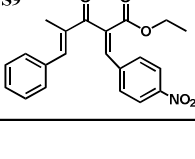
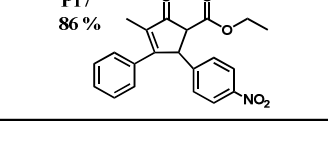
Despite the reported use of silver salts as additives to promote the Nazarov cyclization reaction,¹⁷ the ability of silver salts to act as catalysts in the absence of other metals has not been very much investigated.²⁰ Anthea Miranda¹⁹ showed that AgBAR^F₄, AgSbF₆, and AgOTf can catalyze the cyclization of substrate **S1** to product **P5** using NMR tube experiments in CD₂Cl₂.¹⁷ Therefore, activities of several silver salts were examined using the reaction conditions shown in Scheme 5.2, but with 5 mol% catalyst loading. Reactions were monitored using TLC, and the results are summarized in Table 5.7.

Table 5.7. Nazarov cyclization of substrate **S2** with different silver salts

Silver salt	Time	% Yield
AgSbF ₆	8 min.	94
AgOTf	10 min.	92
AgBF ₄	20 hours	93
AgOAc	4 days	92
AgBAR ^F ₄	5 days	Trace
AgPF ₆	5 days	trace

Silver salts AgSbF₆ and AgOTf showed rapid cyclization, forming **P5** in over 90% yield within 10 minutes. AgBF₄ and AgOAc needed long reaction times (2-4 days) to produce excellent yields (> 90%). Silver salts AgBAR^F₄ and AgPF₆ formed only trace amounts of **P1** after long reaction times (5 days). Using the most active silver salt, AgSbF₆, catalytic activity toward other Nazarov substrates was monitored.

Table 5.8. Substrate scope with AgSbF₆ as catalyst

Entry	Substrate	time	Solvent	Temp. / °C	% Yield ^a
1 ^b		0.5 h	CH ₂ Cl ₂	25	 P6 46 %  P7 48 %
2 ^c		1 h	CH ₂ ClCH ₂ Cl	60	 P8 41 %  P9 52 %
3 ^c		40 h	CH ₂ ClCH ₂ Cl	60	 P10 < 5 %  P11 83 %
4 ^c		40 h	CH ₂ ClCH ₂ Cl	60	 P12 41 %  P13 52 %
5 ^c		5 d	CH ₂ ClCH ₂ Cl	60	 P14 < 5 %  P15 89 %
6 ^b		8 min.	CH ₂ Cl ₂	25	 P5 94 %
7 ^c		1 h	CH ₂ ClCH ₂ Cl	60	 P16 87 %
8 ^c		5 d	CH ₂ ClCH ₂ Cl	60	 P17 86 %

Reaction conditions: substrate (61 mM) in 4 mL solvent. ^aIsolated yield. ^b5.0 mol % catalyst, ^c10.0 mol % catalyst

Even though high catalyst loading was required, AgSbF₆ showed excellent activity towards all substrates. Substrates **S7** and **S9** converted to products **P15** and **P17** in over 85% yields, where it was difficult to achieve good yields with these substrates with palladium catalysts. Substrate **S5** produces the endocyclic product **P11** in high yield with a small amount of hydrolyzed product **P10**. The substrate **S6** produce *exo*- and *endo*-cyclic product in near 50:50 ratio. The exocyclic products were not observed for substrate **S5** and **S6** with the palladium catalysts.

Summary and Conclusion

The acetonitrile adducts of bis(ADC) palladium complexes showed excellent catalytic activities toward Nazarov cyclization of ethyl-4-methyl-3-oxo-5-phenyl-2-(2,4,6-trimethoxybenzylidene)pent-4-enoate (**S2**). The initial rates of the reactions catalyzed by bis(ADC) palladium complexes show a correlation with ligand donicity predicted by a methylisocyanide IR probe study. The highest initial rate and $\Delta\nu_{N\equiv C}$ were observed for the *p*-CF₃ bis(ADC) complex, indicating that the weakest donor ligand results in the highest activity. The strongest donor bis(ADC) complexes with the lowest $\Delta\nu_{N\equiv C}$ values (*p*-CH₃ and *p*-OCH₃) showed the lowest initial rates. The crystal structures of these complexes showed a negligible structural variation upon changing *para* substituents in the phenyl ring. Therefore, bis(ADC) ligands can be tuned to support electrophilic catalysis by the metal without altering the steric properties. The most active bis(ADC) catalyst (*p*-CF₃) showed reasonable substrate scope, but activity decreased when there were less electron donating groups at the vinylic C5 position. A rigid bis(NHC) palladium complex **21** showed slightly improved catalytic activity compared to most bis(ADC) complexes. According to a methylisocyanide IR probe study, this

bis(NHC) ligand showed weaker effective donicity than all studied bis(ADC) ligands. The most active catalysts were those with ligands predicted to have low effective donicity by the MeNC IR probe study. The Silver salts AgSbF₆ and AgOTf showed excellent catalytic activity toward cyclization of **S2**. AgSbF₆ showed excellent activity toward all substrates investigated, even with electron withdrawing substituents at the C5 position.

Experimental

General Considerations. All manipulations were carried out under air unless otherwise noted. Diethyl ether (Acros), *n*-hexane (Acros), and hexanes (Pharmco) were purified by distillation from sodium benzophenone ketyl. Dichloromethane (Pharmco) and dichloroethane were washed with a sequence of concentrated H₂SO₄, de-ionized water, 5% Na₂CO₃ and de-ionized water, followed by pre-drying over anhydrous CaCl₂, then refluxed over and distilled from P₂O₅ under nitrogen. Acetonitrile (Pharmco) was pre-dried over anhydrous CaCl₂ and refluxed over and distilled from CaH₂ under nitrogen. NMR solvents were purchased from Cambridge Isotopes Laboratories. DMSO-*d*₆ and CD₃CN-*d*₃ were dried over activated 4 Å molecular sieves followed by vacuum distillation at room temperature. CD₂Cl₂ was dried over activated 4 Å molecular sieves and stored over P₂O₅ before distillation at room temperature for use. All other reagents were purchased from Acros, Aldrich, or Strem and used as received. Substrates **S2**, **S8** and **S9** were synthesized using published procedures.^{15,19} Substrates **S3-S6** were also synthesized using the same procedure and compared with published data for the same compounds prepared by different synthetic routes.²⁰ New substrate **S7** was also synthesized using the same procedure and characterized by NMR and elemental analysis.

Previously known products (**P5**, **P16** and **P17**) were compared with published data.^{15,19} For new compounds stereo-chemistry, was assigned using DEPT, HMQC and HMBC experiments. NMR spectra were recorded on Varian GEMINI 2000 (300 MHz) and Varian Unity INOVA (400 and 600 MHz) spectrometers. Reported chemical shifts are referenced to residual solvent peaks (¹³C, ¹H). IR spectra were acquired from Nujol mulls on a Perkin Elmer system 2000 FT-IR spectrometer, using 0.5 cm⁻¹ resolution and weak apodization. HPLC spectra were recorded on a Beckman system with a 166 detector (UV detector) using a BDS HYPERSIL C18 column (5 μm particle size, 4.6 mm I.D. and 100 mm length) from Thermo Scientific. Elemental analyses were performed by Midwest Microlab, Indianapolis, Indiana. HRMS were recorded on an Orbitrap tandem mass spectrometer using nano-electrospray ionization.

Nazarov substrate synthesis

Nazarov substrates were synthesized using a common procedure reported for substrate **S2** by Aggarwal¹⁹ and Togni.¹⁵ First, the corresponding acid (alpha-methylcinnamic acid or cyclohexenylcarboxylic acid) was treated with oxalyl chloride in dichloromethane, with a few drops of dimethyl formamide added, at 0 °C for 3 h to form the corresponding acid chloride. The volatiles were evaporated, and the residue was dried under vacuum for a couple of hours and then dissolved in THF. Ethyl acetate was treated with lithium diisopropylamide generated in situ by reaction of *n*-butyl lithium with diisopropylamine in dry THF at -78 °C. The acid chloride solution in THF was added to the above solution, and the mixture was stirred for 3 hours at -78 °C. Acid work up and flash chromatography produced the β-keto esters as yellow oils. A Knoevenagel

condensation was then used to produce Nazarov substrates by reaction between β -keto esters and different aldehydes in the presence of catalytic amounts of acetic acid and piperidine in a Dean-Stark apparatus using benzene as a solvent.

Ethyl 2-(cyclohex-1-enecarbonyl)-3-(2,4,6-trimethoxyphenyl)acrylate S3

Yield: 63% % E / Z (7:3). ^1H NMR (400 MHz, $\text{CDCl}_3\text{-d}_1$): δ 7.95 (s, 1H, CH, major isomer), 7.23 (s, 1H, CH, minor isomer), 6.72 (m, 1H, cyclohexenyl-CH, minor isomer), 6.65 (m, 1H, cyclohexenyl-CH, major isomer), 6.08 (s, 2H, Ar-CH, minor isomer), 6.01 (s, 2H, Ar-CH, major isomer), 4.25 (q, 2H, $^3\text{J}_{\text{HH}} = 9.6$ Hz, OCH_2 , minor isomer), 4.14 (q, 2H, $^3\text{J}_{\text{HH}} = 9.6$ Hz, OCH_2 , major isomer), 3.84 (s, 3H, *p*- OCH_3 , minor isomer), 3.81 (s, 3H, *p*- OCH_3 , major isomer), 3.76 (s, 6H, *o*- OCH_3 , minor isomer), 3.70 (s, 6H, *o*- OCH_3 , major isomer), 2.35-2.04 (s, 4H, cyclohexenyl- CH_2 , major & minor isomer), 2.35-1.70 (s, 4H, cyclohexenyl- CH_2 , major & minor isomer), 1.28 (t, 3H, $^3\text{J}_{\text{HH}} = 9.6$ Hz, CH_3 , major isomer), 1.18 (t, 3H, $^3\text{J}_{\text{HH}} = 9.6$ Hz, CH_3 , minor isomer).

(Z)-Ethyl 2-(cyclohex-1-enecarbonyl)-3-(4-methoxyphenyl)acrylate S4

Yield: 65 % ^1H NMR (400 MHz, $\text{CDCl}_3\text{-d}_1$): δ 7.73 (s, 1H, CH), 6.72 (d, 2H, Ar-CH), 6.72 (s, 1H, cyclohexenyl-CH), 6.72 (d, 2H, Ar-CH), 4.24 (q, 2H, $^3\text{J}_{\text{HH}} = 7.2$ Hz, OCH_2), 3.81 (s, 3H, OCH_3), 2.39-2.36 (m, 2H, cyclohexenyl- CH_2), 2.16-2.13 (m, 2H, cyclohexenyl- CH_2), 1.68-1.64 (m, 2H, cyclohexenyl- CH_2), 1.61-1.56 (m, 2H, cyclohexenyl- CH_2), 1.28 (t, 3H, $^3\text{J}_{\text{HH}} = 7.2$ Hz, CH_3).

(Z)-Ethyl 2-(cyclohex-1-enecarbonyl)-3-phenylacrylate S5

Yield: 67 % ¹H NMR (400 MHz, CDCl₃-d₁): δ 7.79 (s, 1H, CH), 7.34-7.28 (m, 5H, Ar-CH), 6.82 (m, 1H, cyclohexenyl-CH), 6.72 (d, 2H, Ar-CH), 4.26 (q, 2H, ³J_{HH} = 6.8 Hz, OCH₂), 2.38-2.34 (m, 2H, cyclohexenyl-CH₂), 2.14-2.12 (m, 2H, cyclohexenyl-CH₂), 1.66-1.63 (m, 2H, cyclohexenyl-CH₂), 1.63-1.54 (m, 2H, cyclohexenyl-CH₂), 1.28 (t, 3H, ³J_{HH} = 6.8 Hz, CH₃).

(2Z,4E/4Z)-Ethyl 2-(cyclohex-1-enecarbonyl)-5-phenylpenta-2,4-dienoate S6

Yield: 58 % ¹H NMR (400 MHz, CDCl₃-d₁): δ 7.51 (d, 1H, ³J_{HH} = 12 Hz, CH), 7.44-7.42 (m, 2H, Ar-CH), 7.37-7.31 (m, 3H, Ar-CH), 6.97 (d, 1H, ³J_{HH} = 15.2 Hz, CH), 6.78-6.69 (m, 2H, overlapping cyclohexenyl-CH and CH), 4.23 (q, 2H, ³J_{HH} = 9.6 Hz, OCH₂), 2.39 (bm, 2H, cyclohexenyl-CH₂), 2.25-2.23 (m, 2H, cyclohexenyl-CH₂), 1.75-1.62 (m, 4H, cyclohexenyl-CH₂), 1.24 (t, 3H, ³J_{HH} = 9.6 Hz, CH₃).

(Z)-Ethyl 2-(cyclohex-1-enecarbonyl)-3-(4-nitrophenyl)acrylate S7

Yield: 64 % ¹H NMR (400 MHz, CDCl₃-d₁): δ 8.17 (dd, 2H, ³J_{HH} = 8.8 & 2.0 Hz Ar-CH), 7.80 (s, 1H, CH), 7.49 (dd, 2H, ³J_{HH} = 8.8 & 2.0 Hz Ar-CH), 6.72 (m, 1H, cyclohexenyl-CH), 4.29 (q, 2H, ³J_{HH} = 6.8 Hz, OCH₂), 2.34-2.32 (m, 2H, cyclohexenyl-CH₂), 2.17-2.14 (m, 2H, cyclohexenyl-CH₂), 1.66-1.55 (m, 4H, cyclohexenyl-CH₂), 1.29 (t, 3H, ³J_{HH} = 7.2 Hz, CH₃). ¹³C NMR (100 MHz, CD₃CN-d₃): δ 195.50 (C=O), 164.44 (O-C=O), 148.03 (ipso-C-NO₂), 145.88 (Ar-C), 139.54 (ipsoAr-C), 139.43 (HC=C), 138.28 (Ar-C), 135.69 (HC=C), 130.32 (C=CH), 123.81 (C=CH), 61.83 (O-CH₂), 26.26

(CH₂), 22.55 (CH₂), 21.50 (CH₂), 21.31 (CH₂), 14.04 (CH₃). Anal. Calculated for C₁₈H₁₉O₅N: C, 65.64; H, 5.81; N, 4.25 %. Found: C, 65.56; H, 5.84; N, 4.29 %.

General procedure for Nazarov cyclization

Catalyst was placed into a 4 mL reaction vial closed by a screw cap with a PTFE/silicon septum. A bulk solution of substrate and internal standard, 2,7-dimethylnaphthalene, was made with a known molar ratio, in the corresponding solvent. The required amount was then withdrawn and injected into the reaction vial through the septum, and measurement of time started. The reaction was monitored by HPLC or TLC by withdrawing appropriate portions from the reaction mixture. For isolated yields the reaction was set up without internal standard. After aqueous NaHCO₃ workup, products were isolated by flash chromatography.

Kinetic Studies

Experiments were set up as described above for general catalytic procedures. 10 μ L samples were withdrawn at appropriate time intervals and added to excess CH₃CN in acetonitrile to quench the reaction. The mixture was diluted to a known volume and analyzed by HPLC. Concentrations of substrate and products at various times were determined using calibration curves. The rates of reactions and uncertainties were determined from linear least-square regression analysis of plots of concentration of substrate and product versus time. Uncertainties were reported at the 95% confidence level.

Ethyl 1-oxo-3-(2,4,6-trimethoxyphenyl)-2,3,3a,4,5,6-hexahydro-1H-indene-2-carboxylate (P6)

^1H NMR (400 MHz, $\text{CDCl}_3\text{-d}_1$): δ 6.69 (q, 1H, $^3J_{\text{HH}} = 3.2$ Hz, cyclohexenyl-CH), 6.14 (s, 2H, Ar-CH), 4.25 (d, 1H, $^3J_{\text{HH}} = 12$ Hz, CH), 4.20-4.00 (m, 2H, O-CH₂), 4.25 (t, 1H, $^3J_{\text{HH}} = 12$ Hz, CH), 3.80 (s, 3H, OCH₃), 3.78 (s, 6H, OCH₃), 2.97-2.91 (m, 1H, CH), 2.34-2.19 (m, 2H, cyclohexenyl-CH₂), 1.88-1.80 (m, 2H, cyclohexenyl-CH₂), 1.49-1.42 (m, 1H, cyclohexenyl-CH₂), 1.17 (t, 3H, $^3J_{\text{HH}} = 7.2$ Hz, CH₃), 1.49-1.42 (m, 1H, cyclohexenyl-CH₂), ^{13}C NMR (100 MHz, $\text{CDCl}_3\text{-d}_3$): δ 199.63 (C=O), 164.44 (O-C=O), 159.95 (Ar-C), 159.73 (Ar-C), 140.42 (HC=C), 134.30 (C=CH), 107.51 (ipso-Ar), 91.07 (Ar-CH), 60.74 (O-CH₂), 57.87 (CH), 55.79 (O-CH₃), 55.19 (O-CH₃), 40.53 (CH), 39.61 (CH₂), 27.24 (CH₂), 25.72 (CH₂), 21.60 (CH₂), 14.10 (CH₃). HRMS calculated for ($\text{C}_{21}\text{H}_{26}\text{O}_6 + \text{H}^+$) 375.1802, found 375.1794

Ethyl 1-oxo-3-(2,4,6-trimethoxyphenyl)-2,3,4,5,6,7-hexahydro-1H-indene-2-carboxylate (P7)

^1H NMR (400 MHz, $\text{CDCl}_3\text{-d}_1$): δ 6.14 (d, 1H, $^3J_{\text{HH}} = 2$ Hz, Ar-CH), 6.04 (d, 1H, $^3J_{\text{HH}} = 2$ Hz, Ar-CH), 4.81 (bs, CH), 4.24-4.13 (m, 2H, O-CH₂), 3.79 (s, 6H, OCH₃), 3.78 (s, 3H, OCH₃), 3.54 (d, 1H, $^3J_{\text{HH}} = 2.8$ Hz, CH), 2.18-1.94 (m, 4H, cyclohexenyl-CH₂), 1.71-1.56 (m, 4H, cyclohexenyl-CH₂), 1.26 (t, 3H, $^3J_{\text{HH}} = 7.2$ Hz, CH₃), ^{13}C NMR (100 MHz, $\text{CDCl}_3\text{-d}_3$): δ 202.07 (C=O), 177.46 (C=C), 170.66 (O-C=O), 160.70 (Ar-C), 159.80 (Ar-C), 159.58 (Ar-C), 135.27 (C=C), 107.42 (ipso-Ar), 91.03 (Ar-CH), 90.90 (Ar-CH), 61.28 (O-CH₂), 58.72 (CH), 56.26 (O-CH₃), 55.23 (O-CH₃), 55.48 (O-CH₃),

41.78 (CH), 26.52 (CH₂), 22.43 (CH₂), 21.92 (CH₂), 20.53 (CH₂), 14.46 (CH₃). HRMS calculated for (C₂₁H₂₆O₆ + H⁺) 375.1802, found 375.1788

ethyl 3-(4-methoxyphenyl)-1-oxo-2,3,3a,4,5,6-hexahydro-1H-indene-2-carboxylate (P8)

¹H NMR (400 MHz, CDCl₃-d₁): δ 7.21 (d, 2H, ³J_{HH} = 8.8 Hz, Ar-CH), 6.90-6.86 (overlapping d & q, 3H, Ar-CH & cyclohexenyl-CH), 4.20-4.08 (m, 2H, O-CH₂), 3.79 (s, 3H, OCH₃), 3.47 (d, 1H, ³J_{HH} = 12 Hz, CH), 3.18 (t, 1H, cyclohexenyl-CH), 2.65-2.59 (m, 1H, CH), 2.39-2.19 (m, 2H, cyclohexenyl-CH₂), 2.01-1.95 (m, 1H, cyclohexenyl-CH₂), 1.90-1.87 (m, 1H, cyclohexenyl-CH₂), 1.54-1.46 (m, 1H, cyclohexenyl-CH₂), 1.21 (t, 3H, ³J_{HH} = 7.2 Hz, CH₃), 1.15-1.12 (m, 1H, cyclohexenyl-CH₂). HRMS calculated for (C₁₉H₂₂O₄ + H⁺) 315.1589, found 315.1585

Ethyl 1-(4-methoxyphenyl)-3-oxo-2,3,4,5,6,7-hexahydro-1H-indene-2-carboxylate (P9)

¹H NMR (400 MHz, CDCl₃-d₁): δ 7.01(d, 2H, ³J_{HH} = 8 Hz, Ar-CH), 6.85 (d, 2H, ³J_{HH} = 8 Hz, Ar-CH), 4.22-4.19 (overlapping O-CH₂ & CH), 3.79 (s, 3H, OCH₃), 3.32 (d, 1H, ³J_{HH} = 2.8 Hz, CH), 2.24-2.05 (m, 4H, cyclohexenyl-CH₂), 1.68-1.64 (m, 4H, cyclohexenyl-CH₂), 1.28 (t, 3H, ³J_{HH} = 7.2 Hz, CH₃). HRMS calculated for (C₁₈H₂₀O₃ + H⁺) 315.1589, found 315.1573

Ethyl 1-oxo-3-phenyl-2,3,4,5,6,7-hexahydro-1H-indene-2-carboxylate (P11)

^1H NMR (400 MHz, $\text{CDCl}_3\text{-d}_1$): δ 7.28-7.18(m, 3H, Ar-CH), 7.04-7.01(m, 2H, Ar-CH), 4.18-4.11(overlapping O-CH₂ & CH), 3.29(d, 1H, $^3J_{\text{HH}} = 2.8$ Hz, CH), 2.18-1.99 (m, 4H, cyclohexenyl-CH₂), 1.66-1.56 (m, 4H, cyclohexenyl-CH₂), 1.21 (t, 3H, $^3J_{\text{HH}} = 7.2$ Hz, CH₃). ^{13}C NMR (100 MHz, $\text{CDCl}_3\text{-d}_3$): δ 200.61 (C=O), 175.23 (O-C=O), 168.86 (C=C), 140.01(C=C), 137.54 (*ipso*-Ar), 129.00 (*meta*-Ar), 127.47 (*ortho*-Ar), 127.39 (*para*-Ar), 61.57 (O-CH₂), 61.36 (CH), 52.00 (CH), 26.42 (CH₂), 21.93 (CH₂), 21.33 (CH₂), 20.25 (CH₂), 14.13 (CH₃). HRMS calculated for ($\text{C}_{18}\text{H}_{20}\text{O}_3 + \text{H}^+$) 315.1485, found 315.1479

(E)-ethyl 1-oxo-3-styryl-2,3,3a,4,5,6-hexahydro-1H-indene-2-carboxylate (P12)

^1H NMR (400 MHz, $\text{CDCl}_3\text{-d}_1$): δ 7.56-7.38 (m, 5H, Ar-CH), 7.02 (q, 1H, $^3J_{\text{HH}} = 12$ Hz, cyclohexenyl-CH), 6.72 (d, 1H, $^3J_{\text{HH}} = 21.2$ Hz, C=CH), 6.40-6.32 (dd, 1H, $^3J_{\text{HH}} = 21.2$ Hz, $^3J_{\text{HH}} = 12$ Hz, C=CH), 4.45-4.33 (m, 2H, O-CH₂), 3.44 (d, 1H, $^3J_{\text{HH}} = 16$ Hz, CH), 3.00-2.98 (m, 1H, CH), 2.63-2.32 (m, 4H, cyclohexenyl-CH), 2.11-2.08 (m, 2H, cyclohexenyl-CH₂), 1.80-1.64 (m, 2H, cyclohexenyl-CH₂), 1.47 (t, 3H, $^3J_{\text{HH}} = 7.2$ Hz, CH₃),. HRMS calculated for ($\text{C}_{18}\text{H}_{20}\text{O}_3 + \text{H}^+$) 311.1642, found 311.1630

(E)-ethyl 1-oxo-3-styryl-2,3,4,5,6,7-hexahydro-1H-indene-2-carboxylate (P13)

^1H NMR (400 MHz, $\text{CDCl}_3\text{-d}_1$): δ 7.54-7.42 (m, 5H, Ar-CH), 6.76 (d, 1H, $^3J_{\text{HH}} = 21.2$ Hz, C=CH), 6.16-6.07 (dd, 1H, $^3J_{\text{HH}} = 21$ Hz, $^3J_{\text{HH}} = 12$ Hz, C=CH), 4.44-4.37 (m, 2H, O-CH₂), 3.02 (bd, 1H, $^3J_{\text{HH}} = 12$ Hz, CH), 3.45 (d, 1H, $^3J_{\text{HH}} = 3.6$ Hz, CH), 2.59-2.35 (m, 4H, cyclohexenyl-CH), 2.89-2.80 (m, 4H, cyclohexenyl-CH₂), 1.48 (t, 3H, $^3J_{\text{HH}} = 7.2$

Hz, CH_3),. ^{13}C NMR (100 MHz, $\text{CDCl}_3\text{-d}_3$): δ 200.16(C=O), 174.71 (C=C), 169.00 (O-C=O), 137.22 (C=C), 136.27 (*ipso*-Ar), 133.54 (C=CH), 128.62 (Ar-H), 127.87 (C=CH), 126.29 (Ar-H), 61.63 (O- CH_2), 58.75 (CH), 50.10 (CH), 26.66 (CH_2), 22.01 (CH_2), 21.39 (CH_2), 20.29 (CH_2), 14.19 (CH_3). HRMS calculated for ($\text{C}_{18}\text{H}_{20}\text{O}_3 + \text{H}^+$) 311.1642, found 311.1632

Ethyl 1-(4-nitrophenyl)-3-oxo-2,3,4,5,6,7-hexahydro-1H-indene-2-carboxylate (P15)

^1H NMR (300 MHz, $\text{CDCl}_3\text{-d}_1$): δ 8.21 (d, 2H, $^3J_{\text{HH}} = 8.7$ Hz, Ar-CH), 7.29 (d, 2H, $^3J_{\text{HH}} = 8.7$ Hz, Ar-CH), 4.39 (br s, 1H, CH), 4.26-4.19 (m, 2H, O- CH_2), 3.32 (d, 1H, $^3J_{\text{HH}} = 2.7$ Hz, CH), 2.26-1.96 (m, 4H, cyclohexenyl- CH_2), 1.72-1.68 (m, 4H, cyclohexenyl- CH_2), 1.29 (t, 3H, $^3J_{\text{HH}} = 6.9$ Hz, CH_3).

[Pd (1,1'-bis(2,4,6-trimethylbenzyl)-3,3'-(1,2-phenylene)diimidazol-2,2'-diylidene) (CH_3CN) $_2$][BF_4] $_2$ (21)

Methyl isocyanide (17 μL , 0.3037 mmol) was added to a stirred solution of (1,1'-bis(2,4,6-trimethylbenzyl)-3,3'-(1,2-phenylene)diimidazolium dibromide (90 mg, 0.1215 mmol) in acetonitrile (10 mL), and the mixture was stirred for 1 h. AgBF_4 (47 mg, 0.243 mmol) was then added to the reaction mixture, and it was stirred for 2 h. The mixture was filtered through celite, solvent was evaporated, and the residue was dried in vacuum for 12 h. The product was dissolved in dichloromethane (5 mL), the solution was filtered through celite, solvent was evaporated, and the residue was dried in vacuum for 12 h. This sequence was repeated 2 more times. In the final sequence, diethyl ether was added to the filtrate to obtain product as white crystals. The product was isolated by filtration

and dried in vacuo for 12 h. Yield: 84 mg, 84%. ^1H NMR (400 MHz, DMSO- d_6): δ 7.96 (2H, d, $^3J_{\text{HH}} = 2$ Hz, *imid.*), 7.82 (4H, s, *ph.*), 7.05 (4H, s, *m-CH(mes.)*), 6.97 (2H, d, $^3J_{\text{HH}} = 2$ Hz, *imid.*), 5.48-5.34 (4H, AB, CH_2), 3.63 (6H, s, CH_3NC), 2.29 (6H, s, *p-CH}_3*), 2.27 (12H, s, *o-CH}_3*). ^{13}C NMR (101.53 MHz, CD_2Cl_2 - d_2): δ 155.27 (carbene), 138.73 (*Ar-C*), 138.13 (*Ar-C*), 131.06 (*Ar-C*), 130.79 (*Ar-C*), 129.50 (*Ar-C*), 127.52 (*Ar-C*), 126.47 (*Ar-C*), 125.50 (*imid.-C*), 123.37 (CH_3NC), 122.90 (*imid.-C*), 49.21 (N- CH_2), 30.44 (CH_3NC), 20.65 (*p-CH}_3(\text{mes.})*), 19.39 (*o-CH}_3(\text{mes.})*). IR (Nujol, cm^{-1}): 2275 v(m). Anal. Calculated for: $\text{C}_{36}\text{H}_{42}\text{B}_2\text{F}_8\text{N}_6\text{Pd}$: C, 49.85 – 51.67; H, 4.70 – 4.82; N, 9.56 – 10.05%. Found: C, 49.33; H, 5.08; N, 9.45 %. (0.5 mol CH_2Cl_2 trap in the crystals).

References

- (1) Pellissier, H. *Tetrahedron* **2005**, *61*, 6479.
- (2) Frontier, A. J.; Collison, C. *Tetrahedron* **2005**, *61*, 7577.
- (3) Tius, M. A.; Kwok, C. K.; Gu, X. Q.; Zhao, C. W. *Synth. Commun.* **1994**, *24*, 871.
- (4) Casson, S.; Kocienski, P. *J. Chem. Soc.-Perkin Trans. I* **1994**, 1187.
- (5) Kim, S. H.; Cha, J. K. *Synthesis-Stuttgart* **2000**, 2113.
- (6) Marino, J. P.; Linderman, R. J. *Journal of Organic Chemistry* **1983**, *48*, 4621.
- (7) Marino, J. P.; Linderman, R. J. *Journal of Organic Chemistry* **1981**, *46*, 3696.
- (8) Andrews, J. F. P.; Regan, A. C. *Tetrahedron Lett.* **1991**, *32*, 7731.
- (9) Sakai, T.; Miyata, K.; Takeda, A. *Chem. Lett.* **1985**, 1137.
- (10) Jones, T. K.; Denmark, S. E. *Helv. Chim. Acta* **1983**, *66*, 2377.
- (11) Denmark, S. E.; Klis, R. C. *Tetrahedron* **1988**, *44*, 4043.

- (12) Giese, S.; West, F. G. *Tetrahedron* **2000**, *56*, 10221.
- (13) Giese, S.; West, F. G. *Tetrahedron Lett.* **1998**, *39*, 8393.
- (14) Denmark, S. E.; Wallace, M. A.; Walker, C. B. *Journal of Organic Chemistry* **1990**, *55*, 5543.
- (15) Atesin, A. C.; Zhang, J.; Vaidya, T.; Brennessel, W. W.; Frontier, A. J.; Eisenberg, R. *Inorganic Chemistry* **2010**, *49*, 4331.
- (16) Zhang, J.; Vaidya, T.; Brennessel, W. W.; Frontier, A. J.; Eisenberg, R. *Organometallics* **2010**, *29*, 3341.
- (17) Walz, I.; Bertogg, A.; Togni, A. *Eur J Org Chem* **2007**, 2650.
- (18) Wanniarachchi, Y. A. Ph.D. Thesis, Oklahoma State University, 2008.
- (19) Miranda, A. J. Ph.D. Thesis, Oklahoma State University, 2009.
- (20) Huang, J.; Frontier, A. J. *J. Am. Chem. Soc.* **2007**, *129*, 8060.
- (21) Aggarwal, V. K.; Beffield, A. J. *Organic Letters* **2003**, *5*, 5075.
- (22) Canterbury, D. P.; Herrick, I. R.; Um, J.; Houk, K. N.; Frontier, A. J. *Tetrahedron* **2009**, *65*, 3165.

VITA

Sri Skandaraja Subramanium

Candidate for the Degree of

Doctor of Philosophy

Thesis: SYNTHETIC, STRUCTURAL, SPECTROSCOPIC, CATALYTIC AND
MECHANISTIC STUDIES OF PALLADIUM COMPLEXES WITH BIDENTATE
CARBENE LIGANDS

Major Field: Inorganic Chemistry

Biographical:

Education:

Completed the requirements for the Doctor of Philosophy in Inorganic
Chemistry at Oklahoma State University, Stillwater, Oklahoma in May 2011.

B.Sc. Special Degree in Chemistry with first class honors, University of
Kelaniya, Kelaniya, Sri Lanka in 2003.

Professional Memberships:

American Chemical Society

Name: Sri S. Subramaniam

Date of Degree: May, 2011

Institution: Oklahoma State University

Location: Stillwater, Oklahoma

Title of Study: SYNTHETIC, STRUCTURAL, SPECTROSCOPIC, CATALYTIC AND
MECHANISTIC STUDIES OF PALLADIUM COMPLEXES WITH BIDENTATE
CARBENE LIGANDS

Pages in Study: 259

Candidate for the Degree of Doctor of Philosophy

Major Field: Chemistry

Scope and Method of Study:

Findings and Conclusions:

Carbenes are strong donor ligands widely used in metal catalyzed organic reactions. In early work, N-heterocyclic carbenes (NHCs) were considered as mimics for tertiary phosphine ligands, but subsequently they were shown to be superior to phosphine ligands in terms of activity and scope for many catalytic reactions. Bidentate carbenes are potentially more stable than monodentate carbene due to the chelate effect. A possible pathway for tuning the metal reactivity is bite angle variation. Donor abilities of imidazole-derived bis(NHCs), bis acyclic diaminocarbenes, bitriazole bis(NHCs), "abnormal" C4-bound bis(NHCs), and bis(phosphines), and thus their trans influence and effect on metal electrophilicity, were studied using methylisocyanide as an IR probe. Donor abilities of ligands were correlated with structural parameters such as bite angle, and carbene dihedral angle. Acetonitrile adducts of [(chelate)Pd]²⁺ complexes were examined as catalysts for electrophilic cyclizations of acetylenic aldehydes with alcohols to form cyclic alkenyl ethers, hydroarylation of alkynes with aromatic C-H bonds, and polarized Nazarov cyclizations of dialkenyl ketones. The most effective catalysts were those with ligands which were identified as less effective donor ligands by MeNC IR probe studies. The study identified that donor type is the most important determinant of metal electrophilicity, but steric effects are also important. Bis(carbene) ligands can be tuned to support electrophilic catalysis by metals, in contrast to the prevailing use of mono-NHCs to engender electron rich metal centers. Bis(ADC) complexes can be tuned to support electrophilic catalysis by electronic tuning without altering the sterics. Cationic methylpalladium bis(NHC) complexes were synthesized and characterized for first time. Mechanistic details of the migratory insertion of CO into methylpalladium complexes, which is a key step in CO/ethylene polymerization, also have been investigated for the first time with NHC ligands on palladium.

ADVISER'S APPROVAL: Dr. LeGrande M. Slaughter
